Determination of the Velocity of Sound in Reservoir Fluids Using an Equation of State

By

Hoda Tahani

Submitted for the degree of Doctor of Philosophy in

Petroleum Engineering

Heriot-Watt University

Institute of Petroleum Engineering

November 2011

ABSTRACT

Production of oil and gas from hydrocarbon reservoirs results in reduction in reservoir pressure and changes in the fluid composition and saturations. Enhanced oil recovery methods such as Gas Injection, Water Flooding, CO_2 Injection, in-situ Combustion, Water Alternative Gas injection (WAG) and so on have similar effects. Variation of these properties can lead to changes in the velocity of sound in subsurface layers. On the other hand, any change in temperature, pressure, composition and density of pore fluids has strong influence on the seismic elastic properties.

Elastic properties of fluids are usually simplified in geophysics. All existing software employs empirical relations to calculate seismic wave velocities in reservoir fluids. In this study, thermodynamic properties have been considered as first and second order derivative properties of the thermodynamic potentials. For this purpose, a statistical thermodynamic approach, with the Statistical Associated Fluid Theory – Boublik - Alder – Chen – Kreglewski has been used and developed further for mixtures and real oils by proposing new mixing rules, tuning binary interaction parameters, and utilizing the properties of single carbon numbers.

In addition, a large number of experimental data on pure, binary and multi-component systems have been generated in this work. The predictions of the model developed in this work have been validated against the experimental data generated in this work and those reported in the literature. The predictions were found to be in very good agreement with independent experimental data.

Dedicted to my parents, Mohammad and Zahra,

my husband, Siavash and my little daughter Helya.

ACKNOWLEDGEMENT

This thesis is submitted in partial fulfilment of the requirements for the Ph.D. degree at Heriot-Watt University. This work has been conducted at the Institute of Petroleum from February 2007 to February 2011 under the supervision of Professor Bahman Tohidi and Dr. Antonin Chapoy.

The project was financially supported through a Joint Industrial Project (JIP) by TOTAL, Sclumberger and Marathon Oil companies which are gratefully acknowledged.

I specially would like to thank my advisor, Professor Bahman Tohidi, for his guidance during my research and study in Heriot-Watt University. His perpetual energy and enthusiasm in research had motivated all his advisees, including me. I am indebted to many of my colleagues to support me. I was delighted to interact with Dr. Antonin Chapoy by having him as my co-advisor. Speciall thanks go to him for his help and support, and his huge enthusiasm during the time we worked together.

All my lab colleagues at the PVT Laboratory in Institute of petroleum engineering made it a convivial place to work. In particular, I would like to owe my deepest gratitude to my late colleague, Mr. Keith Bell for his collaboration and fruitful discussions. Also, special thanks to Dr. Jinhai Yang, Mr. Ken Malcolm and Mr. Alastair Reid who had inspired me in research through our interactions during the long hours in the lab. I wish to express my thanks to the Institute of Petroleum Engineering, Heriot-Watt University.

My deepest gratitude goes to my parents for their unflagging love and support throughout my life; I have no suitable word that can fully describe their everlasting love to me. I feel proud of my husband, Siavash for his supports; this dissertation is simply impossible without him.

Last, but not least, thanks are to God for my life through all moments in the past five years. You have made my life more beautiful with the little daughter you have given to us in these years.

Hoda Tahani

ACADEMIC REGISTRY

Research Thesis Submission

TABLE OF CONTENTS

LISTS OF TABLES

LISTS OF FIGURES

LIST OF MAIN SYMBOLS

A	Helmholtz free energy
A^{cdis}	The chain formation of dispersion term
$A^{chain,hcb}$	The chain formation term for hard convex body segments
A^{dis}	The dispersion term for hard convex body segments
A^{hcb}	The Helmholtz free energy for a hard convex body fluid
A^{res}	The residual Helmholtz energy for a fluid
AAD	Average of absolute deviation
API	Degree API Gravity of Oil
B_{ol}	Gas volume factor
BACK	Boublik–Alder–Chen–Kreglewski Equation of State
BW	Batzle – Wang Equations
BWR	Benedict-Webb-Rubin Equation of State
°C	Centigrade degree
C_1	Methane
C_2	Ethane
C_3	Propane
iC_4	Iso butene
nC_4	Normal butane
iC_5	Iso pentane
nC_5	Normal pentane
nC_6	Normal hexane
nC_7	Normal heptane
nC_8	Normal octane
nC_9	Normal nonane
nC_{10}	Normal decane
C_P	Isobaric Heat Capacity
C_V	Isochoric Heat Capacity
C_p^{id}	Isobaric Heat capacity at ideal states
C_v^{id}	Isochoric Heat Capacity at ideal states
CAL	Calculated value of a property
CEoS	Cubic Equation of State

D_{nm}	Universal constants in SAFT-BACK EoS
F	Frequency
G	Gibbs free energy
GOR	Gas Oil Ratio
H	Enthalpy
K	Kelvin
K_b	Modulus of gas free brine
K_d	Dead oil modulus
K_{gb}	Modulus of live brine
K_l	Live oil modulus
K_{lm}	Live oil modulus at its Maximum Gas-Oil Ratio
K_{od}	Dead Live oil mixture modulus
K_{ol}	Live oil mixture modulus
K_{olm}	Maximum live oil mixture modulus
K_S	Adiabatic gas modulus
K_w	The Watson Characterisation factor
L	Transit distance of sound
L_f	The intermolecular free length
$LVDT$	Linear Variable Differential Transformer
M	Molecular weight
$Meas.\ u$	Measured speed of sound
N_{AV}	The Avogadro's number
$NIST$	National Institute of Standards and Technology
P	Pressure
P_c	Critical pressure
P_{pr}	Pseudo-reduced pressure
P_{pc}	Pseudocritical pressure
PR	Peng-Robinson Equation of State
PRT	Platinum Resistance Thermometer
R	Universal Gas Constant
S	Entropy
S	Salinity

S_b	Brine Saturation
S_g	Gas Saturation
S_o	Oil Saturation
SAFT	Statistical Associating Fluid Theory
SCN	Single Carbon Number
SG	The specific gravity
SRK	Soave-Redlich- Kwong Equation of State
T	Temperature
T_0	Travel time of sound pulse through the metal of the acoustic cell cap
T_1	Measured transit time of first wave arrival
T_2	Measured transit time of second wave arrival
T_b	The boiling temperature
T_c	Critical temperature
$T_{measured}$	Measured transit time
T_{pc}	Pseudocritical temperature
T_{pr}	Pseudo-reduced temperature
T_R	Reduced temperature
THC	Total Hydrocarbon
U	Internal Energy
V_S	Velocity of Sound
VLE	Vapour-liquid equilibrium
VPT	Valderama Patel Teja
VTPR	Volume-translated Peng-Robinson
V_b	Velocity of brine
V_g	Velocity of gas
V_l	Velocity of live oil
V_{lm}	Velocity of live oil at its Maximum Gas-Oil Ratio
V_{od}	Velocity for Dead oil mixture
V_{ol}	Velocity for live oil mixture
V_{olm}	Velocity for Maximum live oil mixture
V_W	Velocity of water
Z_n	The mole fraction of pseudo-component in splitting the C_7+ fraction

Z_{N_2}	Compressibility factor of Nitrogen
$a(T)$	The attractive parameter in Peng-Robinson Equation of State
b	The co-volume parameter in Peng-Robinson Equation of State
c	The third parameter in Peng-Robinson Equation of State
d	Segment diameter
g^{hcb}	The mean radial distribution function
k_B	Boltzmann constant
k_{ij}	Binary interaction parameter
m	Segment number
s	Shift parameter in Peng-Robinson Equation of State
u	Speed of sound, The interaction energy
u_0	Segment interaction parameter
v	Volume

Greek

ΔT_S	Actual measured, corrected transit times
α	Coefficient of thermal expansion, Segment non-spherical parameter
β_T	Isothermal compressibility
β_S	Adiabatic compressibility
ρ	Molar density
ρ_{dl}	Pseudo Density
ρ_{gl}	Density at saturation
ρ_{md}	Dead oil mixture density
ρ_{mlm}	Max Live oil mixture density
ρ_{ml}	Live oil mixture density
ρ_b	Density of Brine
ρ_o	Density of dead oil at surface conditions
ρ_p	Density at a pressure
ρ_w	Density of fresh water
ρ_{lm}	Live oil density at its Maximum Gas-Oil Ratio

ρ_l	Live oil density
ρ_g	Gas density
ρ_{air}	Density of air
η	Packing factor
μs	Micro Second
u^0/k_B	Segment dispersion parameter
v^{00}	Segment volume
ω	Acentric factor

CHAPTER 1 - INTRODUCTION

Hydrocarbon exploration and development have been more important during recent decades. Also, the importance of extending the life and the maximum recovery from hydrocarbon reservoirs has never been greater. As a reservoir is exploited, pore fluid undergoes changes in temperature, pressure and composition. Production of any fluid typically lowers the fluid pressure, increasing the effective pressure (i.e., the difference between overburden and pore pressures). Tracking the movements of fluids due to production gives valuable information about the depletion of a field, and can indicate areas of bypassed oil or gas. Enhanced oil recovery processes often affect the reservoir properties, such as steam injection which changes the reservoir temperature or gas injection and water flooding mainly change fluid composition and pressure. Changes in fluid saturation and reservoir pressure can be estimated by applying 4D inversion.

4D seismic exploration is a method which involves the acquisition, processing, and interpretation of repeated seismic surveys over a production field with the aim of understanding the change in the reservoir over time, specially its behaviour during production. The objectives of a 4D survey are focused on the production & development stages of a field and are concerned with changes in the reservoir, usually the fluid content and movement within the structures. By tracking these, it is possible to monitor the flow of hydrocarbons within the reservoirs, gain greater understanding of the reservoir behaviour, and optimize its development.

Most of the changes in seismic behaviour come from fluid effects on the formation's seismic velocity rather than on its density. The composition of reservoir fluids changes over the whole lifetime of the reservoir, and this affects the acoustic properties of the rock frame and also the seismic attributes. Introduction of gas into liquid-filled rock or an increase in temperature of hydrocarbon-filled rock both cause a decrease in seismic velocity. Introduction of gas decreases velocity substantially by making the fluid mixture compressible. The effect of increasing temperature makes hydrocarbons less viscous, reducing overall rigidity and therefore reducing seismic velocity.

The seismic response to a change in fluid properties at a reflector can be predicted through seismic forward modelling. Relationships published by many authors can be used to predict density and seismic velocity through fluid substitution which requires knowledge of the properties of the rock frame, rock grains and fluids, all at the pressure and temperature conditions of the reservoirs. These properties can be obtained by either experimental measurements or modelling.

Based on the fact that the available information on experimental data on the speed of sound of different types of fluids such as hydrocarbon mixtures, real oils and several pure non-hydrocarbon gases in literature are limited, it is necessary to generate reliable experimental data of fluids in a wide range of pressure and temperature conditions.

Also, since the direct determination of properties such as density and heat capacity can be quite difficult at high pressures, an indirect technique may be used to obtain these properties.

In this work, Chapter 2 provides an overview of both experimental measurement and modelling of the speed of sound for hydrocarbons such as pure, mixtures and oils extracted from literature. Much fluid velocity data for different pressures, temperatures, measurement frequencies, number of points and error percentages are extracted and presented in this chapter.

New experimental data of the speed of sound for systems of pure, binary, and multi-component mixtures of hydrocarbons, real reservoir oils and CO_2 over a wide range of temperatures, pressures and concentrations are generated and presented. Furthermore, new experimental data of acoustic velocity in sediments saturated with different fluids and sediments in various conditions of pressure and temperature have been generated and presented in this thesis. These results are important for the fundamental theory of liquid mixtures and also for the purpose of validating thermodynamic models. Furthermore, independent measurements of the speed of sound in reservoir fluids (including gas, oil and real oils) are significantly important for the proper analysis of seismic data (Wang and Nur, 1990; Batzle and Wang, 1992).

The experimental procedure used in this work and the generated experimental data have been outlined in Chapter 3, in addition to the equipments which were used for these measurements and their capabilities.

The main aims of this work are improving the prediction of acoustic velocity in fluids and other thermodynamic properties such as heat capacities. Chapter 4 explains the calculation of thermodynamic properties by considering the second order derivatives of thermodynamic potentials and utilizing a new version of SAFT family equations of state. Chen and Mi (2001) combined the BACK EoS with SAFT, introducing a new molecular based equation of state. They made two modifications for better calculation of phase behaviour of chain fluids.

More improvement of this equation was required for mixtures. In this work, some modifications were applied to the SAFT-BACK EoS in order to enable this equation for determination of the above properties in mixtures which are presented in Chapter 4. There are a lot of equations of state for determination of hydrocarbon properties, specially the cubic equations because of their high importance in the industry. The explanation about the ability of cubic equations of state for these properties calculations and also, the ability of SAFT-BACK equation rather than cubic equations of state such as PR, SRK and VPT will be discussed. In this chapter, the model for velocity determination is extended for real fluids using different properties such as single carbon numbers and finding new relationships between equation parameters and physical properties of SCN groups.

Chapter 5 presents the validation of the model by comparing the prediction results with generated data in the laboratory. For pure components such as nC_5, nC_6 and CO_2, the correlated data from NIST and some extracted data from literature were used for this purpose. For mixtures of fluids and real oils, the predictions are compared only with data generated in the laboratory. In Chapter 6, the thermodynamic model is applied for prediction of some pure hydrocarbon fluids, synthetic mixtures and real oils. The results are compared with those obtained by Batzle-Wang model which is the only equation used in seismic modelling and reservoir characterization. Batzle – Wang model calculates the fluid properties such as density, velocity and bulk modulus which are the input data for the Gassmann equations in order to model the properties of bulk frame in

the reservoir. Accurate results of acoustic velocity cannot be obtained for fluid saturated rocks, if the properties of pore fluids are not known precisely.

Another part of Chapter 6 is allocated to the discussion about the effects of pressure and temperature on the speed of sound in a fluid saturated matrix. Different fluids, sediments, temperature and pressure are involved in these experiments in the case of constant and changeable effective pressures to investigate the fluid effects on velocity. For high-pressure reservoirs, pressure depletion during production is associated with compaction within the reservoir causing stretching or extensional stresses in the overburden and underlying formations which leads to porosity variation. A dramatic increase in velocity can occur with decrease in fluid pressure, as typically occurs during oil production. The decrease in fluid pressure increases the effective stress on the reservoir rock, stiffening the matrix and increasing velocity.

The conclusions of this thesis and the recommendations for future work are discussed in Chapter 7.

References:

Batzle M., Wang Z., 1992, *Seismic properties of pore fluids*, Geophysics, **57**, 1396-1408

Chen J., Mi J.g., 2001, *Equation of state extended for SAFT with improved results for non-polar fluids across the critical point fluid,* Phase Equilibria, **186**, 165–184.

Wang Z., Nur A, 1990, *Wave velocities in hydro-carbon saturated rocks: Experimental results,* Geophysics, **55**, 723 – 733

Chapter 2 – OVERVIEW OF EXPERIMETAL MEASUREMENTS AND MODELLING OF SPEED OF SOUND IN LITERATURE

2. 1 Introduction

Knowledge of the thermophysical properties of hydrocarbons is of high importance in various fields of science and technology. As the direct measurement and calculation of properties such as density and heat capacity is quite difficult at elevated pressures, an indirect approach may work better. Acoustic method may be one of such techniques in which the speed of sound can be measured as a function of both temperature T and pressure P. Additionally, the speed of sound is related to derivatives of the thermodynamic properties in equation of states. So, these derivatives are more precise when they are deduced from the speed of sound rather than obtained from the analysis of classical PVT data.

Speed of sound data will give direct and precise information on the adiabatic properties of a liquid. The speed of sound in fluids can be determined by the thermodynamic properties of fluids.

Acoustic measurements can also give valuable information on in situ characterization of reservoir fluids. The possibilities of obtaining the density and/or the viscosity of the oil from acoustic measurements were studied in Ball et al. (2002).

The main aim of this chapter is to provide a review of reported studies on the speed of sound in fluids in the literature and includes the two main sections:

- The first part provides an overview of experimental results of ultrasonic measurements as a function of pressure and temperature in pure hydrocarbons, mixtures and real oils. Major topics of discussion include modern general ultrasonic studies of a broad range of aliphatic liquids. Several tables of 36 pure liquids, 46 liquid mixtures and 17 oils and natural gases are provided by chemical name.

  This review does not focus on instrumentation, as it is not in the objectives of this work. Also, as the review centers solely on liquids and gases, no mention is made of results pertaining to solids.

- The second part of this chapter discusses the methods which are used for calculation of the speed of sound using various equations of state. Different proposed models for determination of the speed of sound in fluids will be introduced and discussed in this chapter.

Review of Available Experimental Data

An extensive literature survey has been performed and the available experimental speed of sound data have been collected from the literature. The experimental data are presented in the tables of this section for different fluids. For each fluid, information about the temperature and pressure range, number of measured points, errors of measurement and frequency of the waves are listed in these tables (if they are provided in the original publications).

The values of *u* which refer to the speed of sound are given for pure fluids of water, carbon dioxide, nitrogen, methane, ethane, propane, n-butane, iso-butane, n-pentane, iso-pentane, neo-pentane, n-hexane, n-heptane, n-octane, n-nonane, n-decane, n-undecane, n-dodecane, n-tridecane, n-tetradecane, n-pentadecane, n-hexadecane, n-heptadecane, n-octadecane, n-nonadecane, n-eicosane, n-docosane, n-tricosane, n-tetracosane, n-octacosane, n-hexatriacontane, benzene, toluene, cyclopentane, cyclohexane and methylcyclohexane in Tables 2.1 – 2.12.

The values of *u* in binary and multi-component mixtures of n-alkanes and CO_2 with n-alkanes are given in Table 2.13 and the synthetic oils, real oils and natural gases are listed in Table 2.14.

Table 2.1 Speed of sound data for pure water

References	T/K	P/MPa	N. Pts	Err.%	F/MHz
		Water			
Wilson (1959)	274.05 - 364.35	0.1 - 97	88	0.05	5
Barlow & Yazgan (1967)	289.15 - 367.15	0.1 - 80	81	0.03	10
Del Grosso (1969)	273.21 - 347.18	0.1	36	0.1	5
Del Grosso (1972)	273.15 - 368.28	0.1	112	0.01 *	5
Alexandrov & Larkin (1976)	373 - 647	0.1 - 60	61	0.02	-
Alexandrov & Kochetov (1979)	266 - 423	50 - 100	59	0.03	-
Ye et al. (1990)	289.65 - 342.65	5 - 47.2	45	0.06	5
Fujii et al. (1993)	293.15 - 348.15	0.1	43	0.03	16
Tsatsuryan (1994)	288.15 - 363.15	0.1 - 60	-	0.01	10
Tsatsuryan (2001)	273 - 373	70 - 200	67	0.023	10
Ball et al. (2002)	292.5	0.1 - 50	8	0.01	5
Benedetto et al. (2005)	274 - 394	0.1 - 90	90	0.05	-
Meier & Kabelac (2006)	240 - 420	0.1- 100		0.004	-
Gedanitz et al. (2009)	303.13 - 323.15	0.1 - 30	21	0.006	8
Vance & Brown (2010)	263.15 - 373.15	0.1 - 700	-	0.5	-

* Errors in m/s

Table 2.2 Speed of sound data for pure carbon dioxide and nitrogen

Non-Hydrocarbon Gases (CO_2 / N_2)					
References	T/K	P/MPa	N. Pts	Err.%	F/MHz
		Carbon Dioxide			
Herget (1940)	301.15 - 311.15	0.5 - 10	195	-	-
Richardson & Tait (1957)	282.15	6.9 -20.7	-	-	5
Ye et al. (1991)	293.15 - 333.15	5 - 50	-	-	5
Daridon et al. (1996)	313 - 393	12 - 70	-	-	2
Alexanders & Trusler (1997)	220 - 450	0.1 - 14	61	0.001	10
Alexanders & Trusler (1998)	220 - 450	0.1 - 14	64	-	10 kHz
Zevnik et al. (2006)	298 - 343	6 - 14	150	0.1 *	0.2
Alexanders & Hurly (2008)	220 - 375	0.1 - 3.4	123	0.005	-
		Nitrogen			
Younglove & McCarty (1980)	80 - 350	0.3 - 0.7	237	0.1	1-30 kHz
Kortbeek et al. (1988)	123 - 298.15	0.1 - 1000	-	0.02	-

Ewing & Trusler (1992)	80 - 373	0.005 - 0.6	99	-	0.1
Daridon et al. (1994)	303.15 - 373.15	0.1 - 100	-	-	3
Costa Gomes & Trusler (1998)	250 - 350	0.1 - 30	136	0.01	5 - 26 kHz
Gedanitz et al. (2009)	250 - 350	20 - 30	20	0.011	8

* Errors in m/s

Table 2.3 Speed of sound data for pure methane, ethane and propane

Hydrocarbon Gases and Liquids					
References	T/K	P/MPa	N. Pts	Err.%	F/MHz
		Methane			
Lacam (1956)	473.15	0.1 - 111	-	-	500 kHz
Van Itterbeek et al. (1967)	91.73-191.15	0.1 - 20	-	-	+ super position
Straty (1974)	100 - 300	25	-	0.05	-
Kortbeek & Schoten (1990)	148.15 - 298.15	100 - 1000	-	0.08 - 0.12	-
Ye et al. (1991)	293.15 - 333.15	5 - 60	-	-	5
Trusler & Zarari (1992)	275 - 375	0.1 - 10	-	0.002	-
Trusler (1994)	200 - 250	0.1 - 1.4	21	-	5 – 25 kHz
Trusler & Zarari (1996)	125 - 250	0.1 - 1.4	64	0.003	
Daridon et al. (1996)	313 - 393	12 - 70	-	-	2
		Ethane			
Tsumura & Straty (1977)	100 - 260	0.1 - 36.8	-	-	-
Alexanders & Trusler (1997)	220 - 450	0.1 - 10.5	187	0.04	-
		Propane			
			-	-	
Noury (1954)	348.15 - 398.15	0.1 - 15	-	-	585 kHz
Lacam (1954)	298.15 - 498.15	0.1 - 111	-	-	3- 4
Lacam (1956)	473.15	0.1 - 111	-	-	500 kHz
Niepmann (1984)	200 - 340	0.1 - 60	241	0.2	2
Trusler & Zarari (1996)	225 - 275	0.01 - 0.85	68	0.001	v

Table 2.4 Speed of sound data for pure n-butane, iso-butane and n-pentane

Hydrocarbon Gases and Liquids					
References	T/K	P/MPa	N. Pts	Err.%	F/MHz
		n- Butane			
Niepmann (1984)	200 - 375	0.1 - 80	249	0.2	2
Ewing et al. (1988)	250 - 320	0.005 - 0.1	78	0.05	-
		Iso-Butane			
Ewing & Goodwin (2003)	251 - 320	0.005 - 0.1	79	0.03	-
		n- Pentane			
Kling et al. (1953)	293 - 433	0.1 - 19.6	-	0.3	-
Richardson & Tait (1957)	288.15 - 317.15	0.1 - 55	-	-	3, 12
Belinskii & Ikramov (1973)	293 - 313	0.1 - 784	48	-	13
Otpushchennikov et al. (1974)	303.15 - 393.15	0.1 - 203			2
Houck (1974)	295	0.1 - 2400	13	-	10
Benson & Handa (1981)	298.15	0.1	1	-	3
Younglove (1981)	90.15 - 290.15	0.1 - 34		-	10
Handa et al. (1981)	298.15	0.1	1	-	3
Sachdeva & Nanda (1981)	298.15	0.1	1	-	-
Ismagilov & Ermakov (1982)	391 - 476	0.1 - 2.5	-	-	2.5
Chavez et al. (1982)	200 - 308	Sat. pres.	44	0.05	7.3- 12
Melikhov (1985)	303 - 433	0.1 - 600	-	-	4
Ewing et al. (1989)	270 - 330	-	-	-	-
Lainez et al. (1990)	263.15 - 433.15	0.1 - 210	220	0.036	3
Ding et al. (1997)	293.15 - 373.15	5 - 100	100	0.37	5
Nath (1998)	298.15	0.1	1		3
Nath (2002)	288.15 –303.15	0.1	1	0.5 *	2
Eden & Richardson (1960), iso-pentane	273.15 - 283.65	0.1 - 55	-	-	3
Houck (1974), iso-pentane	295	0.1 - 2400	-	-	10
Ewing et al. (1986) neo-pentane	250 - 340	7 - 100	-	-	-
Ewing et al. (1987) neo-pentane	250 - 323	-	-	-	-
Lainez et al. (1990) (neo-pentane)	263.15 - 433.15	0.1 - 54	204	0.046	3

* Errors in m/s

Table 2.5 Speed of sound data for pure n-hexane

Hydrocarbon Gases and Liquids					
References	T/K	P/MPa	N. Pts	Err.%	F/MHz
	n- Hexane				
Kling et al. (1953)	293 - 373	0.1 - 49	-	0.3	-
Eden & Richardson (1960)	293.15 - 310.15	0.1 - 55	-	-	3
Boelhouwer (1967)	253.15 - 333.15	0.1 - 140	40	1	2
Hawley et al. (1970)	303.15	0.1 - 392	-	-	31.5
Allegra et al. (1970)	303.15	0.1 - 981	-	-	12– 40
Melikhov et al. (1976)	283 - 393	10 - 300	-	-	4
Kagramanyan & Badalyan, (1978)	303.15 - 343.15	0.1 - 203	42	0.2	2.8
Melikhov et al. (1979)	303 - 423	0.1 - 588	-	-	1 - 5
Sachdeva & Nanda (1981)	298.15	0.1	1	-	-
Benson & Handa (1981)	298.15	0.1	1	-	3
Handa et al. (1981)	298.15	0.1	1	-	3
Ismagilov & Ermakov (1982)	384 - 459	0.1 - 2.5	-	-	2.5
Aicart (1983)	298.15	0.1	1	-	-
Takagi, Teranisih(1985)	298.15	0.1	1	1 *	2
Melikhov (1985)	303 - 423	0.1 - 600	-	-	4
Tardajos et al. (1986)	298.15	0.1	1	-	
Benson & Halpin (1987)	298.15	0.1	1	0.2 *	2
Junquera et al. (1988)	298.15	0.1	1	-	2
Bohidar (1989)	293.15	0.1 - 80	-	-	-
Wang & Nur (1991)	263.15 -341.15	0.1	16	0.2	2.25
Ormanoudis (1991)	298.15	0.1	1	-	4
Aminabhavi et al.(1994)	298.15	0.1	1	2 *	1
Aminabhavi & Gopalkrisha (1995)	298.15	0.1	1	2 *	1
Sastry & Raj (1996)	298.15 - 313.15	0.1	8	0.15	2
Dominguez et al. (1996)	298.15	-	1	0.1 *	-
Nath (1998)	303.15	0.1	1	-	3
Daridon et al. (1998)	293 - 373	0.1 - 150	275	1	3
Orge et al. (1999)	303.15- 318.15	0.1	5	0.1 *	
Khasanshin & Shchemelev (2001)	298.15 - 433.15	0.1 - 50	20	0.1	3
Ball & Trusler (2001)	298.15 - 373.15	0.1 - 100	82	0.1	5
Nath (2002)	288.15 -303.15	0.1	1	0.5 *	2
Oswal et al. (2003)	303.15	0.1	1	1 *	2
Bolotnikov et al. (2005)	293.15 -333.15	Sat. line	17	0.1	1 – 5
Dubey et al. (2008)	298.15 - 308.15	0.1	3	0.1 *	-
Dubey & Sharma (2008)	293.15 - 308.15	0.1	3	0.1 *	-
Khasanshin et al. (2008)	298.15 - 433.15	0.1 - 100	48	0.1	3

* Errors in m/s

Table 2.6 Speed of sound data for pure n-heptane

Hydrocarbon Gases and Liquids					
References	T/K	P/MPa	N. Pts	Err.%	F/MHz
	n- Heptane				
Kling et al. (1953)	293 - 373	0.1 - 49	-	0.3	-
Boelhouwer (1967)	253.15-453.15	0.1 - 140	60	1	2
Takagi (1978a)	283.15-333.15	0.1-210			1
Kiyohara & Benson (1979)	298.15	0.1	1	-	-
Sachdeva & Nanda (1981)	298.15	0.1	1	-	-
Golic et al. (1982)	313 - 453	0.1 - 196	-	0.3	-
Tamura et al. (1983)	298.15	0.1	1	-	-
Aicart (1983)	298.15	0.1	1	-	-
Kumaran et al. (1984)	298.15	0.1	1	-	-
Melikhov (1985)	303 - 433	0.1 - 600		-	4
Muringer et al. (1985)	185.6 - 310.65	0.1 - 263.4	113	0.1 *	2
Tardajos et al. (1986)	298.15	0.1	1	-	-
Ohomuro & Tamura (1987)	298.15	0.1	1	-	-
Akamatsu (1987)	298.15	0.1	1	-	-
Junquera et al. (1988)	298.15	0.1	1	-	2
Rai et al. (1989)	298.15	0.1	1	-	-
Aicart (1990)	298.15	0.1	1	-	-
Wang & Nur (1991)	266.15-368.15	0.1	15	0.2	2.25
Papaioannou (1991)	298.15	0.1	1	-	4
Aminabhavi et al. (1994)	298.15	0.1	1	2 *	1
Aminabhavi & Gopalkrisha (1995)	298.15	0.1	1	2 *	1
Sastry & Raj (1996)	298.15-313.15	0.1	3	0.15	2
Nath (1998)	303.15	0.1	1	-	3
Orge et al. (1999)	303.15-318.15	0.1	3	0.1 *	-
Sastry et al. (1999)	298.15-318.15	0.1	3	0.15	2
Zak et al. (2000)	293 - 318	0.1 - 90		0.5	4
Marino et al. (2000)	298.15	0.1	1	0.1 *	-
Nath (2002)	288.15-303.15	0.1	2	0.5 *	2
Dzida et al. (2005)	293 - 318	0.1 - 90	95	0.5	4
Dzida & Cempa (2008)	293 - 318	0.1 - 101	46	0.04	2

* Errors in m/s

Table 2.7 Speed of sound data for pure n-octane and n-nonane

Hydrocarbon Gases and Liquids					
References	T/K	P/MPa	N. Pts	Err.%	F/MHz
		n- Octane			
Boelhouwer (1967)	253.15 - 473.15	0.1- 140	64	-	2
Badalyan et al. (1970)	303.15 - 413.15	0.1 - 118	-	0.2	2
Badalyan & Otpuschennikov (1971)	303.15 - 393.15	0.1-117.60	78	-	-
Benson & Handa (1981)	298.15	0.1	1	-	3
Handa et al. (1981)	298.15	0.1	1	-	3
Takagi & Teranisih (1985)	298.15	0.1	1	1.5 *	2
Melikhov (1985)	303 - 393	0.1 - 300	-	-	4
Tardajos et al.(1986)	298.15	0.1	1		
Benson & Halpin (1987)	298.15	0.1	1	0.2 *	2
Junquera et al. (1988)	298.15	0.1	1		2
Wang & Nur (1991)	266.15 - 392.15	0.1	16	0.2	2.25
Aminabhavi et al.(1994)	298.15	0.1	1	2 *	1
Daridon et al. (1994)	303.15 - 373.15	0.1 - 100	-	-	3
Daridon (1994)	293.15 - 373.15	5 - 100			1 – 10
Aminabhavi & Gopalkrisha (1995)	298.15	0.1	1	2 *	1
Ding et al. (1997)	293.15 - 363.15	5 - 90	72	0.25	5
Nath (1998)	303.15	0.1	1	-	3
Orge et al. (1999)	303.15 - 318.15	0.1	4	0.1 *	
Khasanshin & Shchemelev (2001)	303.15 - 433.15	0.1 - 50	46	0.1	3
Nath (2002)	288.15 - 303.15	0.1	1	0.5 *	2
Gonzalez et al. (2004)	293.15 - 303.15	0.1	3	0.1 *	-
Dubey et al. (2008)	298.15 - 308.15	0.1	3	0.1 *	-
Khasanshin et al. (2008)	298.15 - 433.15	0.1 - 100	49	0.1	3
Dubey, Sharma (2008)	293.15 - 308.15	0.1	3	0.1 *	-
		n- Nonane			
Kling et al. (1953)	293 - 373	0.1 - 49	-	0.3	-
Boelhouwer (1967)	253.15 - 413.15	0.1 - 140	89	1	2
Melikhov (1985)	303 - 433	0.1 - 600	-	-	4
Tardajos et al. (1986)	298.15	0.1	1	-	-
Aminabhavi & Gopalkrisha (1994)	298.15 - 318.15	0.1	3	2 *	4
Aminabhavi & Gopalkrisha (1995)	298.15	0.1	1	2 *	1
Lago et al. (2006)	293.15 - 393.15	0.1 - 100	66	0.2	-

*Errors in m/s

Table 2.8 Speed of sound data for pure n-decane

Hydrocarbon Gases and Liquids					
References	T/K	P/MPa	N. Pts	Err.%	F/MHz
	n- Decane				
Badalyan et al. (1970)	303.15 - 413.15	0.1 - 118	-	-	2
Badalyan et al. (1970)	303.15 - 413.15	0.1 - 118	-	0.2	2
Badalyan & Otpuschennikov (1971)	303.15 - 413.15	0.1 - 118	91	-	-
Handa et al. (1981)	298.15	0.1	1	-	3
Benson & Handa (1981)	298.15	0.1	1	-	3
Sachdeva & Nanda (1981)	293.15 - 333.15	0.1	6	-	-
Takagi & Teranisihi (1985)	298.15	0.1	1	1.5 *	2
Melikhov (1985)	303 - 393	0.1 - 300	-	-	4
Tardajos et al. (1986)	298.15	0.1	1	-	-
Junquera et al. (1988)	298.15	0.1	1	-	2
Aicart (1990)	298.15	0.1	1	-	-
Ye et al. (1990)	303.15 - 413.15	0.1 - 60	121	0.2	5
Wang & Nur (1991)	268.15 - 391.15	0.1	14	0.2	2.25
Aminabhavi & Gopalkrisha (1994)	298.15 - 318.15	0.1	3	2 *	4
Aminabhavi & Gopalkrisha (1995)	298.15	0.1	1	2 *	1
Khasanshin & Shchemelev (2001)	298.15 - 433.15	0.1 - 50	40	0.1	3
Mosteiro et al. (2001)	288.15 - 308.15	0.1	4	0.5 *	100 kHz
Mosteiro et al. (2001)	288.15 - 308.15	0.1	5	0.5 *	100 kHz
Pineiro et al. (2003)	298.15	0.1	1	-	-
Gonzalez et al. (2004)	293.15 - 303.15	0.1	3	0.1 *	-
Khasanshin et al. (2008)	298.15 - 433.15	0.1 - 100	48	0.1	3
Dubey & Sharma (2008)	293.15 - 308.15	0.1	3	0.1 *	-
Dubey et al. (2008)	298.15 - 308.15	0.1	3	0.1 *	-

* Errors in m/s

Table 2.9 Speed of sound data for pure n-undecane, n-dodecane and n-tridecane

Hydrocarbon Gases and Liquids					
References	T/K	P/MPa	N. Pts	Err.%	F/MHz
		n- Undecane			
Badalyan & Otpuschennikov (1971)	303.15 - 413.15	0.1 - 118	91	-	-
Tardajos et al. (1981)	298.15	0.1	1	-	-
Melikhov (1985)	303 - 393	0.1 - 300		-	4
Junquera et al. (1989)	298.15	0.1	1	-	2
Wang & Nur (1991)	271.15 - 394.15	0.1	15	0.2	2.25
Bessiers & Plantier (2007)	303.15 - 373.15	0.1 - 60	56	0.1	3
		n- Dodecane			
Boelhouwer (1967)	273.15 - 473.15	0.1 - 140	85	1	2
Tardajos et al. (1981)	298.15	0.1	1	-	-
Takagi & Teranisih (1985)	298.15	0.1	1	1.5 *	2
Melikhov (1985)	303 - 433	0.1 - 600	-	-	4
Benson et al. (1986)	298.15	0.1	1	-	3
Junquera et al. (1989)	298.15	0.1	1	-	2
Wang & Nur (1991)	277.15 - 392.15	0.1	14	0.2	2.25
Aminabhavi & Gopalkrisha (1994)	298.15 - 318.15	0.1	3	2 *	4
Aminabhavi & Gopalkrisha (1995)	298.15	0.1	1	2 *	1
Khasanshin &, Shchemelev (2001)	303.15 - 433.15	0.1 - 50	30	0.1	3
Gonzalez-Salgado et al (2002)	283.15 - 323.15	0.1	6	0.1 *	-
Gonzalez et al. (2004)	293.15 - 303.15	0.1	3	0.1 *	-
Dzida & Cempa (2008),	293 - 318	0.1 - 101	50	0.04	2
		n- Tridecane			
Tardajos et al. (1986)	298.15	0.1	1	-	-
Daridon & Lagourette (2000)	293 - 373	0.1 - 150	-	-	3
Khasanshin & Shchemelev (2001)	303.15 - 433.15	0.1 - 50	48	0.1 %	3

* Errors in m/s

Table 2.10 Speed of sound data for pure n-teradecane, n-pentadecane and n-hexadecane

Hydrocarbon Gases and Liquids					
References	T/K	P/MPa	N. Pts	Err.%	F/MHz
		n- Tetradecane			
Takagi &, Teranisih (1985)	298.15	0.1 - 100	-	1.5 *	2
Junquera et al. (1989)	298.15	0.1	1	-	2
Aicart (1990)	298.15	0.1	1	-	
Wang & Nur (1991)	283.15 - 393.15	0.1	14	0.2	2.25
Aminabhavi & Gopalkrisha (1994)	298.15 - 318.15	0.1	3	2 *	4
Daridon & Lagourette (2000)	293 - 373	0.1 - 150	-	-	3
Khasanshin & Shchemelev, (2001)	303.15 - 433.15	0.1 - 50	48	0.1	3
Khasanshin et al. (2004)	303.15 - 433.15	50 - 100	48	0.1	3
		n- Pentadecane			
Tardajos et al. (1986)	298.15	0.1	1	-	-
Wang &, Nur (1991)	287.15 - 394.15	0.1	12	0.2	2.25
Khasanshin & Shchemelev (2001)	303.15 - 433.15	0.1 - 50	54	0.1	3
Daridon et al. (2002)	293.15 - 383.15	0.1 - 150	-	-	3
		n- Hexadecane			
Boelhouwer (1967)	293.15 - 473.15	0.1 - 140	74	1%	2
Benson & Handa (1981)	298.15	0.1	1	-	3
Junquera et al. (1989)	298.15	0.1	1	-	2
Ye et al. (1990)	303.15 - 393.15	0.1 - 70	78	0.5 *	5
Ye et al. (1991)	293.15 - 333.15	5 - 50	-	-	5
Wang & Nur (1991)	300.15 - 392.15	0.1	13	0.2	2.25
Aminabhavi & Gopalkrisha (1994)	298.15 - 318.15	0.1	3	2 *	4
Daridon et al. (1996)	313 - 393	12 - 70	-	-	2
Khasanshin & Shchemelev (2001)	303.15 - 433.15	0.1 - 50	29	0.1	3
Ball & Trusler (2001)	298.15 - 373.15	0.1 - 100	64	0.1	5
Bolotnikov et al. (2005)	298.15 - 373.15	saturation line	17	0.1	1 – 5
Khasanshin et al. (2008)	298.15 - 433.15	0.1 - 100	43	0.1	3
Outcalt et al. (2010)	290.65 - 343.15	0.083	16	0.2	-

* Errors in m/s

Table 2.11 Speed of sound data for pure n-heptadecane and heavier normal hydrocarbons

Hydrocarbon Gases and Liquids					
References	T/K	P/MPa	N. Pts	Err.%	F/MHz
n-Heptadecane and Heavier Hydrocarbons					
Daridon et al. (2002) *(n-heptadecane)*	303.15 - 383.15	0.1 - 150	-	-	3
Wang & Nur (1991) *(n-octadecane)*	303.15 - 395.15	0.1	12	0.2	2.25
Dutour et al. (2000) *(n-octadecane)*	313.15 - 383.15	0.1 - 150	141	0.07	3
Dutour et al. (2000) *(n-nonadecane)*	313.15 - 383.15	0.1 - 150	131	0.05	3
Dutour et al. (2001a) *(n-eicosane)*	323 - 393	0.1 - 150	-	-	3
Wang & Nur (1991) *(n-Docosane)*	317.15 - 393.15	0.1	10	0.2	2.25
Dutour et al. (2001a) *(n-Docosane)*	323 - 393	0.1 - 150	-	-	3
Dutour et al. (2001b) *(n-tricosane)*	333.15 - 393.15	0.1 - 150	112	0.2	3
Dutour et al. (2001b) *(n-tetracosane)*	333.15 - 393.15	0.1 - 150	105	0.2	3
Dutour et al. (2002) *(n-octacosane)*	363.15 - 403.15	0.1 - 150	107	0.2	3
Wang & Nur (1991) *(n-octacosane)*	263.15 - 341.15	0.1	16	0.2	2.25
Dutour et al. (2002) *(n-$C_{36}H_{74}$)*	363.15 - 403.15	0.1 - 150	76	0.2	3

* Errors in m/s

Table 2.12 Speed of sound data for pure benzene, toluene and some cyclic hydrocrbons

Hydrocarbon Gases and Liquids					
References	T/K	P/MPa	N. Pts	Err.%	F/MHz
		Benzene and Toluene			
Takagi (1978b)	283.15 - 313.15	0.1 - 200	-	-	1
Ismagilov & Ermakov (1982)	393 - 467	0.1 - 2.5	-	-	2.5
Asenbaum & Hochheimer (1983)	298.15 - 343.15	0.1 - 130	-	-	-
Tamura et al. (1983)	298.15	0.1	1	-	-
Takagi & Teranishi (1984)	293.15 - 303.15	0.1 - 160	29	-	2
Melikhov (1985)	303 - 393	0.1 - 300	-	-	4
Ohomuro & Tamura (1987)	298.15	0.1	1	-	-
Akamatsu (1987)	298.15	0.1	1	-	-
Sun et al. (1987)	283.15 - 323.15	0.1 - 170	90	-	2
Takagi, Teranishi (1987)	283.15 - 323.15	0.1 - 200	-	-	2
Bohidar (1988)	293.15	0.1 - 82.5	-	-	-
Takagi (1994b)	283.15 - 323.15	0.1 - 200	-	-	2
Dominguez et al. (1996)	298.15		1	0.1 *	-
Sastry et al. (1999)	308.15 -318.15	0.1	2	0.15	2
Takigawa & Tamura (2000)	298.15	0.1	1	0.05	-
George & Sastry (2003)	298.15 , 308.15	0.1	2	2.5 *	multi
Oswal et al. (2003)	303.15	0.1	1	1 *	2
Takagi et al. (2004)	283.15 – 333.15	0.1 - 30	71	0.2	2
Hawley et al. (1970)	303.15 , 348.15	0.1 - 522	-	0.3	22.5
Allegra et al. (1970)	303.15	0.1 - 981	-	1	12- 40
Takagi (1978), (Toluene)	283.15 – 313.15	0.1 - 200	-	-	1
Takagi & Teranishi (1985)	303.15	0.1 - 180	-	0.3	1
Muringer et al. (1985) (Toluene)	173.18 - 320.3	0.1 - 264	88	0.1 *	2
Bohidar (1989)	293.15	0.1 - 82.5	-	1	-
George & Sastry (2003) (Toluene)	298.15 , 308.15	0.1	2	2.5 *	multi
Oswal et al. (2003)	303.15	0.1	1	1 *	2
Takagi et al. (2002) (Cyclopentane)	283 - 343	0.1 - 20	152	0.2	2
Dominguez et al. (1996) (Cyclohexane)	298.15	-	1	0.1 *	-
Takagi et al. (2002) (Cyclohexane)	283 - 333	0.1 - 20	181	0.2	2
Oswal et al. (2003)	303.15	0.1	1	1 *	2
Iloukhani et al. (2006) (Methylcyclohexane)	298.15	0.1	1	1 *	1

Table 2.13 Speed of sound data Binary and multi-component mixture systems

References	T/K	P/MPa	N. Pts	Err.%	F/MHz
Savidge et al. (1988) ($CH_4 + CO_2$)	249.82 -349.82	0.1 - 10	-	-	-
Alexanders & Trusler, (1999) ($0.4C_2H_6 + 0.6CO_2$)	220 - 450	0.1 - 1.2	71	0.0001	-
Ye et al. (1992) ($CO_2 + nC_{16}C_{34}$)	293.15-333.15	2 - 60	317	-	5
Savidge et al. (1988) ($CO_2 + N_2$)	249.82 -349.82	0.1 - 10	-	-	-
Savidge et al. (1988) ($CH_4 + C_2H_6$)	249.82 -349.82	0.1 - 10	-	-	-
Trusler (1994) ($0.8CH_4 + 0.2C_2H_6$)	200 - 375	0.1 – 15	57	-	5 – 25 kHz
Costa Gomes & Trusler (1998) ($0.85CH_4 + 0.15C_2H_6$)	250 - 350	0.1 – 20	40	0.03	-
Savidge et al. (1988) ($CH_4 + C_3H_8$)	249.82 -349.82	0.1 - 10	-	-	-
Trusler et al., (1993) ($CH_4 + C_3H_8$)					
Lagourette et al., (1994) ($CH_4 + C_3H_8$)	262 - 400	10 - 70	244	0.06	2
Plantier et al. (2005) ($CH_4 + nC_4H_{10}$)	311	2 - 17.24	43	0.03	1
Lagourette et al. (1994) ($CH_4 + nC_8H_{18}$)	293.15- 373.15	20 - 100	78	0.06	2
Ye et al. (1992) ($CH_4 + nC_{16}C_{34}$)	292.15- 413.15	6 - 66	398	-	5
Savidge et al. (1988) ($CH_4 + N_2$)	249.82 -349.82	0.1 - 10	-	-	-
Estela-Uribe et al. (2006) ($CH_4 + N_2$)	170 - 400	0.1 - 30	276	0.01	-
Cholpan et al. (1989) ($nC_6H_{14} + nC_7H_{16}$)	253 - 343	0.1	-	0.5	-
Pandey et al. (2007) ($nC_6H_{14} + nC_7H_{16}$)	298.15	0.1	15	-	-
Sperkach et al. (1979) ($nC_6H_{14} + nC_8H_{18}$)	223 - 323	0.1	-	0.5	-
Takagi & Teranishi (1985) ($nC_6H_{14} + nC_{10}H_{22}$)	298.15	0.1 -100	-	0.13	2
Garkusha et al. (1980a) ($nC_6H_{14} + nC_{13}H_{28}$)	251 - 323	0.1	-	0.5	-
Garkusha et al. (1980b) ($nC_6H_{14} + nC_{15}H_32$)	253 - 323	0.1	-	0.5	-
Ye et al. (1991) ($nC_6H_{14} + nC_{16}H_{34}$)	298.15-373.15	0.1- 70	358	0.2	5
Bolotnikov et al. (2005)	298.15 -373.15	Along the	153	0.1	1 - 5

(nC_6H_{14} + $nC_{16}H_{34}$)		saturation line			
Khasanshin et al. (2009) (nC_6H_{14} + $nC_{16}H_{34}$)	298.15 – 433.15	0.1 - 100	102	0.1	3
Sperkach et al. (1979) (nC_7H_{16} + nC_9H_{20})	223 - 323	0.1	-	0.5	-
Golik et al. (1976) (nC_7H_{16} + $nC_{12}H_{26}$)	303 - 413	0.1 - 245	-	0.5	-
Dzida, Cempa, (2008) (nC_7H_{16} + $nC_{12}H_{26}$)	293 - 318	0.1 - 101	410	0.04	2
Cholpan et al. (1981) (nC_7H_{16} + $nC_{13}H_{28}$)	253 - 343	0.1	-	0.5	-
Cholpan et al. (1982) (nC_7H_{16} + $nC_{13}H_{28}$)	253 - 343	0.1	-	0.5	-
Golik et al. (1978) (nC_7H_{16} + $nC_{14}H_{30}$)	333 - 413	0.1 - 245	-	0.5	-
Takagi & Teranishi (1985) (nC_8H_{18} + $nC_{12}H_{26}$)	298.15	0.1 -100	-	0.13	2
Khasanshin et al. (2009) (nC_8H_{18} + $nC_{16}H_{34}$)	298.15 – 433.15	0.1 - 100	88	0.1	3
Takagi & Teranishi (1985) ($nC_{10}H_{22}$ + $nC_{14}H_{30}$)	298.15	0.1 -100	-	0.13	2
Khasanshin et al. (2009) ($nC_{10}H_{22}$ + $nC_{16}H_{34}$)	298.15 – 433.15	0.1 - 100	93	0.1	3
Baragi et al. (2006) (Methylcyclohexane + nC_6H_{14})	298.15	0.1	11	0.002	1
Baragi et al. (2006) (Methylcyclohexane + nC_7H_{16})	298.15	0.1	11	0.002	1
Baragi et al. (2006) (Methylcyclohexane + nC_8H_{18})	298.15	0.1	11	0.002	1
Baragi et al. (2006) (Methylcyclohexane + nC_9H_{20})	298.15	0.1	11	0.002	1
Baragi et al. (2006) (Methylcyclohexane + $nC_{10}H_{22}$)	298.15	0.1	11	0.002	1
Baragi et al. (2006) (Methylcyclohexane + $nC_{12}H_{26}$)	298.15	0.1	11	0.002	1
Baragi & Aralaguppi (2006) (Methylcyclohexane + benzene)	298.15	0.1	11	0.002	1
Baragi & Aralaguppi (2006) (Methylcyclohexane + Toluene)	298.15	0.1	11	0.002	1

Daridon & Lagourette (1996) (CH_4 + C_8H_{18} + C_3H_8)	295.15- 373.15	25 - 100	-	-	3
Daridon et al. (1996a) (CH_4 + $nC_{16}C_{34}$+CO_2)	313.15- 393.15	12 - 70	-	-	2
Costa Gomes & Trusler, (1998) (CH_4 + N_2 + C_2H_6 + C_3H_8 + CO_2)	250 - 350	0.1 - 20	40	0.03	-
Petrauskas (2008) (LPG) (Sample 1: 71.74 % C_3H_8, 25.17 % C_4H_{10})	247.85- 323.65	-	82	-	0.7
Petrauskas (2008) (LPG) (Sample 2: 27.80 % C_3H_8, 67.04 % C_4H_{10})	254.45 -323.65	-	62	-	0.7

Table 2.14 Speed of sound data for real oils, synthetic oils and natural gases

References	T/K	P/MPa	N. Pts	Err.%	F/MHz
Matteson and Vogt (1940) (Oil hydrocarbon)	287.15-372.15	3.4 – 41	-	-	1 kHz
Daridon et al. (1996b) (Hyperbaric reservoir fluid)	313.15-453.15	saturation pressure to 120	136	0.2	3
Wang et al. (1988) (Oil)	295.15-348-15	0.1–20.6	-	-	800 kHz
Daridon et al. (1998b) (Real and synthetic heavy cut)	293.15-373.15	0.1–150	-	-	3
Daridon et al. (1998) (Gas condensate)	273.15-373.15	40–70	176	0.2	2-3
Daridon et al. (1998) (Hyperbaric oil)	313.15-453.15	40–70	136	0.2	2-3
Daridon et al. (1998) (Under-saturated oil)	273.15-413.45	10–70	248	0.2	2-3
Barreau et al. (1997) (Condensate gas)	293 - 373	40 - 100	117	1	3
Ewing & Goodwin (1993) (Natural gas)	255	6.1 – 64 (kPa)	39	0.01	6-27.6 kHz
Labes et al. (1994) (Natural gas)	263 - 413	12 - 70	-	-	3
Lagourette & Daridon (1999) (Quinary synthetic system)	293.15- 373.15	0.1 - 150	297	0.54	3
Lagourette & Daridon (1999) (Natural gas distillation cut)	293.15- 373.15	0.1 - 150	297	0.54	3
Daridon et al. (1998) (Synthetic cuts, S250)	293.15 -373.15	0.1 - 150	279	0.1	3
Daridon et al. (1998) (Synthetic cuts, S300)	293.15 -373.15	0.1 - 100	142	0.1	3
Ball et al. (2002) (Bottom-hole crude oil)	335.1 - 402.1	20 - 70	40	0.01	5
Plantier et al. (2008) (Oil sample 1)	273.15- 383.15	0.1 - 20	110	0.2	2
Plantier et al. (2008) (Oil sample 2)	273.15- 383.15	0.1 - 20	110	0.2	2

2.2 Review of the Modelling of Speed of Sound in Literature

This section deals with the models that are used to calculate the thermodynamic properties of pure fluids and mixtures using different equations of state. Some examples of EoSs are expressed in terms of pressure or Helmholtz free energy.

The advantage of the equations of state method is its applicability over wide ranges of temperature and pressure to mixtures of diverse components, from the light gases to heavy liquids. They can be used for the representation of vapour-liquid, liquid-liquid and supercritical fluid phase equilibria and they can be also applied to the gas, liquid and supercritical phases without encountering any conceptual difficulties.

Many equations of state have been proposed in the literature with either an empirical, semi-empirical or theoretical basis.

The van der Waals equation of state was the first equation to predict vapour –liquid coexistence. Later, the Redlich-Kwong equation of state improved the accuracy of the van der Waals equation by proposing temperature dependence for the attractive term. Soave and Peng and Robinson proposed additional modifications for Redlich-Kwong equation to more accurately predict the vapour pressure, liquid density, and equilibria ratios.

Advances in statistical mechanics and increase of computer power allowed the development of equation of state based on molecular principles that are accurate for real fluids and mixtures. Using Wertheim's theory, Chapman et al. (1990) and Huang and Radosz (1990) developed the Statistical-Associating-Fluid -Theory (SAFT) which is accurate for pure fluids and mixtures containing associating fluids.

In general, equations of state can be classified as being a member of one of three families:

1. Equations of State for Simple Molecules
2. Equations of State for Chain Molecules
3. Equations of State for Associating Fluids

The equations in terms of Helmholtz free energy have an analytical formulation for A (T, ρ). All thermodynamic properties can be calculated simply by differentiation of A

with respect to T and ρ. The other type of equations are in the form of pressure $P = P(T, \rho)$.

In the following section a brief history of the scientists who worked on thermodynamic modelling of fluids and a detailed description and conclusion of their methods is given. This section intends to provide the basic background information for following the discussion in the next chapters.

Thomas et al. (1970) developed an equation of state based on the eight-constant Benedict-Webb-Rubin (BWR) equation for calculation of the speed of sound in natural gases over a broad range of temperatures, pressure and gas gravities. The authors correlated the pseudocritical temperature and pseudocritical pressure with gas gravity using the data from the Phillips Natural Gas and Gasoline Dept. Then the specific heat of gas at constant pressure and constant volume were related to the PVT behaviour of the gas. The acoustic velocities in natural gases with gas gravity of 0.6, 0.8, 1.0 and 1.2 were calculated. The BWR equation of state can be used to calculate heat capacity ratios and in turn the speed of sound with an average error of 0.71 percent.

Picard and Bishnot (1987) used the Peng-Robinson and Soave-Redlich-Kwong equations of state to calculate the thermodynamic speed of sound in single-phase fluid consisting of pure components and mixtures, and in the two-phase region of a multi-component mixture. They compared the predicted results of the acoustic velocity with the experimental data for methane, ethane and propane in different reduced temperatures and reduced pressures. The errors for prediction of this thermodynamic property were as high as approximately 25, 35 and 20% for methane, ethane and propane respectively. The mixture of benzene-hexane liquid-phase was selected to predict the speed of sound and compare the results with experimental data. An error of 10% was observed and the agreement was quite poor. The speed of sound was also predicted for a two-phase multi-component gas. The predicted results showed a rapid decrease in the speed of sound with increasing pressure. This was caused by condensation of gas which decreased the fluid compressibility. The speed of sound, then increased at higher pressures after changing to a single-phase liquid. They concluded that both PR and SRK equations of state are poor in prediction of the speed of sound in fluids.

Savidge et al. (1988) used an equation of state to compute the speed of sound in natural gases. The method used was based on the compressibility factor and was restricted to the vapour phase region. This equation was developed from high accuracy compressibility data and has 27 constants. The uncertainty of the results for pressures less than 1500 psia is around 0.1 % as mentioned by the authors.

Batzle and Wang (1992) examined the seismic properties of different fluids in pores: hydrocarbon gases, hydrocarbon liquids (oils) and brines. They calculated the density, velocity and bulk modulus of gases based on Thomas et al. (1970). The approximation is adequate as long as P_{pr} and T_{pr} are below 0.9. They used the Dodson and Standing (1945) equation to calculate the density of dead oil and Wang (1988) and Wang et al. (1988) empirical relations to calculate the velocity. They estimated seismic properties of live oils by considering them to be a mixture of the original gas-free oil and a light liquid representing the gas component. Velocities can still be calculated using the Wang (1988) and Wang et al. (1988) empirical relation by substituting a pseudodensity based on the expansion caused by gas intake. True densities of live oils are also calculated using a volume factor derived by Standing (1962) but the mass of the dissolved gas must be included. The density of brine is calculated using Rowe and Chou (1970) which is a polynomial to calculate specific volume and compressibility of various salt solutions at pressure over a limited temperature range. They used a simplified form of the velocity function provided by Chen et al. (1978) to calculate the velocity in brine.

Ye et al. (1992) compared the results of the speed of sound calculated by six equations of state and experimental data of linear alkanes from nC_3 to nC_{16}, benzene, toluene and cyclohexane. They calculated the compressibility coefficient, the thermal expansion coefficient and the isobaric heat capacity by differentiation of volume obtained by equations of state with respect to temperature and pressure to determine the speed of sound of these compounds. Finally, they mentioned the deviation between predictions and the experimental data for these compounds as 17.2% for Soave- Redlich, Kwong, 13.8% for Peng- Robinson, 9.8% for translated PR, 15.2% for Simonet- Beher- Rauz, 4.3% for Lee- Kesler and 7.8% for “Chain of Rotators” equation proposed by Chien et al., (1983) for all the 2077 points and the pressures less than 100 MPa.

Then Ye et al. (1992) extended the study to binary mixtures involved in the reservoirs. They used the same equations of state as in their previous paper with various mixing

rules and in particular the rules of pseudocritical parameters as external mixing rules such as: Pederson et al. (1984), Spencer et al. (1972), Hankinson and Thomson (1979), Teja (1980), Lee and Kesler (1975) and Plocker et al. (1978). They reported the AAD % between experimental and calculated data of speed of sound for three binary mixtures of low dissymmetry (nC_6 – nC_{10}, nC_8 – nC_{12}, nC_{10} – nC_{14}) and moderate or very asymmetric systems (nC_6 – nC_{16}, nC_1 – nC_{16}, CO_2 – nC_{16}). They showed the best representation of the data with the Lee – Kesler model with AAD % between 5.5 – 12.9 for the first group and COR model with AAD % between 5.4 – 16.6 for the second one.

Barreau et al. (1997) used a thermodynamic model based on the Peng- Robinson equation of state with a Peneloux volume translation (Peneloux et al., 1982) to model the behaviour of a condensate gas. The calculation of isobaric and isochoric heat capacity and also velocity of sound was achieved by differentiation of pressure with respect to temperature and volume obtained by the equation. They concluded that deviations of calculated results from experimental data are more dependant to temperature than on pressure and varies between +2% and -5%.

Firoozabadi and Pan (2000) proposed a model for calculation of isentropic compressibility and sonic velocity in a number of binary and ternary mixtures and a crude oil in single-phase region. The results were compared for gaseous nitrogen and methane and liquid hexane with experimental data and good agreement was achieved. They, also, presented a model to estimate these properties in the two-phase region. Different molar compositions of C_1/C_3, C_1/C_{10}, $C_1/nC_4/nC_{10}$ and crude oils were investigated. The increment of retrograde dew point pressure and decrement of bubble point pressure were observed as a result of increasing in capillary pressure.

Han and Batzle (2000) improved the velocity and density models of Batzle and Wang (1992) based on a series of new data. These new data suggest that the velocity model developed by Batzle and Wang (1992) overestimated the gas and oil ratio effect on the velocity of hydrocarbon liquids. They used two techniques to fit the data: a model based on engineering concepts of ideal liquids, and one on purely empirical forms.

Llovell and Vega (2006) introduced a molecular based equation of state called Soft-SAFT to calculate the derivative properties of pure components such as methane, propane, n-hexane and n-heptane from n-alkane series and some other compounds from

1-alkanol series. The deviations of the calculated and experimental data are between 5 and 20 percent. This equation is written in terms of residual Helmholtz energy.

Then, Llovell et al. (2006) developed this equation for calculation of second-order thermodynamic properties of selected binary mixtures by using the van der Waals 1-fluid mixing rules in order to evaluate the properties of the reference fluid. The soft-SAFT estimated the speed of sound for both pure compounds at two different constant pressures of 0.1 MPa and 101.3 MPa as compared to experimental data. The AADs% for two constant compositions of propane and isobutane at various temperatures ranging from 260 to 320 K are 3% in both cases.

Llovell and Vega (2007) proposed a crossover Soft-SAFT equation by adding a crossover treatment to the original equation to decrease the deviations of the results near the critical region and applied this equation for calculation of derivative properties.

Queimada et al. (2006) used a model based on a three-parameter corresponding state principle to estimate the speed of sound of pure and mixture hydrocarbons for n-alkanes from ethane to n-hexatriacontane and compared the results with a large number of experimental data as a function of temperature and pressure. The average deviations are approximately 2%, but higher deviations were observed for those n-alkanes with higher reduced temperature / reduced pressure.

Daridon et al. (1998, 1999, 2002), Daridon and Lagourette (2000), Dutour et al. (2000, 2001, 2002) and Lagouretter and Daridon (1999) proposed a correlated function containing nine adjustable constant for each compound over the available experimental temperature and pressure range. The deviations of the results from experimental data using this function are very low, i.e., around 1%.

Nasrifar and Bolland (2006) proposed a new cubic equation of state by matching the critical fugacity coefficient of the EoS to the critical fugacity coefficient of methane. They applied the van der Waals mixing rules and zero binary interaction parameters and could predict compressibility factors and speed of sound of natural gas mixtures with good accuracy. They compared the results with those of some other cubic equations of state such as PR and SRK and showed that their speed of sound results are in better agreement with the experimental data.

Shin et al. (2007) applied a crossover cubic equation of state for the calculation of second-order thermodynamic properties such as speed of sound for pure carbon dioxide and n-alkanes from methane to propane and showed that this equation can give much better results than the original Patel-Teja equation of state. This crossover cubic equation of state which was proposed and improved by Lee et al. (2007) and developed by the other authors, has one adjustable parameter for each pure component. The deviations from experimental data for these 4 compounds are between 1.87 and 10% and are better in comparison with the deviations of the results calculated by Cubic EOS which are between 2.5 and 14%.

Maghari and Sadeghi (2007) used a modified SAFT-BACK equation of state developed by Chen and Mi (2001) to predict thermodynamic properties such as speed of sound for some pure chain fluids from methane to n-decane. They compared the results with the correlated NIST data and determined the AAD% of 2.3% for the speed of sound for these compounds. Also, they compared the results with those obtained by Llovell and Vega (2006) and showed that the modified SAFT-BACK equation of state can give better results than the Soft-SAFT model.

Nichita et al. (2010) derived a method for predicting the isentropic compressibility and the speed of sound of two-phase fluids from an equation of state. They applied their method to various types of reservoir fluid and obtained much lower bulk moduli and speed of sound than predicted values by Wood's approach for low gas content oils in two-phase fluids.

Maghari and Hamzehloo (2011) extended the SAFT-CP model to predict thermodynamic properties including heat capacities and speed of sound of some binary mixtures of hydrocarbons without any additional parameter. The results were compared with correlated data of NIST. The AAD% of speed of sound, density and heat capacities for most n-alkane mixtures are around 3.5%, 1% and 2%, respectively.

2.3 Conclusion

This chapter has investigated all of the work related to measurement and modelling of speed of sound in the past. A lot of experimental data has been measured previously by different authors for various ranges of temperature and pressure, using different frequencies. In order to use the independent experimental data for validation of the

model in this work, all of the data should be consistent. To get the measured values at the right required temperature and pressure and for the purpose of consistency between the data, a considerable amount of laboratory work was performed and the results will be presented in Chapter 3. These data will be then used to evaluate the model in this work.

In modelling the velocity of sound, some equations of state have been used to model the thermodynamic properties. Regarding to the investigation and discussion above, although all of the methods that were used can be useful in prediction of the thermodynamic properties, they have some disadvantages that make the modelling difficult. The problems with the equations of state which were investigated for modelling thermodynamic properties are:

- the use of many constants in some EoSs which need to be regressed;
- poor agreement between model predictions and experimental data;
- the application of some EoSs over a limited range of temperature and pressure;
- the limitation of some EoSs to only natural gases or light hydrocarbons;
- the inability of some EoSs to predict the PVT behaviour near the critical region.

The lack of a comprehensive equation of state which can predict accurate values over a whole range of temperature, pressure and density provided the motivation for this work.

REFERENCES

Aicart E., Costas M., Junquera E., Tardajos G., 1990, *Ultrasonic speeds and isentropic compressibilities of (1,4-dioxane + n-heptane or n-decane or n-tetradecane),* The Journal of Chemical Thermodynamics, **22 (12)**, 1153-1158

Aicart E., Kumaran M.K., Halpin C.J., Benson G.C., 1983, *Ultrasonic speeds and isentropic compressibilities of n-heptane + each of the hexane isomers at 298.15 K*, The Journal of Chemical Thermodynamics, **15 (10)**, 919-925

Akamatsu Y., Ogawa H., Murakami S., 1987, *Molar excess enthalpies, molar excess volumes and molar isentropic compressions of mixtures of 2-propanone with heptane, benzene and trichloromethane at 298.15 K*, Thermochimica Acta, **113(15)**, 141-151

Aleksandrov A.A., Larkin D.K., 1976, *Speed of sound, isochoric heat capacity, and coefficient of isothermal compression of heavy water at atmospheric pressure,* Journal of Engineering Physics and Thermodynamics, **34 (1)**, 73-75

Aleksandrov A.A., Kochetkov A.I., 1979, *The experimental determination of ultrasonic velocity in water at temperatures 266 - 423 K and at pressures up to 100 MPa*, Thermal Engineering, **26,** 558 – 559

Allegra J., Hawley S., Holton G., 1970, *Pressure Dependence of the Ultrasonic Absorption in Toluene and Hexane*, J. Acoust. Soc. Am. **47**, 144

Aminabhavi T.M., Aralaguppi M.I., Gopalakrishna B., Khinnavar R.S., 1994, *Densities, Shear Viscosities, Refractive Indices, and Speeds of Sound of Bis(2-methoxyethyl) Ether with Hexane, Heptane, Octane, and 2,2,4-Trimethylpentane in the Temperature Interval 298.15-318.15 K*, Journal of Chemical Engineering Data, **39**, 522-528

Aminabhavi T.M., Gopalakrishna B., 1994, *Densities, Viscosities, Refractive Indices, and Speeds of Sound of the Binary Mixtures of Bis(2-methoxyethyl) Ether with Nonane, Decane, Dodecane, Tetradecane, and Hexadecane at 298.15,308.15, and 318.15 K*, J. Journal of Chemical Engineering Data, **39**, 529-534

Aminabhavi T.M., Gopalakrishna B., 1995, *Density, Viscosity, Refractive Index, and Speed of Sound in Binary Mixtures of 2-Ethoxyethanol with n-Alkanes (C_6 to C_{12}), 2,2,4-Trimethylpentane, and Cyclohexane in the Temperature Interval 298.15-313.15 K*, Journal of Chemical Engineering Data, **40**, 632-641

Asenbaum A. Hochheimer H., Naturforsch Z., 1983, **38**, 980

Badalyan A.L., Otpushchennikov N.F., Shoitov U.S., 1970, Izv. Akad. Nauk. SSSR Fiz., **5**, 448

Badalyan A., Otpushchennikov N., Shoitov Y., 1970, *The velocity of ultrasound in n-octane and n-decane at high pressure*, Izv. Akad. Nauk Arm. SSSR Fiz. **5**, 448 (In Russian: abstract in English)

Badalyan A.L., Otpuschennikov N.F., 1971, *Sound velocity and some thermodynamic characteristics of liquid octane, decane and undecane at high pressure*, Izv. Akad. Nauk. Arm. SSR, **6**, 207 – 213

Ball S.J., Goodwin A.R.H., Trusler J.P.M., 2002, *Phase behaviour and physical properties of petroleum reservoir fluids from acoustic measurements*, Journal of Petroleum Science and Engineering, **34**, 1– 11

Ball S.J., Trusler J.P.M., 2001, *Speed of Sound of n-Hexane and n-Hexadecane at Temperatures between 298 and 373 K and Pressures up to 100 MPa*, International Journal of Thermophysics, **22 (2)**, 427 - 443

Baragi J.G., Aralaguppi M.I., 2006, *Excess and deviation properties for the binary mixtures of methylcyclohexane with benzene, toluene, p-xylene, mesitylene, and anisole at T = (298.15, 303.15, and 308.15) K*, J. Chem. Thermodynamics, **38**, 1717–1724

Baragi J.G., Aralaguppi M.I., Kariduraganavar M.Y., Kulkarni S.S., Kittur A.S., Aminabhavi T.M., 2006, *Excess properties of the binary mixtures of methylcyclohexane + alkanes (C_6 to C_{12}) at T = 298.15 K to T = 308.15 K*, J. Chem. Thermodynamics, **38**, 75–83

Barlow A.J., Yazgan E., 1967, *Pressure dependence of the velocity of sound in water as a function of temperature*, British Journal of Applied Physics, **18 (5)**, 645 – 651

Barreau A., Gaillard K., Béhar E., Daridon J.L., Lagourette B., Xans P., 1997, *Volumetric properties, isobaric heat capacity and sound velocity of condensate gas measurements and modelling*, Fluid Phase Equilibria **127 (1-2),** 155-171

Batzle M., Wang Z., 1992, *Seismic properties of pore fluids*, Geophysics, **57(11)**, 1396-1408

Belinskii B., Ikramov Sh., 1973, Sov. Phys. Acoust. (a translation of Akusticheskii Zhurnal) **18**, 300

Benedetto G., Gavioso R.M., Giuliano Albo P.A., Lago S., Ripa D.M., Spagnolo R., 2005, *Speed of Sound of Pure Water at Temperatures between 274 and 394 K and Pressures up to 90 MPa*, , International Journal of Thermophysics, **26**, 1667 – 1680

Benson G.C., Halpin C.J., 1987, *Ultrasonic speeds and isentropic compressibilities of binary mixtures of n-octane with each of the hexane isomers at 298.15 K*, Canadian Journal of chemistry, **65**, 322-325

Benson G.C., Halpin C.J., Kumaran M.K., 1986, *Ultrasonic speeds and isentropic compressibilities of each of the mixtures: (n-dodecane + an isomer of hexane) at 298.15 K*, The Journal of Chemical Thermodynamics, **18 (12)**, 1147-1152

Benson G.C., Handa Y.P., 1981, *Ultrasonic speeds and isentropic compressibilities for (decan-1-ol + n-alkane) at 298.15 K*., Journal of Chemical Thermodynamics, **13**, 887–896

Bessières D., Plantier F., 2007, *Thermodynamic consistency between calorimetric acoustic and volumetric measurementents, Application to n –undecane*, Journal of Thermal Analysis and Calorimetry, **89 (1)**, 81-85

Boelhouwer J.W.M., 1967, *Sound velocities in and adiabatic compressibilities of liquid alkanes at various temperatures and pressures*, Physica, **34 (3)**, 484-492

Bohidar H. B., 1988, J. Appl. Phys. **64**, 1810

Bohidar H. B., 1989, *Brillouin scattering study of pressure dependence of hypersonic sound velocity in binary liquids*, J. Phys. D: Appl. Phys. **22**, 1252

Bolotnikov M.F., Neruchev Y.A., Melikhov Y.F., Verveyko V.N., Verveyko M.V., 2005, *Temperature Dependence of the Speed of Sound, Densities, and Isentropic Compressibilities of Hexane + Hexadecane in the Range of (293.15 to 373.15) K*, Journal of Chemical Engineering Data, **50 (3)**, 1095–1098

Chavez M., Palacios J.M., Tsumura R., 1982, *Speed of Sound in Saturated Liquid n-Pentane*, Journal of Chemical and Engineering Data, **27 (3)**

Chen C.T., Chen L.S., Millero F.J., 1978, *Speed of sound in NaCl, MgClz, NazS04, and MgS04 aqueous solutions as functions of concentration, temperature, and pressure*: J. Acoust. Sot. Am., **63**, 1795-1800

Chen J., Mi J., 2001, *Equation of state extended from SAFT with improved results for non-polar fluids across the critical point*, Fluid Phase Equilibria **186**, 165–184

Chien C.H., Greenkorn R.A., Chao K.C., 1983, *Chain-of-rotators equation of state*, AIChE Journal, **29(4)**, 560–571

Cholpan P.F., Sperkach V.S., Garkusha L.N., 1981, *Investigation of Propagation of Ultrasonic Waves in Isoviscous Solutions of n-Paraffins*, in Fizika zhidkogo sostoyaniya (Liquid State Physics), Kiev: Izd. KGU (Kiev State Univ.), **9**, 79

Cholpan P.F., Sperkach V.S., Garkusha L.N., 1982, *Investigation of Propagation of Ultrasonic Waves in Solutions of n-Paraffins*, in Fizika zhidkogo sostoyaniya (Liquid State Physics), Kiev: Izd. KGU (Kiev State Univ.), 1982, **10**, 88

Cholpan P.F., Sperkach V.S., Garkusha L.N., 1989, *The Physical Properties of Solutions of Molecular Liquids of Components of Different Structures*, in Fizika zhidkogo sostoyaniya (Liquid State Physics), Kiev: Izd. KGU (Kiev State Univ.), **17**, 41

Costa Gomes M.F., Trusler J.P.M., 1998, *The speed of sound in nitrogen at temperatures between T = 250 K and T = 350 K and at pressures up to 30 MPa*, The Journal of Chemical Thermodynamics, **30 (5)**, 527-534

Costa Gomes M.F., Trusler J.P.M., 1998, *The speed of sound in two methane-rich gas mixtures at temperatures between 250 K and 350 K and at pressures up to 20 MPa*, The Journal of Chemical Thermodynamics, **30 (9)**, 1121-1129

Daridon J., 1994, Acustica **80**, 416 (In French)

Daridon J., Lagourette B., 1996, Acustica **82**, 32 (In French).

Daridon J., Lagourette B., Gaubert J., Xans P., Montel F., 1996b, Ultrasonics, **34**, 447

Daridon J., Lagourette B., Grolier J., 1998b, International Journal of Thermophysics, **19**, 145

Daridon J., Lagourette B., Labes P., International Journal of Thermophysics, **17**, 851

Daridon J., Lagourette B., Xans P., 1998c, R. Soc. Chem., Great Britain (Special Publication) **222**, 88

Daridon J.L., Carrier H., Lagourette B., 2002, *Pressure Dependence of the Thermophysical Properties of n-Pentadecane and n-Heptadecane*, International Journal of Thermophysics, **23 (3)**, 697-708

Daridon J.L., Lagourette B., 2000, *Ultrasonic velocity of liquid tridecane and tetradecane as a function of temperature and pressure*, High Temperatures - High Pressures, **32(1)**, 83 – 87

Daridon J.L., Lagourette B., Gaubert J. F., Xans P., Montel F., 1996, *Ultrasonic velocity in a hyperbaric reservoir fluid*, Ultrasonics, **34 (2-5)**, 447-449

Daridon J.L., Lagourette B., Grolier J.P.E., 1998, *Experimental Measurements of the Speed of Sound in n-Hexane from 293 to 373 K and up to 150 MPa*, International Journal of Thermophysics, **19 (1)**, 145-160

Daridon J.L., Lagourette B., Labes P., 1996, *Compressibilities of ternary mixtures C_1-nC_{16}-CO_2 under pressure from ultrasonic measurements of sound speed*, International Journal of Thermodynamics, **17 (4)**, 851 - 871

Daridon J.L., Lagourette B., Xans P., 1994, *Thermodynamic properties of liquid mixtures containing gas under pressure based on ultrasonic measurements*, Fluid Phase Equilibria, **100**, 269-282

Daridon J.L., Lagourette B., Xans P., Montel F., 1998, Petroleum characterization from ultrasonic measurement, Journal of Petroleum Science and Engineering, **19 (3-4)**, 281-293

Daridon J.L., Lagrabette A., Lagourette B., 1998, *Speed of sound, density, and compressibilities of heavy synthetic cuts from ultrasonic measurements under pressure*, Journal of Chemical Thermodynamics, **30**, 607-623

Del Grosso V.A., 1970, *Sound speed in pure water and sea water*, The Journal of the Acoustical Society of America, **47 (3)**, 947 – 949

Del Grosso V.A., Mader C.W., 1972, *Speed of sound in pure water*, The Journal of the Acoustical Society of America, **52 (5)**, 1442 – 1446

Ding Z.S., Alliez J., Boned C., Xans P., 1997, *Automation of an ultrasound velocity measurement system in high-pressure liquids*, Measurement Science and Technology, **8 (2)**, 154

Dodson C.R., Standing M.B., 1945, *Pressure - volume - temperature and solubility relations for natural-gas-water mixtures*, Drilling and production practices

Dubey G.P., Sharma M. 2008, *Aoustic thermodynamic, viscometric and volumetric studies in binary systems of 1-decanol with n-hexane, n-octane, n-decane with respect to temperature*, Journal of Molecular Liquids, **143**, 109 - 114

Dubey G.P., Sharma M., Dubey N., 2008, *Study of densities, viscosities, and speeds of sound of binary liquid mixtures of butan-1-ol with n-alkanes (C_6, C_8, and C_{10}) at T = (298.15, 303.15, and 308.15) K*, J. Chem. Thermodynamics, **40**, 309–320

Dutour S., Daridon J.L., Lagourette B., 2000, *Pressure and Temperature Dependence of the Speed of Sound and Related Properties in Normal Octadecane and Nonadecane*, International Journal of Thermophysics, **21 (1)**, 173

Dutour S., Daridon J.L., Lagourette B., 2001a, *Speed of sound, density, and compressibilities of liquid eicosane and docosane at various temperatures and pressures,* High Temperatures - High Pressures, **33(3)**, 371 – 378

Dutour S., Lagourette B., Daridon J.L., 2001, *High-pressure speed of sound and compressibilities in heavy normal hydrocarbons: n-$C_{23}H_{48}$ and n-$C_{24}H_{50}$,* Journal of Chemical Thermodynamics, **33**, 765–774

Dutour S., Lagourette B., Daridon J.L., 2002, *High-pressure speed of sound, density and compressibility of heavy normal paraffins: $C_{28}H_{58}$ and $C_{36}H_{74}$,* Journal of Chemical Thermodynamics, **34**, 475–484

Dzida M., Cempa M., 2008, Thermodynamic and acoustic properties of (heptane + dodecane) mixtures under elevated pressures, The Journal of Chemical Thermodynamics, **40 (10)**, 1531-1541

Dzida M., Żak A., Ernst S., 2005, *Thermodynamic and acoustic properties of binary mixtures of alcohols and alkanes. I. Speed of sound in (ethanol + n-heptane) under elevated pressures,* The Journal of Chemical Thermodynamics, **37 (5)**, 405-414

Eden H., Richardson E., 1960, Acustica **10**, 309

Estela-Uribe J.F., Trusler J.P.M., Chamorro C.R., Segovia J.J., Martin M.C., Villamanan M.A., 2006, *Speeds of sound in {(1 -x)CH_4 + xN_2} with x = (0.10001, 0.19999,and 0.5422) at temperatures between 170 K and 400 K and pressures up to 30 MPa,* J. Chem. Thermodynamics, **38**, 929–937

Estrada-Alexanders A.F., Hurly J.J., 2008, *Kinematic viscosity and speed of sound in gaseous CO, CO_2, SiF_4, SF_6, $C4F_8$, and NH_3 from 220 K to 375 K and pressures up to 3.4 MPa* , Journal of Chemical Thermodynamics, **40**, 193–202

Estrada-Alexanders A.F., Trusler J.P.M., 1997, *The speed of sound and derived thermodynamic properties of ethane at temperatures between 220 K and 450 K and pressures up to 10.5 MPa,* The Journal of Chemical Thermodynamics, **29 (9)**, 991-1015

Estrada-Alexanders A.F., Trusler J.P.M., 1998, *Speed of sound in carbon dioxide at temperatures between (220 and 450) K and pressures up to 14 MPa*, The Journal of Chemical Thermodynamics, **30 (12)**, 1589-1601

Estrada-Alexanders A.F., Trusler J.P.M., 1999, *Speed of sound in ($0.4C_2H_6$ + $0.6CO_2$) at temperatures between T = 220 K and T = 450 K and pressures up top = 1.2 MPa*, The Journal of Chemical Thermodynamics, **31 (5)**, 685-695

Ewing M.B., Goodwin A.R.H., 1991, *Thermophysical properties of alkanes from speeds of sound determined using a spherical resonator 4.2-methylpropane at temperatures in the range 251 K to 320 K and pressures in the range 5 kPa to 114 kPa*, The Journal of Chemical Thermodynamics, **23 (12)**, 1107-1120

Ewing M.B., Goodwin A.R.H., 1993, *Speeds of sound in a natural gas of specified composition at the temperature 255 K and pressures in the range 64 kPa to 6.1 MPa*, The Journal of Chemical Thermodynamics, **25 (12)**, 1503-1511

Ewing M.B., Goodwin A.R.H., McGlashan M.L., Trusler J. P. M., 1988, *Thermophysical properties of alkanes from speeds of sound determined using a spherical resonator 2. n-Butane*, The Journal of Chemical Thermodynamics, **20 (2)**, 243-256

Ewing M.B., Goodwin A.R.H., McGlashan M.L., Trusler J.P.M., 1987, *Thermophysical properties of alkanes from speeds of sound determined using a spherical resonator I. Apparatus, acoustic model, and results for dimethylpropane*, The Journal of Chemical Thermodynamics, **19 (7)**, 721-739

Ewing M.B., Goodwin A.R.H., Trusler J.P.M., 1989, *Thermophysical properties of alkanes from speeds of sound determined using a spherical resonator 3. n-Pentane*, The Journal of Chemical Thermodynamics, **21 (8)**, 867-877

Ewing M.B., McGlashan M.L., Trusler J.P.M., 1986, *The speed of sound in gases II. Acoustic virial coefficients and perfect-gas heat capacities for 2,2-dimethylpropane obtained using a cylindrical interferometer*, The Journal of Chemical Thermodynamics, **18 (6),** 511-517

Ewing M.B., Trusler J.P.M., 1992, *Second acoustic virial coefficients of nitrogen between 80 and 373 K*, Physica A: Statistical and Theoretical Physics, **184 (3-4)**, 415-436

Fujii K., 1993, *Accurate measurements of the sound velocity in pure water by combining phase-detection technique and a variable path-length interferometer*, J. Acoustical Society of America, **93 (1)**, 276 – 282

Gardas R.L., Coutinho J.A.P., 2008, *Estimation of speed of sound of ionic liquids using surface tensions and densities: A volume based approach*, Fluid Phase Equilibria, **267**, 188–192

Garkusha L.N., Sperkach V.S., Cholpan P.F.,1980a, *Investigation of the Acoustic Properties of Solutions of n-Paraffins*, in Fizika zhidkogo sostoyaniya (Liquid State Physics), Kiev: Izd. KGU (Kiev State Univ.), **8**, 41

Garkusha L.N., Sperkach V.S., Cholpan P.F., 1980b, Ukr. Fiz. Zh., 1980b, **25 (9)**, 1559.

Gedanitz H., Dávila M.J., Baumhögger E., Span R., 2010, *An Apparatus for the Determination of Speeds of Sound in Fluids*, J. Chem. Thermodynamics, **42 (4)**, 478 - 483

George J., Sastry N.V., 2003, *Measurements of densities, viscosities, speeds of sound and relative permittivities and excess molar volumes, excess isentropic compressibilities and deviations in relative permittivities and molar polarizations for dibutyl ether + benzene + toluene and + p-xylene at different temperatures*, Journal of Chemical Thermodynamics, **35**, 1837–1853

Golic A.Z., Adamenko I.I., Makhno M.., 1982, *An Integrated facility to study the density and velocity of ultrasound of liquids in a wide range of pressures and temperatures*, in Fizika zhidkogo sostoyaniya (Physics of the liquids state), Kiev, Izd, KGU (Kiev State Univ.), **10**, 3

Golik A.Z., Adamenko I.I., Sokolovskaya S.F., Nesterenko N., 1978, *The Equation of State and Elastic Properties of Solutions of n-Heptane - n-Tetracosane*, in Fizika zhidkogo sostoyaniya (Liquid State Physics), Kiev: Izd. KGU (Kiev State Univ.), **6**, 43

Golik A.Z., Adamenko I.I., Varetskii V.V., 1976, *The Equation of State and Elastic Properties of n-Heptane - n-Dodecane System*, in Fizika zhidkogo sostoyaniya (Liquid State Physics), Kiev: Izd. KGU (Kiev State Univ.), **4**, 91

González B., Dominguez A., Tojo J., 2004, *Dynamic Viscosities of 2-Pentanol with Alkanes (Octane, Decane, and Dodecane) at Three Temperatures T = (293.15, 298.15, and 303.15) K.* New UNIFAC−VISCO Interaction Parameters, J. Chem. Eng. Data, **49 (5)**, 1225–1230

González-Salgado D., Tovar C.A., Cerdeiriña C.A., Carballo E., Roman L., 2002, *Second-order excess derivatives for the 1,3-dichloropropane + n-dodecane system*, Fluid Phase Equilibria, **199**, 121–134

Han D.H., Batzle H.M., 2000, *Velocity, Density and Modulus of Hydrocarbon Fluids - Empirical Modelling*, SEG Expanded Abstracts

Handa Y.P., Halpin C.J., Benson G.C., 1981, *Ultrasonic speeds and isentropic compressibilities for (hexan-1-ol+n-alkane) at 298.15 K*, The Journal of Chemical Thermodynamics, **13 (9)**, 875-886

Hankinson R.W., Thomson G.H., 1979, *A New Correlation for Saturated Liquid Densities of Liquids and Their Mixtures*, AIChE J. **25**, 653- 661

Hawley S.J., Allegra J., Holton G., 1970, *Ultrasonic Absorption and Sound Speed Data for Nine Liquids at High Pressure*, J. Acoust. Soc. Am., 47, 137

Herget C.M., 1940, *Ultrasonic Velocity in Carbon Dioxide and Ethylene in the Critical Region*, Journal of Chemical Physics, **8**, 537

Houck J. C., 1974, J. Res. Natl. Bur. Stand., Sect. A **78**, 617

Iloukhani H., Samiey B., Moghaddasi M.A., 2006, *Speeds of sound, isentropic compressibilities, viscosities and excess molar volumes of binary mixtures of methylcyclohexane + 2-alkanols or ethanol at T = 298.15 K*, J. Chem. Thermodynamics **38,** 190–200

Ismagilov R., Ermakov G., Teplofiz, 1982, Vys. Temp. **20**, 677 (In Russian).

Junquera E., Aicart E., Tardajos G., 1989, *Speed of sound and isentropic compressibility of (1-chlorobutane + n-undecane or n-dodecane or n-tetradecane or n-hexadecane) at 298.15 K*, The Journal of Chemical Thermodynamics, **21 (12)**, 1223-1230

Junquera E., Tardajos G., Aicart E., 1988, *Speeds of sound and isentropic compressibilities of (cyclohexane + benzene and (1-chlorobutane + n-hexane or n-heptane or n-octane or n-decane) at 298.15 K*, The Journal of Chemical Thermodynamics, **20 (12)**, 1461-1467

Kagramanyan L., Badalyan A., 1978, Izv. Akad. Nauk Arm. SSSR Fiz. **13**, 478, (In Russian)

Khasanshin T.S., Poddubskii O.G., Shchemelev A.P., 2004, *Experminetal study of the velocity of sound in liquid n-tetradecane at temperatures from 303.15 to 433.15 K and pressures to 100 MPa*, Journal of Engineering Physics and Thermophysics, **77 (1)**, 185 - 188

Khasanshin T.S., Samuilov V.S. Shchemelev A.P., 2009, *The sound velocity in liquid binary mixtures of n-alkanes*, HIGH TEMPERATURE, 47 (4), 527-532

Khasanshin T.S., Samuilov V.S., Shchemelev A.P., 2008, *Speed of sound in n-hexane, n-octane, n-decane and n-hexadecane in the liquid state*, Journal of Engineering Physics and Thermophysics, **81 (4)**, 760 - 765

Khasanshin T.S., Shchemelev A.P., 2001, *Sound Velocity in Liquid n-Alkanes*, HIGH TEMPERATURE, **39 (1**), 60- 67

Kiyohara O., Benson G.C., 1979, *Ultrasonic speeds and isentropic compressibilities of n-alkanol + n-heptane mixtures at 298.15 K*, The Journal of Chemical Thermodynamics, **11 (9)**, 861-873

Kling R., Nicolini E., Tissot J., Rech. Aeronaut., 1953, **31**, 31

Kortbeek P.J., Schouten J.A., 1990, *Measurements of the compressibility and sound velocity in methane up to 1 GPa*, International Journal of Thermodynamics, **11 (3)**, 455-466

Kortbeek P.J., Trappeniers N.J., Biswas S.N., 1988, *Compressibility and sound velocity measurements on N_2 up to 1 GPa,* International Journal of Thermophysics, **9 (1)**, 103-116

Kumaran M.K., Kimura F., Halpin A.J., Benson G.C., 1984, *Excess volumes and ultrasonic speeds for (3,6-dioxaoctane + n-heptane),* The Journal of Chemical Thermodynamics, **16 (7)**, 687-691

Labes P., Daridon J.L., Lagourette B., Saint-Guirons H., 1994, *Measurement and prediction of ultrasonic speed under high pressure in natural gases*, International Journal of Thermophysics, **15 (5),** 803-819

Lacam P., 1954, J. Phys. Rad. **15**, 830 (In French).

Lacam A., 1956, J. Rech Centre National Recherche Scientifique, **34**, 25 (In French).

Lago S., Giuliano P.A., Albo, Ripa D.M., 2006, *Speed-of-Sound Measurements in n-Nonane at Temperatures between 293.15 and 393.15 K and at Pressures up to 100 MPa*, INTERNATIONAL JOURNAL OF THERMOPHYSICS, **27 (4)** , 1083-1094

Lagourette B., Daridon J. L., Gaubert J. F., Xans P., 1994, *Experimental determination of ultrasonic speeds in (methane + propane)(g) and in (methane + octane)(g) at high pressures*, The Journal of Chemical Thermodynamics, **26 (10)**, 1051-1061

Lagourette B., Daridon J.L., 1999, *Speed of sound, density, and compressibility of petroleum fractions from ultrasonic measurements under pressure*, Journal of Chemical Thermodynamics, **31**, 987–1000

Lainez A., Zollweg J. A., Streett W.B., 1990, *Speed-of-sound measurements for liquid n-pentane and 2,2-dimethylpropane under pressure*, The Journal of Chemical Thermodynamics, **22 (10)**, 937-948

Lee B.I., Kesler M.G., 1975, *A Generalized Thermodynamic Correlation Based on Three-Parameter Corresponding States,* AIChE Journal, **21(3)**, 510–527

Lee Y., Shin M.S., Yeo J.K., Kim H., 2007, *A crossover cubic equation of state near to and far from the critical region*, J. Chem. Thermodynamics, **39**, 1257–1263

Llovell F., Vega L.F., 2007, *Phase equilibria, critical behaviour and derivative properties of selected n-alkane/n-alkane and n-alkane/1-alkanol mixtures by the crossover soft-SAFT equation of state*, J. of Supercritical Fluids, **41**, 204–216

Llovell F., Peters C.J., Vega L.F., 2006, *Second-order thermodynamic derivative properties of selected mixtures by the soft-SAFT equation of state*, Fluid Phase Equilibria, **248**, 115–122

Llovell F., Vega L.F., 2006, *Prediction of Thermodynamic Derivative Properties of Pure Fluids through the Soft-SAFT Equation of State*, J. Phys. Chem. B, **110**, 11427-11437

Maghari A., Sadeghi M.S., 2007, *Prediction of sound velocity and heat capacities of n-alkanes from the modified SAFT-BACK equation of state*, Fluid Phase Equilibria, **252(1-2)**, 152-161

Maghari A., Hamzehloo M., 2011, *Second-order thermodynamic derivative properties of binary mixtures of n-alkanes through the SAFT-CP equation of state Fluid Phase Equilibria*, **302(1-2)**, 195-201

Marino G., Iglesias M., Orge B., Tojo J., Pineiro M.M., 2000, *Thermodynamic properties of the system (acetone + methanol + n-heptane) at T = 298.15 K*, J. Chem. Thermodynamics, **32**, 483–497

Matteson, R. and C. Vogt, J. Appl. Phys. 11, 658 (1940)

Meier K., Kabelac S., 2006, *Speed of sound instrument for fluids with pressures up to 100MPa*, Review of Scientific Instruments , **77 (12)**, 123903 - 123903-8

Melikhov Yu., 1985, Ultrazvuk i Termodinamicheskie Svoitsva Veshchestva, 81– 103 (In Russian).

Melikhov Yu., Kiryakov B., Kuzmin V., 1976, Nauchnye Trudy (Kurskiæi Gosudarstvennyæi Pedagogicheskiæi Institut) **81**, 116 (In Russian).

Melikhov Yu., Kiryakov B., Shoitov Yu., 1979, Nauchnye Trudy (Kurskiæi Gosudarstvennyæi Pedagogicheskiæi Institut) **196**, 147 (In Russian).

Mosteiro L., Casás L.M., Legido J.L., 2009, *Surface tension, density, and speed of sound for the ternary mixture {diethyl carbonate + p-xylene + decane}*, J. Chem. Thermodynamics, **41**, 695–704

Mosteiro L., Mascato E., de Cominges B.E., Iglesias T. P., Legido J.L., 2001, *Density, speed of sound, refractive index and dielectric permittivity of (diethyl carbonate + n - decane) at several temperatures*, The Journal of Chemical Thermodynamics, 33 (7), 787-801

Muringer M.J.P., Trappeniers N.J., Biswas S.N., 1985, *The Effect of Pressure on the Sound Velocity and Density of Toluene and n-heptane up to 2600 bar*, Physics and Chemistry of Liquids, **14 (4),** 273-296

Nasrifar KH., Bolland O., 2006, *Prediction of thermodynamic properties of natural gas mixtures using 10 equations of state including a new cubic two-constant equation of state*, Journal of Petroleum Science and Engineering, **51**, 253–266

Nath J., 1998, *Speeds of sound in and isentropic compressibilities of (n-butanol + n-pentane) at T = 298.15 K, and (n-butanol + n-hexane, or n-heptane, or n-octane, or 2,2,4-trimethylpentane) at T = 303.15 K*, The Journal of Chemical Thermodynamics, **30 (7)**, 885-895,

Nath J., 2002, *Speeds of sound in and isentropic compressibilities of (n-butanol + n-pentane, or n-hexane, or n-heptane, or 2,2,4-trimethylpentane) at T = 288.15 K, (n-hexanol + n-pentane or n-hexane) at T = 298.15 K, and (n-hexanol + n-heptane or n-octane) at T = 298.15 K and T = 303.15 K*, J. Chem. Thermodynamics, **34**, 1857–1872

Nichita D.V., Khalid P., Broseta D.,2010, *Calculation of isentropic compressibility and sound velocity in two-phase fluids*, Fluid Phase Equilibria, **291**,95–102

Niepmann R., 1984, *Thermodynamic properties of propane and n-butane 2. Speeds of sound in the liquid up to 60 MPa*, The Journal of Chemical Thermodynamics, **16 (9)**, 851-860

Noury J., 1954, J. Phys. Paris **55**, 831

Oakley B., Hanna D., Shillor M., Barber G., 2003, *Ultrasonic Parameters as a Function of Absolute Hydrostatic Pressure. II. Mathematical Models of the Speed of Sound in Organic Liquids*, J. Phys. Chem. Ref. Data, **32 (4)** , 1501 - 1533

Ohomuro K., Tamura K., Murakami S., 1987, *Speeds of sound, excess molar volumes, and isentropic compressibilities of "$xCH_3COC_2H_5 + (1 - x)C_7H_{16}$", "$xCH_3COC_2H_5 + (1 - x)c\text{-}C_6H_{12}$", "$xCH_3COC_2H_5 + (1 - x)c\text{-}C_6H_{11}CH_3$", "$xC_2H_5COC_2H_5 + (1 - x)C_7H_{16}$", and "$xC_2H_5COC_2H_5 + (1 - x)c\text{-}C_6H_{12}$" at 298.15 K*, The Journal of Chemical Thermodynamics, **19 (2)**, 163-169

Orge B., Rodríguez A., Canosa J.M., Marino G., Iglesias M., Tojo J., 1999, *Variation of Densities, Refractive Indices, and Speeds of Sound with Temperature of Methanol or Ethanol with Hexane, Heptane, and Octane*, J. Chem. Eng. Data, 1999, **44 (5)**, 1041–1047

Ormanoudis C., Dakos C., Panayiotou C., 1991, *Volumetric properties of binary mixtures. 2. Mixtures of n-hexane with ethanol and 1-propanol*, Journal of Chemical Engineerign Data, **36 (1),** 39–42

Oswal S.L., Patel B.M., Patel A.M., Ghael N.Y., 2003, *Densities, speeds of sound, isentropic compressibilities, and refractive indices of binary mixtures of methyl methacrylate with hydrocarbons, haloalkanes and alkyl amines*, Fluid Phase Equilibria **206**, 313–329

Otpushchennikov N., Kiryakov B., Panin P., 1974, Izv. Vuz. Uchebn. Zaved, Neft Gaz **17**, 73 (In Russian).

Outcalt S., Laesecke A., Fortin T.J., 2010, *Density and speed of sound measurements of hexadecane*, The Journal of Chemical Thermodynamics, **42 (6**), 700-706

Pandey J.D., Sanguri V., Dwivedi D.K., Tiwari K.K., 2007, *Computation of isothermal compressibility, thermal expansivity and ultrasonic velocity of binary liquid mixtures using hole theory*, Journal of Molecular Liquids, **135**, 65–71

Papaioannou D., Ziakas D., Panayiotou C., 1991, *Volumetric properties of binary mixtures. 1. 2-Propanone + 2,2,4-trimethylpentane and n-heptane + ethanol mixtures*, Journal of Chemical Engineerign Data, **36 (1),** 35–39

Pedersen K.S., Fredenslund A, Christensen P.L., Thomassen P., 1984, *Viscosity of Crude Oil*, Chem. Eng. Sci. **39**, 1011-1016

Peneloux A., Rauzy E., Freze R., 1982, A *Consistent Correction for Redlich-Kwong-Soave Volumes,* Fluid Phase Equilibria, **8**, 7-27

Petrauskas A., 2008, Experimental determination of sound velocity in liquefied propane-butane gas mixture (LPG), ISSN 1392 - 2114 ULTRAGARSAS (ULTRASOUND), **63 (3)**, 42 – 46

Picard D.J., Bishnoi P.R., 1987, *Calculation of the thermodynamic sound velocity in two-phase multi-component fluids*, International Journal of Multiphase Flow, **13(3)**, 295-308

Piñeiro M.M., Mascato E., Mosteiro L., Legido J.L., 2003, Mixing Properties for the Ternary Mixture Methyl tert-Butyl Ether + 1-Butanol + Decane at 298.15 K, J. Chem. Eng. Data, **48 (4)**, 758–762

Plantier F., Bessières D., Daridon J.L., Montel F., 2008, *Structure and thermodynamic consistency of heavy oils: A study on the basis of acoustic measurements*, Fuel, **87 (2)**, 196-201

Plantier F., Danesh A., Sohrabi M., Daridon J.L., Gozalpour F., Todd A.C.2005, *Measurements of the Speed of Sound for Mixtures of Methane + Butane with a Particular Focus on the Critical State*, J. Chem. Eng. Data, **50 (2)**, 673–676

Plocker U., Knapp H., Prausnitz J., 1978, *Calculation of High-Pressure Vapor-Liquid Equilibria from a Corresponding-States Correlation with Emphasis on Asymmetric Mixtures*, Ind. Eng. Chem. Process Des. Dev., **17 (3),** 324–332

Queimada A.J., Coutinho J.A.P., Marrucho I.M., Daridon J.L., 2006, *Corresponding-States Modelling of the Speed of Sound of Long-Chain Hydrocarbons*, International Journal of Thermodynamics, **27(4)**, 1095-1109

Rai R.D., Shukla R.K., Shukla A.K., Pandey J.D., 1989, *Ultrasonic speeds and isentropic compressibilities of ternary liquid mixtures at (298.15±0.01) K*, The Journal of Chemical Thermodynamics, **21 (2)**, 125-129

Richardson E., Tait R., 1957, Philos. Mag. **2**, 441

Rowe A.M., Chou J.C.S., 1970, *Pressure – volume – temperature - concentration relation of aqueous NaCl solutions*: J. Chem. Eng. Data, **15**, 61-66

Sachdeva V.K., Nanda V.S., 1981, *Ultrasonic wave velocity in some normal paraffins*, The Journal of Chemical Physics, **75 (9)**, 4745-4746

Sastry N.V., Raj M.M., 1996, *Densities, Speeds of Sound, Viscosities, Dielectric Constants, and Refractive Indices for 1-Heptanol + Hexane and Heptane at 303.15, and 313.15 K*, Journal of Chemical Engineerign Data, **41**, 612-618

Savidge J.L., Starling K.B., MeFall R.L., 1988, *Sound Speed of Natural Gas*, SPE 18396

Shin M.S., Lee Y., Kim H., 2008, *Estimation of second-order derivative thermodynamic properties using the crossover cubic equation of state*, J. Chem. Thermodynamics, **40** , 688–694

Sperkach V.S., Cholpan P.F., Sinilo V.N., Zolotar A.V., 1979, *Propagation of Ultrasonic Waves in Isoviscous Solutions of n-Paraffins*, in Fizika zhidkogo sostoyaniya (Liquid State Physics), Kiev: Izd. KGU (KievState Univ.), **7**, 110

Spencer C.F., Danner R.P., 1972, *Improved Equation for Prediction of Saturated Liquid Density*, Journal of Chem. Eng. Data. **17**, 236 (1972)

Standing M.B., 1962, *Oil systems correlations*, in Frick T.C., Ed., Petroleum production handbook, volume II: McGraw-Hill Book Co., part 19

Straty G.C., 1974, *Velocity of sound in dense fluid methane*, Cryogenics, **14 (7)**, 367-370

Sun, T., Kortbeek P., Trappeniers N., Biswas S., 1987, Physics and Chemistry of Liquids, **16,** 163-178

Takagi T., 1978, Kagaku Kogaku Rombunshu **4** (1), 656 - 658 (In Japanese with abstract, references, tables, and figure titles in English)

Takagi T., 1978, Rev. Phys. Chem. Jpn. **48**, 17

Takagi T., Sakura T., Guedes H.J.R., 2002, *Speed of sound in liquid cyclic alkanes at temperatures between (283 and 343) K and pressures up to 20 MPa*, The Journal of Chemical Thermodynamics, **34 (12)**, 1943-1957

Takagi T., Sawada K., Urakawa H., Ueda M., Cibulka I., 2004, *Speed of sound in liquid tetrachloromethane and benzene at temperatures from 283.15 K to 333.15 K and pressures up to 30 MPa*, Journal of Chemical Thermodynamics, **36**, 659-664

Takagi T., Teranishi H., 1985, *Ultrasonic speeds and thermodynamics for binary solutions of n-alkanes under high pressures*, Fluid Phase Equilibria, **20**, 315-320

Takagi T., Teranishi H., 1987, *Ultrasonic speed in compressed liquid by a sing-around method*, The Journal of Chemical Thermodynamics, **19 (2)**, 1299-1304

Takagi T., Teranishi H., 1984, J. Soc. Mater. Sci. Jpn. **33**, 134 (In Japanese, with abstract, figures, and tables in English).

Takigawa T., Tamura K., 2000, Thermodynamic properties of (1,3 -dioxane, or 1,4-dioxane + a non-polar liquid) at T = 298.15 K; speed of sound, excess isentropic and isothermal compressibilities and excess isochoric heat capacity, The Journal of Chemical Thermodynamics, **32 (8)**, 1045-1055

Tamura K., Ohomuro K., Murakami S., 1983, Speeds of sound, isentropic and isothermal compressibilities, and isochoric heat capacities of {xc-C_6H_{12} + (1−x)C_6H_6}, x{CCl_4 + (1−x)C_6H_6}, and x{C_7H_{16} + (1−x)C_6H_6} at 298.15 K, The Journal of Chemical Thermodynamics, 15 (9), 859-868

Tardajos G., Diaz Peña M., Aicart E, 1986, *Speed of sound in pure liquids by a pulse-echo-overlap method*, The Journal of Chemical Thermodynamics, **18 (7)**, 683-689

Teja A.S., 1980, *A Corresponding States equation for saturated liquid densities. I. Applications to LNG,* AIChE Journal, **26(3)**, 337–341

Teja A.S., Sandler S.I., 1980, *A Corresponding States equation for saturated liquid densities. II. Applications to the calculation of swelling factors of CO_2-crude oil systems*, AIChE Journal, **26(3)**, 341–345

Thomas L.K., Hankinson R.W., Phillips K.A., 1970, *Determination of Acoustic Velocities for Nnatural gas*, Journal of Petroleum Technology, **22(7)**, 1970, 889 – 895

Trusler J. P. M., Zarari M.P., 1996, *The speed of sound in gaseous propane at temperatures between 225 K and 375 K and at pressures up to 0.8 MPa*, The Journal of Chemical Thermodynamics, **28 (3)**, 329-335

Trusler J.P.M. and Zarari M.P., 1995, *Second and third acoustic virial coefficients of methane at temperatures between 125 K and 375 K*, The Journal of Chemical Thermodynamics, **27 (7)**, 771-778

Trusler J.P.M., 1994, *The speed of sound in $(0.8CH_4 + 0.2C_2H_6)(g)$ at temperatures between 200 K and 375 K and amount-of-substance densities up to 5 mol·dm^{-3}*, The Journal of Chemical Thermodynamics, **26 (7)**, 751-763

Trusler J.P.M., Wakeham W.A., Zarari M.P., 1993, *The speed of sound in gaseous mixtures of methane and propane*, High Temperatures High Pressures, **25**, 291-296

Trusler J.P.M., Zarari M., 1992, *The speed of sound and derived thermodynamic properties of methane at temperatures between 275 K and 375 K and pressures up to 10 MPa*, The Journal of Chemical Thermodynamics, **24 (9)**, 973-991

Tsatsuryan Kh.D., 1994, *Experimental Sound Speed investigation in the system KOH-H_2O*, Vestnik IEI., **4**, 47-51 (in Russian)

Tsatsuryan Kh.D., 2001, *Speed of sound in water at high pressures*, XI Session of the Russian Acoustical Society, **60**

Tsumura R., Straty G.C., 1977, *Speed of sound in saturated and compressed fluid ethane*, Cryogenics, **17 (4),** 195-200

Van Itterbeek A., J. Theon A.C., Dael W.V., 1967, Physica **35**, 162

Vance S., Brown J.M., 2010, *Sound velocities and thermodynamic properties of water to 700 MPa and −10 to 100 °C,* Journal of Acoustical Society of America, **127 (1)**,174-180

Wang Z.W., 1988, *Wave velocities in hydrocarbons and hydrocarbon saturated rocks-with applications to EOR monitoring*: Ph.D. thesis, Stanford Univ

Wang Z., Nur A., Batzle M.L., 1988, *Acoustic velocities in petroleum oils*: Sot. Petr. Eng. (SPE) paper 18163, Proc. 63rd Sot. Petr. Eng. Tech. Conf., Formation Eval. Res. Geol. Section, 571-585

Wang Z., Nur A., 1991, *Ultrasonic velocities in pure hydrocarbons and mixtures*, Journal of the Acoustical Society of America, **89 (6)**, 2725-2730

Wang Z., Nur A., Stanford U., Batzle M., 1988, Soc. Petroleum Eng. SPE 18163, 571

Wilson W.D., 1959, *Speed of Sound in Distilled Water as a Function of Temperature and Pressure*, Journal of Acoustical Society of America, **31 (8)**, 1067-1072

Ye S., Lagourette B., Alliez J., Saint-Guirons H., Xans P., Montel F., 1992, *Comparison with experimental data of ultrasound velocity in pure hydrocarbons calculated from equations of state*, Fluid Phase Equilibria, **74**, 157-175

Ye S., Lagourette B., Alliez J., Saint-Guirons H., Xans P., ,Montel F., 1992, *Speed of sound in binary mixtures as a function of temperature and pressure*, Fluid Phase Equilibria, **74**, 177-202

Ye S., Alliez J., Lagourette B., Saint-Guirons H., Arman J., Xans P., 1990, *Réalisation d'un dispositif de mesure de la vitesse et de l'atténuation d'ondes ultrasonores dans des liquides sous pression* , Revue Phys. Appl. **25**, 555 – 565

Younglove B., 1981, J. Res. Natl. Bur. Stand. **86**, 165

Younglove B.A., McCarty R.D., 1980, *Speed-of-sound measurements for nitrogen gas at temperatures from 80 to 350 K and pressures to 1.5 MPa,* The Journal of Chemical Thermodynamics, **12 (12)**, 1121-1128

Żak A., Dzida M., Zorebski M., Ernst S., 2000, *A high pressure device for measurements of the speed of sound in liquid*s, Rev. Sci. Instrum. **71**, 1756 - 1765

Zevnik L., Babic M., Levec J., 2006, *Ultrasound Speed and absorption study in near-critical CO2: A sensor for high-pressure application*, The Journal of Supercritical Fluids, **36(3)**, 245 - 253

CHAPTER 3 – EXPERIMENTAL STUDY

3.1 Introduction

The velocity of sound and in general the characteristics of fluid responses to waves are indicators of the structure and state of the fluid. Hence, they can be related to other properties using thermodynamic concepts. Therefore, one could consider the technique as a general method of fluid property measurements with the added benefits of being non-destructive and far reaching.

Knowledge of the thermophysical properties of organic liquids is of great importance in various fields of science and technology. As the direct determination of properties such as density and heat capacity can be problematic at elevated pressures, an indirect technique therefore may have advantages.

In this work, the speed of sound was measured in pure hydrocarbons, binary mixtures and multi-component hydrocarbon fluids. The velocity of sound was also measured in fluid-saturated matrices, different fluids and matrices were used during these experiments. This chapter describes the equipments used for measurements of the speed of sound either in a fluid, or in a fluid-saturated matrix. The calibration method of the acoustic cell length and the detailed results of all experimental measurements will be also provided.

All of the experiments were conducted using two main set of equipments.

Two sets of measurements were undertaken:

- First, measurements were conducted in the PVT lab to study the acoustic properties of fluids.

This part, first looks at the speed of sound measurement apparatus and then discusses the calibration of the acoustic cell to provide the transit distance (L mm) travelled by the sound wave during the measurements. This value is needed to accurately calculate the speed of sound. In order to obtain a representative value for "L", the transit time has been calculated using various literature values for the speed of sound in our chosen reference fluid. Initially, *n*-hexane was selected as the reference fluid. After finding a

serious problem in the method of measurement, the oscilloscope and also the method of measurement were changed and the acoustic cell was re-calibrated. ‘Deionized pure water’ was chosen as the reference fluid in this stage.

This acoustic cell was used to measure the speed of sound in different hydrocarbon fluids which the results are described in Section 3.3.1.

- Secondly, the speed of sound was measured in a saturated reservoir matrix. The equipment in the Hydrate Lab in Heriot-Watt University was used for the measurement of speed of sound in saturated reservoir matrix.

In this part, the equipments which was used to measure the speed of sound in saturated reservoir matrix is described. A detailed description of the tests procedures and materials is outlined in Section 3.2.2. This equipment was used to measure the velocity of sound in two different matrices saturated with various fluids at different pressures and temperatures and the experimental results will be presented in Section 3.3.2.

3.2 Experimental Equipment and Procedures

3.2.1 PVT lab Equipment and Procedures

Some of experiments were conducted in the PVT laboratory at the Institute of Petroleum Engineering, Heriot-Watt University. In this lab, we were able to measure the speed of sound in a medium which contained only fluid.

3.2.1.1 Apparatus

The experimental apparatus used in this work is shown in Figure 3.1.

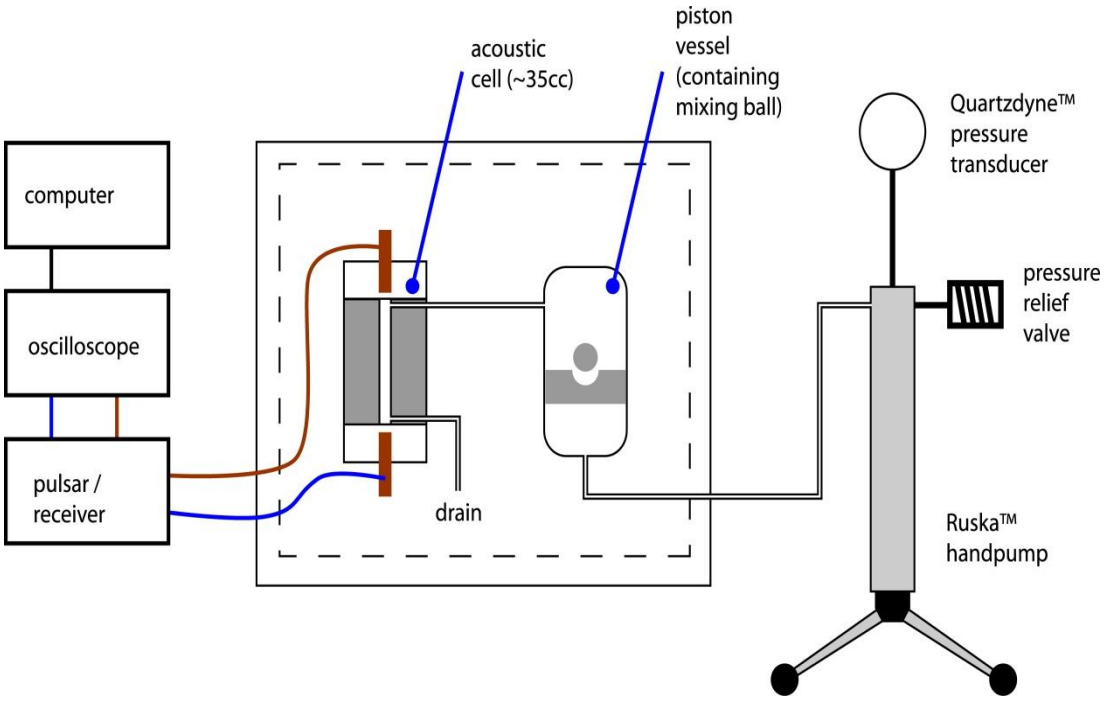

Figure 3.1 Schematic representation of the speed of sound measurement apparatus

The pressure of the sample fluid within the acoustic cell is applied by a single barrelled Ruska 100 ml mercury-free hand pump containing Conosol ® hydraulic fluid. The pump is first attached to a 300cc Proserv "Prolight Ti-690-30-MB" titanium piston vessel which normally contains the study fluid (which is separated from the hydraulic fluid by a sealed piston) and acts as a buffer between the pump and the acoustic cell (see Figure 3.1). This vessel contains a titanium mixing ball that allows the test sample to be thoroughly mixed by careful agitation of the vessel.

The high pressure acoustic cell and piston vessel are located within a Stuart Scientific HT oven which is controlled by a Eurotherm 91e temperature controller to ±1 °C. Additional temperature control and stability is achieved by the use of a large copper heating / cooling coil located within the oven and controlled via a Grant LTC heating /cooling bath which permits temperature control to ±0.1 °C. Temperature is measured using a high precision platinum resistance thermometer (PRT) supplied by SDL (Model T100-250-1D-NA) whose calibration is fully traceable to both UK NPL and USA NIST standard, with a measured maximum uncertainty of ±10 mK. Temperature is displayed on an ASL F250 MkII High Precision Thermometer with a measurement accuracy of ±0.001 °C.

Pressure is measured using a Quartzdyne (model DSB301-20-C85) high precision quartz transducer which is attached to the pump and which is calibrated to conform to internationally recognized standards to within 0.020% of full scale (F.S.) of the pressure standard used in calibration, which is accurate to within 0.01% of reading. This produces an overall accuracy of ±(0.020%F.S. + 0.01% of reading). The actual measured maximum calibration error is 0.0069%F.S.

The technique used to carry out measurements is based on a pulse transmission/reflection technique. Ultrasonic pulses to the transducers are produced using a Panametrics (Model 5077PR) ultrasonic pulsar-receiver which is fully calibrated using methods that conform to the requirements of ISO 9001 using NIST traceable, calibrated test equipment. An ultrasonic pulse passes through the fluid into the chamber and the two end caps of the acoustic cell and is received by the other transducer. The output signal from the acoustic cell is fed to a four channel digital storage oscilloscope (Tektronix, Model TDS 2024B) through 50 ohm co-axial cabling. The oscilloscope signal can also be displayed on a computer using National Instruments "SignalExpress™" software, with a measurement accuracy of ±1 microsecond (μs).

The apparatus used to measure the speed of sound consists primarily of a high pressure cell constructed of 316 stainless steel, which is referred to as the "acoustic cell". This cell was designed and manufactured "in house" by our engineers. (A schematic of the acoustic cell is shown in Figure 3.2). Imbedded within the two end caps of this cell are two piezoelectric ultrasound transducers (Panametrics V114) which have a circular cross section of 19mm and a resonant frequency of 1 MHz. The reason for using this frequency is to neglect the dispersion of the waves and also to compromise between lower

frequencies with lower precision and clearer signals, and higher frequencies with great precision and more attenuated signals. This frequency is within the domain which corresponds to the zero frequency regions for most hydrocarbons

The transducers are located within housing caps that are secured to each end of the acoustic cell. These caps are not subjected to internal pressure but are used as links between the transducers and the fluid sample.

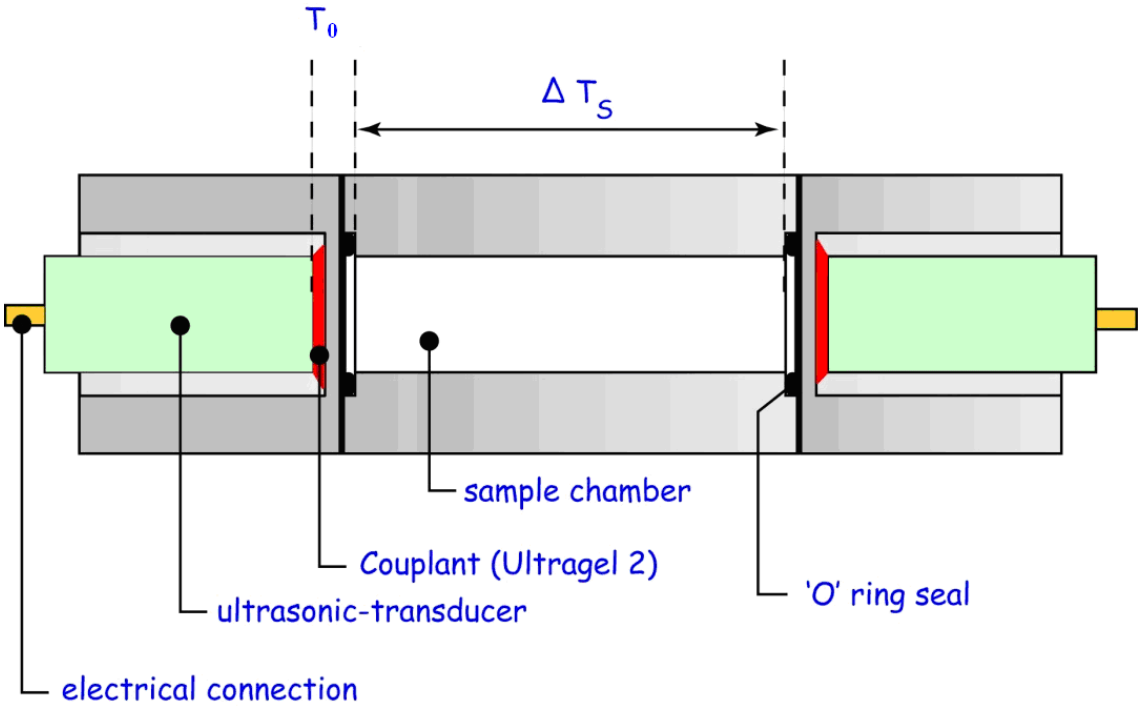

Figure 3.2 Schematic representation of the "Acoustic Cell"

To ensure perfect transmission and reception and also to reduce any attenuation phenomena, an ultrasound couplant (Ultragel II, industrial ultrasound couplant) is used at the interface between the transducers and the housing caps.

3.2.1.2 Calibration of Transit Distance (L mm)

The first measurement to be made is the determination of the travel time for a sound pulse from the transmitter through the metal of the acoustic cell cap. This measurement (T_0) is needed because this travel time has to be subtracted from the measured transit time to give the correct transit time of the sound pulse through the fluid (ΔT_S). So, The value of the end cap transit time (T_0) then has to be subtracted from the measured transit

time through a sample to eliminate the end-cap travel time from experimental readings and so leave the actual transit time (ΔT_S) through the sample.

Determination of the speed of sound is made by direct measurement of the transit times of ultrasound pulses by transmission and reflection within the cell containing the fluid sample.

In this way, it is possible to deduce the transit time (ΔT_S) through the sample and then to calculate the speed of sound (u) given by

$$u = \frac{L}{\Delta T_S} \tag{3.1}$$

where u is the speed of sound in meters per second, ($m.s^{-1}$), L is the transit distance in millimeter, (mm) and ΔT_S is the transit time in microseconds, (μs).

The travelling distance (L mm) for the wave is affected by the pressure and temperature of the system. Therefore it was essential to measure the value of '*L'* and this is achieved by calibrating the acoustic cell against a pure component with known speed of sound values at different temperature and pressure conditions and then simply rearranging Equation 3.1 so that,

$$L = u\Delta T \tag{3.2}$$

For this purpose, the acoustic cell was loaded with pure *n*-hexane (nC_6) supplied by Sigma-Aldrich (ReagentPlus® ≥99%) and the transit time measured at five temperatures (25.2, 30.0, 37.8, 45.0 and 60.0 ±0.1 °C) and ten pressures from 500 to 5000 ±0.5 psia. For the calibration, the cell was calibrated up to 60.0 °C which was considered to be the maximum temperature we could safely operate the transducers without risk of damage.

After several measurements, some deviations of experimental data form the modelling were observed. The procedure of measurement and calculation of the speed of sound using the apparatus in the lab were investigated and a serious problem was found. In earlier works, the measured transit time was considered as the average time of the difference between two sequent arrivals of waves and T_0 was considered as the first

complete waveform. The wrong procedure in calculation of speed of sound appointed us to buy a new simpler, but more accurate oscilloscope for measurement of the transit time.

It was necessary to re-calibrate the cell using deionized pure water (H_2O) in a repeat of the original calibration process. Water is commonly used as a reference fluid for the calibration of a variety of measuring devices including experimental apparatus for the measurement of the speed of sound in liquids.

Therefore, the acoustic cell was loaded with pure *water* (H_2O) and the transit time was measured at three temperatures (30.0, 45.0 and 60.0 ±0.1 °C) and ten pressures from 500 to 5000 ±0.5 psia. The actual measured transit times (ΔT_S) for pure water (H_2O) at the three temperatures and ten pressures are shown in Table 3.1. Values for ΔT_S are given to an accuracy of ±0.1 μs, pressure to ±0.5 psia and temperature to ±0.1 °C.

Table 3.1 Measured transit times Δt_s (microseconds, μs) in deionized pure water (H_2O) at 30.0, 45.0 and 60.0 °C

T (°C) ± 0.1	**30 °C**			**45 °C**			**60 °C**		
Pressure (psia) ±0.5	**T_1 (μs) ±0.1**	**T_2 (μs) ±0.1**	**T_0 (μs) ±0.1**	**T_1 (μs) ±0.1**	**T_2 (μs) ±0.1**	**T_0 (μs) ±0.1**	**T_1 (μs) ±0.1**	**T_2 (μs) ±0.1**	**T_0 (μs) ±0.1**
500	57.2	163.0	4.3	56.2	160.1	4.3	55.8	158.7	4.4
1000	57.0	162.4	4.3	56.1	159.5	4.3	55.6	158.1	4.4
1500	56.8	161.8	4.4	55.9	159.0	4.3	55.4	157.5	4.3
2000	56.6	161.2	4.3	55.7	158.4	4.3	55.2	156.9	4.3
2500	56.5	160.7	4.4	55.5	157.8	4.3	55.0	156.3	4.4
3000	56.2	160.1	4.3	55.3	157.2	4.3	54.8	155.7	4.3
3500	56.1	159.5	4.3	55.1	156.7	4.3	54.7	155.2	4.4
4000	55.9	159.0	4.4	54.9	156.2	4.3	54.5	154.7	4.4
4500	55.7	158.4	4.4	54.8	155.7	4.3	54.3	154.1	4.4
5000	55.5	157.9	4.3	54.6	155.1	4.4	54.1	153.6	4.3

T_1 = measured transit time of first wave arrival
T_2 = measured transit time of second wave arrival

$$T_0 = T_1 - \frac{T_2 - T_1}{2}$$

The measured transit times are used to calculate the transit distance (L mm) within the sample chamber of the acoustic cell, as shown in Table 3.2. In order to calculate this distance the speed of sound in the sample must be known. Therefore, the experimental data by Benedetto et.al.(2005) and Grosso and Mader (1972), and correlated data of

NIST were used to calculate the value of '*L'*. Accuracy of the literature data was generally around ±0.1%. To produce an acceptable value for the transit distance '*L'*, the average of the calculated '*L'* values based on the literature and correlated data at each temperature and pressure were used.

The transit distance 'L' and 'T_0' for all of measurements of speed of sound were considered as the average value of 80 mm and 4.3 μs, respectively.

First and second arrivals of wave travelling through pure deionized water are plotted in Figures 3.3 and 3.4. The cell length determined using the measurements of speed of sound in pure water is plotted in Figure 3.5 in different temperatures.

All the deviations are in the measurement error range. It should be around 0.01 μs for the travel time, and 0.01 mm for the distance. The fluctuations in the distance vs. pressure are in this range.

Table 3.2 Calculated, average transit distance (L mm) in pure water (H_2O) at 30.0, 45.0 and 60.0 °C

T (°C) ± 0.1	**30.0 °C**	**45.0 °C**	**60.0 °C**
P (psia) ±0.5	**L(mm) ±0.01**	**L(mm) ±0.01**	**L(mm) ±0.01**
500	80.10	80.12	80.10
1000	80.11	80.11	80.09
1500	80.09	80.13	80.16
2000	80.14	80.14	80.17
2500	80.13	80.12	80.14
3000	80.18	80.14	80.14
3500	80.16	80.20	80.16
4000	80.17	80.23	80.21
4500	80.16	80.23	80.21
5000	80.19	80.22	80.26

L (mm) – Calculated, average transit distance in the acoustic cell.

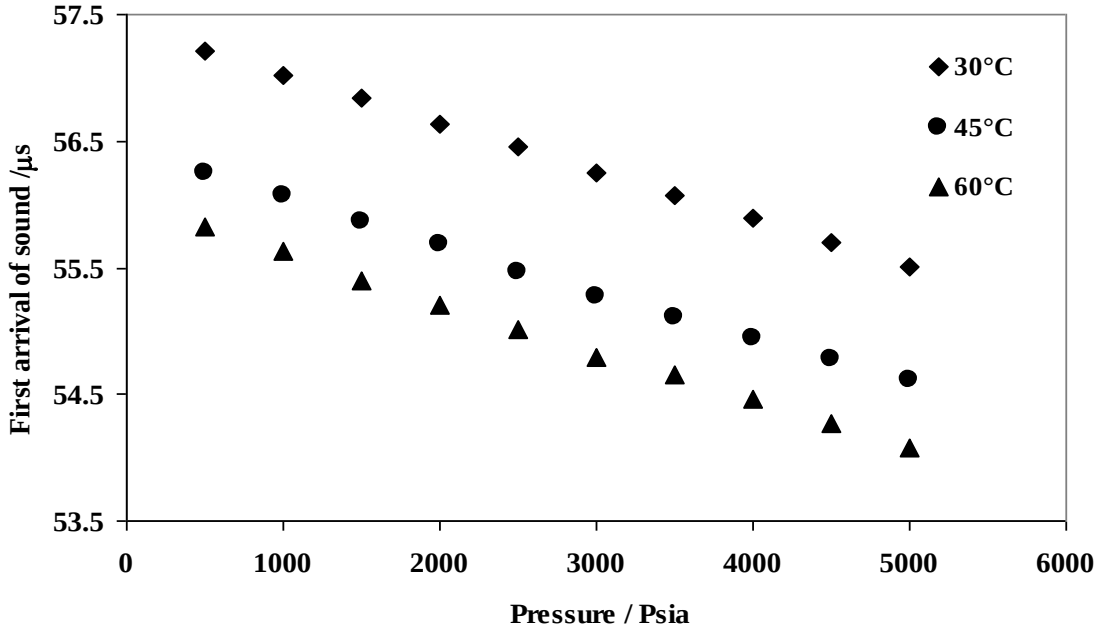

Figure 3.3 First arrival time (µsec) vs. pressure (psia) in pure deionized water (H_2O) at various temperatures

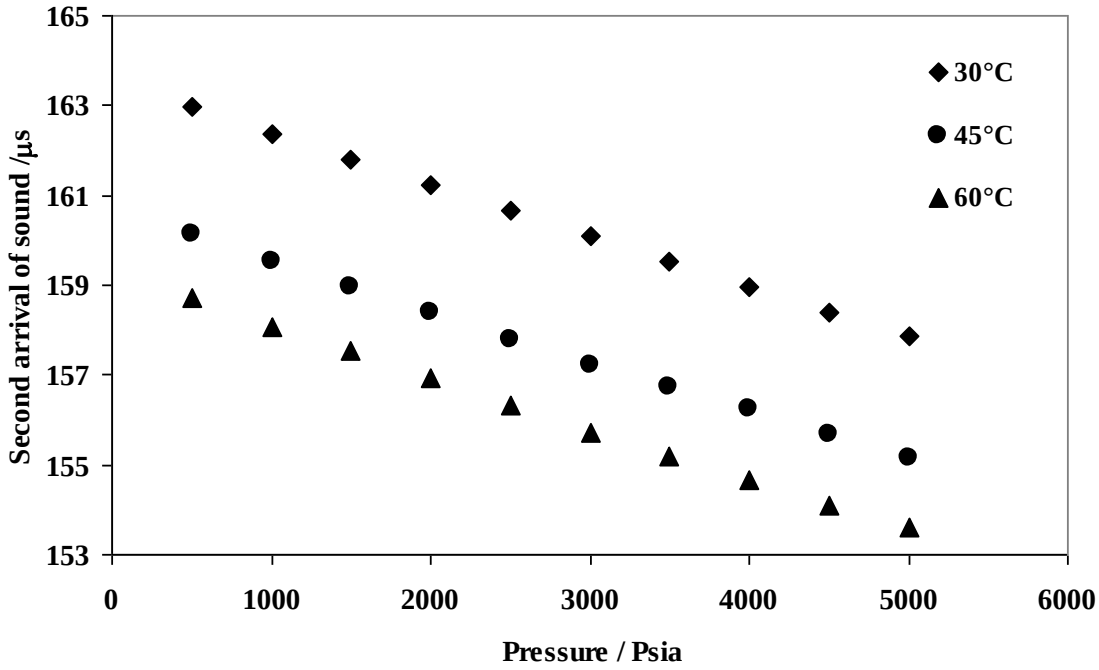

Figure 3.4 Second arrival times (µsec) vs. pressure (psia) in pure deionized water (H_2O) at various temperatures

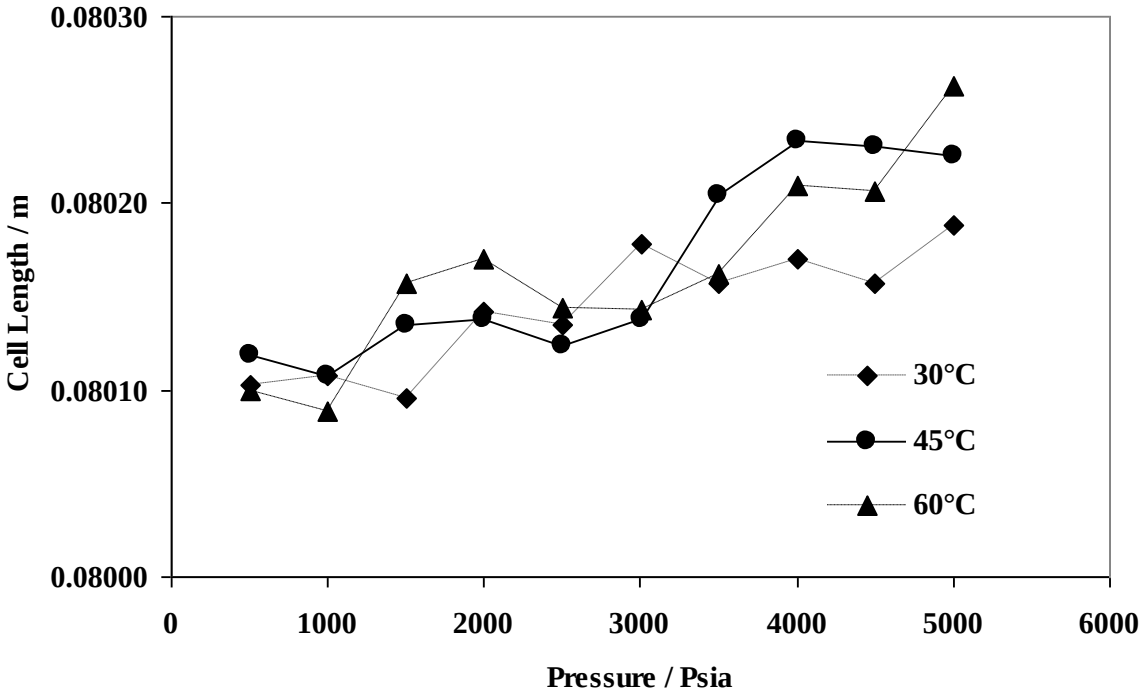

Figure 3.5 Cell Length (m) vs. pressure (psia) in pure deionized water (H_2O) at various temperatures

3.2.1.3 Materials

- Non-hydrocarbon materials
  - Deionized water (H_2O): specified minimum purity of 99.99%
  - Carbon Dioxide (CO_2): >99.995% purity Supplied by Air Products, has impurities of (O_2, H_2O, CO, THC as CH_4, N_2) < 50 ppm

- Hydrocarbon materials
  - Methane (C_1): 99.995% purity supplied by BOC
  - n-Butane (nC_4): >99.9% purity supplied by Aldrich
  - n-Pentane (nC_5): >99% purity supplied by BDH AnalaR™
  - n-Hexane (nC_6) : >99% purity supplied by Aldrich
  - n-Heptane (nC_7) : >99% purity supplied by Aldrich
  - n-Octane (nC_8) : >99% purity supplied by Aldrich
  - n-Nonane (nC_9) : >99% purity supplied by Aldrich
  - n-Decane (nC_{10}) : >99% purity supplied by Aldrich

3.2.1.4 Experimental Procedure

The acoustic cell is emptied, cleaned and evacuated prior to loading the sample fluid of interest. Samples are prepared in the piston vessel initially, both cells are positioned inside the oven and sample transferred into the acoustic cell by opening the connection between these two cells. (Mixtures were prepared gravimetrically by the addition of the components into an evacuated, weighed titanium pressure vessel. The molecular weights of each component used, together with the weight% and mole% compositions for all of prepared binary and multi-component mixtures are given in Section 3.3.1).

The sample is then allowed to reach temperature and pressure stability before starting to make the speed of sound measurements.

For measurements at temperatures lower than 4 °C, an alcohol should be added to water as antifreeze, in these experiments, ethanol was used.

3.2.2 Hydrate lab Equipments and Procedures

3.2.2.1 Apparatus

The experiments with a matrix were conducted using the ultrasonic set-up developed at the Institute's Centre for Gas Hydrate Research. Figure 3.6 shows a schematic of the ultrasonic set-up (Yang et al., 2005). It consists of a cylindrical cell, ultrasonic signal system, a LVDT (Linear Variable Differential Transformer), gas separator and backpressure regulator, Quizix pump and a personal computer. The test cell is 300 mm long with an inner diameter of 75 mm. The set-up can work up to 5800 psia and is surrounded by a cooling jacket connected to a temperature control bath (Cryostat). The cooling jacket is filled with a mixture of water and ethylene glycol as a coolant fluid. The temperature of the cooling jacket can be stabilized to within ± 0.05 °C. One end of the test cell is fitted with a movable piston that can change the cell volume and makes overburden/formation pressure adjustable. The LVDT is fixed to the rod tail of the movable piston to determine the displacement during depressurization and compression. The system pressure can be reduced or increased by withdrawing or injecting desired fluids at a certain rate using a dual-cylinder Quizix pump. The ultrasonic system includes two ultrasonic transducers (a pulsar and a receiver) and a digital storage oscilloscope for measuring the velocities of P-wave and S-wave through the fluid-

saturated sediment samples, as well as for attenuation, and frequency spectrum analysis of acoustic signals in unconsolidated sediments (Yang et al., 2004). A set of test data including pore pressure, overburden pressure, temperature, displacement of the piston, and ultrasonic waveforms, are acquired by the personal computer. The high pressure transducer measuring pore pressure is calibrated using a dead-weight-tester with an accuracy of ± 0.008 MPa in the range of 0 to 138 MPa. The thermal probe is a platinum resistance thermometer (PRT) which is calibrated using a PREMA Precision Thermometer 3040 over a range from 273.15 to 323.15 K. The deviation is within 0.1 K (Salehabadi, 2009). The PRT thermal probe is inserted inside the cell to measure the temperature of the system. All the measurements except for sonic data are logged using a LabView programme. The time interval of data logging is adjustable through the interface of the LabView programme (set to one minute in all experiments).

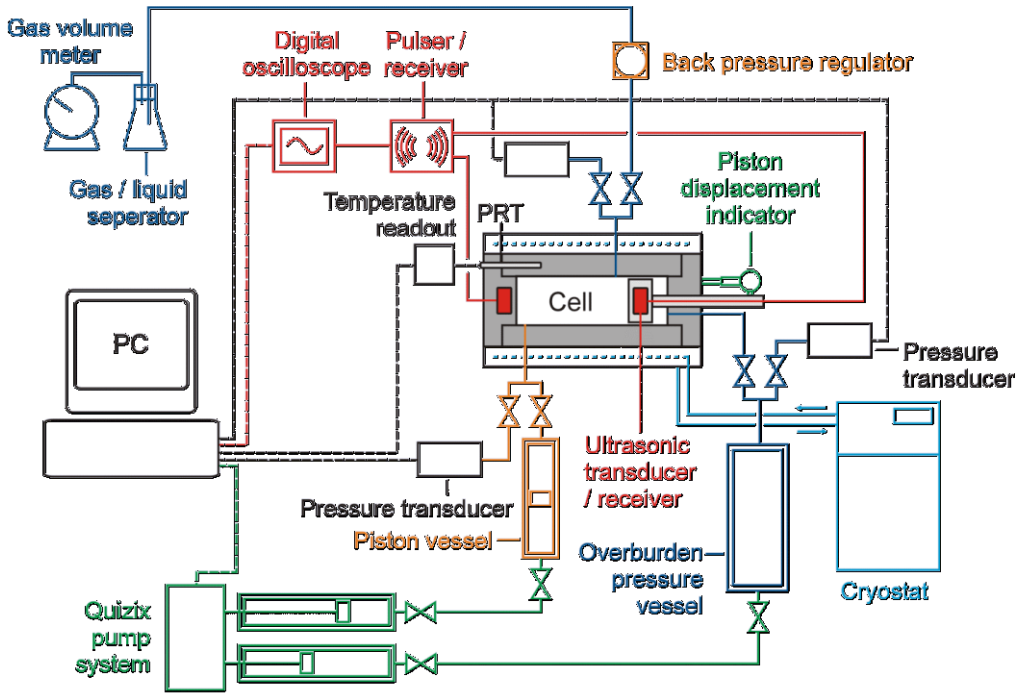

Figure 3.6 Schematic diagram of the ultrasonic set-up

3.2.2.2 Test Materials

- Sediments

  During this work, two different sediments were used:

  - Sand: the mean particle size of the silica sand was 259.68 μm.
  - Glass beads: the mean particle size of the glass beads was 0.1mm in diameter provided by Biospec products Cat. No. 11079101

- Fluids
  - $nC_6 + nC_{10}$
  - CO_2
  - $nC_4 + nC_{10} + CO_2$

  All of these fluids were in liquid state during the experiment. Pure CO_2 was kept in the lab under a pressure above 800 psia and was injected into the cylinder at pressure of 3000 psia. The measurements started from 0 °C to the upper temperatures to ensure the liquid state of CO_2. All the measurements were performed above the bubble point pressure for the last fluid.

3.2.2.3 Experimental Procedure

The acoustic cell was filled with dry sediments and then evacuated. The pore spaces between the sediment particles were then filled with nitrogen then compression was applied to the sediment at the overburden pressure prior to calculating the porosity of the porous media.

The nitrogen was then dumped and the system re-evacuated before loading the test fluid, which was injected at a constant rate of +0.1 ml/min until reaching the required pore pressure while keeping the effective pressure constant and changing the overburden pressure by the hand pump. The Quizix pumps were then used to maintain a constant pore pressure.

At each stage of the measurement, pressure and temperature should be stable for at least 20 minutes, before P-wave and S-wave velocities were measured with the following oscilloscope settings: Low-Pass filter, at the frequency of 500 KHz and +20 db gain for P-wave and Low-Pass filter at frequency of 100 KHz and +50 db gain for S-wave. Also,

cumulative volume of the Quizix pump was recorded for calculation of the density of the fluid inside the pores.

There was no problem associated with injection the fluid if it was liquid at atmospheric temperature and pressure conditions. Otherwise, the fluid should have been prepared either in at least 3 times of pore volume, injected into the cell and emptied from the back-pressure valve, or twice the pore spaces and injected into the cell and emptied in the cylinder 2 at the back-pressure, then the injection started for the second cycle from the cylinder 2 to the cell and continued these cycling for at least 3 times. During these cycling, the pore, effective and overburden pressures should have been kept constant. For maintaining the pressure constant at cylinder 2, it was connected to a Syringe HPLC pump.

The system pressure should be reduced either by withdrawing the fluid at constant rate of 0.5 ml/min using the Quizix pump at the end of each experiment or connecting a venting line to the cell and removing the gas inside the pores, if the fluid has been converted to two-phase.

3.3 Experimental Results

3.3.1 PVT Lab Experimental Results

3.3.1.1 Speed of sound in n-Pentane

Measurements of speed of sound in n-Pentane were performed at different temperatures and pressures and the corrected measured speed of sound (*u, m.s^{-1})* in *n*-pentane (nC_5) at five temperatures (25.2, 30.0, 37.8, 45.0 and 60.0 ±0.1 °C) is given in Table 3.3, and shown graphically in Figure 3.7.

The measured values (which have a calculated accuracy of ±0.07%) are also compared against extrapolated literature data (Ding *et al*. 1997 and Lainez *et al*. 1990). Our measured values for speed of sound data (*u,* in m.s^{-1}) show a generally good agreement with the literature data but are in better agreement with the data of Lainez *et al*. 1990. Differences are generally around ±0.1 to ±0.2% from the measured values with a maximum difference of -0.6% with Ding *et al*. 1997 data and 0.4% with Lainez *et al*. 1990 data (Table 3.4).

Table 3.3 Measured speed of sound (u, $m.s^{-1}$) in n-pentane in different temperatures

Temperature (°C) ±0.1	**25.2**	**30.0**	**37.8**	**45.0**	**60.0**
Pressure (psia) ±0.5	**Measured Velocity ±0.08%**				
500	1038.0	1014.3	975.2	942.2	873.8
1000	1066.5	1044.5	1008.9	976.6	912.9
1500	1096.5	1073.3	1038.2	1008.7	947.1
2000	1121.4	1101.6	1068.1	1039.0	977.5
2500	1147.7	1128.2	1096.8	1067.8	1007.2
3000	1173.4	1154.2	1123.9	1096.1	1036.6
3500	1196.0	1178.0	1146.7	1120.5	1063.1
4000	1220.4	1199.7	1170.0	1142.9	1087.8
4500	1240.9	1222.3	1193.9	1167.6	1112.9
5000	1260.1	1242.7	1214.9	1190.4	1136.6

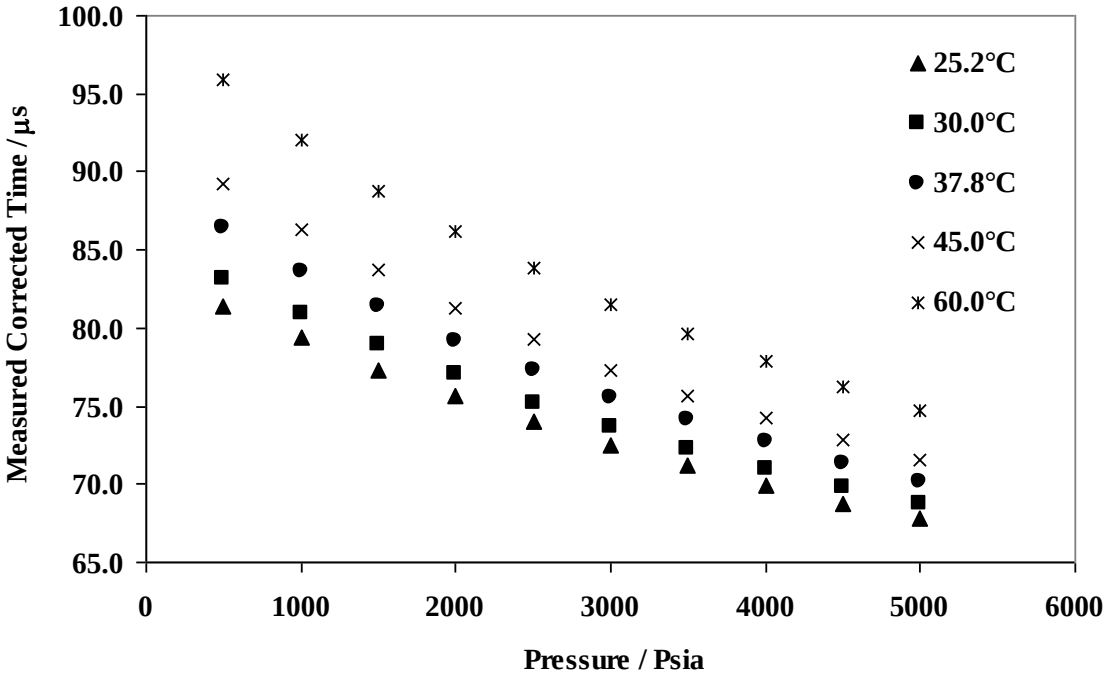

Figure 3.7 Transit time vs. pressure for n-pentane at various temperatures

To check the reliability and repeatability of the experimental measurements the fluid was removed from the acoustic cell and the cell cleaned before a fresh sample of *n*-pentane was re-loaded to the cell. The experimental measurements were then repeated at the same temperatures and pressures. In all cases the re-measured transit times (ΔT_S) were found to be the same as in the previous test (within the experimental error of ±0.1 µs). This result gave us confidence in both our measurement technique and in the repeatability of measured data points.

Table 3.4 Percentage deviations of measured speed of sound of n-pentane from literature data in various Temperatures

P (psia)	Average Deviation from Literatures [1]					[2]				
±0.5	25.2 °C	30.0 °C	37.8 °C	45.0 °C	60.0 °C	25.2 °C	30.0 °C	37.8 °C	45.0 °C	60.0 °C
500	dna*	dna*	dna*	dna*	dna*	0.2	0.1	-0.2	-0.1	dna*
1000	-0.3	-0.4	-0.5	-0.5	-0.4	0.0	0.0	-0.1	-0.2	-0.1
1500	-0.2	-0.4	-0.6	-0.6	-0.5	0.2	0.0	-0.2	-0.1	-0.1
2000	-0.3	-0.3	-0.4	-0.4	-0.6	0.0	0.1	0.0	0.0	-0.3
2500	-0.3	-0.3	-0.3	-0.4	-0.6	0.1	0.1	0.0	0.0	-0.4
3000	-0.2	-0.2	-0.2	-0.2	-0.5	0.2	0.2	0.2	0.1	-0.3
3500	-0.2	-0.2	-0.3	-0.3	-0.5	0.1	0.2	0.0	0.1	-0.3
4000	-0.1	-0.3	-0.3	-0.4	-0.6	0.2	0.0	0.0	0.0	-0.2
4500	-0.1	-0.2	-0.2	-0.3	-0.5	0.2	0.1	0.1	0.0	-0.2
5000	-0.3	-0.3	-0.3	-0.2	-0.5	0.0	0.0	0.1	0.1	-0.3

[1] Ding et al 1997, [2] Lainez et al 1990, dna - data not available*

$$\textit{Average deviation between runs} = \frac{\Delta u_{\exp} - \Delta u_{lit}}{\Delta u_{\exp}} * 100$$

3.3.1.2 Speed of sound in n-Hexane

The calculated speed of sound in n-Hexane (nC_6) at five temperatures (25.2, 30.0, 37.8, 45.0 and 60.0 ±0.1 °C) are given in Table 3.5.

Table 3.5 Measured speed of sound (u, $m.s^{-1}$) in n-hexane in different temperatures

Temperature (°C) ±0.1	25.2 °C	30.0 °C	37.8 °C	45.0 °C	60.0 °C
Pressure (psia) ±0.5	Measured Velocity ±0.08%				
500	1105.5	1082.5	1048.5	1017.6	953.4
1000	1131.4	1109.2	1076.3	1046.5	988.1
1500	1156.7	1135.2	1103.7	1074.6	1017.8
2000	1181.0	1160.0	1129.4	1101.4	1045.4
2500	1204.6	1184.2	1154.7	1127.4	1072.2
3000	1227.2	1207.3	1178.5	1152.1	1097.9
3500	1248.1	1228.5	1200.9	1174.8	1122.1
4000	1268.5	1249.3	1221.8	1196.8	1145.5
4500	1288.6	1269.7	1242.9	1218.2	1168.2
5000	1308.2	1289.6	1263.7	1239.1	1189.9

Table 3.6 Percentage deviations of measured speed of sound of n-hexane from literature data in various Temperatures

Pressure (psia) ±0.5			**[1]**					**[2]**		
	25.2	**30.0**	**37.8**	**45.0**	**60.0**	**25.2**	**30.0**	**37.8**	**45.0**	**60.0**
500	0.2	0.0	0.0	0.0	-	-0.3	-0.4	-0.4	-0.3	-
1000	0.0	-0.1	-0.1	-0.1	-	-0.1	-0.3	-0.3	-0.2	0.2
1500	0.0	-0.2	-0.1	-0.2	-	-0.1	-0.2	-0.2	-0.1	0.1
2000	0.0	-0.2	-0.2	-0.2	-	0.0	0.1	-0.1	0.0	0.0
2500	0.0	-0.1	-0.1	-0.1	-	0.1	0.0	0.0	0.0	0.0
3000	0.0	-0.1	-0.1	-0.1	-	0.2	0.0	0.0	0.1	0.0
3500	0.0	-0.2	-0.1	-0.1	-	0.2	0.0	0.0	0.1	0.0
4000	0.0	-0.2	-0.1	-0.1	-	0.2	0.0	0.0	0.0	0.0
4500	0.0	-0.1	-0.1	-0.1	-	0.2	0.0	0.0	0.0	0.0
5000	0.0	-0.1	0.0	-0.1	-	0.2	0.0	0.1	0.0	0.0
			[3]					**[4]**		
	25.2	**30.0**	**37.8**	**45.0**	**60.0**	**25.2**	**30.0**	**37.8**	**45.0**	**60.0**
500	0.1	0.0	0.0	0.0	-	0.3	0.5	0.4	0.4	-
1000	0.0	-0.1	-0.1	-0.1	-0.2	0.3	0.5	0.5	0.5	-
1500	0.0	-0.1	-0.1	-0.2	-0.1	0.3	0.5	0.5	0.4	-
2000	0.0	-0.1	-0.1	-0.1	0.0	0.2	0.4	0.3	0.3	-
2500	0.1	0.0	0.0	0.0	0.0	0.1	0.2	0.2	0.1	-
3000	0.1	0.0	0.0	0.0	0.0	0.0	0.1	0.0	0.0	-
3500	0.0	-0.1	0.0	0.0	0.0	0.1	0.2	0.2	0.1	-
4000	0.0	-0.1	-0.1	0.0	0.0	0.1	0.2	0.1	0.1	-
4500	0.0	-0.1	-0.1	-0.1	0.0	0.1	0.2	0.1	0.1	-
5000	0.0	-0.1	0.0	0.0	0.0	0.0	0.1	0.1	0.1	-

[1] Plantier 2005, [2] Ball et al 2000, [3] Daridon et al 1997, [4] Khasanshin et al 2001

The measured values (which have a calculated accuracy of ±0.08%) are also compared against extrapolated literature data (Plantier 2005, Ball *et al* 2000, Daridon *et al* 1998 and Khasanshin *et al* 2001). The measured values for speed of sound are in a good agreement with the literature data with differences of around ±0.1% from the measured values. The maximum difference of -0.4% is seen in the data of Ball *et al* 2000 and 0.5% in the data of Khasanshin *et al* 2001 at lower pressures. The literature data are generally in better agreement with the measured data at higher pressures (above 1500 psia) (Table 3.6).

3.3.1.3 Speed of sound in binary mixtures of n-Pentane and n-Hexane

A series of binary mixtures of *n*-pentane (nC_5) (Spectrophotometric Grade ≥99%) and *n*-hexane (nC_6) (Reagent Plus® ≥99%) were prepared and studied as the first step in this experimental program. The mixtures were prepared gravimetrically by the addition of the components into an evacuated, weighed titanium pressure vessel. The molecular weights of each component used, together with the mole% compositions for the three prepared binary mixtures are given in Table 3.7.

Table 3.7 Compositions of three n-pentane (nC_5) and n-hexane (nC_6) Binaries

	Molecular weight		**Density**		**Moles**		**Mole%**	
	nC_5	**nC_6**	**nC_5**	**nC_6**	**nC_5**	**nC_6**	**nC_5**	**nC_6**
Composition 1	72.15	86.18	0.626	0.659	0.36	0.36	50.19	49.81
Composition 2	72.15	86.18	0.626	0.659	0.63	0.16	79.97	20.03
Composition 3	72.15	86.18	0.626	0.659	0.14	0.57	20.22	79.78

The measured speeds of sound in the three binary mixtures given in Table 3.7, at four temperatures and various pressures, are given in Tables 3.8 – 3.11.

Table 3.8 Measured speed of sound (u $m.s^{-1}$) in various binary mixtures of n-pentane (nC_5) and n-hexane (nC_6) at 30.0 °C

Composition Mole %	**100.00% *n*C_5**	**79.97% *n*C_5**	**50.19% *n*C_5**	**20.22% *n*C_5**	**0 % *n*C_5 (100%*n*C_6)**
Pressure (psia) ±0.5	**Measured *u* ($m.s^{-1}$) ±0.08%**				
500	1014.3	1029.8	1054.1	1071.1	1082.5
1000	1044.5	1059.5	1083.0	1098.7	1109.2
1500	1073.3	1087.7	1110.1	1125.8	1135.2
2000	1101.6	1115.2	1136.3	1151.1	1160.0
2500	1128.2	1140.8	1162.1	1175.7	1184.2
3000	1154.2	1165.6	1186.1	1198.5	1207.3
3500	1178.0	1188.1	1207.5	1220.4	1228.5
4000	1199.7	1210.2	1229.5	1241.8	1249.3
4500	1222.3	1231.3	1250.2	1262.0	1269.7
5000	1242.7	1252.0	1269.5	1281.7	1289.6

Table 3.9 Measured speed of sound (u m.s^{-1}) in various binary mixtures of n-pentane (nC_5) and n-hexane (nC_6) at 37.8 °C

Composition Mole %	**100.00% *n*C$_5$**	**79.97% *n*C$_5$**	**50.19% *n*C$_5$**	**20.22% *n*C$_5$**	**0 % *n*C$_5$ (100%*n*C$_6$)**
Pressure (psia) ±0.5	**Measured *u* (m.s^{-1}) ±0.08%**				
500	975.2	992.6	1019.2	1035.0	1048.5
1000	1008.9	1024.8	1049.6	1065.0	1076.3
1500	1038.2	1053.0	1077.0	1091.8	1103.7
2000	1068.1	1082.4	1104.6	1118.5	1129.4
2500	1096.8	1109.4	1131.2	1144.1	1154.7
3000	1123.9	1134.7	1155.8	1169.3	1178.5
3500	1146.7	1157.9	1178.2	1190.4	1200.9
4000	1170.0	1181.8	1200.1	1211.9	1221.8
4500	1193.9	1204.3	1222.3	1234.6	1242.9
5000	1214.9	1225.6	1242.4	1254.1	1263.7

Table 3.10 Measured speed of sound (u m.s^{-1}) in various binary mixtures of n-pentane (nC_5) and n-hexane (nC_6) at 45.0 °C

Composition Mole %	**100.00% *n*C$_5$**	**79.97% *n*C$_5$**	**50.19% *n*C$_5$**	**20.22% *n*C$_5$**	**0 % *n*C$_5$ (100%*n*C$_6$)**
Pressure (psia) ±0.5	**Measured *u* (m.s^{-1}) ±0.08%**				
500	942.2	959.0	986.2	1003.6	1017.6
1000	976.6	993.4	1018.6	1034.5	1046.5
1500	1008.7	1023.9	1048.0	1063.3	1074.6
2000	1039.0	1052.4	1076.4	1089.6	1101.4
2500	1067.8	1082.0	1102.7	1118.1	1127.4
3000	1096.1	1107.9	1128.8	1142.5	1152.1
3500	1120.5	1132.8	1152.2	1165.6	1174.8
4000	1142.9	1154.9	1174.1	1187.2	1196.8
4500	1167.6	1179.3	1197.5	1209.3	1218.2
5000	1190.4	1200.7	1218.7	1229.9	1239.1

Table 3.11 Measured speed of sound (u m.s^{-1}) in various binary mixtures of n-pentane (nC_5) and n-hexane (nC_6) at 60.0 °C

Composition Mole %	**100.00% nC_5**	**79.97% nC_5**	**50.19% nC_5**	**20.22% nC_5**	**0 % nC_5 (100%nC_6)**
Pressure (psia) ±0.5	**Measured *u* (m.s^{-1}) ±0.08%**				
500	873.8	893.4	921.6	939.0	953.4
1000	912.9	930.2	956.9	974.4	988.1
1500	947.1	964.1	989.0	1005.2	1017.8
2000	977.5	993.7	1017.6	1032.7	1045.4
2500	1007.2	1022.4	1045.7	1060.3	1072.2
3000	1036.6	1051.3	1073.0	1086.8	1097.9
3500	1063.1	1077.1	1097.6	1111.4	1122.1
4000	1087.8	1101.7	1121.6	1134.3	1145.5
4500	1112.9	1125.9	1145.0	1158.3	1168.2
5000	1136.6	1150.2	1168.4	1180.4	1189.9

Table 3.12 Comparison of measured and NIST correlated speed of sound in binary mixtures of 79.97 % nC_5 and 20.03 % nC_6 at different temperatures

Pressure	**30.0 °C**		**37.8 °C**		**45.0 °C**		**60.0 °C**	
(psia)±0.5	**NIST *u***	**%Dif**	**NIST *u***	**%Dif**	**NIST *u***	**%Dif**	**NIST *u***	**%Dif**
500	1026.7	0.3	992.0	0.1	960.1	-0.1	894.0	-0.1
1000	1056.4	0.3	1023.0	0.2	992.5	0.1	929.6	0.1
1500	1084.4	0.3	1052.2	0.1	1022.8	0.1	962.5	0.2
2000	1111.0	0.4	1079.8	0.2	1051.4	0.1	993.3	0.0
2500	1136.4	0.4	1106.1	0.3	1078.5	0.3	1022.4	0.0
3000	1160.7	0.4	1131.2	0.3	1104.4	0.3	1049.8	0.1
3500	1184.0	0.3	1155.2	0.2	1129.0	0.3	1076.0	0.1
4000	1206.5	0.3	1178.3	0.3	1152.7	0.2	1100.9	0.1
4500	1228.1	0.3	1200.5	0.3	1175.5	0.3	1124.9	0.1
5000	1249.1	0.2	1222.0	0.3	1197.4	0.3	1147.9	0.2

Table 3.13 Comparison of measured and NIST correlated speed of sound in binary mixtures of 50.19 % nC_5 and 49.81 % nC_6 at different temperatures

Pressure	**30.0 °C**		**37.8 °C**		**45.0 °C**		**60.0 °C**	
(psia)±0.5	**NIST *u***	**%Dif**	**NIST *u***	**%Dif**	**NIST *u***	**%Dif**	**NIST *u***	**%Dif**
500	1040.7	1.3	1007.2	1.2	976.6	1.0	913.2	0.9
1000	1069.2	1.3	1036.9	1.2	1007.5	1.1	946.9	1.0
1500	1096.2	1.3	1065.0	1.1	1036.6	1.1	978.4	1.1
2000	1121.9	1.3	1091.7	1.2	1064.1	1.1	1007.9	1.0
2500	1146.5	1.3	1117.1	1.2	1090.3	1.1	1035.8	0.9
3000	1170.1	1.4	1141.4	1.2	1115.3	1.2	1062.3	1.0
3500	1192.8	1.2	1164.7	1.1	1139.3	1.1	1087.6	0.9
4000	1214.7	1.2	1187.2	1.1	1162.3	1.0	1111.8	0.9
4500	1235.9	1.1	1208.9	1.1	1184.5	1.1	1135.1	0.9
5000	1256.4	1.0	1229.9	1.0	1205.9	1.0	1157.4	0.9

Table 3.14 Comparison of measured and NIST correlated speed of sound in binary mixtures of 20.22 % nC_5 and 79.78 % nC_6 at different temperatures

Pressure	30.0 °C		37.8 °C		45.0 °C		60.0 °C	
(psia)±0.5	NIST *u*	%Dif	NIST *u*	%Dif	NIST *u*	%Dif	NIST *u*	%Dif
500	1053.6	1.6	1021.1	1.3	991.4	1.2	930.1	0.9
1000	1081.1	1.6	1049.8	1.4	1021.1	1.3	962.4	1.2
1500	1107.3	1.6	1076.9	1.4	1049.2	1.3	992.6	1.3
2000	1132.4	1.6	1102.8	1.4	1075.9	1.3	1021.1	1.1
2500	1156.3	1.7	1127.5	1.5	1101.3	1.5	1048.1	1.1
3000	1179.4	1.6	1151.2	1.5	1125.6	1.5	1073.8	1.2
3500	1201.6	1.5	1174.0	1.4	1149.0	1.4	1098.4	1.2
4000	1223.0	1.5	1196.0	1.3	1171.5	1.3	1122.0	1.1
4500	1243.8	1.4	1217.2	1.4	1193.2	1.3	1144.7	1.2
5000	1263.9	1.4	1237.8	1.3	1214.2	1.3	1166.6	1.2

As no literature data was available for this set of binary mixtures the experimental results were compared against values obtained from a commercially available programme from NIST called "REFPROP, Reference Fluid Thermodynamic and Transport Properties". The results of these comparisons are given in Tables 3.12 – 3.14.

Comparisons between our measured and the NIST predicted speed of sound values as shown in Tables 3.12 – 3.14 are generally good with a spread of differences ranging from -0.1 to +1.7%.

3.3.1.4 Speed of Sound in Multi-Component Mixtures of Methane, n-Pentane, n-Hexane

A volatile mixture of Methane, *n*-Pentane (nC_5) and *n*-Hexane (nC_6) was prepared and studied. The weights of each component which was used, with the mole% of the prepared mixture are given in Table 3.15.

Table 3.15 Compositions of methane, n-pentane (nC_5) and n-hexane (nC_6) in the mixture

Compound	Molecular weight	Weight /Grams	Moles	Mole%
Methane	16.03	2.008	0.12	21.25
nC_5	72.15	16.652	0.23	39.14
nC_6	86.18	20.128	0.23	39.61

The measured transit time and speeds of sound in this mixture at three temperatures and various pressures (above bubble pressure), are given in Table 3.16 and also plotted against pressure in Figure 3.8.

Table 3.16 Measured transit time and speed of sound (u m.s^{-1}) in volatile mixture of methane, n-pentane (nC_5) and n-hexane (nC_6) at 30.0 °C, 45.0 °C and 60.0 °C

T (°C)±0.1	30.0 °C		45.0 °C		60.0 °C	
Pressure (psia)±0.5	T_1 (µs) ±0.1	Meas. u (m/s)	T_1 (µs) ±0.1	Meas. u (m/s)	T_1 (µs) ±0.1	Meas. u (m/s)
1000	85.3	987.96	91.4	918.54	98.3	851.24
1500	82.8	1020.15	88.2	954.20	94.3	889.73
2000	80.5	1050.28	85.4	987.35	90.8	925.55
2500	78.5	1078.97	82.9	1018.27	87.8	958.54
3000	76.7	1105.89	80.7	1047.33	85.3	988.69
3500	75.1	1131.38	78.8	1074.19	82.9	1017.81
4000	73.6	1155.82	77.1	1099.81	80.9	1044.93
4500	72.2	1179.07	75.5	1124.54	79.0	1071.17
5000	70.9	1201.20	74.0	1148.02	77.3	1096.42
1000	85.3	987.96	91.4	918.54	98.3	851.24

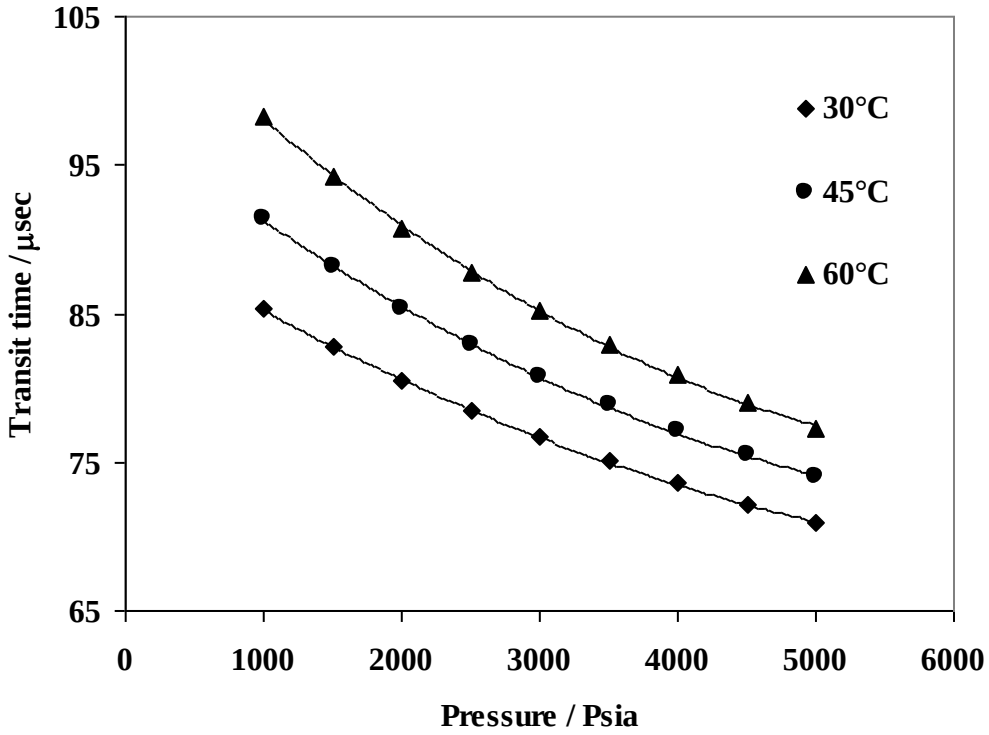

Figure 3.8 Measured transit time (µsec) vs. pressure (psia) in volatile mixture of methane, n-pentane (nC_5) and n-hexane (nC_6) at various temperatures

- **Measurement of GOR and density of live oil**

The speed of sound of this synthetic live oil was measured above the bubble point. The measurements were done at pressures above 1000 psia and in 500 psia pressure increments. After the test, the Gas Oil Ratio (GOR) of the volatile oil was measured and is given in Table 3.17. Density of dead oil was also determined using AntonPaar Densitometer and is 0.6275 gr/cm^3.

Table 3.17 GOR of the volatile oil

Gas Volume cc	Oil Weight gr	Oil Density g/cc	Oil Volume cc	atm. Pressure mmHg	Lab Temperature °C	GOR cc/cc	GOR ft^3/barrel
185	2.1534	0.6275	3.432	756	21.3	53	295

The density of the oil was determined before in this calculation and gas and liquid volume are the amount of liquid and gas which was accumulated.

$$\text{Oil Volume} = \text{Oil Weight} / \text{Oil Density} \tag{3.8}$$

$$\text{GOR (cc/cc)} = \left(\frac{Gas Volume(cc)}{Oil Volume(cc)}\right)\left(\frac{Atm.Pres}{760}\right)\left(\frac{288.65}{273.15 + Lab\ Temperature}\right) \tag{3.9}$$

$$\text{GOR } (ft^3/\text{barrel}) = \text{GOR(cc/cc)} * 5.615 \tag{3.10}$$

3.3.1.5 Speed of sound in binary mixture of n-Hexane and n-Decane

A mixture of *n*-Hexane (nC_6) and n-Decane (nC_{10}) was prepared and studied. The weights of each component which were used, with the mole% of the prepared mixture are listed in Table 3.18.

Table 3.18 Compositions of n-hexane (nC_6) and n-decane (nC_{10}) binary mixture

Compound	Density g/cm^3	Molecular weight	Weight grams	Moles	Mole%	Volume cm^3
nC_6	0.66	86.18	110.20	1.28	50.04	167.22
nC_{10}	0.73	142.28	181.70	1.28	49.96	248.90

The measured transit time and speeds of sound in this mixture at three temperatures and various pressures are given in Table 3.19 and also plotted against pressure in Figure 3.9.

Table 3.19 Measured transit time and speed of sound (u $m.s^{-1}$) in binary mixture of n-hexane (nC_6) and n-decane (nC_{10}) at 30.0 °C, 45.0 °C and 60.0 °C

T (°C)±0.1	30.0 °C		45.0 °C		60.0 °C	
Pressure (psia)±0.5	T_1 (µs) ±0.1	Meas. u (m/s)	T_1 (µs) ±0.1	Meas. u (m/s)	T_1 (µs) ±0.1	Meas. u (m/s)
500	72.6	1172.76	76.2	1113.18	80.2	1054.46
1000	71.2	1196.44	74.6	1137.98	78.4	1080.64
1500	70.0	1218.58	73.2	1161.91	76.7	1106.32
2000	68.9	1240.21	71.9	1184.83	75.1	1130.93
2500	67.8	1261.23	70.6	1207.07	73.6	1154.67
3000	66.8	1281.95	69.5	1228.77	72.3	1177.27
3500	65.9	1300.71	68.4	1249.14	71.1	1198.36
4000	65.0	1319.87	67.4	1269.12	69.9	1219.66
4500	64.1	1338.58	66.5	1288.04	68.9	1239.54
5000	63.3	1356.07	65.6	1306.76	67.9	1259.33

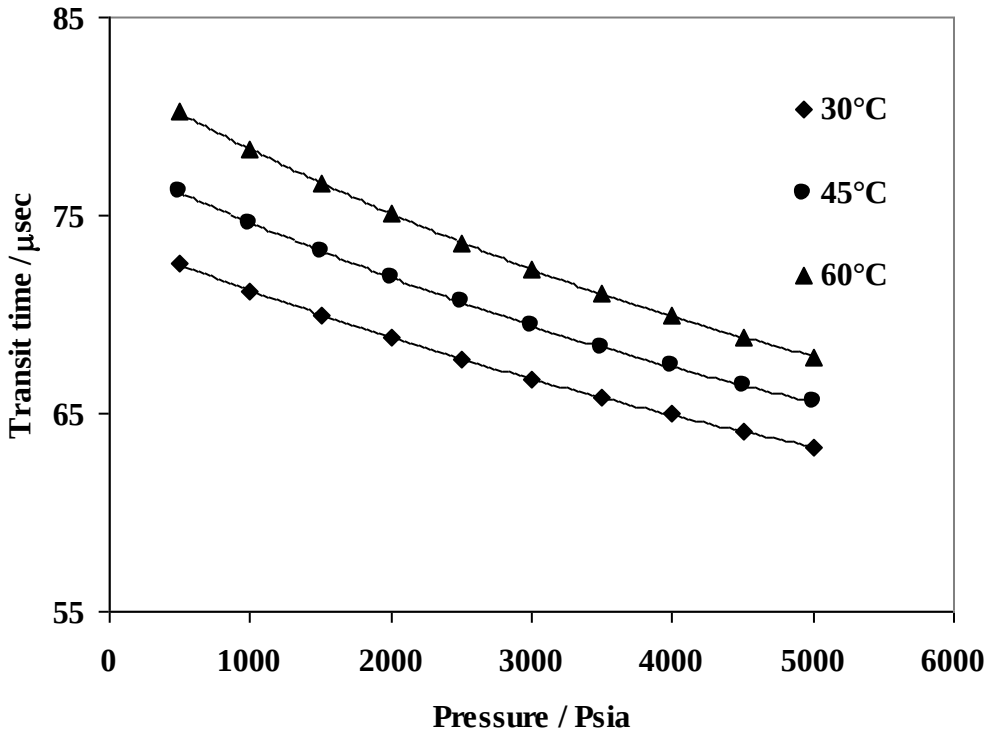

Figure 3.9 Measured transit time (µsec) vs. pressure (psia) in binary mixture of n-hexane (nC_6) and n-decane (nC_{10}) at various temperatures

3.3.1.6 Speed of Sound in CO_2

Speed of sound measurements in CO_2 were carried out over a wide range of temperature at 2500 psia. Liquid CO_2 was loaded into the piston vessel and the pressure maintained at 2500 psia to ensure that CO_2 stays liquid above its vapour pressure. The measured transit times and speeds of sound in the CO_2 are listed in Table 3.20 and displayed in

Figure 3.10. The measurements were performed in steps of 5 to 10 °C between 10 and 50 °C but more measurements were made around the critical temperature of CO_2, which is 31.1 °C.

Table 3.20 Measured transit time and speed of sound (u m.s^{-1}) in carbon dioxide (CO_2) at different temperatures

Temperature (°C) ±0.01	Pressure (psia)±0.5	T_1 (µs) ±0.1	Meas. u (m/s)
9.97	2500.0	122.2	654.50
15.02	2500.0	126.0	634.79
25.02	2500.2	139.8	572.16
28.02	2499.8	145.5	549.83
29.00	2500.0	149.9	533.78
29.99	2500.2	150.8	530.70
30.58	2500.1	150.8	530.54
31.10	2500.2	153.8	520.21
31.58	2500.1	154.4	518.00
32.10	2500.1	155.4	514.67
35.00	2500.0	158.3	505.31
39.98	2500.4	168.7	474.37
45.00	2500.0	182.9	437.37
49.16	2502.0	194.0	412.49

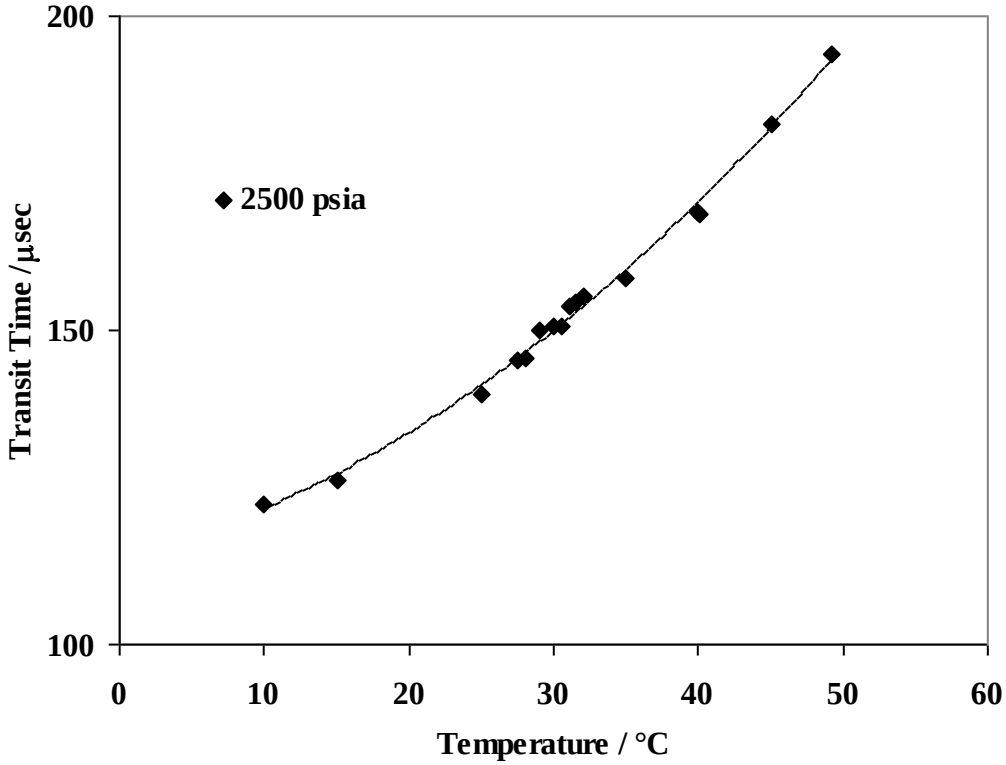

Figure 3.10 Measured transit time (µsec) vs. pressure (psia) in CO_2 at various temperatures

3.3.1.7 Speed of Sound in CO_2, n-Butane and n-Decane

To prepare this mixture, n-Decane was first added to the weighted evacuated cylinder. Then, n-butane and CO_2 were injected into two other different cells at a specified required weight. These cells were compressed to a high pressure and the fluids injected into the first cylinder using Quizix pump. The mixture was made with the composition given in Table 3.21.

Table 3.21 Compositions of n-butane (nC_4) and n-decane (nC_{10}) and CO_2 mixture

Compound	Density g/cm^3	Molecular weight	Weight grams	Moles	Mole%	Volume cm^3
nC_4	0.63	58.12	21.00	0.36	39.0	33.5
nC_{10}	0.73	142.28	54.30	0.38	41.2	74.4
CO_2	-	44.01	8.10	0.18	19.8	-

The experimental results for this system are given in Table 3.22 and also plotted in Figure 3.11.

Table 3.22 Measured transit time and speed of sound (u m.s^{-1}) in ternary mixture of n-butane (nC_4) and n-decane (nC_{10}) and CO_2 at different temperatures

Temperature (°C) ±0.01	Pressure (psia)±0.5	T_1 (µs) ±0.1	Meas. u (m/s)
10.03	1000.0	69.6	1148.68
10.01	2000.1	66.9	1195.46
9.98	3000.0	64.6	1238.29
10.00	4000.1	62.6	1277.54
10.04	5000.1	60.9	1314.17
20.00	1000.0	72.5	1104.82
20.00	2000.1	69.3	1154.32
20.02	3000.1	66.7	1199.22
20.02	4000.0	64.6	1238.78
19.97	5000.0	62.6	1278.57
29.99	1000.0	75.3	1061.92
30.00	2000.1	71.8	1114.13
30.00	3000.0	68.9	1160.43
29.99	4000.0	66.5	1203.46
30.00	5000.1	64.3	1243.39
40.00	1000.0	78.3	1021.12
40.02	2000.0	74.4	1075.63
40.04	3000.0	71.1	1124.54
40.06	4000.0	68.4	1168.82
40.07	5000.0	66.1	1210.28
49.96	1000.0	81.7	979.73
50.00	2000.0	77.1	1037.34
50.01	3000.1	73.5	1088.51
49.99	4000.0	70.5	1134.67
50.01	5000.0	67.9	1177.42

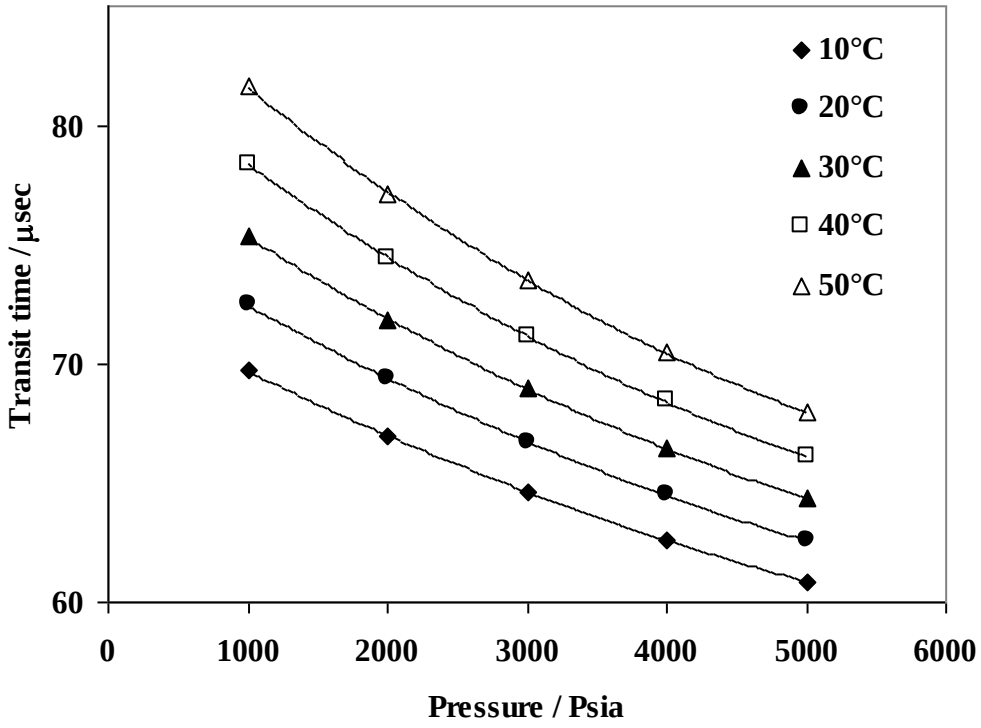

Figure 3.11 Measured transit time (µsec) vs. pressure (psia) in ternary mixture of n-butane (nC_4) and n-decane (nC_{10}) and CO_2 at various temperatures

3.3.1.8 Speed of sound in a Synthetic Mixture of $nC_7 + nC_8 + nC_9 + nC_{10}$

To extend the modelling to real oils with petroleum fractions, one synthetic fluid was made to test the model. The composition of this fluid was defined based on the Katz (1983) fitting method. Several methods exist for C_7+ characterization. Those methods are grouped into two main categories: correlation and splitting and lumping *(Naji, 2006)*. Correlation refers to the process of predicting C_7+ properties solely from specific gravity and molecular weight and/or true boiling point. However, a single C_7+ fraction was found unsuitable for PVT predictions and phase behaviour calculations. Splitting refers to the process of breaking down C_7+ fraction into a number of pseudo-components with a single carbon number: C_7, C_8, C_9, C_n. Pseudo-components are described by the same physical properties used for pure components; which were measured and compiled over the years. The exponential molar distribution (mole fraction/molecular weight relation) is perhaps the simplest method for splitting the C_7+ fraction into a number of pseudo-components. The mole fraction of pseudo-component *n* in the extended analysis is given by:

$$Z_n = Z_{C7+}\ Ae^{-Bn} \tag{3.11}$$

where A and B are fitting parameters. Katz (1983) proposed a simple graphical correlation, which is represented in a mathematical form as follows:

$$Z_n = Z_{C7+}(1.38205)e^{-0.25903n} \tag{3.12}$$

This equation was used to determine the mole fraction of the components in the fluid. Table 3.23 and Figure 3.12 show the mole fraction of each component in the fluid.

Table 3.23 Compositions of nC_7 + nC_8 + nC_9 + nC_{10} mixture

Compound	Target Mole%	Molecular weight	Weight grams	Moles	Mole%	Volume cm^3
nC_7	36	100.20	43.15	0.26	36.00	63.34
nC_8	27	114.23	36.88	0.20	26.99	52.71
nC_9	21	128.25	32.22	0.15	21.01	45.05
nC_{10}	16	142.28	27.23	0.12	16.00	37.42

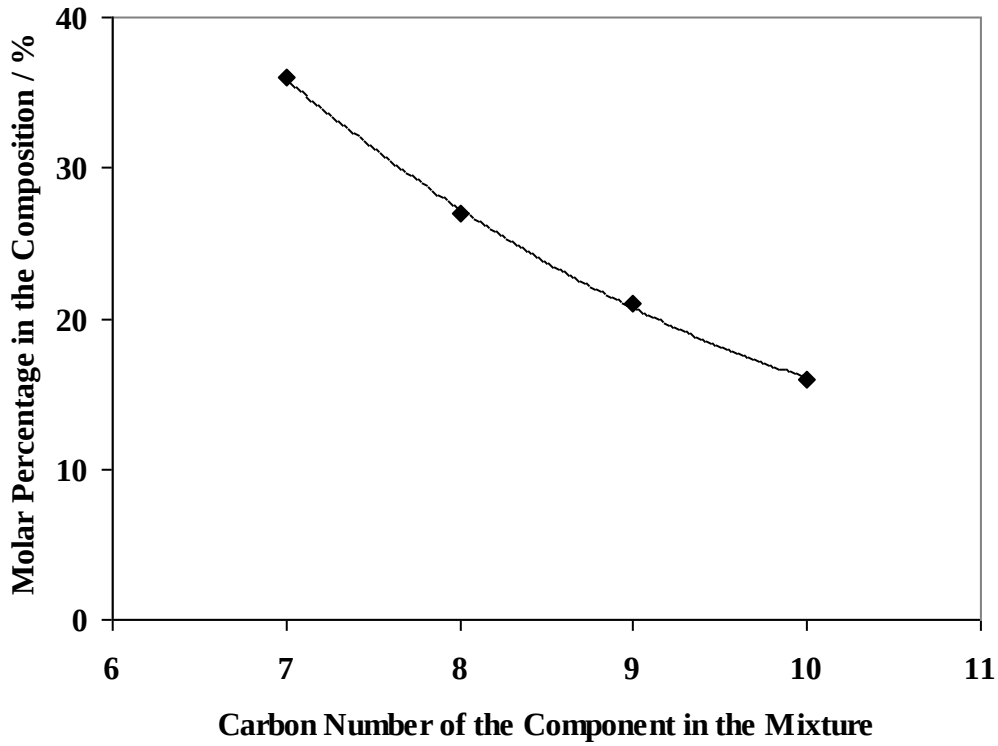

Figure 3.12 Molar percentage of each component in the mixture. This figure shows the exponential decay of hydrocarbon concentration in the mixture with increasing carbon number.

The measured transit times and speed of sound are listed in Table 3.24 and displayed in Figure 3.13.

Table 3.24 Measurement of transit time and speed of sound in the synthetic mixture of nC_7- nC_8- nC_9- nC_{10} at various temperatures and pressures

Temperature (°C) ±0.01	Pressure (psia)±0.5	T_1 (μs) ±0.1	Meas. u (m/s)
30.00	1000.3	66.6	1200.75
30.01	2000.2	64.3	1244.94
29.99	3000.8	62.3	1285.04
29.99	4000.2	60.4	1323.69
29.98	5000.5	58.9	1358.35
44.98	1000.0	70.0	1142.53
44.99	2000.1	67.3	1189.06
45.00	3000.1	64.9	1232.29
44.99	4000.0	62.9	1272.67
45.01	5000.2	61.1	1310.40
59.98	1000.0	73.6	1087.10
60.00	2000.0	70.4	1136.36
59.99	3000.1	67.7	1181.68
59.97	4000.1	65.4	1223.90
60.00	5000.0	63.3	1263.62

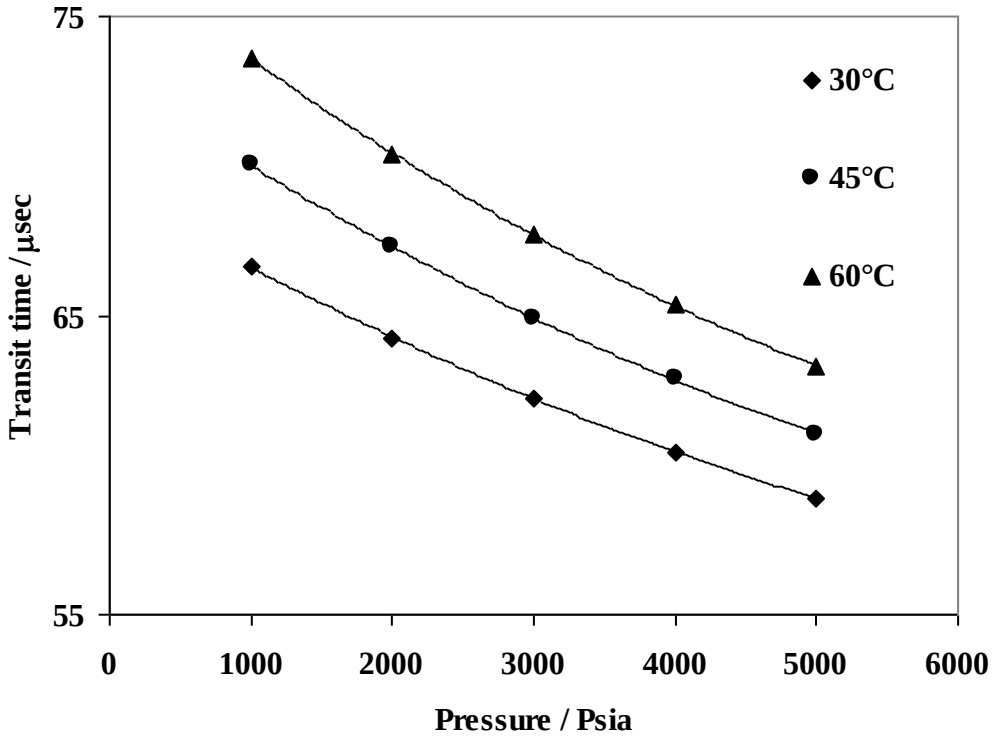

Figure 3.13 Measured transit time (μsec) vs. pressure (psia) in the synthetic mixture of nC_7- nC_8- nC_9- nC_{10} at various temperatures

3.3.1.9 Speed of sound in real oil 1

The next stage in this work was to measure the speed of sound in a real oil. For this purpose, three real oils were selected and their speeds of sound were measured. The composition of the real oil1 is indicated in Table 3.25.

Table 3.25 Composition of real oil 1

SCN	MW	Weight%	Mole%	SCN	MW	Weight%	Mole%
C_1	16.04	0.00	0.00	C_{13}s	175	7.86	9.47
C_2	30.07	0.00	0.00	C_{14}s	190	8.71	9.66
C_3	44.10	0.00	0.00	C_{15}s	206	9.27	9.48
iC_4	58.12	0.00	0.00	C_{16}s	222	9.09	8.63
nC_4	58.12	0.00	0.00	C_{17}s	237	8.59	7.64
iC_5	72.15	0.00	0.00	C_{18}s	251	8.43	7.08
nC_5	72.15	0.00	0.00	C_{19}s	263	7.16	5.74
C_6s	84	0.02	0.05	C_{20}s	275	6.61	5.07
C_7s	96	0.11	0.24	C_{21}s	291	7.55	5.47
C_8s	107	0.54	1.06	C_{22}s	300	3.85	2.70
C_9s	121	2.13	3.71	C_{23}s	312	2.61	1.76
C_{10}s	134	3.42	5.38	C_{24}s	324	1.69	1.10
C_{11}s	147	4.59	6.58	C_{25}s	337	0.95	0.59
C_{12}s	161	6.34	8.30	C_{26}s	349	0.47	0.28
Calculated Molecular Weight = 211				Total		100.00	100.00

The measured transit times and speeds of sound for this oil are indicated in Table 3.26.

Table 3.26 Measurement of transit time and speed of sound in real oil 1 at various temperatures and pressures

Temperature (°C) ±0.01	Pressure (psia)±0.5	T_1 (μs) ±0.1	Meas. u (m/s)
30.01	1000.0	58.4	1370.24
30.01	2000.0	56.9	1405.28
30.01	3000.0	55.7	1436.88
30.00	4000.0	54.5	1468.43
30.00	5000.1	53.4	1497.34
44.80	1000.0	60.6	1319.57
44.98	1000.0	60.7	1318.83
45.01	2000.0	59.1	1353.98
44.98	3000.0	57.6	1387.93
44.97	4000.1	56.3	1420.20
44.99	5000.1	55.2	1450.19
59.98	1000.1	63.1	1267.83
60.00	2000.0	61.3	1305.06
60.00	3000.1	59.7	1340.03
59.98	4000.0	58.2	1373.63
60.00	5000.1	56.9	1405.85

3.3.1.10 Speed of sound in real oil 2

The composition of the real oil 2 is listed in Table 3.27. The measured transit time and speed of sound are indicated in Table 3.28.

Table 3.27 Composition of real oil 2

SCN	MW	Weight%	Mole%	SCN	MW	Weight%	Mole%
C_1	16.04	0.00	0.00	$C_{13}s$	175	3.87	5.69
C_2	30.07	0.00	0.00	$C_{14}s$	190	4.16	5.62
C_3	44.10	0.00	0.02	$C_{15}s$	206	4.40	5.49
iC_4	58.12	0.02	0.11	$C_{16}s$	222	4.18	4.84
nC_4	58.12	0.05	0.22	$C_{17}s$	237	3.76	4.08
iC_5	72.15	0.16	0.58	$C_{18}s$	251	3.94	4.03
nC_5	72.15	0.15	0.54	$C_{19}s$	263	3.61	3.53
C_6s	84	0.59	1.81	$C_{20}s$	275	3.35	3.13
C_7s	96	2.21	5.90	$C_{21}s$	291	3.11	2.74
C_8s	107	2.75	6.61	$C_{22}s$	300	2.78	2.38
C_9s	121	2.33	4.96	$C_{23}s$	312	2.69	2.21
$C_{10}s$	134	2.72	5.22	$C_{24}s$	324	2.53	2.00
$C_{11}s$	147	2.78	4.87	$C_{25}s$	337	2.65	2.02
$C_{12}s$	161	3.19	5.09	$C_{26}+$	599	38.02	16.31
Measured Molecular Weight = 257				Total		100.00	100.00

Table 3.28 Measurement of transit time and speed of sound in real oil 2 at various temperatures and pressures

Temperature (°C) ±0.01	Pressure (psia)±0.5	T_1 (μs) ±0.1	Meas. u (m/s)
30.01	1000.6	56.4	1419.45
30.01	2000.0	55.2	1449.54
30.02	3000.0	54.2	1476.97
30.00	4000.0	53.1	1507.59
30.00	5000.0	52.1	1535.66
44.98	1000.0	58.9	1358.58
45.00	2000.1	57.4	1392.88
45.00	3000.1	56.1	1425.90
45.00	4000.0	54.9	1456.80
45.00	5000.0	53.8	1486.85
59.98	1000.0	60.9	1313.31
60.02	2000.0	59.4	1347.60
59.98	3000.1	57.9	1380.62
59.96	4000.0	56.7	1411.31
59.96	5000.0	55.5	1442.61

3.3.1.11 Speed of sound in real oil 3

The composition of the real oil 3 is listed in Table 3.29. The measured transit time and speed of sound are indicated in Table 3.30.

Table 3.29 Composition of real oil 3

SCN	MW	Weight%	Mole%	SCN	MW	Weight%	Mole%
C_1	16.04	0.00	0.00	$C_{18}s$	251	2.49	1.93
C_2	30.07	0.03	0.19	$C_{19}s$	263	1.96	1.45
C_3	44.10	0.32	1.41	$C_{20}s$	275	2.02	1.43
iC_4	58.12	0.27	0.91	$C_{21}s$	291	1.89	1.27
nC_4	58.12	1.00	3.35	$C_{22}s$	300	1.79	1.16
iC_5	72.15	0.93	2.51	$C_{23}s$	312	1.71	1.07
nC_5	72.15	1.37	3.70	$C_{24}s$	324	1.59	0.96
C_6s	84	2.90	6.73	$C_{25}s$	337	1.46	0.84
C_7s	96	4.40	8.93	$C_{26}s$	349	1.43	0.80
C_8s	107	5.41	9.86	$C_{24}s$	360	1.35	0.73
C_9s	121	5.41	8.72	$C_{25}s$	372	1.30	0.68
$C_{10}s$	134	4.61	6.71	$C_{26}s$	382	1.25	0.64
$C_{11}s$	147	3.74	4.96	$C_{30}s$	394	1.17	0.58
$C_{12}s$	161	3.24	3.92	$C_{31}s$	404	1.08	0.52
$C_{13}s$	175	3.39	3.78	$C_{32}s$	415	0.99	0.47
$C_{14}s$	190	3.17	3.25	$C_{33}s$	426	0.93	0.43
$C_{15}s$	206	2.98	2.82	$C_{34}s$	437	0.86	0.38
$C_{16}s$	222	2.65	2.33	$C_{35}s$	445	0.83	0.36
$C_{17}s$	237	2.98	2.45	$C_{36}+$	630	25.10	7.77
Measured Molecular Weight = 195				Total		100.00	100.00

Table 3.30 Measurement of transit time and speed of sound in real oil 3 at various temperatures and pressures

Temperature (°C) ±0.01	Pressure (psia)±0.5	T_1 (µs) ±0.1	Meas. u (m/s)
30.01	1000.0	58.9	1358.93
30.00	2001.0	57.5	1392.27
30.00	2999.3	56.1	1425.01
30.02	4000.2	55.0	1455.60
30.00	5000.0	53.9	1485.61
44.99	1000.0	61.5	1301.02
44.99	2000.0	59.8	1337.57
45.01	3000.0	58.3	1372.21
44.94	4000.0	56.9	1404.99
45.00	5000.0	55.7	1436.01
59.90	1000.0	63.6	1257.07
59.97	2000.0	61.9	1293.24
60.00	3000.0	60.2	1329.79
60.02	4000.1	58.7	1364.02
60.06	5000.0	57.3	1396.16

3.3.2 Hydrate Lab Experimental Results

Three experiments to measure the velocity of sound in a fluid-saturated matrix were performed in the hydrate lab. The fluids were different in each test and the matrix was made of either sand or glass beads. The porosity of these systems was determined using nitrogen injection. Porosity was calculated using the following equations:

$$Porosity = \frac{Pore\ volume}{Total\ volume} \times 100 \tag{3.13}$$

$$Pore\ Volume = \frac{nZRT}{P} \tag{3.14}$$

$$Total\ volume = \frac{\pi\ d^2}{4}\left(L - Displacement\right) \tag{3.15}$$

Where T, P, Z, R and *n* are temperature, pressure, compressibility factor of the gas we used in the pore spaces, universal gas constant and number of nitrogen moles in the pores, respectively. L is the length of the acoustic cell which is 148 mm and "Displacement" is the value shown by the LVDT that determines the displacement during depressurization and compression. In all of above calculations, SI units were used, T (K), P (MPa), etc.

$$number\ of\ \ N_2\ \ Moles = \frac{gram\ of\ \ N_2\ \ injected\ \ \text{int}\, o\ the\ cell}{28} \tag{3.16}$$

The compressibility factor of pure nitrogen can be calculated directly by the following correlations (Obeida, 1997):

$$Z_{N2} = a_0 + a_1 P + a_2 P \tag{3.17}$$

The parameters of a_0, a_1 and a_2 are functions of temperature which can be calculated from the following equations:

$$a_0(T) = b_0 + b_1 T + b_2 T^2 \tag{3.18}$$

$$a_1(T) = c_0 + c_1 T + c_2 T^2 \tag{3.19}$$

$$a_2(T) = d_0 + d_1 T + d_2 T^2 \tag{3.20}$$

b_0, b_1, …, d_2 are constants obtained from regression and listed in Table 3.31.

Table 3.31 Constants obtained from regression for determination of compressibility factor of N_2

b_0	9.902E-01	c_0	-2.078E-04	d_0	2.273E-06
b_1	7.827E-05	c_1	7.450E-06	d_1	-2.051E-8
b_2	-1.791E-07	c_2	-2.534E08	d_2	6.790E-11

Temperature and pressure should be in °C and bar in above equations.

Speed of sound in a saturated reservoir matrix can be calculated via the following equation:

$$V_S = \frac{0.148 - Displacement}{T_{measured} - T_0} \tag{3.21}$$

Where 0.148 m is the length of the acoustic cell and T_0 is the transit time of the wave through the end caps of the acoustic cell which is:

$T_0 = 2.42\ \mu s$ For the P-wave

In all experiments, effective pressures of around 700-800 psia were exerted to prevent the matrix from collapsing. The effective pressure should be less than the elastic limit and in the elasticity region of the solid.

3.3.2.1 Sand + (nC_6 + nC_{10})

This test was performed at 45 °C and at several different pore pressures. Effective pressure was maintained constant at 800 psia during the experiment. The porosity was 46.46%. The measurement of transit time and the calculations of speed of sound in the saturated matrix are listed in Table 3.32.

Table 3.32 Measurement of transit time in matrix saturated with nC_6 + nC_{10} and calculated speed of sound at different pressures and 45.0 °C

Temperature (°C)±0.01	Overburden Pressure (psia)±0.5	Pore Pressure (psia)±0.5	Displacement mm	T (μs) ±0.1	Meas.u (m/s)
45.00	1301	500.0	5.017	107.0	1367.8
45.00	1803	1000.2	5.025	105.4	1387.8
45.00	2302	1501.4	5.029	104.0	1407.3
45.00	2801	1999.7	5.038	102.7	1426.3
45.00	3299	2500.3	5.041	101.4	1444.8
44.92	3803	3003.3	4.967	100.2	1462.8
44.98	4301	3500.7	5.004	99.0	1480.3
44.98	4800	3998.5	5.025	97.9	1497.3
45.02	5300	4500.9	5.031	96.9	1513.8
45.02	5803	5000.2	5.074	95.9	1529.8

3.3.2.2 Glass Beads + (CO_2)

In this experiment, porosity was determined as 50.68%, matrix particles were glass beads and liquid CO_2 was injected into the pores between the glass beads. The overburden pressure was maintained at above 700 psia above the test pore pressure, throughout the test. The pore pressure was kept constant at 2500 psia during the test.

The measurement of transit time and the calculations of speed of sound in the saturated matrix with CO_2 were listed in Table 3.33.

Table 3.33 Measurement of transit time in matrix saturated with CO_2 and calculated speed of sound at 2500 psia and different temperatures

Temperature (°C)±0.01	Overburden Pressure (psia)±0.5	Pore Pressure (psia)±0.5	Displacement mm	T (μs)	Meas.u (m/s)
9.97	3200	2500.3	11.471	136.5	1018.1
15.02	3200	2499.2	11.481	141.5	981.8
25.02	3199	2501.2	11.535	151.6	915.1
28.02	3201	2499.4	11.553	154.5	896.9
29.00	3199	2502.2	11.555	155.7	890.5
29.99	3200	2499.9	11.561	156.7	884.6
30.58	3199	2499.7	11.562	157.3	880.9
31.10	3203	2500.1	11.574	157.8	878.2
31.58	3199	2499.9	11.573	158.3	875.3
32.10	3201	3200.6	11.586	158.8	872.3
35.00	3201	2500.2	11.601	161.8	855.9
39.98	3202	2500.9	11.625	167.0	828.7
45.00	3199	2500.5	11.644	172.1	803.6
49.16	3200	2499.6	11.656	176.3	783.9

3.3.2.3 Glass Beads + (nC_4 + nC_{10} + CO_2)

Porosity was 44.83% in this test. At 20.18 °C, 5.4 grams of nitrogen were injected into the cell. The velocity of sound before and after nitrogen injection were 847.25 and 839.97 m/s, respectively. The matrix was made of glass beads and the fluid sample was a mixture of nC_4 + nC_{10} + CO_2. The effective pressure was maintained at 800 psia during the test. These measurements were performed at six temperatures from 0 to 50 °C and 5 pressures, 1000 to 5000 psia.

In this test, at first, several circulations of the sample fluid were applied to make sure that the sample inside the pores is homogeneous and single phase. For circulating the fluid, the sample fluid was prepared in amount of at least twice of the pore spaces. Then two piston vessels were connected to the two sides of the acoustic cell. Injection started from one cylinder and after filling the pore spaces with the sample, the other cylinder was filled with the residual fluid. During the circulation of the fluid, the transit time was monitored and investigated. The temperature and pressure was kept constant during this process and they were 20 °C and 2500 psia, respectively. The main part of the test started when the velocity of sound measurements stabilized.

Table 3.34 Measurement of transit time in matrix saturated with nC_4 + nC_{10} +CO_2 and calculated speed of sound at different pressures and temperatures

Temperature (°C)±0.01	Overburden Pressure (psia)±0.5	Pore Pressure (psia)±0.5	Displacement mm	T (μs)	Meas.u (m/s)
-0.04	1799	1000.1	38.616	84.1	1339.2
-0.04	2803	2001.2	38.625	82.0	1374.8
-0.02	3801	3000.3	38.630	81.3	1386.9
-0.02	4803	4000.4	38.637	79.8	1413.7
-0.02	5802	4998.3	38.597	78.8	1432.7
10.03	1799	1000.0	38.641	86.9	1294.8
10.01	2803	2000.1	38.653	85.1	1322.2
9.98	3799	3000.0	38.660	83.7	1345.6
10.00	4802	4000.1	38.663	82.1	1373.0
10.04	5800	5000.1	38.615	80.8	1395.9
20.00	1799	1000.0	38.660	89.5	1256.0
20.00	2799	2000.1	38.672	87.6	1284.1
20.02	3801	3000.1	38.675	86.1	1307.1
20.02	4798	4000.0	38.680	84.5	1332.5
19.97	5803	5000.0	38.666	83.0	1357.5
29.99	1800	1000.0	38.715	91.6	1226.0
30.00	2802	2000.1	38.729	89.7	1252.7
30.00	3798	3000.0	38.733	87.9	1278.9
29.99	4802	4000.0	38.744	86.4	1301.2

30.00	5800	5000.1	38.715	84.7	1327.5
40.00	1802	1000.0	38.737	93.6	1198.9
40.02	2798	2000.0	38.744	91.6	1225.7
40.04	3800	3000.0	38.759	89.8	1250.8
40.06	4800	4000.0	38.769	87.9	1277.3
40.07	5801	5000.0	38.766	86.2	1304.2
49.96	1799	1000.0	38.772	95.5	1173.0
50.00	2799	2000.0	38.785	93.2	1203.4
50.01	3803	3000.1	38.800	91.2	1230.6
49.99	4801	4000.0	38.811	89.3	1256.6
50.01	5803	5000.0	38.819	87.6	1282.4

The measurement of transit time and the calculations of speed of sound in the saturated matrix with this mixture are listed in Table 3.34.

3.4 Conclusion

An acoustic cell for the experimental determination of the speed of sound (u m.s-1) in liquid *n*-alkanes has been set up and calibrated to determine the transit distance (L mm) within the cell. This data has then been used together with the measured values of transit time ΔT_S (μs) to measure the speed of sound in liquid pure compounds, binary and multi-component of hydrocarbon mixtures at different temperatures and pressures. These experiments were performed principally to assist in the development of an equation of state to accurately predict the speed of sound.

The experimental data have been compared, where possible, with literature data and shows generally good agreement with the published speed of sound data.

Another set up was used to measure the velocity of sound in a fluid-saturated porous media. Different fluids and matrices were used in these experiments at various temperature and pressure conditions. These kinds of experiments help to investigate the effects of fluid substitution on velocity of saturated sediments with reservoir fluids in various temperatures and pressures that will be disscused in Chapter 6.

REFERENCES

Ball S.J., Trusler J.P.M., 2000, *The speed of sound and derived thermodynamic properties of n-Hexane and n-Hexadecane at temperatures between 298 K and 373 K and pressures up to 100 MPa,* 14th Symposium on Thermophysical Properties, June 25-30, Boulder, Colorado, USA

Benedetto G., Gavioso R.M., Giuliano Albo P.A., Lago S., Madonna Ripa D., Spagnolo R., 2005, *Speed of sound in pure water at temperatures between 274 and 394 K and at pressures up to 90 MPa*, International Journal of Thermophysics, **26(6)**, 1667-1680

Daridon J.L., Lagourette B., Grolier J-P.E., 1998, *Experimental measurements of the speed of sound in n-Hexane from 293 to 373 K and up to 150 MPa,* International Journal of Thermophysics, **19(1)**, 145 – 160

Ding Z.S., Alliez J., Boned C., Xans P., 1997, *Automation of an ultrasound velocity measurement system in high pressure liquids,* Measurement Science and Technology, **8**, 154 – 161

Grosso V.A.D., Mader C.W., 1972, Speed of sound in pure water, Naval Research Laboratory, Washington D.C., 20390

Hakim S.E.A., Comley W.J., 1965, *Acoustic velocity dispersion in some non-associated organic liquids*, Nature, **208**, 1082-1083

Katz D., 1983, *Overview of phase behaviour of oil and gas production*, JPT, 1205-1214.

Khasanshin T.S., Shchemelev A.P., 2001, *Sound velocity in liquid n-Alkanes, High Temperature*, **39(1)**, 60 – 67

Lainez A., Zollweg J.A., Streett W.B., 1990, *Speed of sound measurements for liquid n-Pentane and 2,2-dimethylpropane under pressure*, Journal of Chemical Thermodynamics, **22**, 937 – 948

Lamb J., 1965, *Physical Acoustics: Principles and Methods*; Mason, W.P., Ed.; Academic Press: New York

Naji H.S., 2006, *A polynomial fit to the continuous distribution for C7+ characterization*, Emirates Journal for Engineering Research, **11(2)**, 73-79

NIST, http://webbook.nist.gov/chemistry/fluid

NIST "REFPROP, Reference Fluid Thermodynamic and Transport Properties".

Obeida T.A., AGOCO, Heinemann Z.E., 1997, *Accurate calculation of compressibility factor for pure gases and gas mixtures*, SPE 37440

Plantier F., 2005, *Laboratoire des fluide complexes, groupe haute pression, Université de Pau et des Pays de l'Adour*, Personal Communication

Reservoir Fluids Studies, Institute of Petroleum Engineering, Heriot-Watt University, Edinburgh, UK, Report Number PVT/00/1.

Reservoir Fluid Studies, Institute of Petroleum Engineering, Heriot-Watt University, Edinburgh, UK, Report Number PVT/03/1.

Reservoir Fluid Studies, Institute of Petroleum Engineering, Heriot-Watt University, Edinburgh, UK, Report Number PVT/06/1.

Reservoir Fluid Studies, Institute of Petroleum Engineering, Heriot-Watt University, Edinburgh, UK, Report Number PVT/07/1.

Reservoir Fluid Studies, Institute of Petroleum Engineering, Heriot-Watt University, Edinburgh, UK, Report Number PVT/07/2

Salehabadi M., 2009, *Hydrates in sediments: Their role in wellbore/casing integrity and CO_2 sequestration*, PhD Thesis

Yang J., Tohidi B., Clennell B., 2004, *Micro and macro-scale investigation of cementing characteristics of gas hydrates.* The AAPG Hedberg Research Conference: 'Natural Gas Hydrates - Energy Resource Potential and Associated Geologic Hazards', Vancouver, British Columbia, Canada

Yang J., Llamedo M., Marinakis D., Tohidi B., Varotsis N., 2005, *Successful applications of a versatile ultrasonic test system for gas hydrates in unconsolidated*

sediments. Proceedings of the Fifth International Conference on Gas Hydrates, Tronheim, Norway June 13-16

CHAPTER 4 – THERMODYNAMIC MODELLING

4.1 Introduction

An equation of state is a thermodynamic equation describing the state of matter under a given set of physical conditions. This equation usually relates the thermodynamic variables of pressure, temperature, volume and number of atoms to one another. Equations of state are useful in describing the properties of fluids and mixtures of fluids. Moreover, the equations of state (EoS) are used to estimate the thermodynamic properties of gases, liquids, and solids necessary for phase behaviour calculations. Among all of the equations of state proposed by different researchers, only a few are based on a fundamental theory, and the majority have been developed as a result of the mathematical processing of experimental data (Maghari & Sadeghi, 2007).

For non polar systems, cubic equations of state (CEoS) have been shown to predict with reasonable accuracy the phase equilibrium of pure and multi-component mixtures, whereas they are incapable of describing the observed singularities in variation of the second order derivatives such as the density in isothermal variation of isochoric heat capacity and speed of sound (Gregorowicz et al., 1996). Cubic equations of state (CEoS) have shown poor performances also in predicting the regularities in dense fluids (Maghari and Hosseinzadeh-Shahri 2003).

To improve the predictions near the critical point, crossover equations of state based on the critical scaling law (Landau & Lifshitz, 1980) and renormalization group theory (Wilson, 1971) have been proposed by some investigators (Kiselev, 1998; Lee et al., 2007; Kiselev, 2004; Kostrowicka et al., 2004; Shin et al., 2008) to combine the known behaviour of fluids in the critical region with EoS that are successful far away from the critical point. Crossover cubic equations of state improve predictions compared to classical EoS without these crossover methods. But those EoS are basically acceptable in the calculation of *PVT* and phase equilibria for spherical molecular fluids such as argon and methane. (Landau et al., 1980)

It has been long recognized that molecular-based equations of state can present better results than cubic EoS, due to their statistical mechanical basis. Statistical Associating Fluid Theory (SAFT) can be used to describe the properties of fluids with good accuracy. Based on the first-order theory of Wertheim (1984 and 1986), the SAFT EoS

has been proposed by Chapman et al. (1989) and converted to a more applicable equation in industry and engineering by Huang and Radosz (1990 and 1991) and different versions of SAFT have been widely used in the past decade.

The modified SAFT-BACK EoS is an equation combining the SAFT and BACK equations. This equation can calculate not only the phase equilibria, but also the PVT lines in a wide range and the vaporization enthalpies with good accuracy for single *n*-alkane (Chen and Mi., 2001). In the SAFT-BACK EoS, the residual Helmholtz energy for a fluid can be considered as a sum of the separate contributions to the energy.

In spite of all its advantages, the SAFT-BACK EoS is more complex algebraically and computationally intensive, so its practical use in industrial applications have been limited. The detail description of this equation of state for modelling of thermodynamic properties and especially speed of sound are outlined in this chapter. At first, the SAFT-BACK equation for calculation and modelling of the speed of sound will be investigated using thermodynamic properties such as related pressure, isobaric and isochoric heat capacities for several types of (alkanes and cyclic compounds) and other non-hydrocarbon compounds such as CO_2, N_2. Also, the SAFT-BACK EoS was extended for binary and multi-component mixture calculations and real fluids.

Then, because of the high importance placed on the use of cubic equations of state in the oil industry, a cubic equation will be used to predict and model these properties in parallel.

4.2 Thermodynamic Modelling

The thermodynamic properties of materials are intensive parameters pertinent to a given material. Isobaric and isochoric heat capacities, reduced bulk modulus, isothermal expansion coefficient, Joule-Thomson coefficient and the speed of sound are some derivative properties of fluids that are of technological importance. In fact, these properties are essential for the accurate design and optimization of several industrial processes. Speed of sound is also commonly employed for aerodynamic calculations. As their names specify, derivative properties are second derivatives of a thermodynamic potential function (Internal energy, U, Enthalpy, H, Gibbs free energy, G, or Helmholtz

free energy, A). They can be obtained by differentiation with respect to the temperature and density and are related to thermodynamic potentials as follows:

$$\beta_T = -\frac{1}{v}\left(\frac{\partial v}{\partial P}\right)_T = -\frac{1}{v}\frac{\partial^2 G}{\partial P^2} \tag{4.1}$$

$$\beta_S = -\frac{1}{v}\left(\frac{\partial v}{\partial P}\right)_S = -\frac{1}{v}\frac{\partial^2 H}{\partial P^2} \tag{4.2}$$

$$C_P = T\left(\frac{\partial S}{\partial T}\right)_P = -T\frac{\partial^2 G}{\partial T^2} \tag{4.3}$$

$$C_V = T\left(\frac{\partial S}{\partial T}\right)_V = -T\frac{\partial^2 A}{\partial T^2} \tag{4.4}$$

$$\alpha = \frac{1}{v}\left(\frac{\partial v}{\partial T}\right)_P = \frac{1}{v}\frac{\partial^2 G}{\partial P \partial T} \tag{4.5}$$

$$V_S = \sqrt{-\left(\frac{v^2 C_P}{C_V M}\right)\left(\frac{\partial P}{\partial v}\right)_T} = \sqrt{\frac{C_P}{C_V}\frac{v}{M\beta_T}} \tag{4.6}$$

Where β_T and β_S are the isothermal and adiabatic compressibility, respectively. C_P is isobaric heat capacity, C_V is isochoric heat capacity, α is thermal expansion coeffient and V_S is the speed of sound (Heriot-Watt University- Report PVT/08/1). In above relations, *P* is pressure, *T* is temperature, *v* is molar volume, *S* is entropy and *M* is molecular weight. For pure compounds, only three of these parameters are required to calculate the other parameters, as they are mathematically related.

In addition to technical interest, there is also a serious scientific concern in accurately obtaining these parameters. It has been shown that these parameters are very sensitive to the errors in comparison to the first order derivative properties. For instance, while determining the first derivative properties such as phase equilibrium calculation through equality of the chemical potentials using a thermodynamic function (e.g. an equation of state such as Peng-Robinson, PR (Peng and Robinson, 1976)) may result in reasonable predictions, its second order derivative property may not necessarily yield accurate results (e.g., speed of sound).

In the present work, the modified SAFT-BACK equation of state is employed and extended to model second-order derivative thermodynamic properties for different hydrocarbon mixtures.

4.3 Introduction to SAFT-BACK

The great success of SAFT is rooted in its reliable predictions where other models fail. More details are available in Muller-Gubbins (2001) and Economou (2002). The inability of other equations of state for prediction of the thermodynamic properties near critical region is basically due to the difficulty in describing the critical compressibility factor Z_C and using equations of state (Sengers 1991). An equation of state has its own theoretical compressibility factor Z_C, but because of failure of the expression of the critical exponent, the equations of state cannot satisfactorily describe phase equilibria and thermodynamic properties in the near-critical region.

The statistical associating fluid theory (SAFT) has been proposed by Chapman et al. (1989, 1990) and Huang and Radosz (1990, 1991) converted it into a very useful engineering equation. In SAFT a molecule is composed of m segments corresponding to atoms or functional groups that have the same volume v^{00} and interaction energy parameter u_0. So it includes four parameters for every non-polar fluid: the segment number m, the segment non-spherical parameter α, the segment volume v^{00} and the segment interaction parameter u_0.

Based on a statistical mechanical description, an equation of state for hard convex body (hcb) fluids was proposed by Boublik (1975) from the scaled particle theory for systems composed of non-spherical molecules to take into account the non-sphericity of the molecules. Chen and Kreglewski (1977) used the equation proposed by Boublik (1975) combined with the equation of Alder et al. (1972) to establish an equation of state called Boublik–Alder–Chen–Kreglewski (BACK).

The BACK EoS is quite successful in describing the equilibrium behaviour of fluids up to the critical point for systems of non-associating molecules and mixtures (Machet & Boublik, 1985; Aim & Boublik, 1986), such as carbon dioxide, nitrogen, ethane, etc. But this EoS cannot be used for long chain fluids.

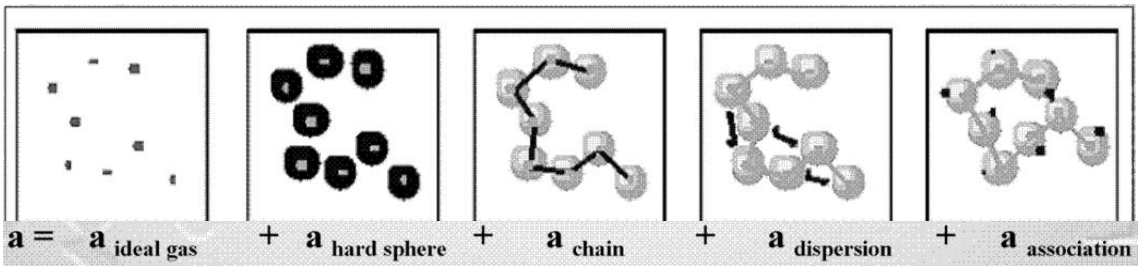

Figure 4.1 Sum of different helmhotlz energies in SAFT EoS

Figure 4.1 shows the separate contribution of Helmholtz energy. The SAFT equation of state can express the properties of spherical molecules, such as argon and methane, over the wide range of temperature and pressure including the near-critical region within relatively small errors. When a molecule is not a sphere (for example, carbon dioxide), the BACK equation of state can give quite good results including the near-critical region as pointed out by Chen and Kreglewski (1977) and Pfohl and Brunner (1998). In BACK, the term for hard-sphere is replaced by the equation for hard convex body, and the term for dispersion energy is the same as that used in SAFT. The first modification on SAFT was to use the equation of state for hard convex body to take into account the non-sphericity of segments.

Chen and Mi (2001) combined BACK with SAFT and proposed a new equation of state. For one-segment molecular fluids, such as spherical fluids as argon and methane or non-spherical fluids as carbon dioxide and ethane, SAFT or BACK can express their phase equilibria and *PVT* properties with good accuracy even in the near-critical region. This means that an analytic equation of state as SAFT can be used for the calculation in the near-critical region. The problem for the description in the critical region appears when the segment number is larger than 1. So in order to establish an EOS for chain fluids, a further modification about the contribution of chain formation should be considered. Only the hard-sphere term is corrected with a term accounting for the effect of chain formation, and the term for dispersion energy is not corrected. The dispersion term includes all interactions between segments in the fluid, which is expressed by the segment density. In other words, although the segments have been bonded to be chain molecules, the dispersion energy is not corrected and still includes the energy between intermolecular segments and between intramolecular segments. But for any EOS, its reference state is the ideal gaseous state of molecules, not of segments. The interaction between intramolecular segments occupies a large part in the whole interaction because

they are usually near to each other in the fluid. So the intramolecular segment interaction should be excluded in the dispersion term.

With the two following modifications, SAFT-BACK can be known in order to describe phase equilibrium behaviour of chain fluids in the whole region:

(i) The chain formation term is modified for describing the long chain fluids;

(ii) The consideration of the effect of chain formation on the dispersion term. This modification improves the expression of critical points for non-polar chain fluids.

Figure 4.2 shows the modification to this equation.

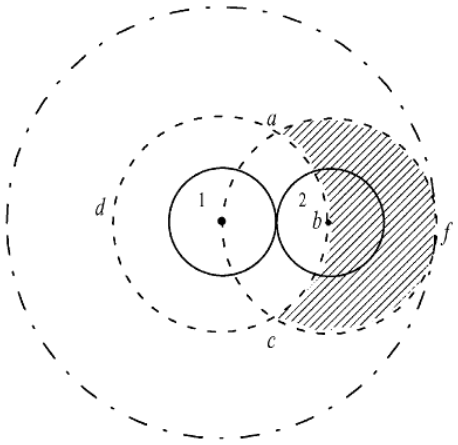

Figure 4.2 Diatomic molecular diagram. The segments 1 and 2 are bonded with each other. When the dispersion energy is calculated between the segment 1 and all other segments except the segment 2, the center of a third segment cannot be in the sphere 'abcda' and the shaded space 'abcfa' which is occupied by the bonded segment 2. (Chen & Mi, 2001)

The new equation after these modifications can describe the properties of chain fluids in the whole region and the results are better near critical region in comparison with SAFT. In the SAFT-BACK EoS, the residual Helmholtz energy for a fluid is written as a sum of separate contributions to the energy

$$A^{res} = A - A^{ideal} = A^{hcb} + A^{chain,hcb} + A^{dis} + A^{chain,dis} \qquad (4.7)$$

where A and A^{ideal} are the total and ideal gas Helmholtz energy at the same condition of temperature and density. Four terms of this equation are described as:

- A^{hcb} : the Helmholtz free energy for a hard convex body fluid

$$\frac{A^{hcb}}{RT} = m\left[\frac{\alpha^2}{(1-\eta)^2} - \frac{\alpha^2 - 3\alpha}{1-\eta} - (1-\alpha^2)\ln(1-\eta-3\alpha)\right] \tag{4.8}$$

where α is a shape factor and related to the geometry of the hard convex body and packing factor η is defined as

$$\eta = \frac{1}{6}\pi N_{AV} m \rho d^3 \tag{4.9}$$

in which ρ is the molar density, m is the segment number and N_{AV} is the Avogadro's number. The segment diameter d is calculated via the following equation:

$$d = \sigma\left[1 - 0.12\exp\left(-\frac{3u^0}{k_B T}\right)\right] \tag{4.10}$$

where u^0/k_B is the segment dispersion parameter, k_B is Boltzmann constant and σ is related to the segment volume parameter v^{00} by

$$v^{00} = \frac{1}{6}\pi N_{AV}\sigma^3 \tag{4.11}$$

- A^{chcb} : The chain formation term for hard convex body segments, with the mean radial distribution function g^{hcb} for the hard convex body fluids

$$\frac{A^{chain,hcb}}{RT} = (1-m)\ln g^{hcb}(d) \tag{4.12}$$

$$\text{Where } g^{hcb}(d) = \frac{1}{1-\eta} + \frac{3\alpha(1+\alpha)}{(1-\eta)^2(1+3\alpha)} + \frac{2\alpha^2\eta^2}{(1-\eta)^3(1+3\alpha)} \tag{4.13}$$

- A^{dis} : The dispersion term which can be expressed with the results of Alder et al. (1972) for square-well fluid as

$$\frac{A^{dis}}{RT} = m\sum_i\sum_j D_{ij}\left(\frac{u}{k_B T}\right)^i\left(\frac{\eta}{\tau}\right)^j \tag{4.14}$$

the interaction energy u is

$$u = u^0\left(1 + \frac{e}{k_B T}\right) \tag{4.15}$$

where e/k_B = 10.0, except for small molecules such as argon, nitrogen, oxygen and methane which is m = 1, and e/k_B = 1.0.

Also, D_{ij} are universal constants which were regressed from the experimental data of argon by Chen and Kreglewski (1977) and are shown in Table 4.1, $\tau = \sqrt{2}\pi/6$.
The dispersion term includes all interactions between segments in the fluid, which is expressed by the segment density.

- A^{cdis} : The chain formation of dispersion term is

$$\frac{A^{chain,dis}}{RT} = m\frac{\lambda A^{chani,hcb}}{A^{hcb}}\sum_i\sum_j D_{ij}\left(\frac{u}{k_BT}\right)^i\left(\frac{\eta}{\tau}\right)^j \tag{4.16}$$

After several regression, the best result for non-polar fluids is λ = 1.75.

For every fluid, four parameters (α, m, v^{00}, u_0) are necessary to be regressed to account for segment non-spherical degree, segment number, segment volume and segment dispersion energy. Critical properties and vapour–liquid equilibria were calculated with the initial parameters. These parameters were then regressed with the minimization of the objective:

$$F = \left(\frac{T^{C,ca} - T^{C,ex}}{T^{C,ex}}\right)^2 + \left(\frac{P^{C,ca} - P^{C,ex}}{P^{C,ex}}\right)^2 + \left(\frac{\rho^{C,ca} - \rho^{C,ex}}{\rho^{C,ex}}\right)^2 + \sum_{j=1}^{NP}\left[\left(\frac{P^{ca} - P^{ex}}{P^{ex}}\right)^2 + \left(\frac{\rho_j^{liq,ca} - \rho_j^{liq,ex}}{\rho_j^{liq,ex}}\right)^2\right] \tag{4.17}$$

The correlation results for *n*-alkanes, branched alkanes, cycloalkanes, alkenes, alkynes and aromatics are listed in Table 4.2.

Table 4.1 Universal constants D_{nm} in SAFT-BACK EoS

D_{11} = -8.8043	D_{21} = +2.9396	D_{31} = -2.8225	D_{41} = +0.3400
D_{12} = +4.1646270	D_{22} = -6.0865383	D_{32} = +4.7600148	D_{42} = -3.1875014
D_{13} = -48.203555	D_{23} = +40.137956	D_{33} = +11.257177	D_{43} = +12.231796
D_{14} = +140.43620	D_{24} = -76.230797	D_{34} = -66.382743	D_{44} = -12.110681
D_{15} = -195.23339	D_{25} = -133.70055	D_{35} = +69.248785	
D_{16} = +113.51500	D_{26} = +860.25349		
	D_{27} = -1535.3224		
	D_{28} = +1221.4261		
	D_{29} = -409.10539		

Table 4.2 Parameters of SAFT-BACK EoS for 44 non-polar fluids (Chen & Mi, 2001)

Component	***m***	***α***	v^{00}	u_0/k_B
Argon	1.000	1.000	12.08	149.2
Nitrogen	1.000	1.031	14.02	128.9
Oxygen	1.000	1.017	11.80	155.9
Carbon dioxide	1.348	1.067	10.95	324.3
n-Alkanes				
Methane	1.000	1.012	15.93	191.2
Ethane	1.070	1.028	21.43	308.4
Propane	1.240	1.051	25.46	387.4
Butane	1.340	1.071	29.88	457.9
Pentane	1.446	1.083	33.80	517.6
Hexane	1.573	1.097	36.64	570.7
Heptane	1.682	1.108	39.65	617.8
Octane	1.814	1.117	42.05	659.7
Nonane	1.905	1.123	45.06	698.0
Decane	2.018	1.130	47.37	732.0
Dodecane	2.255	1.137	55.10	787.5
Tetradecane	2.434	1.148	60.00	841.4
Hexadecane	2.524	1.157	65.61	893.9
Octadecane	2.786	1.162	71.14	926.5
Eicosane	3.039	1.163	84.15	950.9
Branched alkanes				
Isobutene	1.319	1.066	30.69	435.8
2-Methylbutane	1.411	1.073	34.33	501.0
2,2-Dimethylpropane	1.353	1.060	36.55	463.9
2-Metylpentane	1.541	1.088	37.41	553.3
2,2-Dimethylbutane	1.433	1.074	39.68	533.3
2,3-Dimethylbutane	1.474	1.081	38.29	550.3
3-Methylhexane	1.640	1.100	39.68	606.0
3-Ethylpentane	1.623	1.096	40.02	609.0
2,2Dimethylpentane	1.563	1.090	41.93	581.1
2,2,3-Trimethylbutane	1.488	1.080	43.04	585.0
3-Methylheptane	1.742	1.110	43.01	647.4
3,3-Dimethylhexane	1.642	1.096	44.35	635.5
3-Ethyl-2-methylpentane	1.661	1.097	43.73	642.4
2,2,3-Trimethylpentane	1.600	1.086	45.40	630.5
2,3,3-Trimethylpentane	1.575	1.087	45.92	640.6
Cycloalkanes				
Cyclopropane	1.171	1.052	21.99	416.0
Ethyl cyclopropane	1.550	1.085	38.48	632.4
Alkenes				
Ethylene	1.039	1.034	20.03	283.4
Propylene	1.202	1.047	24.22	379.5
1-Pentene	1.424	1.082	32.21	510.3
Alkynes				
Acetylene	1.254	1.064	14.18	326.6
Methyl acetylene	1.355	1.076	18.63	435.5
Aromatics				
Benzene	1.403	1.078	28.70	615.8

Toluene	1.503	1.076	33.34	655.9
p-Xylene	1.576	1.101	37.15	703.4

4.3.1 Extension to Mixtures

Mixing rules are very important for the calculation of fluids properties using different equations of state. When equations of state are used for mixtures, the mixing rules for the parameters are necessary. The parameters of SAFT-BACK EoS are considered to represent the attractive and repulsive forces between the segments.

Some researchers have used different mixing rules for the SAFT type equations of state (Chen et al (1997), Llovell et al (2006), Llovell and Vega (2007), Zhang et al (2003)), but no mixing rules have been found for the SAFT-BACK equation of state. Therefore, mixing rules are proposed in this work for the parameters of this equation.

The reference fluid is the hard-sphere (hs) which is described by the Carnahan–Starling (1969) EOS for pure fluids and Boublik–Mansoori EOS (1970, 1971) for fluid mixtures. In BACK, the term for hard-sphere is replaced by the equation for hard convex body. To take the non-sphericity of segments into account, Pfohl and Brunner (1998) used the equation of state for a hard convex body .Since the Helmholtz free energy is calculated by adding different terms, each of them should be expressed as a function of composition for mixtures studies. For the parameter *m*, the simple linear mixing rule is proposed:

$$m_{mix} = \sum_i m_i x_i \tag{4.18}$$

where x_i is the mole fraction of component *i*.

The non-sphericity parameter of a solution can be obtained from:

$$\alpha_{mix} = (\sum_i \alpha_i m_i x_i) / (\sum_i m_i x_i) \tag{4.19}$$

While for the energetic parameter, (u_{0x}), the van der Waals-like mixing rule is adopted:

$$(u_0 / k)_{mix} = \sum_i \sum_j x_i x_j (u_0 / k)_{ij} \tag{4.20}$$

Associated with the quadratic equation:

$$(u_0/k)_{ij} = \sqrt{(u_0/k)_i (u_0/k)_j}(1-k_{ij}) \tag{4.21}$$

Where k_{ij} is a binary interaction parameter and $k_{ij} = k_{ji}, \quad k_{ii} = k_{jj} = 0$

The volume fractions $\eta = \pi N_A m \rho d^3/6$ are based on the diameter of an equivalent one-component mixture:

$$d_{mix} = \left(\frac{\sum_i x_i m_i d_i^3}{\sum_i x_i m_i} \right)^{1/3} \tag{4.22}$$

Where the individual d_i are temperature-dependant segment diameters.

Binary interaction parameters were regressed for 3 different compositions of each binary mixture of normal alkanes from C_1 to nC_{10}, iC_4, iC_5, N_2 and CO_2-hydrocarbons. These regressed k_{ij} were used to predict pressure, isobaric and isochoric heat capacities and speed of sound of the investigated mixtures.

These mixing rules were proposed based on the investigations of the other molecular based equations of state (Boublik, 2007; Chen et al., 1997; Koushoumvekaki, 2004; Economou, 2002; Economou et al, 1996; Maghari et al, 2010; Llovell et al., 2006, 2007)

The isomorphism approach is used in order to apply the equation to mixtures. Following this approach the one-component density is replaced by the total density of the mixture. In addition, as shown by Kiselev and Friend (1999), choosing mole fractions as independent variables provides a good approximation to the original isomorphism assumption, although some scaling behaviour is not correctly represented.

4.4 Speed of Sound Modelling

The speed of sound has been increasingly employed to model fluid properties. Perhaps one of the main reasons is the significant improvement in experimental techniques where the measurements can be made quickly and with a high accuracy over wide ranges of temperature and pressure for the liquid and vapour phases. The literature contains several fluid modelling approaches using the speed of sound as input data

(Goodween-Moldover 1990, Trusler 1991, Estrada-Alexanders et al. 1995, Gillis-Moldover 1996, Grigiante et al. 2000, Benedetto et al. 2001, Hurly 2002, Scalabrin et al. 2002, Monago 2005). For example, Monago (2005) demonstrated that virial coefficients could be precisely calculated using measured speed of sound data. The approach was applied to gaseous argon and using the determined virial coefficients, the developed EoS could accurately predict all the interesting thermodynamic properties of the gaseous argon over a wide range of temperature.

To make use of high quality measured speed of sound data in the petroleum industry, a research study was planned using the following steps:

- Prediction of the speed of sound using various equations of state (EOS). This provides a good understanding about the capabilities and limitations of the available models, particularly CEOS.
- Developing new EOS or new potential functions using the measured speed of sound data. This can be made simply by improving the available models through fitting the parameters of EOS to experimental speed of sound data (rather than using phase equilibrium data i.e. vapour pressure and/or density data). More rigorously, a molecular thermodynamic model based on statistical mechanic theory can be designed regarding the potential energies, and its second derivatives can be matched with the measured speed of sound data.
- Molecular basis of speed of sound, however, must be understood carefully. A molecular model, therefore, explaining molecular speed of sound would be of paramount importance. Using this model the speed of sound and consequently the potential energies can be found.

Accurate modelling of speed of sound in real fluids has a special interest in reservoir fluid research as it offers an indirect way to obtain information on related thermodynamic properties, like density and heat capacity, whose direct measurement (especially at high pressure) is extremely difficult.

The speed of sound v_s can be written as

$$v_s = \left[\left(\frac{\gamma}{M} \right) \left(\frac{\partial p}{\partial \rho} \right)_T \right]^{1/2} \tag{4.23}$$

Where M is the molecular mass and $\gamma \equiv C_p/C_V$ is the heat capacity ratio.

As it is evident from Eq. (4.23), calculation of the speed of sound entails calculation of the heat capacities at constant pressure and volume and the differentiation of the pressure with respect to the volume at constant temperature. An EOS such as the PR can be used for this purpose. Since CEOS are explicit in pressure, the following exact expressions can be utilised in order to reach the required items:

$$C_v^{id} - C_v = -T\int_{\infty}^{v}\left(\frac{\partial^2 P}{\partial T^2}\right)_v dv \tag{4.24}$$

where superscript *id* stands for the ideal state. The difference between C_P and C_v can be calculated as;

$$C_P - C_v = -T\frac{\left(\frac{\partial P}{\partial T}\right)_v^2}{\left(\frac{\partial P}{\partial v}\right)_T} \tag{4.25}$$

and the heat capacity at constant pressure can be deduced as,

$$C_v^{id} = C_p^{id} - R \tag{4.26}$$

where R is the universal gas constant. Heat capacities in ideal states are just functions of temperature, and are obtainable as,

$$C_P^{id} = R\left(a_0 + a_1 T + a_2 T^2 + a_3 T^3 + a_4 T^4\right) \tag{4.27}$$

The constant values of a_0 –a_4 are available in Poling et al. (2001). There are some other functions that can be used to calculate C_P^{id}, such as: Aly and Lee (1981) and Passut and Danner (1972), but no significant difference between the ultrasound velocity values calculated using the three representations was observed.

Using an EOS, which relates the pressure to the volume and the temperature, the speed of sound can be easily calculated through the above equations.

An alternative route to obtain the second derivative properties is to employ the statistical based equations and theories such as Statistical Associating Fluid Theory (SAFT) and its derivatives. The thermodynamic properties can be obtained by differentiation of this potential with respect to temperature and density. Once the Helmholtz energy has been obtained, the pressure can be calculated through first order derivatives:

$$P = \rho^2 \left(\frac{\partial A^{res}}{\partial \rho} \right)_T \tag{4.28}$$

$$C_v = C_v^{id} - T \frac{\partial^2 A^{res}}{\partial T^2} \tag{4.29}$$

$$C_p = C_v + \frac{T}{\rho^2} \left(\left(\frac{\partial P}{\partial T} \right)_\rho^2 \Big/ \left(\frac{\partial P}{\partial \rho} \right)_T \right) \tag{4.30}$$

The compressibility factor is derived as:

$$Z = \rho \left(\frac{\partial \left(A^{res} / NkT \right)}{\partial \rho} \right)_{N,T} \tag{4.31}$$

where k is Boltzmann constant, T the temperature, ρ the number density of molecules, and N is total number of molecules.

To determine the thermodynamic properties for mixtures, the isomorphism theory is applied and the density of the total mixture is employed. Other relations are the same as the formulas for pure hydrocarbons, with the difference of using mixture parameters like m_{mix}, α_{mix}, u_{0mix} and d_{mix} in all of the formulas in the equation. The exception is calculation of ideal heat capacity which is determined as a summation of individual' ideal heat capacities of each component in the mixture:

$$P = \rho^2 \left(\frac{\partial A^{res}}{\partial \rho} \right)_{T(mixture)} \tag{4.32}$$

$$(C_p^{id})_{mixture} = \sum_i C_p^{id}(i) \tag{4.33}$$

$$(C_v^{id})_{mixture} = (C_p^{id})_{mixture} - R \tag{4.34}$$

$$(C_v)_{mixture} = (C_v^{id})_{mixture} - T(\frac{\partial^2 A^{res}}{\partial T^2})_{mixture} \tag{4.35}$$

$$(C_p)_{mixture} = (C_v)_{mixture} + \frac{T}{\rho^2}\left(\left(\frac{\partial P}{\partial T}\right)_\rho^2 \Big/ \left(\frac{\partial P}{\partial \rho}\right)_T\right)_{mixture} \tag{4.36}$$

$$v_{mixture} = \left[\left(\frac{\gamma}{M}\right)\left(\frac{\partial p}{\partial \rho}\right)_T\right]_{mixture}^{1/2} \tag{4.37}$$

The modelling of thermodynamic properties and especially speed of sound was performed for some pure and mixtures of hydrocarbon and non-hydrocarbon compounds in sub and supercritical regions. The experimental data for several pure components and mixtures were generated in this work and some corresponding values are found in NIST chemistry web book (http://webbook.nist.gov/chemistry/fluid). The modelling results will be compared with experimentally generated data and data from the literature and with correlated data in NIST in the next chapter. A table will show the average absolute percentage of results deviations from the experimental values.

4.4.1 Modelling Speed of Sound using Cubic Equations of State

In practice, the cubic equations of state generally give results in good agreement with experimental data for pure hydrocarbon and mixtures. Since amongst available CEoS, the Peng-Robinson EoS (PR) is maybe the most widely used in the petroleum industry to predict the phase and volumetric behaviour of reservoir fluids. The, PR EoS was selected for this work.

The expression for the PR-EOS is the following (Peng – Robinson, 1976):

$$P = \frac{RT}{(v-b)} - \frac{\alpha}{v(v+b)+b(v-b)} \tag{4.38}$$

Where P is pressure, v the molar volume, T the temperature, $a(T)$ the attractive parameter, b the co-volume parameter of the fluid and R is the ideal gas constant. The co-volume parameter, b, is temperature independent and is calculated using the critical temperature (Tc) and critical pressure (Pc) of the fluid as follows:

$$b = 0.0778\frac{RT_c}{P_c} \tag{4.39}$$

The temperature dependant attractive parameter, alpha (α) is calculated by the Soave-type expression:

$$\alpha = a(T_c, P_c)[1 + m(1 - T_R^{0.5})]^2 \tag{4.40}$$

Where $a(T_c, P_c) = 0.45724\frac{(RT_c)^2}{P_c}$ and $T_r = \frac{T}{T_c}$ (4.41)

Peng and Robinson correlated the parameter *m* to the acentric factor ω for light non-polar compounds, hydrocarbons up to decane and some aromatics and achieved the following expression (Robinson-Peng, 1978):

$$m = 0.37646 + 1.54226\omega - 0.26992\omega^2 \tag{4.42}$$

When $\omega > 0.49$, $m = 0.379642 + 1.485030\omega - 0.164423\omega^2 + 0.0116666\omega^3$ (4.43)

The volumetric estimations obtained through these two-parameter equations of state generally show the systematic deviations.

Peneloux et al. (1982) developed a method of improving the volumetric predictions by introducing a third parameter into a two-parameter cubic EOS. It modifies the phase volume by employing certain translations along the volume axis. This method introduces a third mixture parameter, c, into the two-parameter EOS:

$$v_{cor} = v - c \tag{4.44}$$

The third parameter has the same unit as the second parameter, so, the dimensionless shift parameter, *s*, is defined as:

$$s = \frac{c}{b} \tag{4.45}$$

For well-defined lighter hydrocarbons, the shift parameters are presented in Table 4.3. Jhaveri and Youngren (1988), introduced "*s*" as a power function in *M* as:

$$s = 1 - \frac{d}{M^e} \tag{4.46}$$

where d and e are positive correlation coefficients and are given in Table 4.4.

Table 4.3 Shift parameter for hydrocarbons

COMPONENT	s
Methane	-0.154
Ethane	-0.1002
Propane	-0.085
Isobutane	-0.0794
Normal butane	-0.0641
Isopentane	-0.0435
Normal pentane	-0.0418
Normal hexane	-0.0148

Table 4.4 Shift parameter correlation coefficients for hydrocarbons heavier than hexanes

Component type	Correlation coefficient		D (%)
	D	*e*	
n-alkanes	2.258	0.1823	0.19
n-alkylcyclohexanes	3.004	0.2324	0.28
n-alkylbenzenes	2.516	0.2008	0.24

Using the three-parameter Peng-Robinson equation of state, the pressures of 10 light normal-alkanes were modelled over a wide range of density and temperatures 300, 400 and 500 K and the results are indicated in Table 4.11.

Deviations of calculated pressure using Peng-Robinson equation of state from correlated data are not negligible (up to 45% deviation). Improving this equation employs applicable variations in some parameters and functions, such as utilizing different alpha functions, various correlations of shift parameter and other tuning methods. In this way, the Mathias-Copeman (1983) alpha function, the Lin and Duan (2005) correlation method for shift parameter and some other correlations were used. These different alpha functions and correlations could give a small improvement to the results. But these improvements are not applicable for a wide range of temperature. This certainly affects the other properties obtained by differentiation of pressure with respect to density and temperature like C_p, C_v and V_s. These thermodynamic properties can be calculated using Equations 4.23 - 4.27 described earlier in this chapter.

Tuning parameters of the Peng-Robinson equation of state can improve the results over a limited range of temperature. So many different theories and functions were proposed

for the volume translation parameter. Some of authors could show the negligible effects of temperature-dependant volume translation function (Peneloux et.al., 1982), some others decided not to use temperature-dependency in volume translation and used the constant volume translation only (Ahlers et. al., 2001). On the other hand, it was shown (Frey et. al., 2007) that only using a temperature-dependent volume translation is not sufficient to predict the phase behaviour of fluids, but it should be a function of density. The approach of dependency of volume translation to both temperature and density was originally attributed to Mathias et al (1989). Chou and Prausnitz (1989) with this approach, created a new volume translation that was a function of temperature and density for each hydrocarbon to enable this equation to predict thermodynamic properties with high accuracy. The new equation of state no longer remains cubic, so the complexity of the equation is increased. With this variation, for improvement of phase equilibrium calculations, alpha function should be re-regressed Kutney et al (1997). Because this translation could not easily be used to calculate fugacities and other derived thermodynamic properties, the limitations of Mathias et al. (1989) approach caused this function to be used only for volume corrections, not for other derived properties.

Here, the results of modelling with another alpha functions such as Mathias and Copeman (1983), Twu et al. (1995) and Chapoy (2004) are presented.

- The Mathias-Copeman alpha function is written as below:

IF $T<T_c$ $$\alpha(T_R) = \left[1 + c_1(1 - T_R^{1/2}) + c_2(1 - T_R^{1/2})^2 + c_3(1 - T_R^{1/2})^3\right]^2 \quad (4.47)$$

IF $T>T_c$ $$\alpha(T_R) = \left[1 + c_1(1 - T_R^{1/2})\right]^2 \quad (4.48)$$

T_R and T_c are reduced and critical temperatures, respectively. c_1, c_2, and c_3 are three constants for each component which are tuned and listed in Table 4.5 below.

Table 4.5 Parameters C_1, C_2 and C_3 for the Mathias-Copeman alpha function in Peng-Robinson equation of state

Component	C_1	C_2	C_3
Methane	0.41574	-0.17265	0.34842
Ethane	0.53125	-0.06181	0.21424
Propane	0.60007	-0.00630	0.17390
n-Butane	0.67734	-0.08109	0.29854
n-Pentane	0.76286	-0.22431	0.66951
n-Hexane	0.87026	-0.58796	1.50392
n-Heptane	0.87765	-0.03073	0.30187
n-Octane	0.95827	-0.13407	0.48666
n-Nonane	1.00870	-0.08230	0.46275
n-Decane	1.09326	-0.23359	0.71649

- Twu et al. (1995) created this alpha function for the Peng-Robinson equation of state:

$$\alpha(T_R) = \alpha^{(0)}(T_R) + \omega(\alpha^{(1)}(T_R) - \alpha^{(0)}(T_R)) \tag{4.49}$$

Where $$\alpha^{(i)}(T_R) = T_R^{N(M-1)}[\exp(L(1-T_R^{NM}))] \tag{4.50}$$

Parameters L, M and N are listed in Table 4.6.

Table 4.6 Parameters L, M and N for the Twu et al. alpha function in Peng-Robinson equation of state

Parameters	$T_R \le 1$		$T_R > 1$	
	$\alpha^{(0)}(T)$	$\alpha^{(1)}(T)$	$\alpha^{(0)}(T)$	$\alpha^{(1)}(T)$
L	0.125283	0.511614	0.401219	0.024955
M	0.911807	0.784054	4.963075	1.248088
N	1.948153	2.812522	-0.200000	-8.000000

- Chapoy (2004) proposed a new alpha function which is a combination of both mathematical forms of TB and Mathias-Copeman alpha functions and is related to acentric factor of the fluid:

$$\alpha(T) = \exp[c_1(1-T_R)] \times \left[1 + c_2(1-T_R^{1/2})^2 + c_3(1-T_R^{1/2})^3\right]^2 \tag{4.51}$$

Where

$$C_1 = 0.1441\omega^2 + 1.3838\omega + 0.387 \tag{4.52}$$

$$C_2 = -2.5214\omega^2 + 0.6939\omega + 0.0325 \quad (4.53)$$

$$C_3 = 0.6225\omega + 0.2236 \quad (4.54)$$

- Jhaveri and Youngren (1988) proposed a third parameter function which was earlier shown in this chapter:

$$c = s.b$$

where $s = 1 - \frac{d}{M^e}$ and "d" and "e" are positive correlation coefficients and are given in Table 4.4.

- Lin et al. (2005) presented an empirical correction to improve the Peng-Robinson equation of state. A temperature-dependent volume correction is employed to improve the original PR-EOS which is generalized as a function of critical parameters and the reduced temperature, because a constant volume translation, c, cannot satisfy the entire saturated region (Ahlers and Gmehling, 2001), a temperature dependent parameter is considered as follows:

$$c(T) = c_c f(T_r) \quad (4.55)$$

Where c_c is the critical volume translation:

$$c_c = (vPR)_c - (v\exp)_c = (0.3074 - Z_c)\frac{RT_c}{P_c} \quad (4.56)$$

where Z_c is the critical compressibility factor. At the reduced temperature T_r =1.0, the *f*-function in Equation (4.55) should be unity, because the volume translation must be equal to the critical volume translation in Equation (4.56). Therefore, the form of the temperature-dependant function $f(T_r)$ is assumed to be:

$$f(T_r) = \beta + (1-\beta)\exp(\gamma|1 - T_r|) \quad (4.57)$$

Where β and γ are two parameters which can be determined by fitting experimental liquid densities, also they can be generalized by the following functions:

$$\beta = -2.8431\exp[-64.2184(0.3074 - Z_c)] + 0.1735 \quad (4.58)$$

$$\gamma = -99.2558 + 301.6201 Z_c \tag{4.59}$$

- Tsai and Chen (1998) applied a volume-translated PR (VTPR) EOS to vapour-liquid equilibrium (VLE) calculations for non-polar and polar components with good liquid density predictions. "*t*", is taken as the following temperature-dependent form in correlating the saturated properties:

$$t = \frac{RT_c}{P_c}\left[k_1 + k_2(1 - T_R^{2/3}) + k_3(1 - T_R^{2/3})^2\right] \tag{4.60}$$

It is found that k_1 can be expressed as a function of the acentric factor, k_3 is left as another pure fluid parameter, and k_2 can be expressed as a function of k_3:

$$k_1 = 0.00185 + 0.00438\omega + 0.36322\omega^2 - 0.90831\omega^3 + 0.55885\omega^4 \tag{4.61}$$

$$k_2 = -0.00542 - 0.51112k_3 + 0.04533k_3^2 + 0.07447k_3^3 - 0.03831k_3^4 \tag{4.62}$$

k_3 have been regressed for over 130 pure components and their values are listed in tabular form in their paper (Tsai & Chen, 1998).

- Hoyos (2004) proposed a new correction equation to calculate the specific volume of liquid hydrocarbons from C_1 to C_8, which does not require additional parameters for each substance and can be applied in a wide temperature range:

$$V_{corr} = C_{PR} + \left(\frac{C_1}{C_2}\right)C_2 + C_2(T_r - C_3)^2 \tag{4.63}$$

At the particular reduced temperature value where the PR equation does not need correction, the C_1/C_2 ratio can be calculated as a polynomial function of the acentric factor as follows:

$$\frac{C_1}{C_2} = 110.07\omega^4 - 83.807\omega^3 + 18.926\omega^2 - 1.6348\omega - 0.0066 \tag{4.64}$$

The C_2 constant remains as a degree of freedom, which is found as the value that minimizes the average of absolute of relative deviations for all substances, yielding:

$$C_2 = 2.013645 * 10^{-3} \ m^3/kg \tag{4.65}$$

The value of C_3 is obtained as the average of reduced temperature where the maximum deviation of the original PR equation for saturated liquid volumes occurs, yielding:

$$C_3 = 0.89. \tag{4.66}$$

For comparison between the performance of these different alpha functions and shift parameters, the pressure modelling was performed for liquid n-pentane using these different third parameters equations. The results are displayed in Figure 4.3.

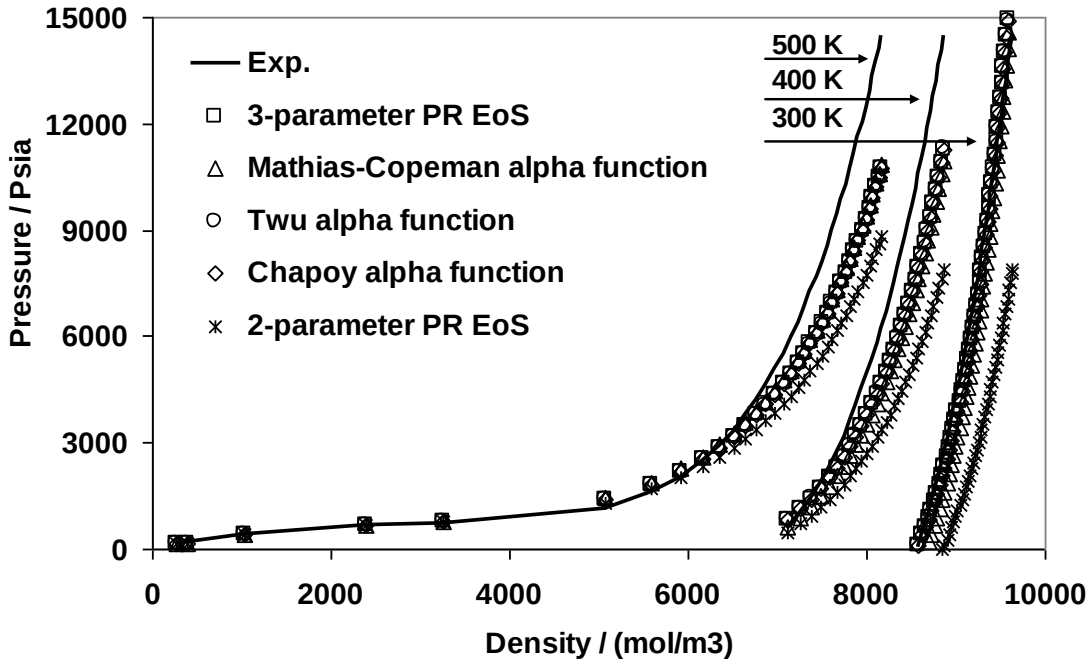

Figure 4.3 Pressure vs. density for n-Pentane in different temperatures and densities using various alpha functions

This figure shows the equal effects of alpha functions on pressure. In Figure 4.3, the Peng-Robinson equation of state was used to calculate the pressure of n-pentane for different temperatures and densities using four alpha functions. No significant improvement can be observed compared to the original PR EoS.

Also, to investigate the performance of other cubic equations of state, two equations of state were selected to model these properties, i.e., SRK and VPT. The results are discussed and displayed in Figure 4.4. This figure indicates the monotonous performance of SRK EoS with different alpha functions. Results obtained by SRK EoS

are reasonable at higher temperatures and are better than the results by PR EoS, but they are not reliable at lower temperatures than 500 K (226.85 °C). These figures proved that the 3-parameter PR gives the best performance in comparison with two other cubic equations of state for modelling of thermodynamic properties. The next section provides mixing rules for calculation of thermodynamic properties of hydrocarbon mixtures using PR EoS.

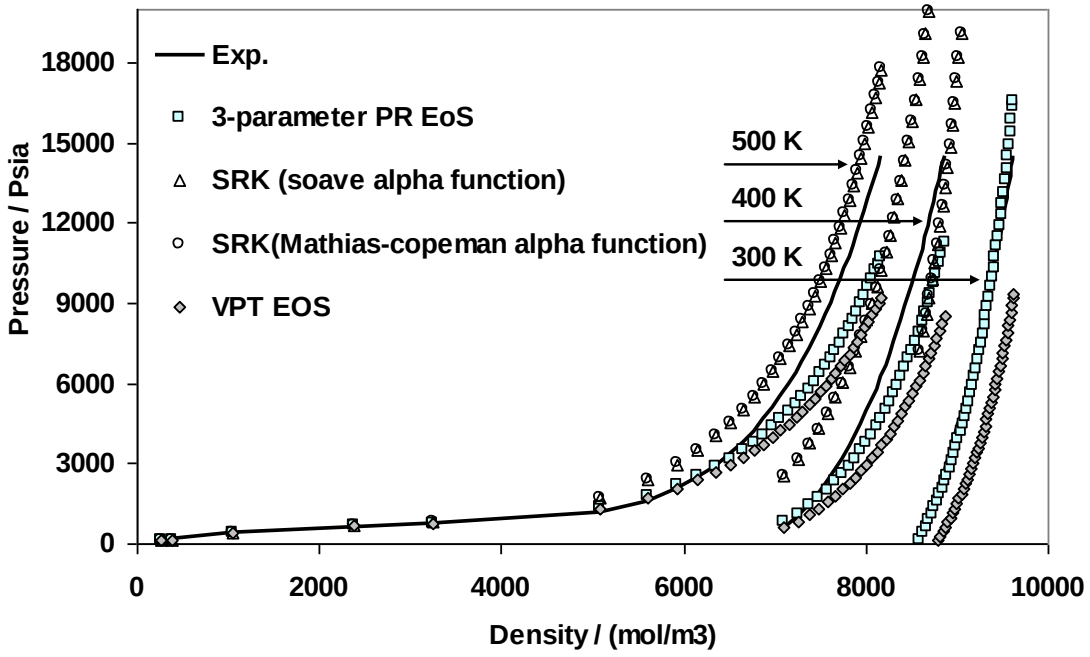

Figure 4.4 Pressure vs. density for n-Pentane in different temperatures and densities using three various cubic EoS (PR-SRK-VPT)

4.4.2 Extension of Peng-Robinson Equation of State to Mixtures

For mixtures, cubic EOS like PR, are widely applied using the van der Waals one fluid mixing rules:

$$a_{mix} = \sum_i \sum_j x_i x_j a_{ij} \tag{4.67}$$

$$a_{ij} = (a_i a_j)^{0.5}(1 - k_{ij}) \tag{4.68}$$

$$b_{mix} = \sum_i x_i b_i \tag{4.69}$$

k_{ij} is a binary interaction parameter.

The third parameter in a mixture is related through a linear mixing rule to a third parameter of each component:

$$c = \sum_i x_i c_i \tag{4.71}$$

The simplest mixing rule is applied to isobaric and isochoric heat capacities:

$$C_V^m = \sum_i C_{Vi} . x_i \tag{4.72}$$

$$C_P^m = \sum_i C_{Pi} . x_i \tag{4.73}$$

The speed of sound can be calculated using the above data and Equation 4.23.

Using the above equations, pressure modelling was done using PR EoS for three binary mixtures: *n*C_5-*n*C_6, *n*C5-*n*C_7 and *n*C_6-*n*C_7. The results are presented in Tables 4.7-4.9. The displayed results in these tables are predicted values of pressure at three different temperatures and only one pressure, i.e., 4,351.13 psi (30 MPa). Note that the results of these predictions for pressures of 10 and 20 MPa will not be indicated here. Therefore, AD%s in the last columns of these tables are the average of deviations of predicted values from the experimental data at three pressures, i.e., 1,450.37, 2,900.75, 4,351.13 Psia (10, 20, 30 MPa). However, the results did not match the experimental data very accurately and the AAD% varies from 0.49% to more than 20% depending on the temperature and composition. This indicates that further work is required in order to extend the PR EOS to mixtures.

Table 4.7 Pressure calculations using PR EoS for different mixtures of nC_5-nC_6

T / K	C_5 (mole %)	C_6 (mole %)	P/ psia (CAL) *	AD%
298.15	12.2	87.8	4214.27	3.20
	12.4	87.6	4196.33	3.63
	25.0	75.0	4197.75	3.28
	24.8	75.2	4174.19	3.82
	37.2	62.8	4080.50	6.58
	37.4	62.6	4156.75	4.02
	49.9	50.1	4063.92	6.75
	49.7	50.3	4083.27	5.83
	62.2	37.8	4013.94	7.96
	62.4	37.6	4027.81	7.38
	75.0	25.0	3954.36	9.47
	74.3	25.7	3972.22	8.88
	87.4	12.6	3934.84	9.71
	87.2	12.8	3932.83	9.85
323.15	12.2	87.8	3496.52	23.06
	12.4	87.6	3476.63	23.73
	25.0	75.0	3536.59	21.47
	24.8	75.2	3509.59	22.33
	37.2	62.8	3469.07	23.22
	37.4	62.6	3529.65	21.32
	49.9	50.1	3508.48	21.55
	49.7	50.3	3508.41	21.45
	62.2	37.8	3500.63	21.38
	62.4	37.6	3492.88	21.66
	75.0	25.0	3477.25	21.77
	74.3	25.7	3498.70	21.14
	87.4	12.6	3495.23	20.90
	87.2	12.8	3467.10	20.06
348.15	12.2	87.8	3100.54	30.94
	12.4	87.6	3083.72	31.35
	25.0	75.0	3152.27	28.88
	24.8	75.2	3115.51	28.82
	37.2	62.8	3089.19	30.44
	37.4	62.6	3137.11	28.96
	49.9	50.1	3160.04	27.90
	49.7	50.3	3147.66	28.29
	62.2	37.8	3181.04	26.87
	62.4	37.6	3175.73	27.03
	75.0	25.0	3192.13	26.17
	74.3	25.7	3193.11	26.09
	87.4	12.6	3224.27	24.73
	87.2	12.8	3183.03	25.97
			AAD%	**18.76**

* Calculated pressure using PR EoS (experimental pressure = 4351.13 Psia)

Table 4.8 Pressure calculations using PR EoS for different mixtures of nC_6-nC_7

T / K	C_6 (mole %)	C_7 (mole %)	P/ psia (CAL)	AD%
298.15	12.4	87.6	5837.08	45.18
	12.5	87.5	5848.73	46.28
	24.9	75.1	5589.05	38.65
	24.9	75.1	5516.37	35.91
	37.5	62.5	5363.38	31.64
	37.6	62.4	5361.88	31.57
	49.8	50.2	5037.79	21.51
	49.8	50.2	5131.04	24.55
	62.5	37.5	4935.86	18.88
	62.5	37.5	4841.52	15.44
	75.0	25.0	4691.36	11.08
	73.4	26.6	4724.61	12.40
	87.4	12.6	4473.53	4.39
	84.0	16.0	4549.95	6.78
323.15	12.4	87.6	4417.09	3.19
	12.5	87.5	4425.75	3.32
	24.9	75.1	4257.33	2.89
	24.9	75.1	4238.82	2.84
	37.5	62.5	4144.64	5.13
	37.6	62.4	4149.36	4.92
	49.8	50.2	3973.89	9.95
	49.8	50.2	4024.11	8.53
	62.5	37.5	3913.55	11.55
	62.5	37.5	3883.35	12.52
	75.0	25.0	3803.04	14.73
	73.4	26.6	3812.95	14.57
	87.4	12.6	3670.68	18.37
	84.0	16.0	3696.27	17.79
348.15	12.4	87.6	3554.61	19.55
	12.5	87.5	3548.59	19.91
	24.9	75.1	3456.65	22.53
	24.9	75.1	3418.44	23.65
	37.5	62.5	3431.34	23.05
	37.6	62.4	3404.46	23.74
	49.8	50.2	3323.50	25.86
	49.8	50.2	3322.21	25.99
	62.5	37.5	3282.23	26.76
	62.5	37.5	3304.92	26.12
	75.0	25.0	3239.57	27.78
	73.4	26.6	3239.28	27.62
	87.4	12.6	3165.00	29.76
	84.0	16.0	3164.75	29.76
			AAD%	**19.68**

Table 4.9 Pressure calculations using PR EoS for different mixtures of nC_5-nC_7

T / K	C_5 (mole %)	C_7 (mole %)	P/ psia (CAL)	AD%
298.15	12.6	87.4	5800.38	45.38
	12.2	87.8	5638.59	39.63
	25.0	75.0	5492.89	36.35
	25.0	75.0	5538.00	37.24
	37.1	62.9	5170.47	26.42
	37.3	62.7	5258.85	29.44
	50.2	49.8	4925.58	19.90
	49.7	50.3	4922.35	19.48
	62.5	37.5	4737.34	14.57
	62.5	37.5	4679.39	12.92
	74.9	25.1	4434.39	5.32
	75.1	24.9	4395.03	4.24
	87.7	12.3	4135.61	3.48
	87.4	12.6	4104.26	4.73
323.15	12.6	87.4	4424.52	3.59
	12.2	87.8	4364.29	2.71
	25.0	75.0	4287.06	3.19
	25.0	75.0	4294.25	3.11
	37.1	62.9	4147.17	3.86
	37.3	62.7	4170.30	3.84
	50.2	49.8	4024.13	6.76
	49.7	50.3	4035.58	6.45
	62.5	37.5	3944.10	8.77
	62.5	37.5	3908.81	9.77
	74.9	25.1	3788.99	12.66
	75.1	24.9	3748.17	13.93
	87.7	12.3	3619.65	17.32
	87.4	12.6	3603.04	17.76
348.15	12.6	87.4	3592.76	18.27
	12.2	87.8	3537.33	19.93
	25.0	75.0	3532.26	19.32
	25.0	75.0	3528.26	19.46
	37.1	62.9	3488.89	19.96
	37.3	62.7	3497.29	19.79
	50.2	49.8	3451.40	20.24
	49.7	50.3	3468.88	19.77
	62.5	37.5	3433.14	20.06
	62.5	37.5	3411.08	20.77
	74.9	25.1	3371.94	21.24
	75.1	24.9	3342.15	22.13
	87.7	12.3	3289.51	22.98
	87.4	12.6	3285.07	23.22
			AAD%	**16.67**

Regarding the comparison of AAD% of the results of modelling using the PR and SAFT-BACK equations (Tables 4.10 and 4.11), it is clear that SAFT-BACK gives better results than PR over this range of temperature and density. Therefore, SAFT-BACK was selected as a reliable and accurate equation of state to model thermodynamic properties of pure, binary and multi-component mixtures. The results of the modelling will be discussed in the next chapter.

Table 4.10 Absolute average deviations for modelling thermodynamic properties using the SAFT-BACK equation of state for 10 n-alkanes (Heriot-Watt University- Report PVT/08/1)

Component	No. of Samples	AAD% (P)*	AAD% (C_V)*	AAD% (C_P)*	AAD% (V_S)*
Methane	908	1.91	1.97	1.43	1.35
Ethane	806	1.16	0.79	0.15	1.28
Propane	808	1.63	0.93	0.47	1.32
n-Butane	805	1.33	0.71	0.75	1.40
n-Pentane	805	1.31	0.58	0.28	1.17
n-Hexane	806	1.61	0.45	0.28	1.31
n-Heptane	803	1.41	0.73	0.26	1.47
n-Octane	604	1.72	1.46	0.90	0.80
n-Nonane	255	1.42	0.91	1.07	0.87
n-Decane	370	1.46	0.93	0.59	1.60

** P, C_V, C_P and Vs stand for pressure, isochoric heat capacity, isobaric heat capacity and the speed of sound respectively.*

Table 4.11 Absolute average deviations for modelling thermodynamic properties using the Peng-Robinson equation of state for 10 n-alkanes (Heriot-Watt University- Report PVT/08/2)

Component	AAD% (P)*	AAD% (CV)*	AAD% (CP)*	AAD% (VS)*
Methane	3.32	1.40	1.01	7.70
Ethane	7.28	2.51	1.43	8.01
Propane	14.95	3.13	1.29	11.65
n-Butane	18.35	4.03	1.35	13.58
n-Pentane	17.14	4.03	2.06	13.96
n-Hexane	21.86	4.09	2.38	16.01
n-Heptane	43.78	3.45	2.52	19.26
n-Octane	44.92	2.89	2.92	16.68
n-Nonane	34.30	3.03	3.40	23.46
n-Decane	38.12	2.63	1.81	21.22

**- P, C_V, C_P and Vs stand for pressure, isochoric heat capacity, isobaric heat capacity and the speed of sound respectively.*

4.5 Modelling of thermodynamic properties of Pseudo-components and real oils using SAFT-BACK Equation of State

Petroleum reservoir fluids can be composed of thousands of hydrocarbon components and non-hydrocarbon components such as N_2, CO_2 and H_2S . A full description of the fluid by identifying all its constituents may not be possible. So, a real reservoir oil is commonly described by discrete hydrocarbon components up to C_6 and the non-hydrocarbon gases, such as N_2, CO_2, H_2S and hydrocarbon groups for heavier fractions. Most pressure-temperature-volume (PVT) studies investigate the fluids composed of components with carbon numbers from 1 to 6 individually listed and hydrocarbon fractions with carbon numbers greater than 6 are characterized in several groups of single carbon numbers (SCN). The hydrocarbon groups are generally determined according to their boiling points by distillation and/or gas chromatography. The distilled hydrocarbon groups are characterized by measuring some of their properties such as the average boiling point temperature, molecular weight and density (Danesh, 1998).

Katz and Firoozabadi (1978) presented a generalized set of boiling point, specific gravity and molecular weight for the petroleum fractions from C_6 through C_{45}. Whitson revised the original physical data and the inconsistency of the molecular weight was improved by using Riazi and Daubert (1980) correlations to extrapolate data from C_{22} to C_{45}. Physical properties of SCNs are listed in Table 4.12.

Table 4.12 Physical properties of single carbon number groups (Whitson, 1983)

SCN	Molecular Weight	Boiling Point	Specific Gravity	Acentric Factor	Watson Char. Fact.
	kg/kmol	K	Rel.dens.@ 288K		
C_6	84	337	0.690	0.251	12.27
C_7	96	366	0.727	0.28	11.97
C_8	107	390	0.749	0.312	11.87
C_9	121	416	0.768	0.352	11.82
C_{10}	134	439	0.782	0.389	11.82
C_{11}	147	461	0.793	0.429	11.85
C_{12}	161	482	0.804	0.467	11.86
C_{13}	175	501	0.815	0.501	11.85
C_{14}	190	520	0.826	0.536	11.84
C_{15}	206	539	0.836	0.571	11.84
C_{16}	222	557	0.843	0.61	11.87
C_{17}	237	573	0.851	0.643	11.87
C_{18}	251	586	0.856	0.672	11.89
C_{19}	263	598	0.861	0.698	11.90

C_{20}	275	612	0.866	0.732	11.93
C_{21}	291	624	0.871	0.759	11.93
C_{22}	300	637	0.876	0.789	11.95
C_{23}	312	648	0.881	0.815	11.95
C_{24}	324	659	0.885	0.841	11.96
C_{25}	337	671	0.888	0.874	11.99
C_{26}	349	681	0.892	0.897	12.00
C_{27}	360	691	0.896	0.944	12.00
C_{28}	372	701	0.899	0.968	12.02
C_{29}	382	709	0.902	0.986	12.03
C_{30}	394	719	0.905	1.008	12.04
C_{31}	404	728	0.909	1.026	12.04
C_{32}	415	737	0.912	1.046	12.05
C_{33}	426	745	0.915	1.063	12.05
C_{34}	437	753	0.917	1.082	12.07
C_{35}	445	760	0.920	1.095	12.07
C_{36}	456	768	0.922	1.114	12.08
C_{37}	464	774	0.925	1.124	12.07
C_{38}	475	782	0.927	1.142	12.09
C_{39}	484	788	0.929	1.154	12.09
C_{40}	495	796	0.931	1.172	12.11
C_{41}	502	801	0.933	1.181	12.11
C_{42}	512	807	0.934	1.195	12.13
C_{43}	521	813	0.936	1.207	12.13
C_{44}	531	821	0.938	1.224	12.14
C_{45}	539	826	0.940	1.232	12.14

The Watson characterization factor, K_w, is an empirical tool for expressing the approximate relative paraffinicity of a petroleum fraction by a single number. The magnitude of K_w provides the information about an oil fraction such as the type of crude oil. Physical properties such as density, or specific gravity, average boiling point can be used for estimating the Watson K_w factor of a particular oil fraction.

The Watson Characterisation factor which is sometimes recognized as the UIP (Universal Oil Products) characterisation factor, K_w, is calculated via various equations and properties. In this work, K_w is calculated as follows:

$$K_w = \frac{(1.8T_b)^{1/3}}{SG} \tag{4.74}$$

Where T_b and SG are the boiling temperature in K and the specific gravity, respectively.

The SAFT-BACK EoS parameters for pure fluids were obtained by regression with the minimization of the objective function after calculation of critical properties and

vapour-liquid equilibria (Chen & Mi, 2001). It can be shown that these parameters are in a linear relation with molecular weight of each type of hydrocarbons. Since all of the single carbon numbers have K_w less than 12.5 and it is assumed that they are in Naphthenic and Aromatics range, the relations between the SAFT-BACK parameters of naphthenic and Aromatic compounds and Molecular weight are used to determine these parameters for single carbon numbers as follow:

$$m = 0.0065 * MW + 0.8983 \tag{4.75}$$

$$m\alpha = 0.0079 * MW + 0.8986 \tag{4.76}$$

$$mu^0 = 9.3892 * MW + 102.66 \tag{4.77}$$

Mixing rules 4.17 – 4.21 are used for calculation of these parameters in mixtures.

By minimizing the deviations between experimental and predicted values of speed of sound in real oils, a temperature-molecular weight dependant binary interaction parameter, k_{ij}, has been established for the calculation of the dispersion energy between the segments in a mixture:

$$k_{ij} = a + b * T + c * MW \tag{4.78}$$

Where a, b and c are the following constants:

$$a = 9.439E - 01 \tag{4.79}$$

$$b = -1.830E - 03 \tag{4.80}$$

$$c = -7.826E - 04 \tag{4.81}$$

Thermodynamic properties of mixtures containing SCNs are calculated using Equations 4.28 – 4.37. A new equation is suggested for calculation of the ideal isobaric heat capacity of SCNs which is a function of the Watson characterisation number, acentric factor and temperature:

$$C_p^0 = -0.33886 + 0.02827K - \left(0.9291 - 1.1543K + 0.0368K^2\right)\times 10^{-4}T - 1.6658\times 10^{-7}T^2 - A\times\left[0.26105 - 0.59332\omega - \left(4.56 - 9.48\omega\right)\times 10^{-4}T - \left(0.536 - 0.6828\omega\right)\times 10^{-7}T^2\right] \quad (4.82)$$

The factor 'A' is given by:

$$A = \left[\left(12.8 - K\right)\left(10 - K\right)/\left(10\omega\right)\right]^2 \quad (4.83)$$

Therefore, modelling of speed of sound of real oils should be done for the calculation of the properties of real oil. At this step, the parameters of equation of state will be related to the physical properties of SCNs such as molecular weight of each compound. The next step is to develop this method to the properties of petroleum fractions and modify the equation in order to enable them for calculation of velocity of sound for real reservoir fluids. The experimental results of speed of sound of petroleum fractions are required to develop this correlation for mixtures. Some researchers measured speed of sound in synthetic and a real distillation cut (Lagourette et al., 1999). These results and other useful data will be used in the future to model the velocity in real oils.

4.6 Summary about the programming

An extensive programming was performed for the modelling of the thermodynamic properties in this work from the beginning. The language used for this purpose was FORTRAN. All of the SAFT-BACK parameters have been added to the program. First, the code asks for the components and their molar percentage for the composition, temperature and also, density as input data. The program starts to run, calculating four terms of equation, differentitaion of Helmholtz energy with respect to temperature and density, calculating pressure, differentiation of pressure with respect to temperature and density, calculating ideal isobaric heat capacity, isochoric and isobarik heat capacity and finally the speed of sound. The binary interaction parameters for this modelling were regressed using a Simplex method with a lot of data for binary mixtures from NIST webbook and the literatures. They have been defined in the program after regression. The program can also work and give the results if the pressure and temperature of the mixture are entered as input data, instead of density and temperature.

4.7 Conclusion

This chapter of the thesis aimed to review and develop a reliable thermodynamic model capable of describing accurately thermodynamic properties and especially speed of sound multi-component mixtures. Several equations from different classes of thermodynamic functions in terms of simplicity and complexity of functional forms were evaluated for their capability in predicting second order derivative properties such as speed of sound. The Peng-Robinson, VPT, SRK equations from the simple class, and SAFT-BACK equation from the complex family are selected for this purpose.

The results have demonstrated the superiority of the SAFT-BACK equation of state over the cubic equations, especially at the liquid region or the high density conditions.

These results imply the deficiency of cubic equations of state in predicting second derivative properties. It must be noted that the capability of cubic equations of state in performing phase equilibrium calculation of pure and multi-components mixtures, including petroleum fluids have been demonstrated. Moreover, main advantages of CEOS over the statistical based equations such as SAFT is simple mathematical form. Superiority of simple CEOS over complex SAFT equation has been demonstrated through applying these approached in calculating vapour liquid equilibrium of binary and multi-component mixtures by Voutsas et al. (2006), showing that complexity offers no significant advantages over simplicity when dealing with first order derivative properties. However, based on the results of this study, the second order derivatives of fluids cannot be predicted reliably by CEOS.

REFERENCES:

Ahlers J., Gmehling J., 2001, *Development of an universal group contribution equation of state: I. Prediction of liquid densities for pure compounds with a volume translated Peng–Robinson equation of state*, Fluid Phase Equilibria, **191(1-2)**, 177-188

Aim K., Boublik T., 1986, *Vapor-liquid equilibrium calculations with the back equation of state*, Fluid Phase Equilibria, **29**, 583–591.

Alder B.J., Young D.A., Mark M.A., 1972, *Studies in molecular dynamics. X. Correction to the augmented van der Waals theory for the square well fluid*, Chem. Phys., **56**, 3013–3029.

Aly F.A., Lee L., 1981, *Self-Consistent equations for calculating the ideal gas heat capacity, enthalpy, and entropy*, Fluid Phase Equilibria **6**, 169-179

Benedetto G.; Gavioso R. M.; Spagnolo R.; Grigiante M.; Scalabrin G.; 2001, *Vapour-phase helmholtz equation for HFC-227ea from speed-of-sound measurements*, Int. J. Thermophys., **4**, 1073-1088.

Boublik T., 1970, *Hard-sphere equation of state*, Journal of Chemical Physics, **53**, 471-472

Boublik T., 1975, *Hard convex body equation of state*, The Journal of Chemical Physics, **63**, 4084.

Boublik T., 2007, *BACK eqution of state for simple compounds*, Journal of Molecular Liquids, **134**, 151-155

Carnahan N.F., Starling K.E., 1969, *Equation of state for nonattracting rigid spheres*, The Journal of Chemical Physics, **51(2)**, 635-636

Chapman W.G., Gubbins K.E., Jackson G., Radosz M., 1989, *Equation of state solution model for associating fluids*, Fluid Phase Equilibria. **52**, 31.

Chapman W.G., Gubbins K.E., Jackson G., Radosz M., 1990, *New reference equation of state for associating liquids*, Ind. Eng. Chem. Res. **29**, 1709.

Chapoy A., 2004, *Phase behaviour in water/hydrocarbon mixtures involved in gas production systems*, PhD thesis

Chen J., Mi J.g., 2001, *Equation of state extended for SAFT with improved results for non-polar fluids across the critical point fluid,* Phase Equilibria, **186**, 165–184.

Chen S.S., Kreglewski A., 1977, *Applications of the augmented van der Waals theory of fluids. I. Pure fluids. Ber. Bunsen-Ges.* Phys. Chem., **81**, 1048–1052.

Chen J., Lu J., Li Y., 1997 , *Mixing rules for hardsphere chain mixtures and their extension to heteronuclear hardsphere polyatomic fluids and mixtures*, Fluid Phase Equilibria, **140**, 37-51

Chou G., Prausnitz J.M., 1989, *A phenomenological correction to an equation of state for the critical region,* AICHE Journal, **35**, 1487-1496

Danesh A., 1998, *PVT and phase behaviour of petroleum reservoir fluids*.

Economou I.G., Tsonopoulos C., 1996, *Associating models and mixing rules in equations of state for water/hydrocarbon mixtures*, Chemical Engineering Science, **52(4)**, 511-525

Economou I.G., 2002, *Statistical Associating Fluid Theory: A successful model for the calculation of thermodynamic and phase equilibrium properties of complex fluid mixtures,* Ind. Eng. Chem. Res., **41**, 953-962.

Estrada-Alexanders A.F., Trusler J.P.M., Zarari M.P., 1995, *Determination of thermodynamic properties from the speed of sound*, Int. J. Thermophysical., **16**, 663-673.

Frey K., Augustine C., Ciccolini R.P., Paap S., Modell M., Tester J., 2007, *Volume translation in equation of state as a means of accurate property estimation*, Fluid Phase Equilibria, **260**, 316-325

Gillis K.A., Moldover M.R., 1996, *Practical determination of gas densities from the speed of sound using square-well potentials*, Int. J. Thermophysical, **17**, 1305-1324.

Goodwin A.R.H., Moldover M.R., 1990, *Thermophysical properties of gaseous refrigerants from speed of sound measurement. I. Apparatus, model, and results for 1,1,1,2-tetrafluroethane R134a*, J. Chem. Phys., **93**, 2741-2753.

Gregorowicz J., O'Connell J.P., Peters C.J., 1996, *Some characteristics of pure fluid properties that challenge equation-of-state models*, Fluid Phase Equilibria, **116**, 94-101

Grigiante M., Scalabrin G., Benedetto G., Gavioso R.M., Spagnolo R., 2000, *Vapour phase acoustic measurements for R125 and development of a Helmholtz free energy equation*, Fluid Phase Equilibria, **174**, 69-79.

Heriot-Watt University, Reservoir Fluid Studies, 2005 – 2008 Programme, Progress Report, January 2008, Report Number PVT/08/1 (2008)

Heriot-Watt University, Reservoir Fluid Studies, 2005 – 2008 Programme, Progress Report, August 2008, Report Number PVT/08/2 (2008)

Hoyos B., 2004, *Generalized liquid volume shifts for the Peng-Robinson equation of state for C_1 to C_8 hydrocarbons*, Latin American Applied Research **34**, 83-89

Huang S.H., Radosz M., 1990, *Equation of state for small large, polydisperse and associating molecules*, Ind. Eng. Chem. Res. **29**, 2284.

Huang S.H., Radosz M., 1991, *Equation of state for small large, polydisperse and associating molecules: extensions to mixtures*, Ind. Eng. Chem. Res. **30**, 1994.

Hurly J.J., 2002, *Thermophysical properties of chlorine from speed-of-sound measurements*, Int. J. Thermophysical, **23**, 455-475.

Jhaveri B., Youngren G., 1988, *Three-parameter modification of the Peng-Robinson equation of state to improve volumetric predictions*, SPE Reservoir Engineering,

Katz D.L., Firoozabadi A., 1978, *Predicting phase behaviour of condensate/crude oil systems using methane interaction coefficients*, JPT, 1649-1655.

Kiselev S.B., 1998, *Cubic crossover equation of state*, Fluid Phase Equilibria, **147**, 7-23

Kiselev S.B., Ely J.F., 2004, *Crossover description of the thermodynamic and transport properties in pure fluids*, Fluid Phase Equilibria, **222–223**, 149–159

Kiselev S.B., Friend D.G., 1999, *Cubic crossover equation of state for mixtures*. Fluid Phase Equilibria, **162 (1–2)**, 51–82

Kostrowicka Wyczalkowska A., Sengers J.V., Anisimov M.A., 2004, *Critical fluctuations and the equation of state of Van der Waals*, Physica **A 334**, 482 – 512

Koushoumvekaki I.A., Solms N.V., Michelsen M.L., Kontogeorgis G.M., 2004, *Application of the perturbed chain SAFT equation of state to complex polymer systems using simplifies mixing rules*, Fluid Phase Equilibria, **215**, 71-78

Kutney M.C., Dodd V.S., Smith K.A., Herzog H.J., Tester J.W., 1997, *A hand-sphere volume-translated van der Waals equation of state for supercritical process modelling 1. Pure components*, Fluid Phase Equilibria, **128**, 149-171

Lagourette B., Daridon J.L., Alliez J., 1999, *Thermophysical properties of petroleum distillation fractions up to 150 MPa. Comparative analysis of some equations of state*, Physica B, **265**, 282-286

Landau L.D., Lifshitz E.M., 1980, *Statistical physics, 3rd Edition*, Pergamon Press, New York

Lee Y., Shin M. S., Yeo J.K., Kim H., 2007, *A crossover cubic equation of state near to and far from the critical region*, J. Chem. Thermodynamics **39**, 1257–1263

Lin H., Duan Y.Y., 2005, *Empirical correction to the Peng–Robinson equation of state for the saturated region*, Fluid Phase Equilibria **233**, 194–203

Llovell F., Peters C.J., Vega L.F., 2006, *Second-order thermodynamic derivative properties of selected mixtures by soft-SAFT equation of state*, Fluid Phase Equilibria **248**, 115-122

Llovell F., Vega L.F., 2007, *Phase equilibria, critical behaviour and derivative properties of selected n-alkanes / n-alkanes and n-alkanes/1-alkanol mixtures by the crossover soft-SAFT equation of state*, Fluid Phase Equilibria, **41**, 204-216

Machet V., Boublik T., 1985, *Vapour—liquid equilibrium at elevated pressures from the BACK equation of state. I. One-component systems*, Fluid Phase Equilibria, **21,** 1–9.

Maghari A., Hamzehloo M., 2010, *Second-order thermodynamic derivative properties of binary mixtures of n-Alkanes through the SAFT-CP equation of state*, Fluid Phase Equilibria, Fluid Phase Equilibria, **302(1)**, 195-201

Maghari A., Hosseinzadeh-Shahri L., 2003, *Evaluation of the performance of cubic equations of state in prediction the regularities in dense fluids*, Fluid Phase Equilibria, **206**, 287-311.

Maghari A., Sadeghi M.S., 2007, *Prediction of sound velocity and heat capacities of n-alkanes from the modified SAFT-BACK equation of state*, Fluid Phase Equilibria, **252**, 152–161

Mansoori G.A., Carnahan K.E., Leland T.W., 1971, *Equilibrium thermodynamic properties of the mixture of hard spheres*, The Journal of Chemical Physics, **54(4)**, 1523-1525

Mathias P.M., Copeman T.W., 1983, *Extension of the Peng-Robinson equation of state to complex mixtures: Evaluation of the various forms of the local composition concept*, Fluid Phase Equilibria, **13**, 91-108

Mathias P.M., Naheiri T., Oh E.M., 1989, *A density correction for the Peng-Robinson equation of state*, Fluid Phase Equilibria, **47**, 77-87

Monago K.O., 2005, *An equation of state for gaseous Argon determined from the speed of sound*, Chem. Phys., **316**, 9-19.

Muller E.A.; Gubbins K.E., 2001, *Molecular-based equations of state for associating fluids: A review of SAFT and related approaches*, Ind. Eng. Chem. Res., **40**, 2193-2211.

NIST, http://webbook.nist.gov/chemistry/fluid

Passut C.A., Danner R.P., 1972, *Correlation of ideal gas enthalpy, heat Capacity, and entropy*, Industrial and Engineering Chemistry Process Design and Development, **11(4),** 543-546

Peneloux A., Rauzy A.E., Freze R., 1982, *A consistent correction for Redlich-Kwong-Soave volumes,* Fluid Phase Equilibria, **8**, 7-23

Peng D.Y., Robinson D.B., 1976, *A new two-constant equation of state*, Ind. Eng. Chem. Fundam., **15**, 58-64

Pfohl O., Brunner G., 1998, *2. Use of BACK to modify SAFT in order to enable density and phase equilibrium calculations connected to gas-extraction processes,* Ind. Eng. Chem. Res., **37**, 2966–2976

Poling B.P., Prausnitz J.M., O'Connell J.P., 2001, *Properties of gases and liquids,* 5th Edition. McGraw-Hill

Riazi M.R., Daubert T.E., 1980, *Simplify property predictions*, Hydrocarbon Processing, 115-116

Robinson D.B., Peng D.Y., 1978, *The characterization of the Heptanes and heavior fractions for the GPA Peng-Robinson programs*, GPA Research report 28, Tulsa,

Scalabrin G., Marchi P., Benedetto G., Gavioso R.M., Spagnolo R., 2002, *Determination of a vapour phase helmholtz equation for 1,1,1-trifluroethane (HFC-143a) from speed of sound mesurements*, J. Chem. Thermodynamics, **34**, 1601-1619.

Sengers J.M.H.L., Bruno T.J., Ely J.F., 1991, *Supercritical fluid technology reviews. I. Modern theory and applications*, CRC Press, Boca Raton, 1.

Shin M.S., Lee Y., Kim H., 2008, *Estimation of second-order derivative thermodynamic properties using the crossover cubic equation of state*, Journal of Chemical Thermodynamics, **40**, 68-694

Trusler J.P.M., 1991, *Physical acoustics and metrology*, Adam Hihler, Bristol.

Tsai J.C., Chen Y.P., 1998, *Application of a volume-translated Peng-Robinson equation of state on vapour-liquid equilibrium calculations*, Fluid Phase Equilibria, **145**, 193-215

Twu C.H., Coon J.E., Cunningham J.R., 1995, *A new generalized Alpha function for a cubic equation of state, Part 1: Peng-Robinson equation*, Fluid Phase Equilibria, **105**, 49-59

Voutsas E., Pappa G. D., Magoulas K., Tassios D. P., 2006, *Vapour liquid equilibrium modelling od alkane systems with Equations of State: "Simplicity versus Complexity",* Fluid Phase Equilibria, **240 (2),** 127-139

Wertheim M.S., 1984, *Fluids with highly directional attractive forces. I. Statistical thermodynamics*, Journal of Statistical Physics, **35**, 19

Wertheim M.S., 1984, *Fluids with highly directional attractive forces. II. Thermodynamic perturbation theory and integral equations,* Journal of Statistical Physics, **35**, 35

Wertheim M.S., 1986, *Fluids with highly directional attractive forces. III. Multiple attraction sites,* Journal of Statistical Physics, **42,** 459

Wertheim M.S., 1986, *Fluids with highly directional attractive forces. IV. Equilibrium polymerization,* Journal of Statistical Physics, **42,** 477

Wertheim M.S., 1986, *Fluids of dimerizing hard spheres and fluid mixtures of hard spheres and dispheres*, Journal of Chemical Physics, **85,** 2929

Whitson C.H., 1983, *Characterizing the hydrocarbon plus fractions*. SPE Journal, **23**, 683-701

Wilson K.G., 1971, *Renormalization group and critical phenomena. I. Renormalization group and the Kadanoff scaling picture*, Phys. Rev. **B 4**, 3174.

Zhang Q.Y., Mi J.G., Yu Y.M., Chen J., 2003, *A study for phase equilibria of fluid mixtures with a component near its critical point,* Computer and applied chemistry 20

CHAPTER 5- VALIDATION OF THERMODYNAMIC MODEL USING INDEPENDENT DATA

5.1 Introduction

The main objective of this work was to develop a thermodynamic model to improve the prediction of thermodynamic properties of fluids, and in particular speed of sound. In order to accomplish this goal, the thermodynamic properties were defined as the derivatives of thermodynamic potential functions in Chapter 4. In this regards, the SAFT-BACK equation of state used Helmholtz free energy for differentiation with respect to density and temperature to calculate pressure, isobaric and isochoric heat capacities and the speed of sound. This modelling was performed for 10 pure normal hydrocarbons, some cyclic hydrocarbons such as benzene, toluene, cyclopropane, carbon dioxide and branched alkanes such as isobutane and isopentane. Then it was extended to binary mixtures with implementation of binary interaction parameters which were tuned using physical properties of the mixtures. Therefore, this model was able to calculate the thermodynamic properties of multi-component mixtures. Finally, the physical properties of single carbon numbers were employed to calculate the thermodynamic properties of pseudo-components and real oils. A detailed description of the modelling for the fluid system has been illustrated previously in Chapter 4.

The new experimental data for various pure hydrocarbons, binary and multi-component mixtures and real oils measured in this work (Chapter 3), in addition to the data from the literature, have been used for evaluating the model. In this chapter, the validation of the model will be achieved by comparing the predictions with the experimental data generated in this work and data from the literature. These data can be referred to the independent data as they were not used for tuning and improving the model.

In this chapter, the modelling results will be compared with experimental data of this work and other data obtained from the literature and the validity of the thermodynamic model will be examined for pure components, binary and multi-component mixtures and real reservoir oils which their experimental data are available and the measurement results were presented in Chapter 3.

5.2 Thermodynamic Model for Pure Compounds

Pure component thermodynamic properties were calculated with the parameters regressed using NIST correlated and data from literature. Among all of the pure hydrocarbon and non-hydrocarbon components, n-pentane, n-hexane and CO_2 were selected to test and validate the predictions of the speed of sound as several experimental data were found in the literature for nC_5 and nC_6 and because also of the high importance of CO_2 in industry and reservoir engineering.

Figures 5.1 - 5.3 and Tables 5.1 - 5.3 show the comparison of predicted values using this thermodynamic model with experimental data which were generated in this work, literature data and NIST correlated data.

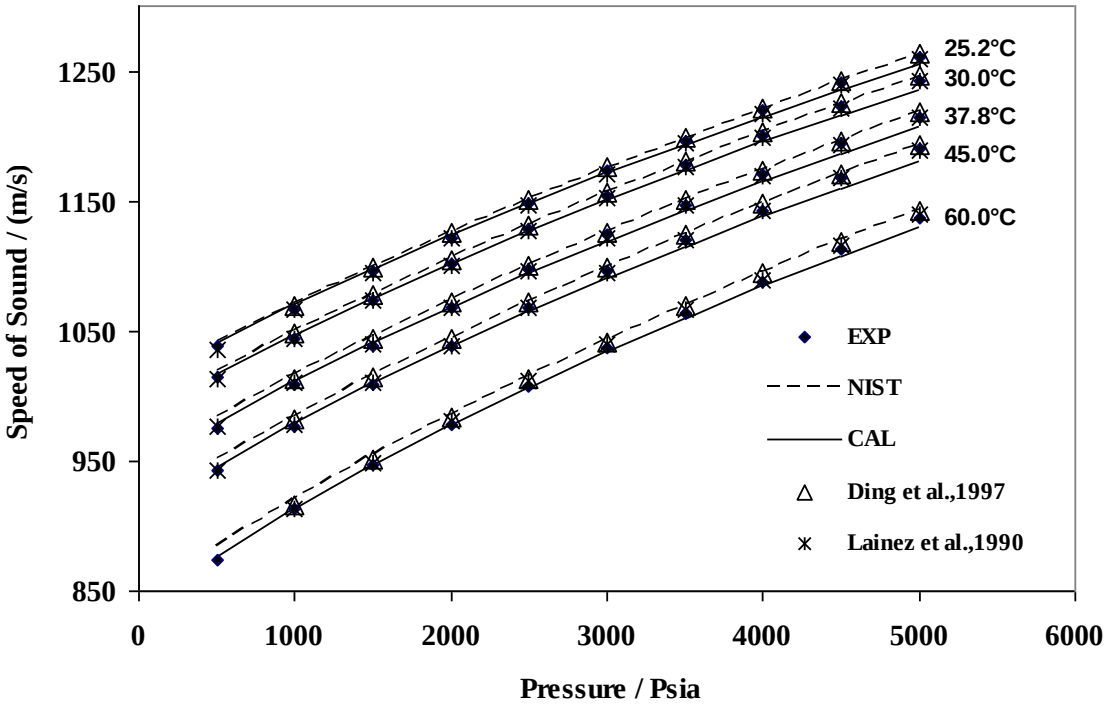

Figure 5.1 Comparison of the predicted values of the speed of sound for n-pentane at different temperatures and pressures

Table 5.1 Comparison of the predicted values of speed of sound for n-pentane using thermodynamic model with literature and experimental data

T (°C)	P (psia)	u (m/s) CAL	AAD% EXP	AAD% NIST	AAD% Ding et al	AAD% Lainez et al
25.2	500	1040.9	0.28	0.02	-	0.50
25.2	1000	1070.2	0.35	0.04	0.04	0.38
25.2	1500	1097.3	0.07	0.12	0.12	0.26
25.2	2000	1123.6	0.20	0.13	0.15	0.22

25.2	2500	1148.1	0.03	0.20	0.25	0.11
25.2	3000	1171.5	0.16	0.27	0.35	0.02
25.2	3500	1193.7	0.19	0.34	0.43	0.09
25.2	4000	1214.9	0.45	0.43	0.51	0.22
25.2	4500	1235.2	0.46	0.53	0.60	0.30
25.2	5000	1254.5	0.44	0.65	0.72	0.40
30.0	500	1017.1	0.27	0.21	-	0.38
30.0	1000	1047.5	0.29	0.19	0.07	0.28
30.0	1500	1075.7	0.22	0.23	0.21	0.19
30.0	2000	1102.2	0.05	0.28	0.26	0.12
30.0	2500	1127.6	0.05	0.32	0.32	0.02
30.0	3000	1151.1	0.27	0.41	0.47	0.10
30.0	3500	1173.7	0.37	0.50	0.56	0.21
30.0	4000	1195.3	0.37	0.58	0.64	0.34
30.0	4500	1216.0	0.52	0.68	0.74	0.44
30.0	5000	1235.7	0.57	0.79	0.84	0.52
37.8	500	980.0	0.50	0.37	-	0.31
37.8	1000	1011.7	0.28	0.37	0.18	0.16
37.8	1500	1040.8	0.25	0.43	0.36	0.04
37.8	2000	1068.4	0.03	0.48	0.40	0.00
37.8	2500	1094.5	0.21	0.53	0.49	0.16
37.8	3000	1119.3	0.41	0.59	0.61	0.24
37.8	3500	1142.7	0.35	0.66	0.69	0.32
37.8	4000	1164.9	0.43	0.75	0.77	0.42
37.8	4500	1186.3	0.64	0.84	0.85	0.56
37.8	5000	1206.6	0.68	0.93	0.93	0.61
45.0	500	946.0	0.40	0.53	-	0.27
45.0	1000	979.2	0.27	0.51	0.27	0.11
45.0	1500	1009.8	0.11	0.55	0.45	0.00
45.0	2000	1038.2	0.07	0.61	0.51	0.07
45.0	2500	1065.1	0.26	0.67	0.61	0.27
45.0	3000	1090.8	0.48	0.71	0.71	0.34
45.0	3500	1114.8	0.51	0.79	0.81	0.44
45.0	4000	1137.8	0.44	0.87	0.88	0.45
45.0	4500	1159.9	0.66	0.94	0.96	0.63
45.0	5000	1180.9	0.80	1.02	1.02	0.70
60.0	500	877.3	0.40	0.68	-	-
60.0	1000	913.4	0.06	0.71	0.32	0.02
60.0	1500	946.7	0.04	0.74	0.54	0.18
60.0	2000	977.8	0.03	0.77	0.59	0.27
60.0	2500	1006.7	0.05	0.83	0.66	0.44
60.0	3000	1034.0	0.25	0.87	0.76	0.55
60.0	3500	1059.7	0.32	0.95	0.85	0.64
60.0	4000	1084.2	0.33	1.01	0.92	0.49
60.0	4500	1107.4	0.49	1.08	1.01	0.72
60.0	5000	1129.7	0.60	1.14	1.10	0.87

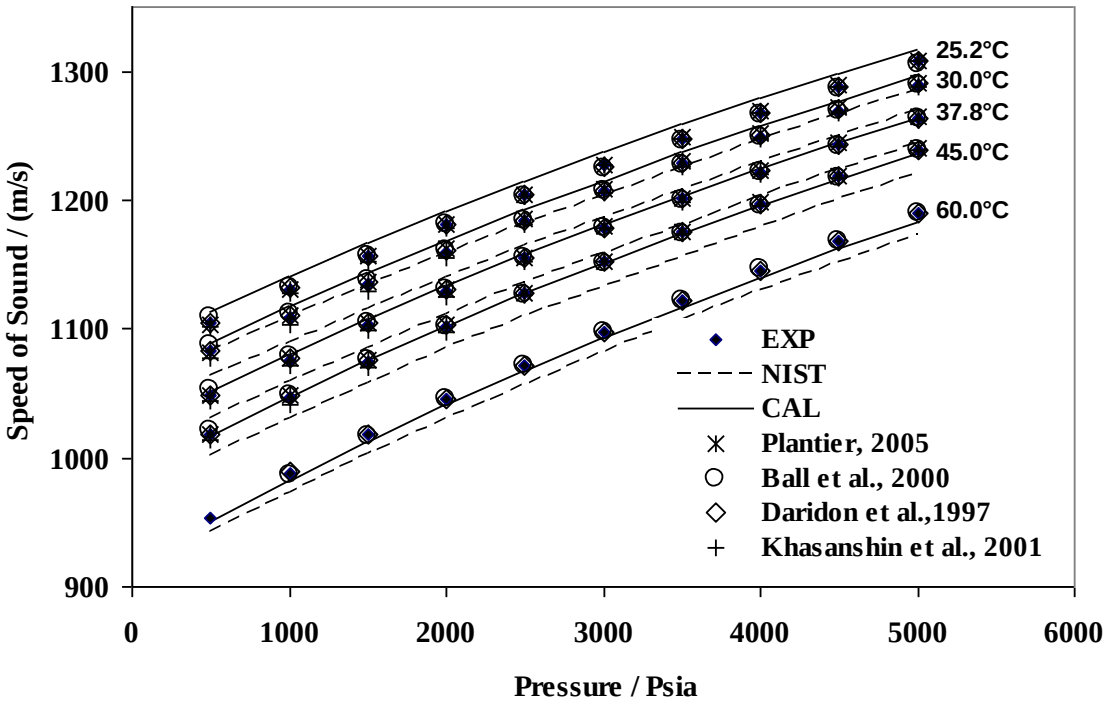

Figure 5.2 Comparison of the predicted values of the speed of sound for n-hexane at different temperatures and pressures

Table 5.2 Comparison of the predicted values of speed of sound for n-hexane using thermodynamic model with literature and experimental data

T (°C)	P (psia)	u (m/s) CAL	AAD% EXP	AAD% NIST	AAD% Plantier	AAD% Bell	AAD% Daridon	AAD% Khasanshin
25.2	500	1113.6	0.74	2.91	0.89	0.44	0.83	1.00
25.2	1000	1141.3	0.87	2.95	0.89	0.74	0.80	1.20
25.2	1500	1167.5	0.93	2.97	0.90	0.87	0.93	1.24
25.2	2000	1191.4	0.88	2.89	0.84	0.90	0.89	1.11
25.2	2500	1215.1	0.87	2.88	0.85	0.99	0.92	0.96
25.2	3000	1237.1	0.81	2.80	0.81	0.99	0.87	0.80
25.2	3500	1258.8	0.86	2.76	0.83	1.07	0.88	0.92
25.2	4000	1278.8	0.82	2.65	0.78	1.03	0.82	0.90
25.2	4500	1298.1	0.73	2.53	0.71	0.95	0.73	0.81
25.2	5000	1317.1	0.68	2.45	0.70	0.89	0.69	0.71
30	500	1089.0	0.60	2.50	0.61	0.14	0.57	1.06
30	1000	1117.3	0.73	2.56	0.61	0.45	0.62	1.25
30	1500	1143.5	0.73	2.55	0.57	0.53	0.62	1.23
30	2000	1168.7	0.75	2.54	0.57	0.62	0.65	1.13
30	2500	1192.3	0.68	2.49	0.54	0.65	0.64	0.91
30	3000	1215.1	0.64	2.45	0.54	0.67	0.62	0.74
30	3500	1237.0	0.69	2.41	0.53	0.73	0.62	0.85
30	4000	1257.5	0.66	2.32	0.49	0.70	0.59	0.85
30	4500	1277.1	0.58	2.21	0.44	0.61	0.51	0.76
30	5000	1296.2	0.51	2.11	0.40	0.55	0.43	0.65

37.8	500	1050.8	0.22	1.98	0.21	0.20	0.18	0.62
37.8	1000	1079.9	0.33	2.02	0.19	0.07	0.21	0.79
37.8	1500	1107.5	0.34	2.06	0.20	0.18	0.24	0.82
37.8	2000	1133.0	0.32	2.04	0.15	0.23	0.21	0.66
37.8	2500	1157.9	0.28	2.05	0.18	0.29	0.25	0.45
37.8	3000	1180.9	0.20	1.97	0.13	0.25	0.20	0.24
37.8	3500	1203.3	0.20	1.93	0.12	0.27	0.20	0.35
37.8	4000	1224.2	0.20	1.83	0.06	0.23	0.13	0.34
37.8	4500	1244.7	0.15	1.76	0.04	0.18	0.08	0.28
37.8	5000	1264.0	0.03	1.65	0.02	0.09	0.01	0.14
45	500	1017.0	0.06	1.57	0.06	0.40	0.09	0.32
45	1000	1047.3	0.08	1.65	0.06	0.11	0.06	0.53
45	1500	1075.5	0.08	1.68	0.08	0.04	0.07	0.52
45	2000	1102.0	0.06	1.67	0.11	0.02	0.06	0.37
45	2500	1127.3	0.01	1.66	0.11	0.03	0.04	0.11
45	3000	1151.2	0.08	1.62	0.14	0.01	0.07	0.10
45	3500	1174.2	0.05	1.59	0.16	0.01	0.09	0.03
45	4000	1195.6	0.10	1.50	0.21	0.05	0.15	0.02
45	4500	1216.5	0.14	1.42	0.24	0.10	0.20	0.04
45	5000	1236.7	0.19	1.35	0.26	0.16	0.23	0.14
60	500	949.9	0.37	0.92	-	-	-	-
60	1000	982.0	0.62	0.97	-	0.47	0.77	-
60	1500	1012.5	0.52	1.04	-	0.46	0.59	-
60	2000	1041.3	0.39	1.11	-	0.39	0.40	-
60	2500	1067.9	0.40	1.10	-	0.41	0.39	-
60	3000	1093.2	0.43	1.07	-	0.46	0.39	-
60	3500	1117.0	0.46	1.01	-	0.50	0.41	-
60	4000	1139.9	0.48	0.97	-	0.53	0.44	-
60	4500	1161.9	0.54	0.92	-	0.58	0.50	-
60	5000	1182.8	0.59	0.84	-	0.64	0.54	-

As shown in Figures 5.1 and 5.2, the model can accurately predict the speed of sound in these pure hydrocarbons. A good agreement with most of the published experimental data and the data generated in this work is observed. The total average deviations of the predicted results from available data for n-pentane and n-hexane are 0.44 and 0.72, respectively.

To investigate the accuracy of the thermodynamic model for non-hydrocabon gases, the speed of sound of CO_2 was modelled over a wide range of temperature and pressure. The results are plotted in Figure 5.3 and listed in Table 5.3. The agreements between the

experimental (*EXP*) and calculated (*CAL*) data are good with the typical AAD% $\left(\frac{1}{n}\sum\left|\frac{X_{EXP}-X_{CAL}}{X_{EXP}}\right|\times 100\right)$ of 0.74.

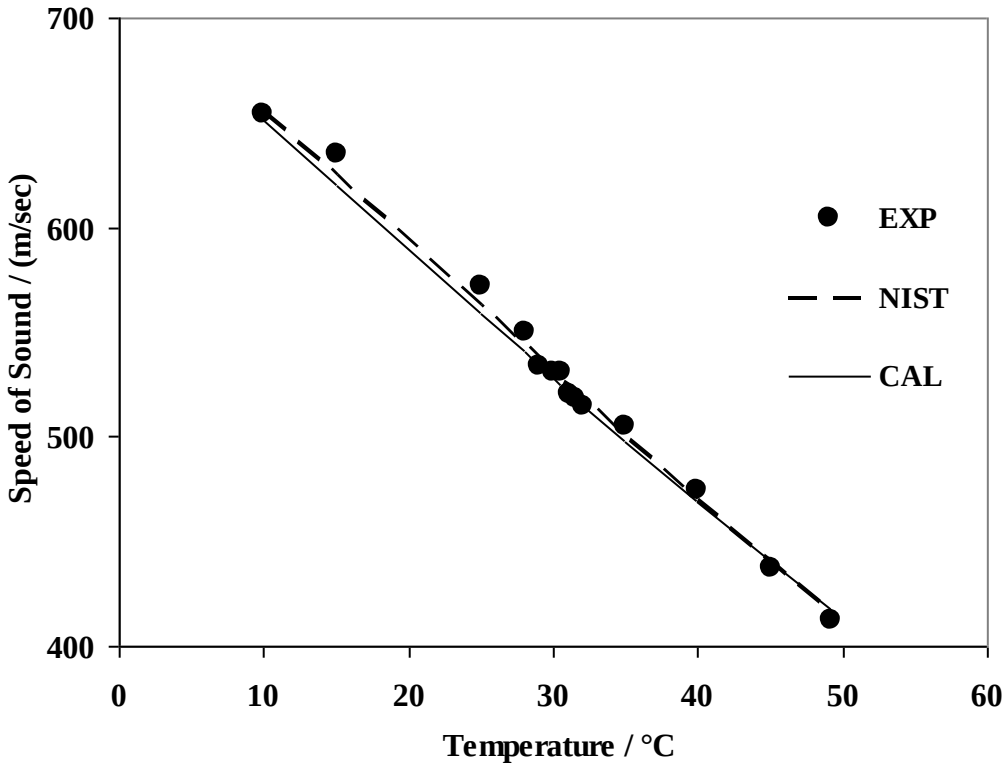

Figure 5.3 Comparison of the predicted values of the speed of sound for pure CO_2 at different temperatures and 2500 psia

Table 5.3 Measured transit time and speed of sound (u in $m.s^{-1}$) in carbon dioxide (CO_2) at different temperatures and comparison with experimental and NIST data

T (°C)	P (psia)	T_1 (μs)	u (m/s) (CAL)	AAD% (EXP)	AAD% (NIST)
9.97	2500.0	122.2	651.64	0.44	0.53
15.02	2500.0	126.0	620.16	2.31	0.66
25.02	2500.2	139.8	558.31	2.42	0.69
28.02	2499.8	145.5	540.03	1.78	0.64
29.00	2500.0	149.9	533.79	0.00	0.65
29.99	2500.2	150.8	527.97	0.51	0.58
30.58	2500.1	150.8	524.45	1.15	0.55
31.10	2500.2	153.8	521.23	0.20	0.57
31.58	2500.1	154.4	518.40	0.08	0.53
32.10	2500.1	155.4	515.03	0.07	0.58
35.00	2500.0	158.3	497.93	1.46	0.44
39.98	2500.4	168.7	468.61	1.21	0.20
45.00	2500.0	182.9	440.12	0.63	0.08
49.16	2502.0	194.0	417.58	1.23	0.50

5.3 Thermodynamic Model for Binary Mixtures

The next step is to evaluate the performance of the developed model in predicting the speed of sound in binary mixtures. The first mixtures were made of various concentrations of n-pentane and n-hexane.

5.3.1 Binary Mixtures of n-Pentane (nC_5) and n-Hexane (nC_6)

Figures 5.4 - 5.6 display the comparison of the calculated results with the experimental and NIST data for three different concentrations of nC_5-nC_6.

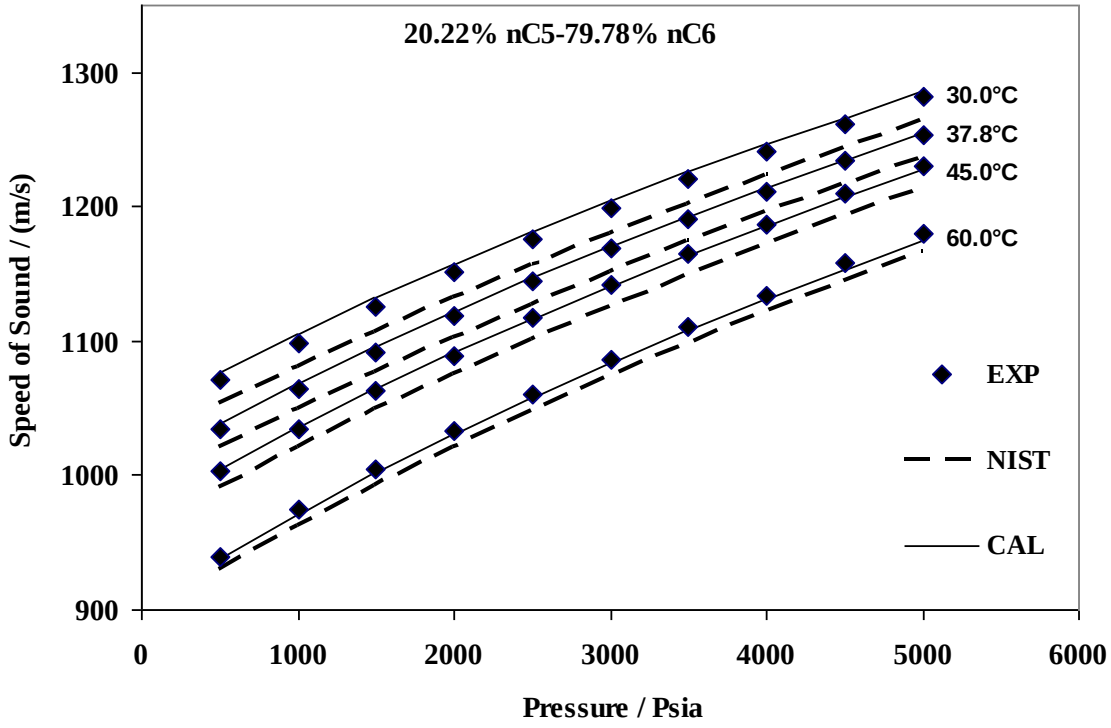

Figure 5.4 Comparison of the predicted values of the speed of sound for mixture of 79.78 mole% of n-hexane and 20.22 mole% of n-pentane at different temperatures and pressures

To investigate the effect of n-pentane concentration in the mixture on the speed of sound, the results for these three mixtures are plotted in one diagram at 45 °C and a wide range of pressure. Decreasing n-pentane increases the speed of sound because of the higher density of the mixture which is caused by n-hexane. Figure 5.7 shows a direct relation between pressure and the speed of sound for each composition.

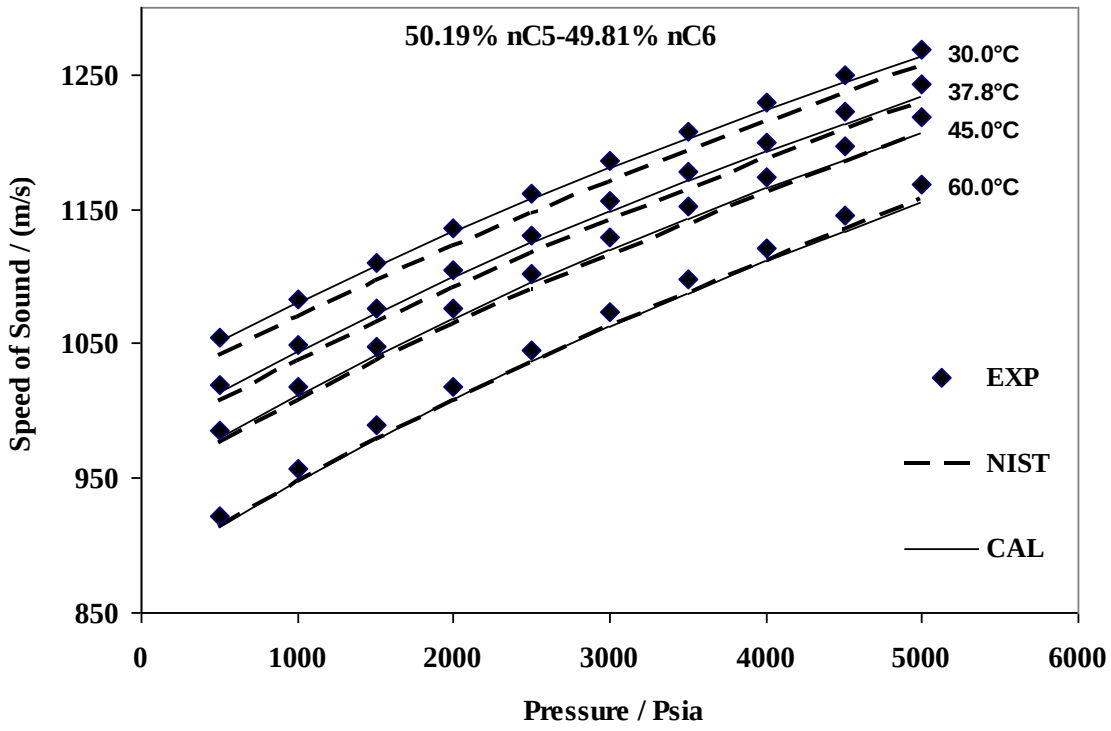

Figure 5.5 Comparison of the predicted values of the speed of sound for mixture of 49.81 mole% of n-hexane and 50.19 mole% of n-pentane at different temperatures and pressures

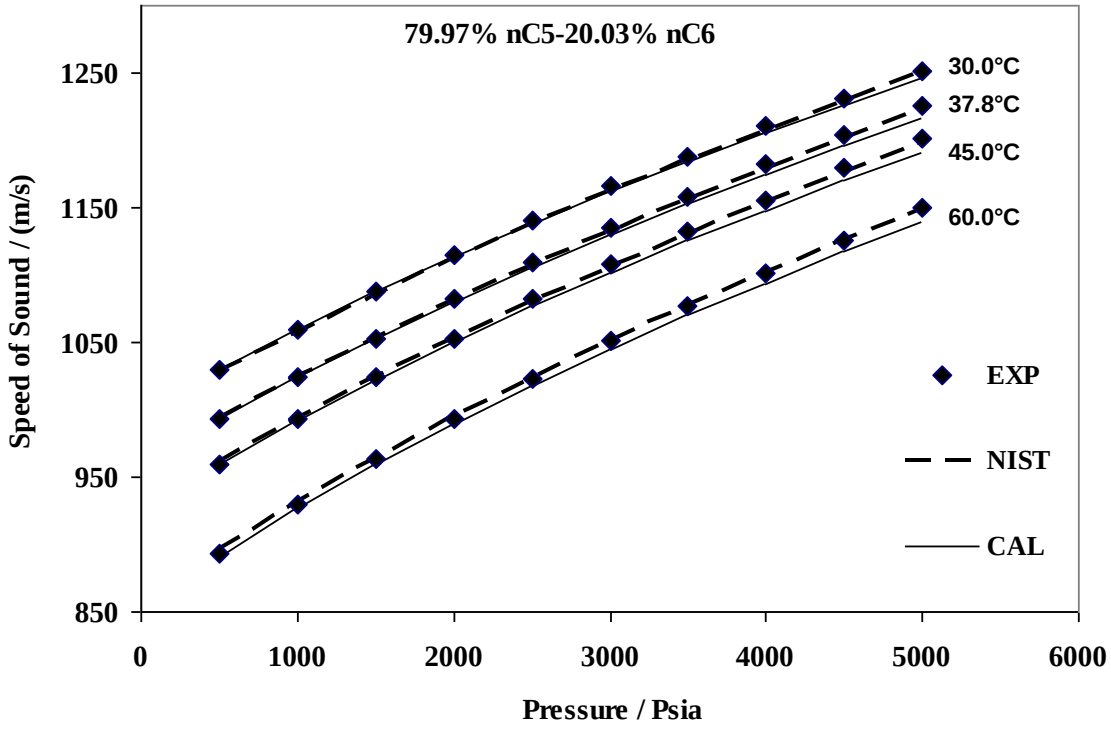

Figure 5.6 Comparison of the predicted values of the speed of sound for mixture of 20.03 mole% of n-hexane and 79.97 mole% of n-pentane at different temperatures and pressures

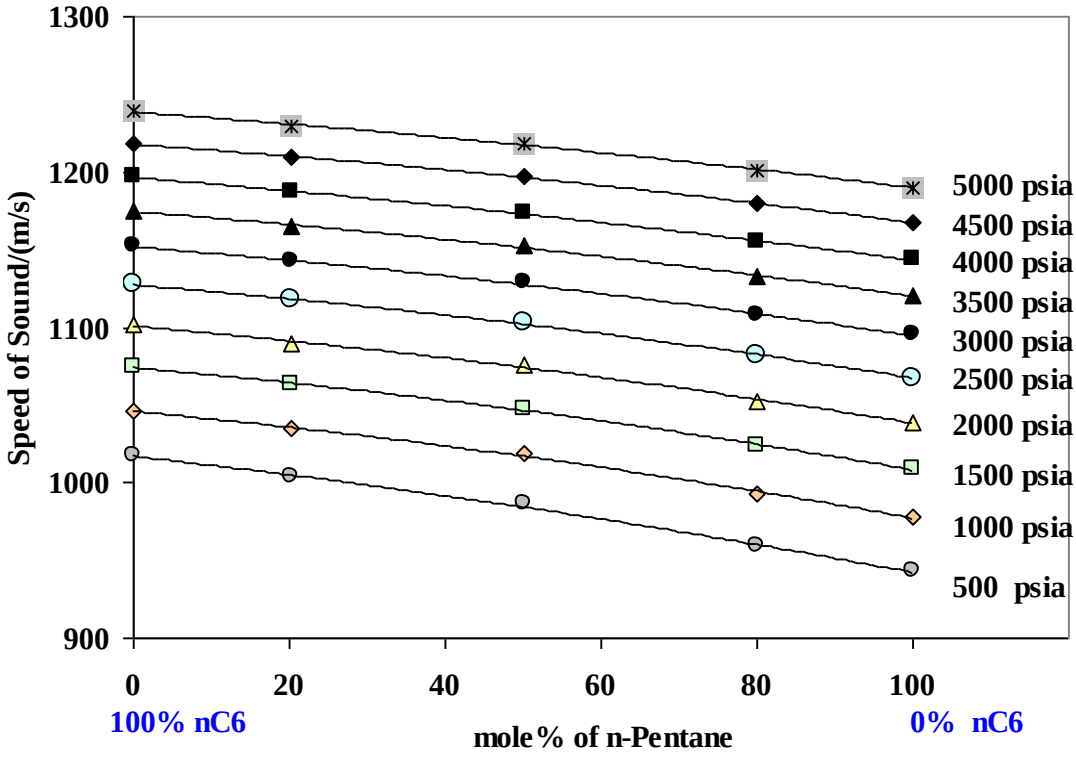

Figure 5.7 Effect of different concentrations of nC_5 in binary mixture of nC_5-nC_6 at various pressures and 45 °C

Table 5.4 Comparison of the predicted values of speed of sound with the experimental and NIST data for three compositions of nC_5-nC_6 binary mixtures

P (psia)	u (m/s) (CAL)	AAD% (EXP)	AAD% (NIST)	u (m/s) (CAL)	AAD% (EXP)	AAD% (NIST)
	T = 30.0 °C			**T = 37.8 °C**		
		X(nC_5) = 20.22%, X(nC_6) = 79.78%				
500	1076.52	0.51	2.18	1038.87	0.37	1.74
1000	1105.29	0.60	2.24	1068.07	0.29	1.74
1500	1131.97	0.55	2.23	1096.05	0.39	1.78
2000	1157.13	0.52	2.18	1122.06	0.32	1.75
2500	1181.31	0.48	2.16	1147.16	0.27	1.74
3000	1204.11	0.47	2.10	1170.42	0.10	1.67
3500	1225.69	0.43	2.00	1192.90	0.21	1.61
4000	1246.57	0.38	1.93	1214.34	0.20	1.53
4500	1266.17	0.33	1.80	1234.96	0.03	1.46
5000	1285.55	0.30	1.71	1254.23	0.01	1.33
		X(nC_5) = 50.19%, X(nC_6) = 49.81%				
500	1051.65	0.23	1.05	1014.49	0.46	0.72
1000	1080.39	0.24	1.05	1044.48	0.49	0.73
1500	1107.73	0.21	1.05	1072.52	0.42	0.71
2000	1133.79	0.22	1.06	1099.31	0.48	0.70
2500	1157.67	0.38	0.97	1124.52	0.59	0.66
3000	1180.87	0.44	0.92	1148.53	0.63	0.62
3500	1203.04	0.37	0.86	1170.99	0.61	0.54
4000	1224.22	0.43	0.78	1192.80	0.61	0.47

4500	1244.36	0.47	0.68	1213.60	0.71	0.39
5000	1263.64	0.46	0.58	1233.45	0.72	0.29
			X(nC$_5$) = 79.97%, X(nC$_6$) = 20.03%			
500	1030.16	0.03	0.22	993.04	0.04	0.02
1000	1059.63	0.01	0.21	1023.72	0.11	0.05
1500	1087.38	0.03	0.18	1052.64	0.03	0.06
2000	1113.71	0.13	0.16	1079.55	0.26	0.12
2500	1138.50	0.20	0.11	1105.62	0.34	0.12
3000	1162.12	0.30	0.05	1129.89	0.42	0.19
3500	1184.30	0.32	0.03	1152.91	0.43	0.27
4000	1205.71	0.37	0.12	1174.92	0.58	0.35
4500	1226.05	0.43	0.22	1196.19	0.67	0.42
5000	1245.73	0.50	0.31	1216.24	0.76	0.52
	T = 45.0 °C			**T = 60.0 °C**		
			X(nC$_5$) = 20.22%, X(nC$_6$) = 79.78%			
500	1005.35	0.17	1.41	938.04	0.10	0.85
1000	1035.63	0.11	1.42	971.00	0.35	0.90
1500	1064.53	0.12	1.46	1001.71	0.35	0.92
2000	1091.43	0.17	1.44	1030.40	0.22	0.91
2500	1116.84	0.11	1.41	1057.61	0.25	0.91
3000	1140.94	0.14	1.36	1083.35	0.32	0.89
3500	1163.91	0.15	1.30	1107.97	0.31	0.87
4000	1186.15	0.09	1.25	1131.09	0.28	0.81
4500	1207.27	0.17	1.18	1153.30	0.43	0.75
5000	1227.26	0.22	1.08	1174.31	0.52	0.66
			X(nC$_5$) = 50.19%, X(nC$_6$) = 49.81%			
500	980.73	0.55	0.43	913.45	0.88	0.02
1000	1011.96	0.65	0.44	947.54	0.98	0.06
1500	1041.64	0.61	0.49	979.12	1.00	0.08
2000	1068.79	0.71	0.44	1008.53	0.89	0.06
2500	1094.98	0.70	0.43	1036.44	0.89	0.06
3000	1119.47	0.83	0.37	1062.50	0.98	0.02
3500	1143.18	0.78	0.34	1087.65	0.91	0.00
4000	1165.52	0.73	0.28	1111.20	0.93	0.05
4500	1186.50	0.92	0.17	1133.65	0.99	0.13
5000	1206.93	0.97	0.09	1155.07	1.14	0.21
			X(nC$_5$) = 79.97%, X(nC$_6$) = 20.03%			
500	959.14	0.01	0.24	891.07	0.26	0.51
1000	991.51	0.19	0.22	926.42	0.41	0.50
1500	1021.42	0.24	0.25	959.15	0.51	0.49
2000	1049.81	0.25	0.26	989.22	0.45	0.54
2500	1076.47	0.51	0.28	1017.90	0.44	0.55
3000	1101.56	0.57	0.34	1044.73	0.63	0.59
3500	1125.23	0.67	0.41	1070.07	0.65	0.63
4000	1147.85	0.61	0.49	1093.91	0.71	0.72
4500	1169.69	0.81	0.55	1117.06	0.78	0.77
5000	1190.02	0.89	0.67	1138.85	0.99	0.85

Comparisons of the predicted speed of sound values with NIST and experimental speed of sound values (as shown in Table 5.4) are generally good. However, there is a general trend of increasing differences with decreasing nC_5 (or increasing nC_6) concentration. One reasonable explanation for this is given by Takagi *et al*, 2002, where this difference is attributed, in part, to the differences in the intermolecular free length (L_f).

This process is well illustrated in Figure 5.7 for the *n*-alkanes, nC_5 and nC_6, which have intermolecular lengths of 6.85 pm and 6.31 pm, respectively (Takagi *et al*, 2002). This figure shows that C_6H_{12} (which has the shorter intermolecular free length, L_f) has the higher speed of sound.

5.3.2 Binary mixture of n-Hexane (nC_6) and n-Decane (nC_{10})

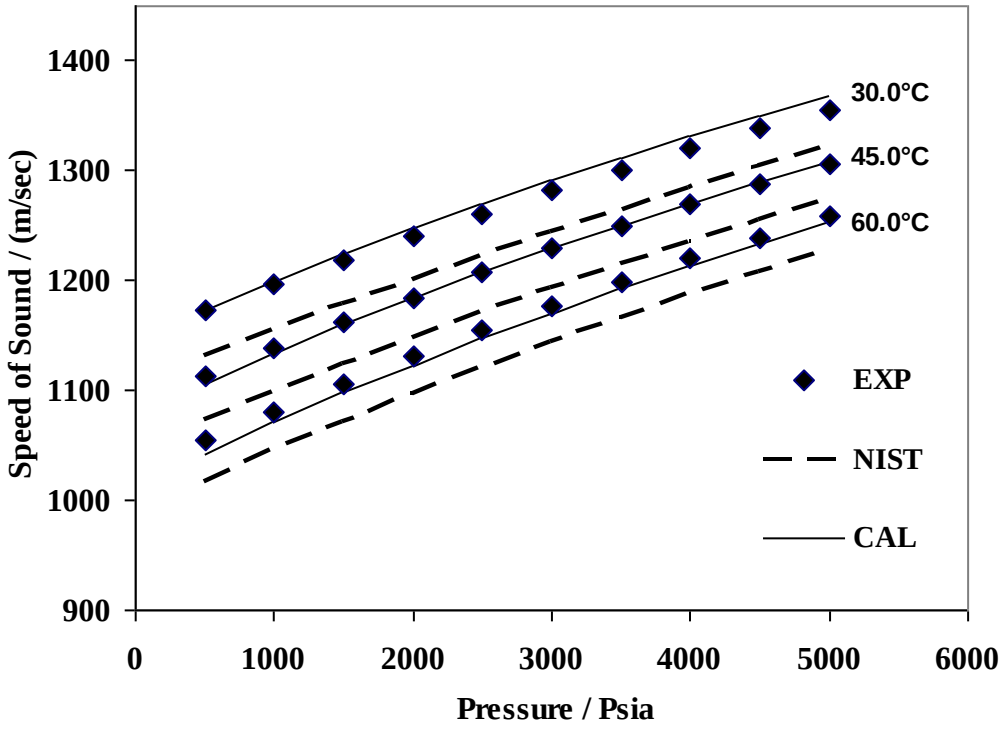

Figure 5.8 Comparison of the predicted values of the speed of sound for mixture of nC_6-nC_{10} at different temperatures and pressures

Figure 5.8 and Table 5.5 display the comparison of the predicted results with the experimental and NIST data at different temperatures and pressures of nC_6-nC_{10}.

Table 5.5 Comparison of the predicted values of speed of sound with the experimental and NIST data for nC_6-nC_{10} binary mixture

T (°C)	P (psia)	u (CAL) m/s	AAD% (EXP)	AAD% (NIST)
30.0	500	1173.35	0.05	3.75
30.0	1000	1199.25	0.24	3.80
30.0	1500	1223.98	0.44	3.83
30.0	2000	1247.24	0.57	3.82
30.0	2500	1269.76	0.68	3.81
30.0	3000	1290.85	0.69	3.75
30.0	3500	1311.29	0.81	3.68
30.0	4000	1330.88	0.83	3.61
30.0	4500	1349.85	0.84	3.54
30.0	5000	1367.41	0.84	3.40
45.0	500	1106.68	0.58	3.11
45.0	1000	1133.87	0.36	3.14
45.0	1500	1159.67	0.19	3.16
45.0	2000	1183.62	0.10	3.10
45.0	2500	1207.15	0.01	3.09
45.0	3000	1229.12	0.03	3.03
45.0	3500	1250.42	0.10	2.97
45.0	4000	1270.22	0.09	2.85
45.0	4500	1289.39	0.10	2.74
45.0	5000	1307.66	0.07	2.60
60.0	500	1041.90	1.19	2.42
60.0	1000	1070.63	0.93	2.44
60.0	1500	1097.65	0.78	2.44
60.0	2000	1123.07	0.69	2.41
60.0	2500	1147.35	0.63	2.38
60.0	3000	1170.16	0.60	2.30
60.0	3500	1192.42	0.50	2.25
60.0	4000	1213.26	0.52	2.15
60.0	4500	1233.44	0.49	2.06
60.0	5000	1252.69	0.53	1.95

Investigation of the AAD in the above tables, show better prediction accuracies at higher temperatures for each mixture. The deviations from either experimental or NIST data are negligible and can be neglected.

Pressure, isobaric and isochoric heat capacities and speed of sound for a full-range of binary mixtures of hydrocarbon - hydrocarbon and CO_2 - hydrocarbon were calculated using the thermodynamic model and the results were compared with the NIST

correlated data at different temperature and pressure conditions. The average absolute deviations for these mixtures are indicated in Tables 5.6 - 5.9.

Table 5.6 Absolute average percentage deviations for modelling pressure of binary mixtures of 10 n-Alkanes using SAFT-BACK equation of state

	CO_2	C_1	C_2	C_3	nC_4	nC_5	nC_6	nC_7	nC_8	nC_9
C_1	2.58									
C_2	2.44	1.48								
C_3	3.53	0.72	1.34							
nC_4	4.72	2.78	1.27	2.21						
nC_5	3.36	3.95	2.33	1.33	2.81					
nC_6	3.39	4.6	2.11	2.44	2.16	2.58				
nC_7	3.88	3.14	3.67	1.23	2.84	1.83	2.11			
nC_8	2.11	4.07	3.23	2.57	2.67	2.77	3.77	2.11		
nC_9	3.18	-	3.13	2.29	3.05	3.29	3.37	1.97	4.81	
nC_{10}	4.49	-	3.22	1.39	1.25	3.27	3.98	3.44	5.16	4.64

Table 5.7 Absolute average percentage deviations for modelling C_v of binary mixtures of 10 n-Alkanes using SAFT-BACK equation of state

	CO_2	C_1	C_2	C_3	nC_4	nC_5	nC_6	nC_7	nC_8	nC_9
C_1	3.56									
C_2	3.28	1.54								
C_3	2.72	1.66	1.39							
nC_4	2.76	2.98	1.55	0.98						
nC_5	2.74	1.39	1.25	1.26	1.26					
nC_6	2.97	1.57	1.83	0.97	1.19	1.33				
nC_7	3.05	1.57	2.77	1.24	1.26	0.96	1.18			
nC_8	3.4	1.85	3.29	1.28	1.45	1.06	1.16	1.32		
nC_9	3.11	-	2.38	1.47	1.48	1.38	1.43	1.76	1.73	
nC_{10}	3.28	-	2.46	1.75	3.29	1.66	1.48	1.63	1.62	1.73

Table 5.8 Absolute average percentage deviations for modelling C_p of binary mixtures of 10 n-Alkanes using SAFT-BACK equation of state

	CO_2	C_1	C_2	C_3	nC_4	nC_5	nC_6	nC_7	nC_8	nC_9
C_1	1.67									
C_2	2.89	1.49								
C_3	2.01	1.28	1.69							
nC_4	1.66	2.98	1.52	1.14						
nC_5	1.87	1.39	1.49	1.19	1.45					
nC_6	2.17	1.50	2.36	1.27	0.96	1.06				
nC_7	2.46	1.48	3.24	3.05	1.45	1.48	1.72			
nC_8	2.93	1.85	2.70	1.92	2.32	1.90	2.38	2.42		
nC_9	3.91	-	2.88	2.72	2.90	2.84	2.74	3.21	3.09	
nC_{10}	2.51	-	2.90	2.98	3.07	2.35	3.75	3.26	3.97	3.25

Table 5.9 Absolute average percentage deviations for modelling speed of sound of binary mixtures of 10 n-Alkanes using SAFT-BACK equation of state

	CO_2	C_1	C_2	C_3	nC_4	nC_5	nC_6	nC_7	nC_8	nC_9
C_1	3.81									
C_2	2.66	0.84								
C_3	2.20	0.70	0.82							
nC_4	2.16	1.82	1.11	1.09						
nC_5	1.25	1.23	2.23	1.15	1.42					
nC_6	1.41	1.88	2.01	1.28	1.59	1.03				
nC_7	1.96	2.84	2.08	1.32	1.77	1.26	2.38			
nC_8	2.08	3.60	2.13	1.49	1.49	2.34	3.22	3.08		
nC_9	2.06	-	2.17	1.50	1.65	2.67	2.30	1.92	2.32	
nC_{10}	2.21	-	2.46	1.48	2.98	2.38	2.98	2.72	2.90	2.84

The above tables show the deviations of calculated values of pressure, heat capacities and the speed of sound from the NIST correlated data for a lot of binary mixtures. The results are in a very good agreement with the minimum deviations from the NIST data. Only the values of CV show a little higher deviations in Table 5.7.

5.4 Thermodynamic Model for Multi-Component Mixtures

Validation of the speed of sound modelling using the model developed in this work will continue by investigating multi-component mixtures, both live and synthetic oils. This section, examines at the modelling of the speed of sound for three multi-component mixtures.

5.4.1 Multi-component Mixture of Methane (C_1), n-Pentane (nC_5) and n-Hexane (nC_6)

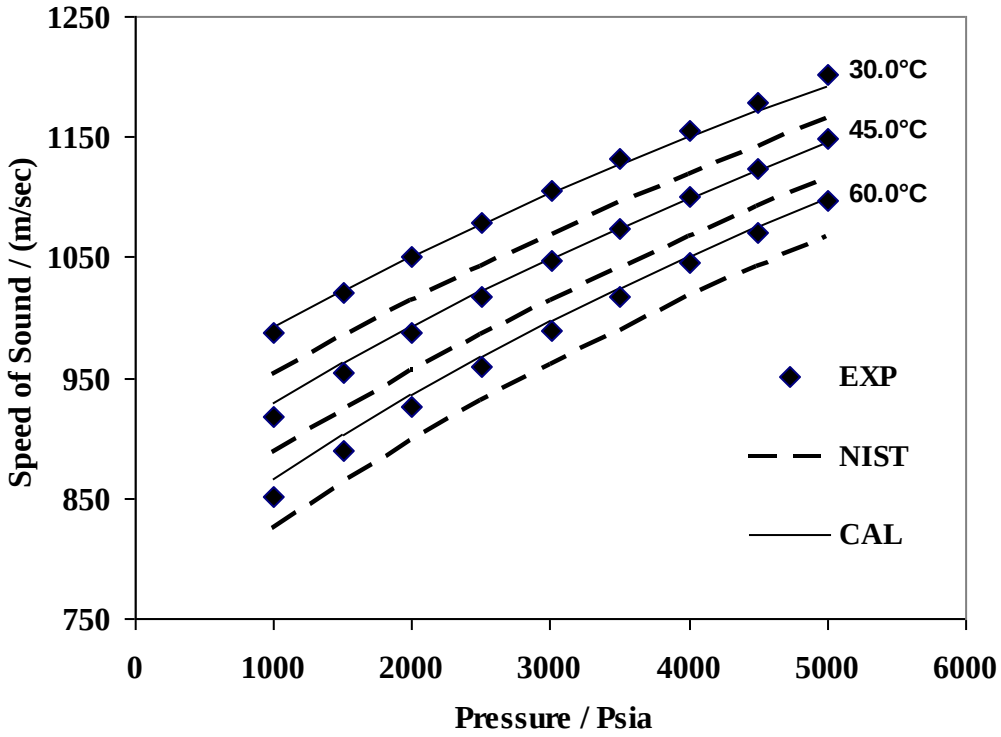

Figure 5.9 Comparison of the predicted values of the speed of sound for mixture of C_1-nC_5-nC_6 at different temperatures and pressures

Table 5.10 Comparison of predicted values of speed of sound with the experimental and NIST data for C_1-nC_5-nC_6 mixture

T (°C)	P (psia)	u (CAL) m/s	AAD% (EXP)	AAD% (NIST)
30.0	500	-	-	-
30.0	1000	992.24	0.43	4.11
30.0	1500	1022.77	0.26	3.85
30.0	2000	1050.95	0.06	3.56
30.0	2500	1077.85	0.10	3.35
30.0	3000	1103.06	0.26	3.12
30.0	3500	1127.00	0.39	2.91
30.0	4000	1149.62	0.54	2.69
30.0	4500	1171.42	0.65	2.50
30.0	5000	1192.17	0.75	2.31
45.0	500	-	-	-
45.0	1000	928.83	1.12	4.55
45.0	1500	962.12	0.83	4.21
45.0	2000	993.07	0.58	3.92
45.0	2500	1022.06	0.37	3.66
45.0	3000	1049.23	0.18	3.42
45.0	3500	1074.74	0.05	3.19

45.0	4000	1099.40	0.04	3.01
45.0	4500	1122.23	0.21	2.78
45.0	5000	1144.58	0.30	2.61
60.0	500	-	-	-
60.0	1000	866.28	1.77	5.10
60.0	1500	902.94	1.49	4.67
60.0	2000	936.75	1.21	4.34
60.0	2500	967.95	0.98	4.03
60.0	3000	997.36	0.88	3.78
60.0	3500	1024.74	0.68	3.53
60.0	4000	1050.79	0.56	3.32
60.0	4500	1075.37	0.39	3.11
60.0	5000	1098.82	0.22	2.91

The first live oil is a mixture of methane, n-pentane and n-hexane (composition is shown in Table 3.15). The predicted speed of sound are compared with the NIST and experimental data and the accuracy of the modelling is illustrated in Figure 5.9 and Table 5.10.

5.4.2 Multi-component mixture of n-Butane (nC_4), n-Decane (nC_{10}) and CO_2

Table 5.11 and Figure 5.10 show the results of the modelling for determination of the speed of sound in comparison with the experimental and NIST data for a mixture of n-butane, n-decane and carbon dioxide.

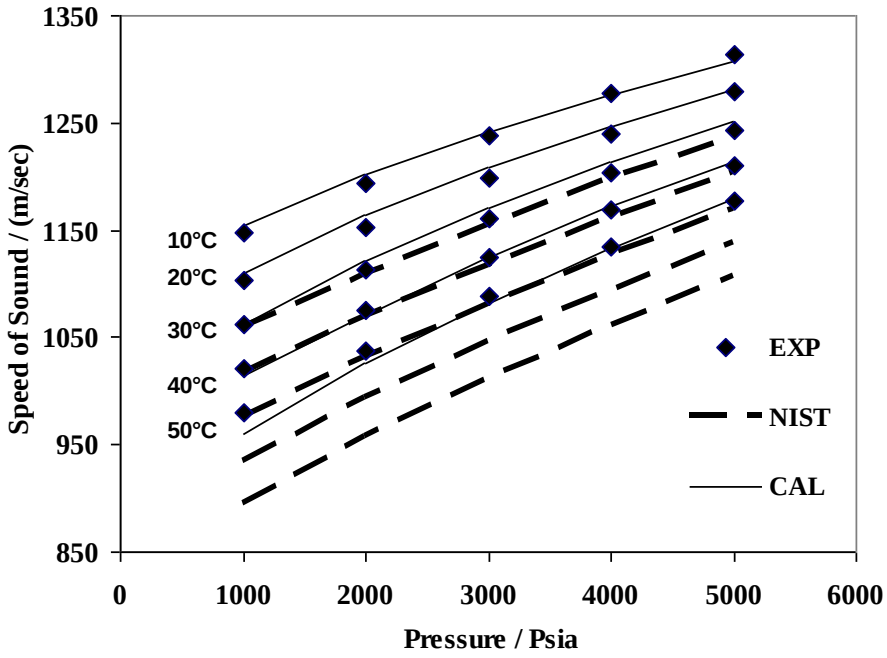

Figure 5.10 Comparison of predicted values of the speed of sound for mixture of nC_4-nC_{10}-CO_2 at different temperatures and pressures

In all of the above mixtures, comparison of the predicted results with the NIST and measured data show that more deviations are observed between the NIST data and experimental data than between these predictions and experimental data. The reason is in the type of binary interaction parameters, which were regressed using physical properties of each binary mixture using the available NIST data. k_{ij} for each mixture at specified temperature and density were regressed in order to enable the equation to predict the pressure accurately. The same k_{ij} was used later in the program to model other thermodynamic properties such as speed of sound. Therefore, the observed deviations of the calculated data from NIST data are because of the different method which NIST uses for its calculations. However, the experimental data that were generated in the lab are an important and accurate reference for validation of the model.

Table 5.11 Comparison of the predicted values of the speed of sound with the experimental and NIST data for nC_4-nC_{10}-CO_2 mixture

T (°C)	P (psia)	u (CAL) m/s	AAD% (EXP)	AAD% (NIST)
10.1	1000	1154.63	0.60	9.10
10.1	2000	1201.54	0.59	8.39
10.1	3000	1241.45	0.32	7.53
10.1	4000	1276.51	0.07	6.62
10.0	5000	1307.30	0.52	5.67
20.1	1000	1110.63	0.61	9.29
20.0	2000	1163.34	0.88	8.83
20.0	3000	1208.21	0.81	8.16
20.0	4000	1246.72	0.56	7.34
20.0	5000	1281.00	0.19	6.50
30.0	1000	1062.17	0.02	8.95
30.0	2000	1121.21	0.71	8.79
30.0	3000	1170.77	0.89	8.32
30.0	4000	1213.93	0.90	7.72
30.0	5000	1250.63	0.58	6.93
40.0	1000	1013.96	0.64	8.51
40.0	2000	1070.41	0.41	7.80
40.0	3000	1125.45	0.12	7.65
40.1	4000	1172.94	0.35	7.28
40.1	5000	1213.66	0.28	6.70
49.9	1000	960.81	1.97	7.40
50.0	2000	1025.22	1.16	7.21
50.0	3000	1081.32	0.59	6.95
50.0	4000	1133.07	0.13	6.83
50.0	5000	1178.14	0.06	6.50

The above table shows decreasing deviations from both NIST and experimental data at higher pressures and temperatures.

5.4.3 Multi-component mixture of n-Heptane (nC_7), n-Octane (nC_8), n-Nonane (nC_9) and n-Decane (nC_{10})

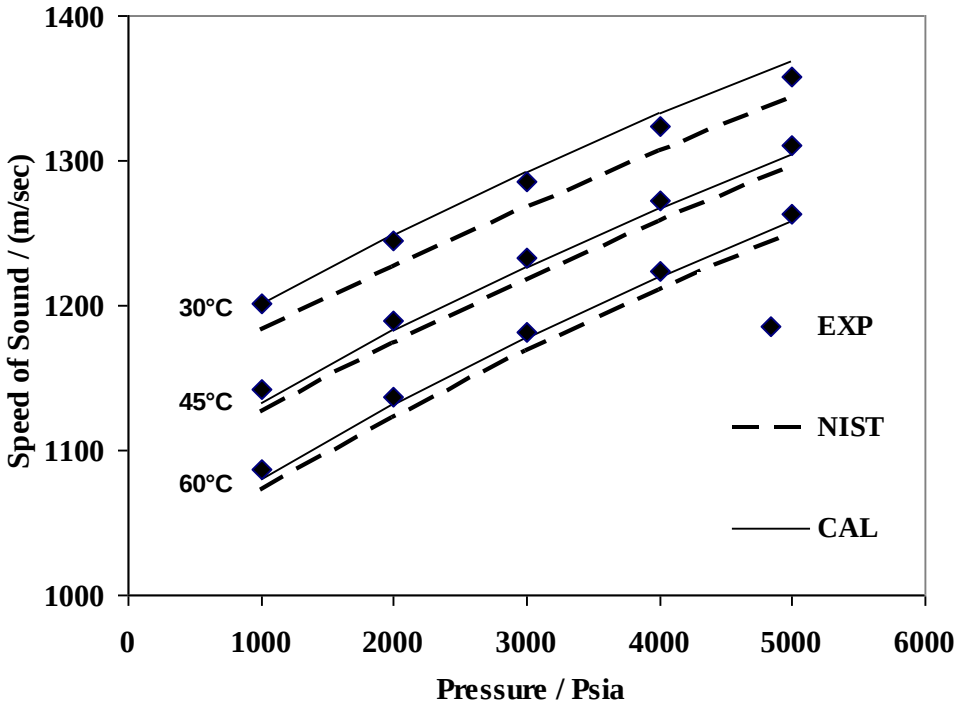

Figure 5.11 Comparison of the predicted values of speed of sound for the synthetic mixture of nC_7- nC_8- nC_9- nC_{10} at different temperatures and pressures

Table 5.12 Comparison of the predicted values of speed of sound with the experimental and NIST data for the synthetic mixture of nC_7- nC_8- nC_9- nC_{10}

T (°C)	P (psia)	u (CAL) m/s	AAD% (EXP)	AAD% (NIST)
30.0	1000	1201.26	0.04	1.60
30.0	2000	1248.79	0.31	1.82
30.0	3001	1292.60	0.59	1.96
30.0	4000	1332.37	0.66	1.98
30.0	5001	1368.65	0.76	1.89
45.0	1000	1133.36	0.80	0.58
45.0	2000	1182.41	0.56	0.77
45.0	3000	1226.92	0.44	0.83
45.0	4000	1267.43	0.41	0.81
45.0	5000	1304.48	0.45	0.69
60.0	1000	1080.41	0.62	0.71
60.0	2000	1131.48	0.43	0.82
60.0	3000	1177.24	0.38	0.81
60.0	4000	1219.33	0.37	0.76
60.0	5000	1257.67	0.47	0.62

The following figure and table show the predictions of speed of sound in a n-Heptane (nC_7), n-Octane (nC_8), n-Nonane (nC_9) and n-Decane (nC_{10}) synthetic mixture (composition given in 36, 27, 21, 16 mole%).

In all of the above mixtures, the thermodynamic model developed in this work can predict the speed of sound accurately, with deviation typically less than 2% from independent experimental data.

5.5 Validation of Thermodynamic Model for Real Reservoir Fluids

For further investigation of the capability of the developed model, real reservoir oils have been modelled and compared with the experimental data generated in this work at different temperatures and pressures. The compositions of the real oils (named real oil 1, 2 and 3) used in this work can be found in Tables 3.25, 3.27 and 3.29.

5.5.1 Speed of Sound in Real Oil 1

Equations 4.75 – 4.83 were used to predict the thermodynamic properties of real oil 1. Table 5.13 and Figure 5.12 show the calculated speed of sound through real oil 1 at three temperatures and five pressures and comparison with experimental data. Table 5.13 also indicates the density of the fluid at each temperature and pressure which was calculated using the SAFT-BACK equation of state. Figure 5.13 shows the calculated density of this oil at different temperature and pressure.

Table 5.13 Comparison of the predicted values of speed of sound with the experimental data of real oil 1 and calculated density at each temperature and pressure

T (°C)	P (psia)	u (CAL) m/s	AAD% (EXP)	Density (CAL) (mol/m^3)
30.0	1000	1370.01	0.02	4140
30.0	2000	1409.35	0.29	4170
30.0	3001	1444.05	0.50	4197
30.0	4000	1476.10	0.52	4223
30.0	5001	1509.45	0.81	4250
45.0	1000	1322.13	0.25	4106
45.0	2000	1361.41	0.55	4135
45.0	3000	1395.46	0.54	4162
45.0	4000	1430.21	0.70	4190
45.0	5000	1460.90	0.74	4215
60.0	1000	1267.23	0.05	4065
60.0	2000	1305.04	0.00	4095
60.0	3000	1340.07	0.00	4122
60.0	4000	1373.26	0.03	4148
60.0	5000	1404.52	0.09	4174

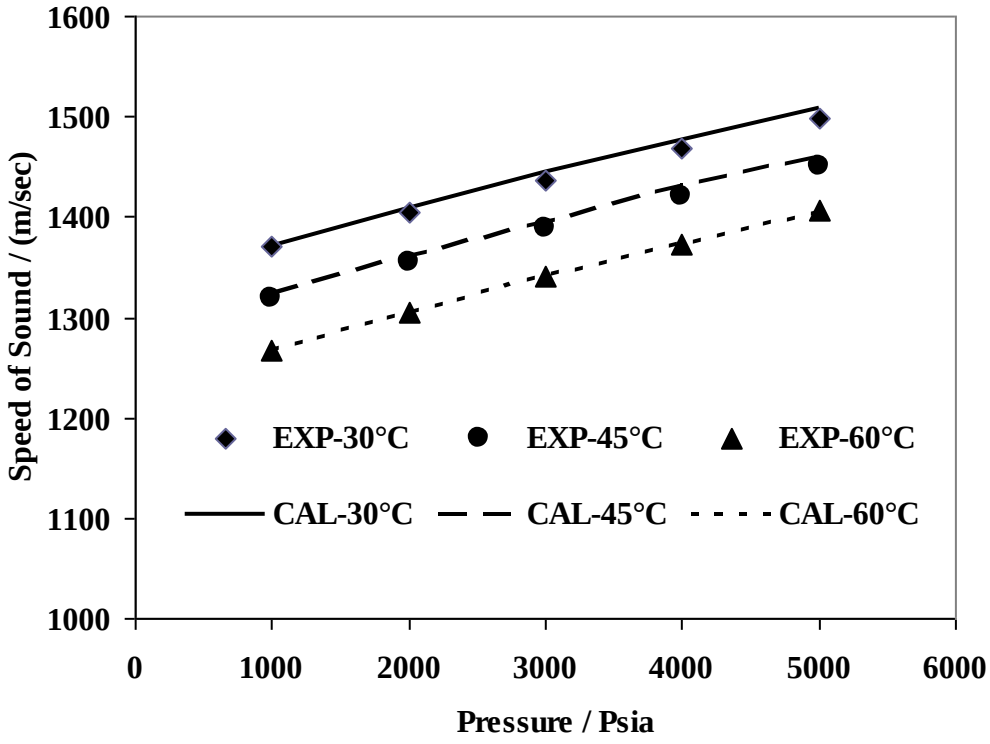

Figure 5.12 Calculated speed of sound for real oil 1 and comparison with experimental data

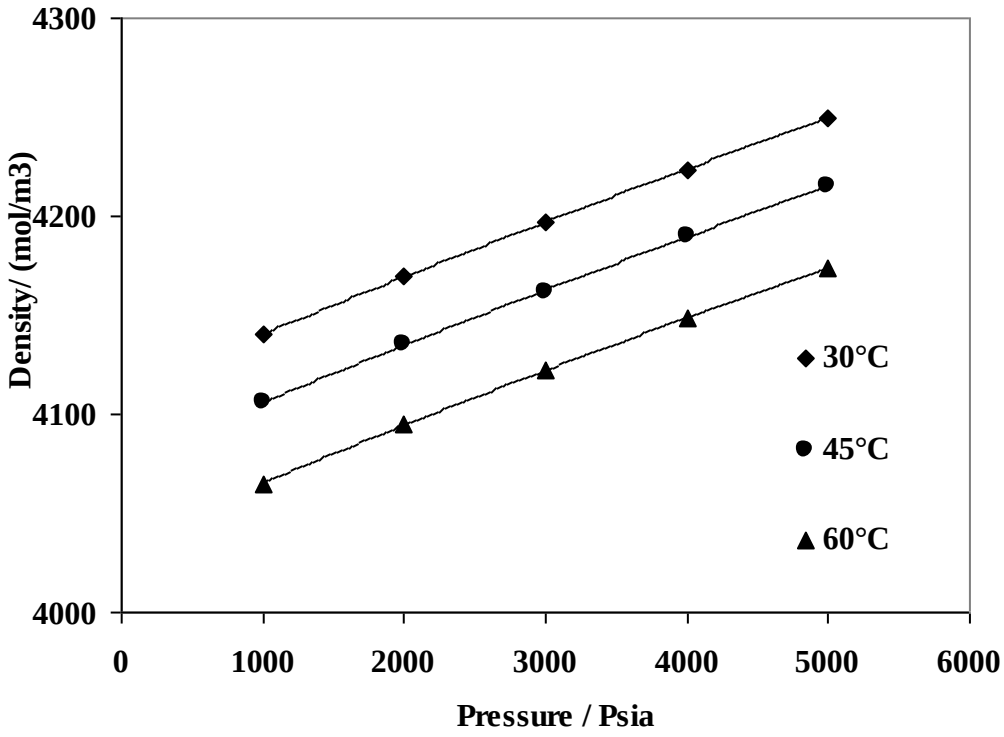

Figure 5.13 Calculated density of real oil 1 in different pressures and temperatures

5.5.2 Speed of Sound in Real Oil 2

Table 5.14 and Figures 5.14 and 5.15 show the predicted speed of sound through real oil 2 and also predicted density of this fluid at various temperatures and pressures and comparison with experimental data.

Table 5.14 Comparison of the predicted values of speed of sound with the experimental data of real oil 2 and calculated density at each temperature and pressure using this work

T (°C)	P (psia)	u (CAL) m/s	AAD% (EXP)	Density (CAL) (mol/m^3)
30.0	1000	1410.98	0.60	4057
30.0	2000	1450.37	0.06	4085
30.0	3001	1485.14	0.55	4111
30.0	4000	1517.76	0.67	4136
30.0	5001	1547.00	0.74	4160
45.0	1000	1352.84	0.42	4021
45.0	2000	1391.56	0.09	4048
45.0	3000	1425.43	0.03	4074
45.0	4000	1457.11	0.02	4099
45.0	5000	1487.31	0.03	4123
60.0	1000	1310.55	0.21	3988
60.0	2000	1348.76	0.09	4016
60.0	3000	1383.35	0.20	4042
60.0	4000	1414.21	0.21	4067
60.0	5000	1444.34	0.12	4091

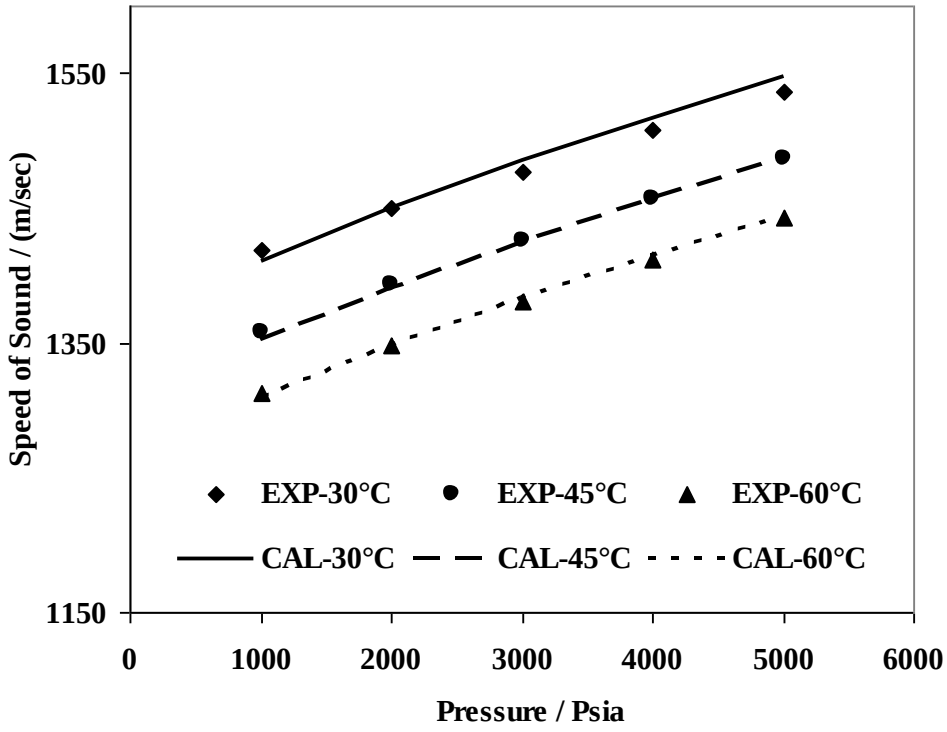

Figure 5.14 Calculated speed of sound for real oil 2 and comparison with experimental data

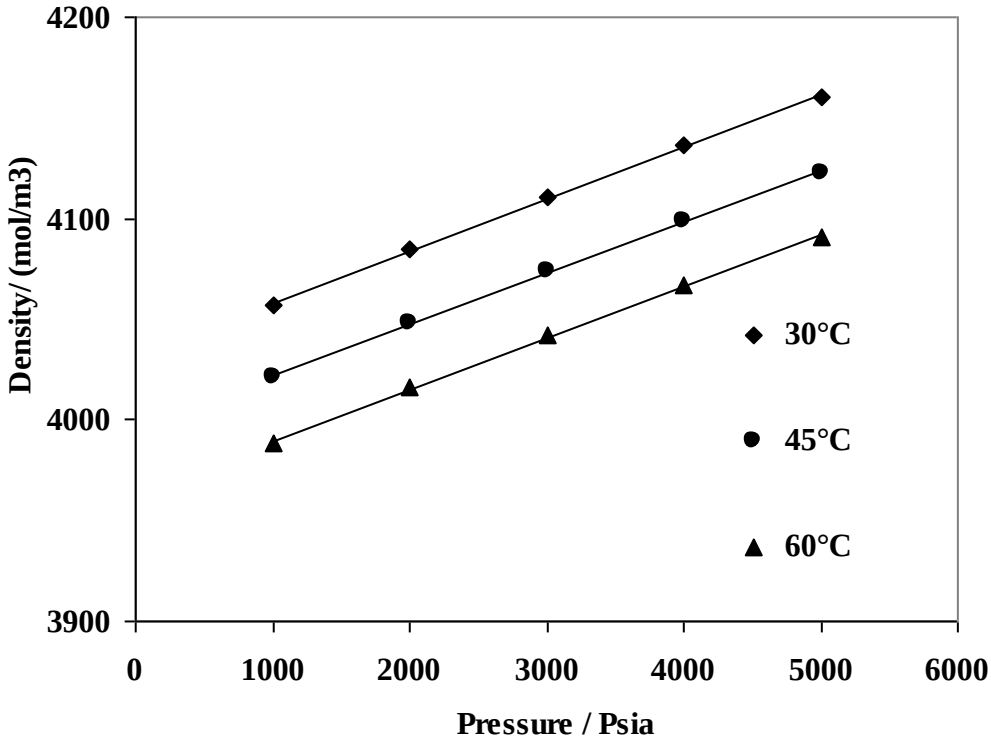

Figure 5.15 Calculated density of real oil 2 in different pressures and temperatures

5.5.3 Speed of Sound in Real Oil 3

Table 5.15 and Figures 5.16 - 5.17 show the results of the modelling for this fluid.

Table 5.15 Comparison of the predicted values of speed of sound with the experimental data of real oil 3 and calculated density at each temperature and pressure using this work

T (°C)	P (psia)	u (CAL) m/s	AAD% (EXP)	Density (CAL) (mol/m^3)
30.0	1000	1365.02	0.45	4836
30.0	2000	1395.12	0.20	4867
30.0	3001	1422.31	0.19	4896
30.0	4000	1449.17	0.44	4924
30.0	5001	1475.11	0.71	4952
45.0	1000	1313.53	0.96	4796
45.0	2000	1341.14	0.27	4826
45.0	3000	1370.35	0.14	4855
45.0	4000	1397.21	0.55	4883
45.0	5000	1425.74	0.72	4910
60.0	1000	1265.43	0.67	4758
60.0	2000	1297.23	0.31	4788
60.0	3000	1329.84	0.00	4817
60.0	4000	1355.14	0.65	4844
60.0	5000	1384.62	0.83	4872

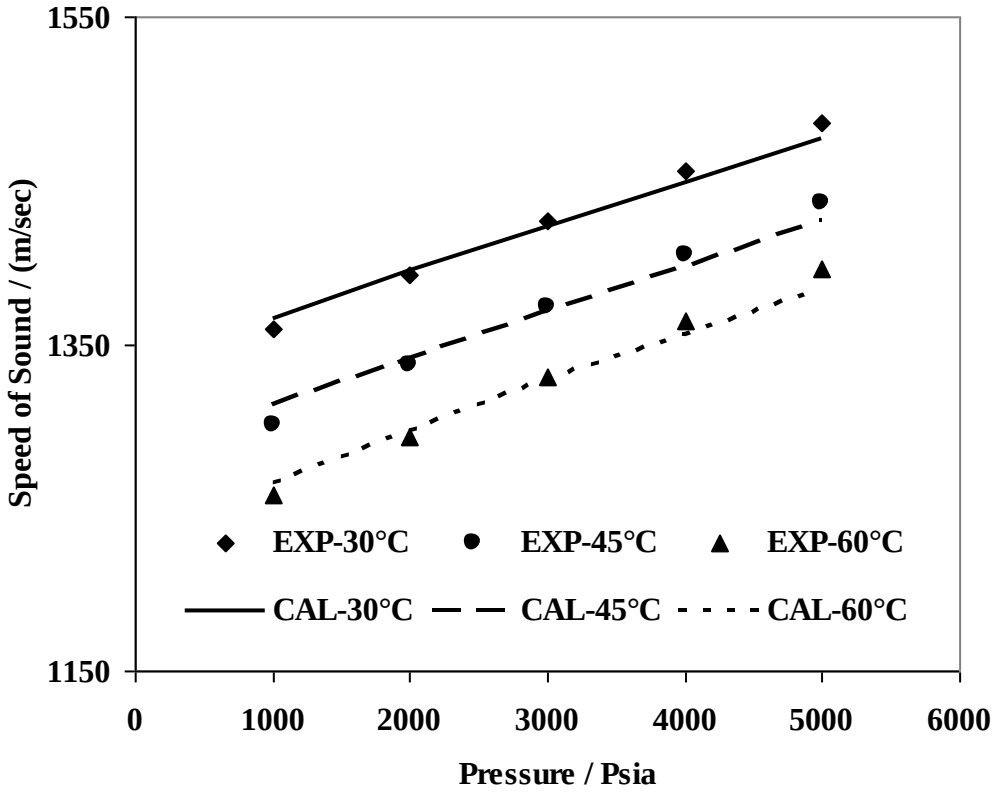

Figure 5.16 Calculated speed of sound for real oil 3 and comparison with experimental data

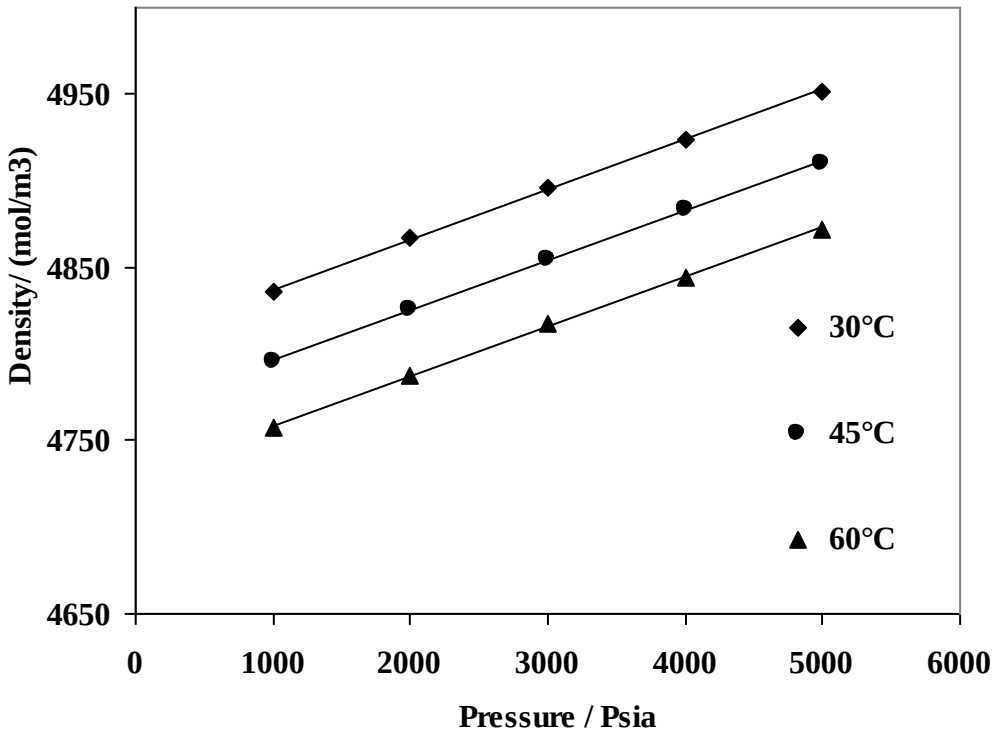

Figure 5.17 Calculated density of real oil 3 in different pressures and temperatures

Similar to real oil 1 and real oil 2, only the calculated values for densities of real oil 3 are displayed in Figure 5.17.

Considering Figures 5.12, 5.14 and 5.16, it is evident that SAFT-BACK equation predicts the speed of sound of reservoir real fluids with acceptable accuracy and the average absolute deviation (AAD %) is less than 1%.

For the last section of this chapter, results of the modelling for different compositions of n-pentane and carbon dioxide mixtures are discussed and will be compared with the NIST webbook data at three temperatures and in a wide range pressure.

The concentrations of n-pentane were 20, 50 and 80 mol%. The variation of speed of sound with changing temperature, density and composition is observed in Figure 5.18. All of these data in this figure are in liquid phase. Table 5.16 indicates the bubble point pressure of these mixtures at each temperature.

Table 5.16 Bubble point pressure for each composition in different temperatures

T (°C)	Bubble Point Pressure (Psia)		
	nC_5 (20%)-CO_2 (80%)	nC_5 (50%)-CO_2 (50%)	nC_5 (80%)-CO_2 (20%)
26.85 °C	696.18	485.88	221.91
126.85 °C	-	1325.64	639.62
226.85 °C	-	-	-

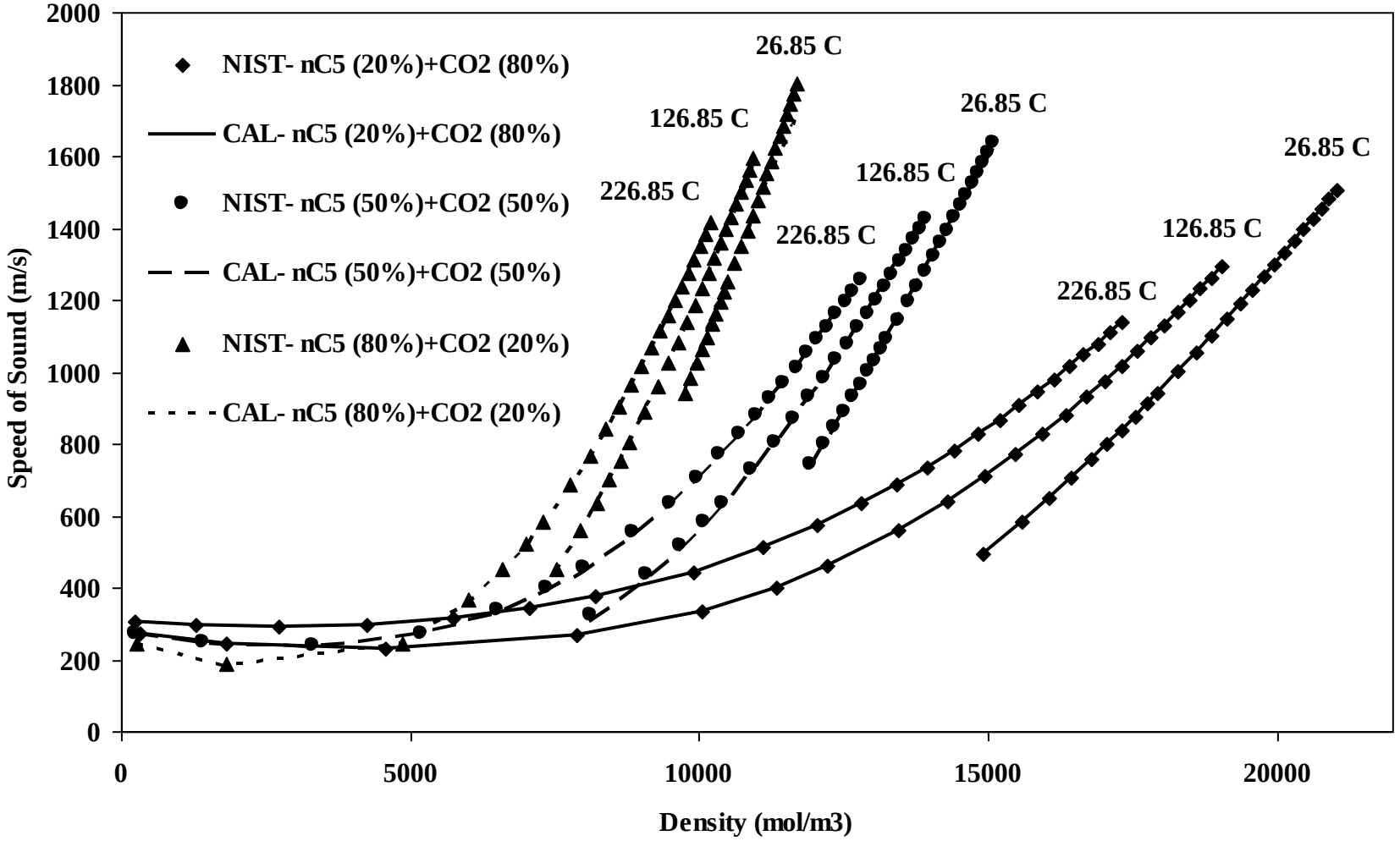

Figure 5.18 Speed of sound in three different compositions of n-pentane and carbon dioxide in a wide range of temperature and density, comparison of the predicted result by SAFT-BACK equation of state with NIST data

5.6 Conclusion

In this chapter the SAFT-BACK equation of state has been applied to different single, binary and multi-component mixtures of hydrocarbons and a non-hydrocarbon gas (CO_2). The predictions of the developed SAFT-BACK model have been compared, where possible, with literature data and validated against experimental data which were generated in this work over a wide range of temperature and pressure conditions.

Additionally, the compositions of real reservoir fluids containing pseudo-components and single carbon numbers of hydrocarbons were used to predict their speed of sound. A good agreement between the predicted values and experimental data was observed. The SAFT-BACK equation of state was shown to be a very successful equation of state for calculation of speed of sound through the real reservoir fluids.

REFERENCES:

Ball S.J., Trusler J.P.M., 2000, *The speed of sound and derived thermodynamic properties of n-Hexane and n-Hexadecane at temperatures between 298 K and 373 K and pressures up to 100 MPa,* 14th Symposium on Thermophysical Properties, June 25-30, Boulder, Colorado, USA

Daridon J.L., Lagourette B., Grolier J-P.E., 1998, *Experimental measurements of the speed of sound in n-Hexane from 293 to 373 K and up to 150 MPa,* International Journal of Thermophysics, **19(1)**, 145 – 160

Ding Z.S., Alliez J., Boned C., Xans P., 1997, *Automation of an ultrasound velocity measurement system in high pressure liquids,* Measurement Science and Technology, **8**, 154 – 161

Khasanshin T.S., Shchemelev A.P., 2001, *Sound velocity in liquid n-Alkanes, High Temperature*, **39(1)**, 60 – 67

Lainez A., Zollweg J.A., Streett W.B., 1990, *Speed of sound measurements for liquid n-Pentane and 2,2-dimethylpropane under pressure*, Journal of Chemical Thermodynamics, **22**, 937 – 948

NIST, http://webbook.nist.gov/chemistry/fluid

Plantier F., 2005, *Laboratoire des fluide complexes, groupe haute pression, Université de Pau et des Pays de l'Adour*, Personal Communication

Takagi T., Sakura T., Guedes H.J.R., 2002, *Speed of Sound in Liquid Cyclic Alkanes at temperatures between (283 and 343) K and pressures up to 20 MPa*, Journal of Chemical Thermodynamics, **34**, 1943 – 1957

Chapter 6 – APPLICATION TO THE RESERVOIRS

6.1 Introduction

Seismic data are used for interpreting subsurface structural or stratigraphic features. The physical properties of pore fluids strongly influence the seismic properties of rocks and which vary with composition, pressure, and temperature. The fluids within the pores of the sedimentary rocks can vary widely in composition and physical properties. Pore fluids form a dynamic system in which both composition and physical phases change with pressure and temperature (Batzle & Wang, 1992). Density, bulk modulus, and viscosity of oil increase with molecular weight and pressure, but decrease with temperature. Gas has a similar behaviour, except at lower pressures where the viscosity increases with temperature. A good understanding of the changes in the P & S-wave velocities and density as a function of fluid or rock properties is necessary for reliable determination of seismic wave amplitudes and travel time.

In fact, P- wave velocity is different in gas and oil in comparison with brine. Oil or gas fill will reduce the P velocity significantly compared with the brine case. Also, the density decreases linearly as gas saturation increases.

Several mathematical models were used and developed in order to describe pore fluid effects on rock density and seismic velocity (Gassmann, 1951, Biot 1956, Batzle & Wang 1992).

Equations for the calculation of fluid properties in seismic exploration have been given by Batzle and Wang (1992). The properties in these equations depend on pressure and temperature. Also, they are dependant on API gravity and GOR (gas-oil ratio) for oils and specific gravity for gases. They proposed simple equations for the calculation of density, bulk modulus, velocity and viscosity of pore fluids and used a combination of thermodynamic relationships, empirical trends, and published data to examine the effects of pressure, temperature and composition on these important seismic properties of hydrocarbon gases and oils and brines.

This chapter is in two parts:

First, the results of the speed of sound calculations using the SAFT-BACK equation of state and the Batzle – Wang model will be compared with experimental data for different fluid types, i.e., ten pure hydrocarbons, a volatile oil, four multi-component mixtures and three real oils. The objective of this study is to investigate the efficiency of the SAFT-BACK EoS in determination of thermodynamic properties compared to Batzle – Wang model which has been used for many years.

Then, the effects of fluid substitution on the velocity of saturated sediments saturated with reservoir fluids in various temperatures and pressures are described. In this part, three different fluids were used as pore fluids in sediments and the results of the measurements are presented.

6.2 Batzle and Wang Fluid Property Model

The Batzle and Wang (1992) model predicts the effects of pressure, temperature, and composition on the seismic properties of fluids using a combination of thermodynamic relationships and empirical trends. They investigated the properties of gases, oils and brine and predicted density, bulk modulus and velocity as functions of fluid temperature and pressure, when the pore fluid composition is known or estimated. A summary of these models will be explained in this section and include gas, live oil, dead oil, brine, and mixtures of these fluids. There is one assumption in this model: at any point below the bubble point, the gas that comes out of solution has the same properties and composition as the total liberated gas at the surface conditions. It means that the remaining liquid oil has the same composition as the original live oil.

First, some input variables are necessary for all Batzle and Wang model calculations that are determined from PVT testing of an oil/fluid sample.

6.2.1 Basic Input Variables

T = Reservoir Temperature, °C
P = Reservoir Pressure, MPa
G = Specific Gravity of the Gas
R_g = Gas - Oil Ratio (GOR), vol/vol
°API = Degree API Gravity of Oil
S = Salinity (ppm of NaCl)

Mixture Saturation Variables:

S_g = Gas Saturation
S_o = Oil Saturation
S_b = Brine Saturation

Constants:

ρ_{air} = Density of air, g/cm^3 = 0.00122 at 15.6 °C
R = Gas Constant, m^3.Pa/(mol.°K) = 8.3145

6.2.2 Gas Model

Hydrocarbon gases usually consist of alkanes such as methane, ethane, and propane. The specific gravity (G) of typical gases is between 0.56 and greater than 1.8 which is measured relative to air, taken as 1.0 (Bulloch, 1999). In this method, the modelling is performed as adiabatic, rather than isothermal, because of the large coefficient of thermal expansion in most fluids.

Gases are simpler to model than oils because the composition and phase behaviour of gases has been examined more thoroughly.

Using the equations listed below with the input variables previously listed allow calculation of gas phase properties.

6.2.2.1 The Gas Equations:

Adiabatic gas modulus, K_S, in MPa:

$$K_S = \frac{P}{1 - \frac{P_{\mathrm{Pr}}}{Z}\frac{\partial Z}{\partial P_{\mathrm{Pr}}}}\gamma_0 \tag{6.1}$$

Where

$$P_{\mathrm{Pr}} = \frac{P}{P_{Pc}} \tag{6.2}$$

$$P_{PC} = 4.892 - 0.4048G \tag{6.3}$$

$$\frac{\partial Z}{\partial P_{\mathrm{Pr}}} = A + 0.1308(3.85 - T_{\mathrm{Pr}})^2 \exp\left(DP_{\mathrm{Pr}}^{1.2}\right)DP_{\mathrm{Pr}}^{0.2} \tag{6.4}$$

$$\mathrm{A} = 0.03 + 0.00527(3.5\mathrm{T}_{\mathrm{Pr}})^3 \tag{6.5}$$

$$D = \left(\frac{-1}{T_{\mathrm{Pr}}}\right)\left(0.45 + 8\left(0.56 - \frac{1}{T_{\mathrm{Pr}}}\right)^2\right) \tag{6.6}$$

$$T_{\mathrm{Pr}} = \frac{T_a}{T_{PC}} \tag{6.7}$$

$$T_a = T(^{\circ}C) + 273.15 \tag{6.8}$$

$$T_{PC} = 94.72 + 170.75G \tag{6.9}$$

$$\gamma_0 = 0.85 + \frac{5.6}{(P_{\mathrm{Pr}} + 2)} + \frac{27.1}{(P_{\mathrm{Pr}} + 3.5)^2} - 8.7\exp\left[-0.65(P_{\mathrm{Pr}} + 1)\right] \tag{6.10}$$

$$Z = A.P_{\mathrm{Pr}} + \left(0.642\,T_{\mathrm{Pr}} - 0.007\,T_{\mathrm{Pr}}^{4} - 0.52\right) + E \tag{6.11}$$

$$E = 0.109\left(3.85 - T_{\mathrm{Pr}}\right)^{2} \exp\left\{-\left[0.45 + 8\left(0.56 - \frac{1}{T_{\mathrm{Pr}}}\right)^{2}\right]\frac{P_{\mathrm{Pr}}^{1.2}}{T_{\mathrm{Pr}}}\right\} \tag{6.12}$$

Gas density, ρ_g, in g/cm^3:

$$\rho_g = \frac{28.8\,G\,P}{ZRT_a} \tag{6.13}$$

P-wave Velocity, V_g, in m/s:

$$V_g = \sqrt{\frac{K_S}{\rho_g}} \tag{6.14}$$

Where T_{pc} and P_{pc} are pseudocritical temperature and pressure, T_{pr} and P_{pr} are pseudo-reduced temperature and pressure, respectively.

6.2.3 Live and Dead Oil Models

Crude oils have a wide range of different properties such as API, density, composition, velocity and other characterizations that affect the seismic responses. The variation in API gravity can be from 5 for very heavy tars to near 80 for very light condensate. Densities can vary from 0.5 g/cm^3 to greater than 1 g/cm^3 for dead oil in surface conditions of temperature and pressure. The effect of temperature is greater than pressure on seismic properties. Wang (1988) and Wang et. al. (1988) developed a relationship for ultrasonic velocities within dead oils. This calculation method uses the temperature and pressure of the reservoir, the API gravity of the oil, and the density of dead oil at surface conditions for calculation of the density in reservoir or other pressures. For determination of density of live oil in reservoirs, the model requires the density at saturation, GOR, gas volume factor and specific gravity.

6.2.3.1 Dead Oil Equations:

$$\rho_d = \frac{\rho_P}{\left[0.972 + \left(3.81\times10^{-4}\right)\left(T + 17.78\right)^{1.175}\right]} \tag{6.15}$$

Where

$$\rho_P = \rho_O + \left(0.00277\ P - \left(1.71\times10^{-7}\right)P^3\right)\left(\rho_O - 1.15\right)^2 + \left(3.49\times10^{-4}\right)P \tag{6.16}$$

$$\rho_O = \frac{141.5}{API + 131.5} \tag{6.17}$$

Where ρ_O is the density of dead oil at surface conditions.

P-wave Velocity, V_d, in m/s:

$$V_d = 15450\left(77.1 + API\right)^{-0.5} - 3.7\,T + 4.64\,P + 0.0115\left(0.36\,API^{0.5} - 1\right)TP \tag{6.18}$$

Dead oil modulus, K_d, in MPa:

$$K_d = V_d^2\rho_d \tag{6.19}$$

6.2.3.2 Live Oil Equations:

Live oil density, ρ_l, in g/cm^3:

$$\rho_l = \frac{\rho_{Pl}}{[0.972 + (3.81\times10^{-4})(T + 17.78)^{1.175}]} \tag{6.20}$$

Where

$$\rho_{Pl} = (\rho_{gl} + 0.00277P - 1.71\times10^{-7}\,P^3)(\rho_{gl} - 1.15)^2 + (3.49\times10^{-4})P \tag{6.21}$$

Where ρ_{Pl} is the density at saturation and is:

$$\rho_{gl} = \frac{(\rho_0 + 0.0012GR_g)}{B_{ol}} \tag{6.22}$$

$$B_{ol} = 0.972 + 0.0003812[2.4955R_g(\frac{G}{\rho_o})^{0.5} + T + 17.778]^{1.175} \quad (6.23)$$

P-wave Velocity, V_l, in m/s:

$$V_l = 2096\left(\frac{\rho_{dl}}{2.6-\rho_{dl}}\right)^{0.5} - 3.7\,T + 4.64\,P + 0.0115\left(4.12\left(\frac{1.08}{\rho_{dl}}\right)^{0.5} - 1\right)TP \quad (6.24)$$

$$\rho_{dl} = \frac{\rho_o}{B_{ol}}(1 + 0.001R_g)^{-1}$$

(6.25)

Where ρ_{dl} is pseudo density and R_g is the gas-oil ratio.

Live oil modulus, K_l, in MPa:

$$K_l = V_l^2\rho_l \quad (6.26)$$

6.2.3.3 The Equations for Live Oil at its Maximum Gas-Oil Ratio:

Live oil density, ρ_{lm},in g/cm^3:

$$\rho_{lm} = \frac{\rho_{Pm}}{[0.972 + (3.81\times10^{-4})(T + 17.78)^{1.175}]} \quad (6.27)$$

Where

$$\rho_{Pm} = (\rho_{gm} + 0.00277P - 1.71\times10^{-7}P^3)(\rho_{gm} - 1.15)^2 + (3.49\times10^{-4})P \quad (6.28)$$

$$\rho_{gm} = \frac{\left(\rho_o + 0.0012GR_{g\max}\right)}{B_{olm}} \quad (6.29)$$

$$B_{olm} = 0.972 + 0.0003812[2.4955R_{g\max}(\frac{G}{\rho_o})^{0.5} + T + 17.778]^{1.175} \quad (6.30)$$

$$R_{g\max} = 2.028G\left[P\exp\left(0.02877API - 0.003772T\right)\right]^{1.204} \quad (6.31)$$

P-wave Velocity, V_l, in m/s:

$$V_{lm} = 2096\left(\frac{\rho_{pdm}}{2.6-\rho_{pdm}}\right)^{0.5} - 3.7\,T + 4.64\,P + 0.0115\left(4.12\left(\frac{1.08}{\rho_{pdm}}\right)^{0.5} - 1\right)TP \qquad (6.32)$$

$$\rho_{pdm} = \frac{\rho_o}{B_{om}}(1 + 0.001R_{g\max})^{-1} \qquad (6.33)$$

Live oil modulus, K_{lm}, in MPa:

$$K_{lm} = V_{lm}^2\rho_{ml} \qquad (6.34)$$

6.2.4 Brine Model

Brine is in the most common fluid in the pore of subsurface sediments with different compositions ranging from pure water to saturated saline solutions. Increasing salinity increases the brine density. Batzle and Wang (1992) proposed a simple polynomial model using salinity and reservoir temperature and pressure for calculation of brine density, but it is only applicable for sodium chloride solutions. Also, they extended and modified the equations to fit additional higher salinity and higher temperature data for calculation of velocity of brine.

Velocity in waters and brines are different from the other reservoir fluids, as their velocities decrease in very high pressures. The amount of gas that can be dissolved in brine increases with an increase in pressure and decreases with an increase in salinity.

6.2.4.1 Brine/Water Equations:

Density of fresh water, ρ_w, in g/cm^3:

$$\rho_w = 1 + ((1\times10^{-6})(-80T - 3.3T^2 + 0.00175T^3 + 489P - 2TP + 0.016T^2P - (1.3\times10^{-5})T^3P - 0.333P^2 - 0.002TP^2)) \qquad (6.35)$$

Density of Brine, ρ_b, in g/cm^3:

$$\rho_b = \rho_w + S\{0.668 + 0.44S + (1\times10^{-6})[300P - 2400PS + T(80 + 3T - 3300S - 13P + 47PS)]\} \qquad (6.36)$$

Velocity of water, V_W in m/s (constants w_{ij} are provided in Table 6.1)

$$V_W = \sum_{i=0}^{4}\sum_{j=0}^{3} w_{ij}T^iP^j \qquad (6.37)$$

Velocity of brine, V_b, in m/s:

$$V_b = V_w + S(1170 - 9.6T + 0.055T^2 - (8.5\times10^{-5})T^3 + 2.6P - 0.0029TP - 0.0476P^2) + S^{1.5}(780 - 10P + 0.16P^2) - 1820S^2 \tag{6.38}$$

Modulus of gas free brine, K_b, in MPa:

$$K_b = V_b^2 \rho_b \tag{6.39}$$

Modulus of live brine, K_{gb}, in MPa:

$$K_{gb} = \frac{K_b}{1 + 0.0494 R_{gb}} \tag{6.40}$$

Where

$$R_{gb} = 10^{\log_{10}\left\{0.712P\left|T-76.71\right|^{1.5}+3676P^{0.64}\right\}-4-7.786S(T+17.78)^{-0.5}} \tag{6.41}$$

Table 6.1 Coefficients for velocity of water calculation

w_{00}	1402.85	w_{02}	3.437×10^{-3}
w_{10}	4.871	w_{12}	1.739×10^{-4}
w_{20}	-0.04783	w_{22}	-2.135×10^{-6}
w_{30}	1.487×10^{-4}	w_{32}	-1.455×10^{-8}
w_{40}	-2.197×10^{-7}	w_{42}	5.230×10^{-11}
w_{01}	1.524	w_{03}	-1.197×10^{-5}
w_{11}	-0.0111	w_{13}	-1.628×10^{-6}
w_{21}	2.747×10^{-4}	w_{23}	1.237×10^{-8}
w_{31}	-6.503×10^{-7}	w_{33}	1.327×10^{-10}
w_{41}	7.987×10^{-10}	w_{43}	-4.614×10^{-13}

6.2.5 Mixture Model

Pore fluid properties are very important in seismic characterization. Most of the pore fluids are hydrocarbon mixtures and their properties may change in the reservoir during the time, since some dissolved gases may be released as the pressure drops during the production and this can cause changes in the seismic properties.

If the properties of the individual fluids and their volume fraction are known, the mixture properties can be calculated.

6.2.5.1 The Fluid Mixture Equations:

Live oil mixture density, ρ_{ml}, in g/cm^3:

$$\rho_{ml} = S_g\rho_g + S_o\rho_l + S_b\rho_b \tag{6.42}$$

Max Live oil mixture density, ρ_{mlm}, in g/cm^3:

$$\rho_{mlm} = S_g\rho_g + S_o\rho_{lm} + S_b\rho_b \tag{6.43}$$

Dead oil mixture density, ρ_{md}, in g/cm^3:

$$\rho_{md} = S_g\rho_g + S_o\rho_d + S_b\rho_b \tag{6.44}$$

Live oil mixture modulus, K_{ol}, in MPa:

$$K_{ol} = \frac{1}{\left(\frac{S_g}{K_S} + \frac{S_o}{K_l} + \frac{S_b}{K_g}\right)} \tag{6.45}$$

Maximum live oil mixture modulus, K_{olm}, in MPa:

$$K_{olm} = \frac{1}{\left(\frac{S_g}{K_S} + \frac{S_o}{K_{lm}} + \frac{S_b}{K_g}\right)} \tag{6.46}$$

Dead Live oil mixture modulus, K_{od}, in MPa:

$$K_{od} = \frac{1}{\left(\frac{S_g}{K_S} + \frac{S_o}{K_{ld}} + \frac{S_b}{K_g}\right)} \tag{6.47}$$

Velocity for live oil mixture, V_{ol}, in m/s:

$$V_{ol} = \sqrt{\frac{K_{ol}(1000)}{\rho_{ml}}} \tag{6.48}$$

Velocity for Maximum live oil mixture, V_{olm}, in m/s:

$$V_{olm} = \sqrt{\frac{K_{olm}(1000)}{\rho_{mlm}}} \tag{6.49}$$

Velocity for Dead oil mixture, V_{od}, in m/s:

$$V_{od} = \sqrt{\frac{K_{od}(1000)}{\rho_{md}}} \tag{6.50}$$

6.2.6 Comparison of Measured Fluid Properties with the Results of SAFT-BACK Equation of State and Batzle-Wang Equations

In the previous section of this chapter, Batzle - Wang equations were listed for different types of fluids for calculation of fluid properties. Chapter 3 indicated the measurement of sound velocities for several hydrocarbons, pure, mixtures and real oils. In Chapter 4, SAFT-BACK equation of state was described to model the thermodynamic properties of fluids. Also, the results of other cubic equations of state were compared with SAFT-BACK EoS and the priority of this work was explained. Then, the obtained results were compared with experimental data in Chapter 5.

Now, in this part, the result of Batzle-Wang equations which is the only equation in seismic reservoir characterization for calculating fluid elastic properties will be compared with experimental and calculated data using SAFT-BACK EoS. This chapter will show the efficiency of this technique in reservoir fluid modelling. To obtain a good understanding of the reservoir modelling, a seismic flow chart (Figure 6.1) shows the relationship of fluid properties to seismic responses. Based on these input values, the fluid properties of the reservoir are calculated using the Batzle and Wang (1992) model. Once the fluid properties (modulus, density, velocity) are known, a model must be used to determine the properties of the fluids within the reservoir rock matrix under differing conditions, such as saturation. The Gassmann-Biot model can be used for this and it can also be used to determine the correction necessary to convert well log values from logging conditions (invaded conditions, mostly water or brine) to reservoir conditions.

The P- and S- wave velocities and density for the fluid saturated reservoir rock, predicted by the Gassmann-Biot model, may then be used along with the overlying rock property information (determined from logs or estimated) for AVO modeling, to compare a calculated response to seismic observations.

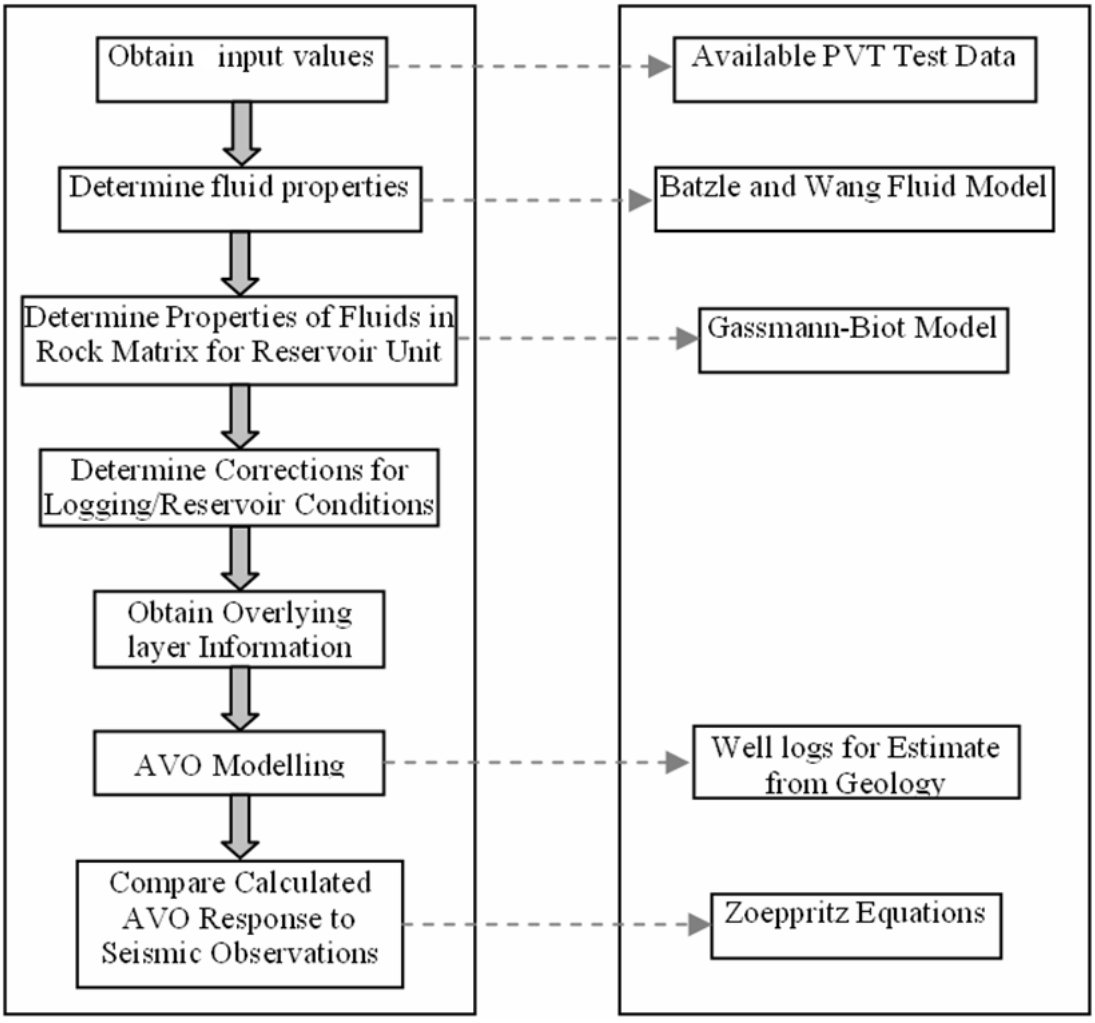

Figure 6.1 Flow Chart showing the relationship of fluid properties to seismic response (Bulloch,1999)

To know the effects of these different equations on fluid properties, this chapter will discuss the results obtained by SAFT-BACK equation of state and Batzle-Wang equations and show the efficiency of this work in reservoir fluid modelling. For this purpose, the results of two pure hydrocarbons (methane gas and n-heptane in liquid state), a volatile oil ($C_1 + nC_5 + nC_6$), four multi-component mixtures ([$nC_5 + nC_6$], [$nC_6 + nC_{10}$], [$CO_2 + nC_4 + nC_{10}$] and [$nC_7 + nC_8 + nC_9 + nC_{10}$]) and three real oils will be displayed here and compared with experimental data. Table 6.2 shows the average deviation of calculated values of density, velocity and bulk module from experimental data and NIST correlated data when experimental data are not available. The application of the SAFT-BACK equation of state in reservoirs in comparison with the Batzle – Wang equations will be discussed later in this chapter. The results of these two

equations in calculating speed of sound are compared with experimental data and displayed in Figures 6.2 – 6.11.

Table 6.2 Absolute average percentage deviations from experimental data predicted values are calculated using the Batzle-Wang and SAFT-BACK model.

Component	Eq.	Fluid density	Fluid velocity	Bulk module
Methane	B&W	1.17	9.87	18.48
	S&B	0.72	1.88	4.56
Ethane	B&W	4.80	11.47	22.83
	S&B	0.57	0.32	4.57
Propane	B&W	5.33	115.42	677.53
	S&B	0.86	1.01	2.54
Butane	B&W	23.74	13.08	112.52
	S&B	0.09	0.57	1.12
n-Pentane	B&W	3.75	5.42	7.98
	S&B	0.15	0.70	1.39
n-Hexane	B&W	4.47	4.82	7.90
	S&B	0.21	2.04	4.32
n-Heptane	B&W	5.13	4.04	7.90
	S&B	0.21	2.74	5.48
n-Octane	B&W	5.73	4.13	8.09
	S&B	0.29	3.41	7.60
n-Nonane	B&W	5.88	5.13	11.51
	S&B	0.45	4.43	10.49
n-Decane	B&W	6.34	5.66	13.48
	S&B	0.74	4.74	6.56

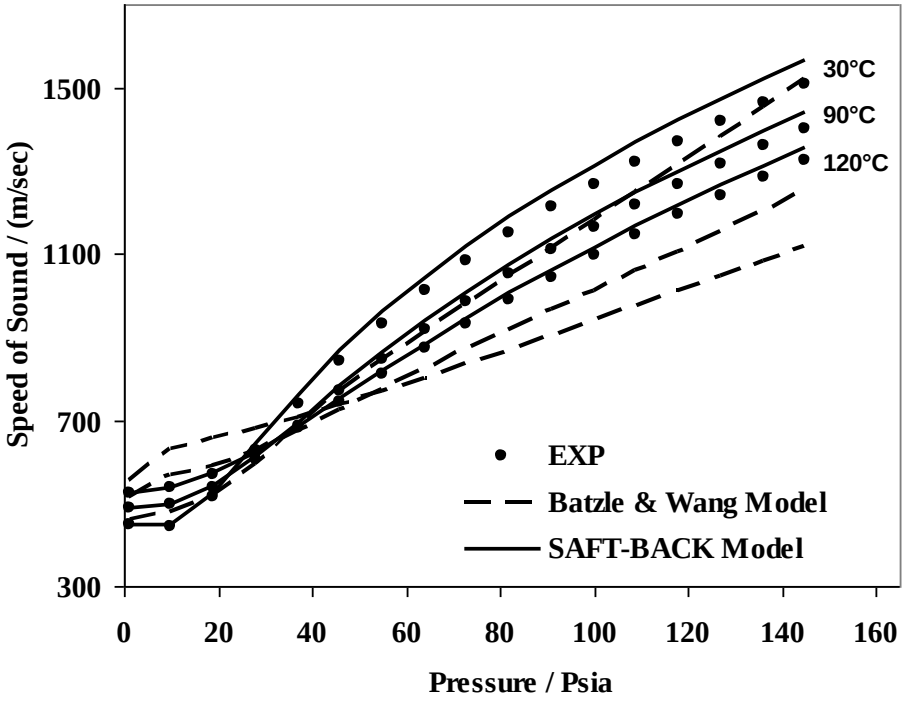

Figure 6.2 Comparison of the speed of sound in methane at different temperatures and pressures using the Batzle and Wang equations and the SAFT-BACK equation of state

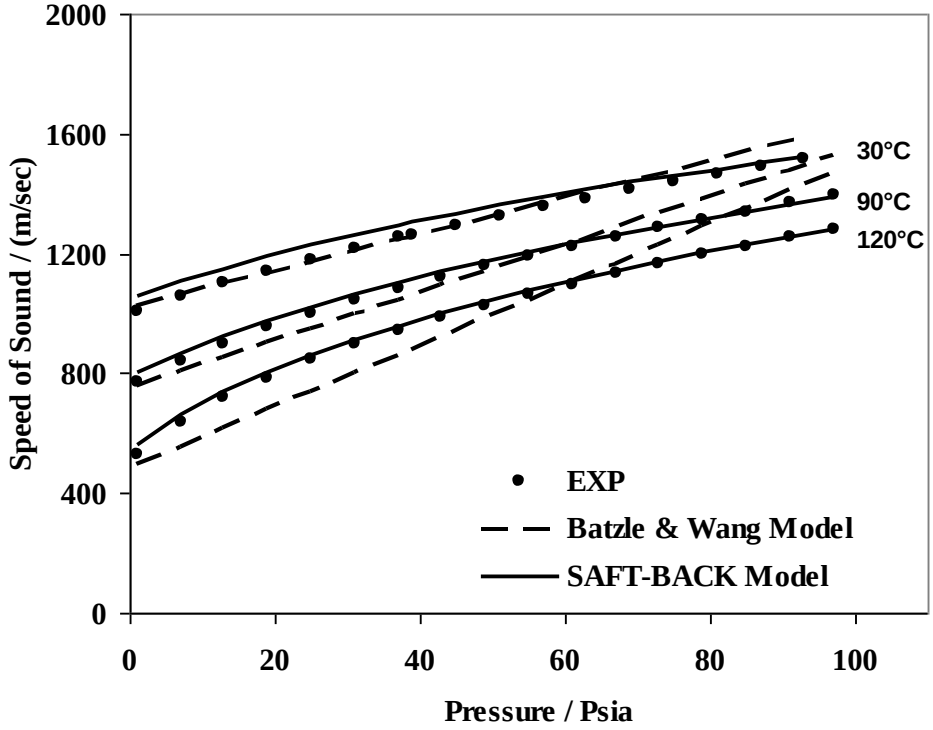

Figure 6.3 Comparison of speed of sound in n-heptane in different temperatures and pressures using Batzle and Wang equations and SAFT-BACK equation of state

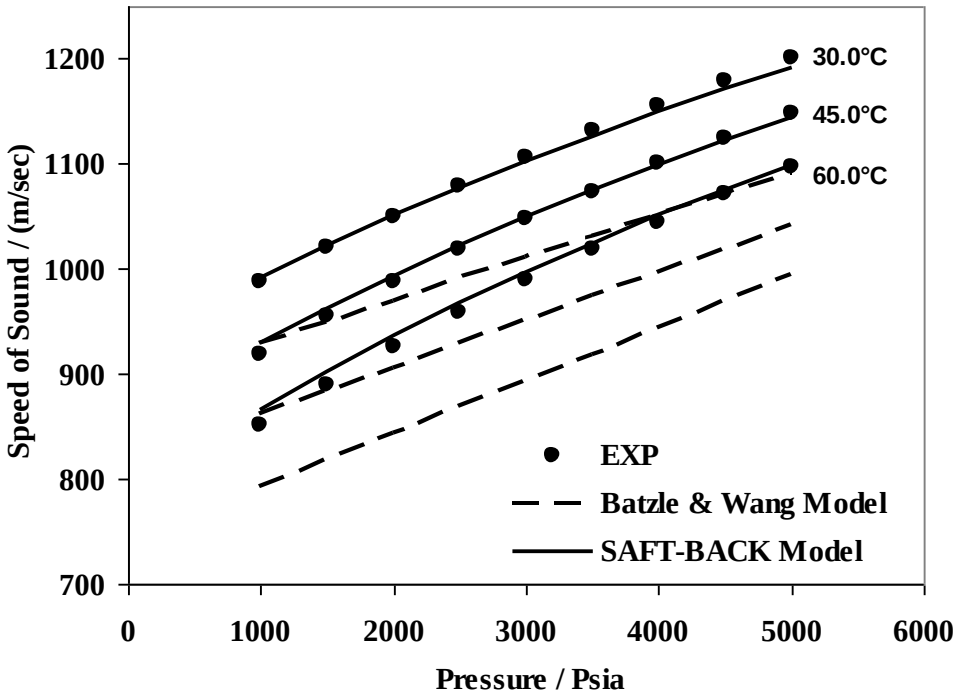

Figure 6.4 Comparison of speed of sound in a volatile oil of methane + n-pentane + n-hexane in different temperatures and pressures using Batzle and Wang equations and SAFT-BACK equation of state

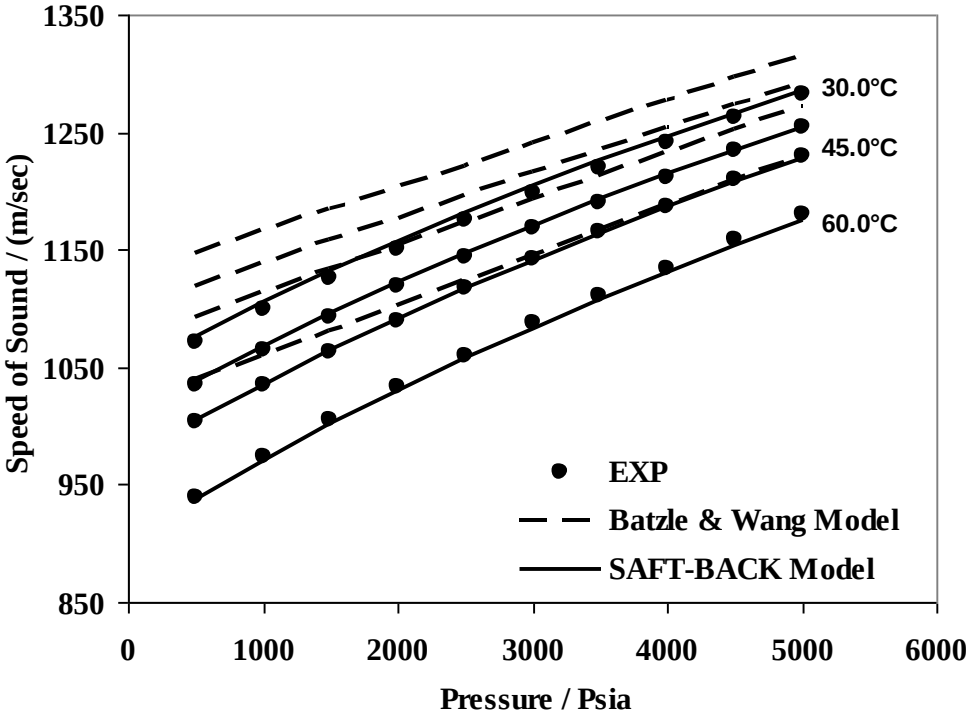

Figure 6.5 Comparison of speed of sound in a binary mixture of n-pentane + n-hexane in different temperatures and pressures using Batzle and Wang equations and SAFT-BACK equation of state

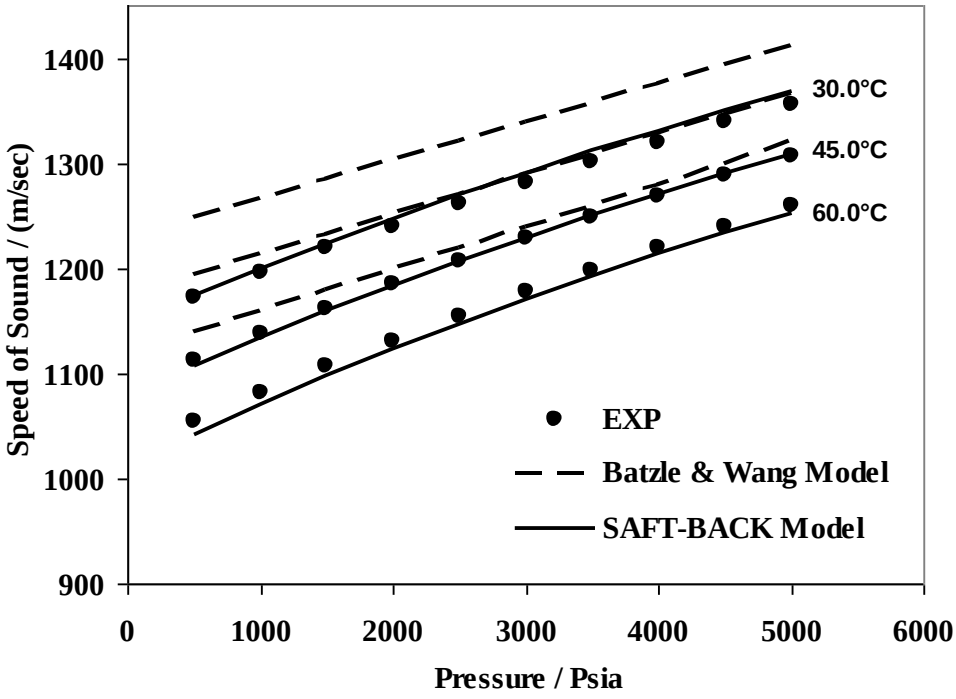

Figure 6.6 Comparison of speed of sound in a binary mixture of n-hexane + n-decane in different temperatures and pressures using Batzle and Wang equations and SAFT-BACK equation of state

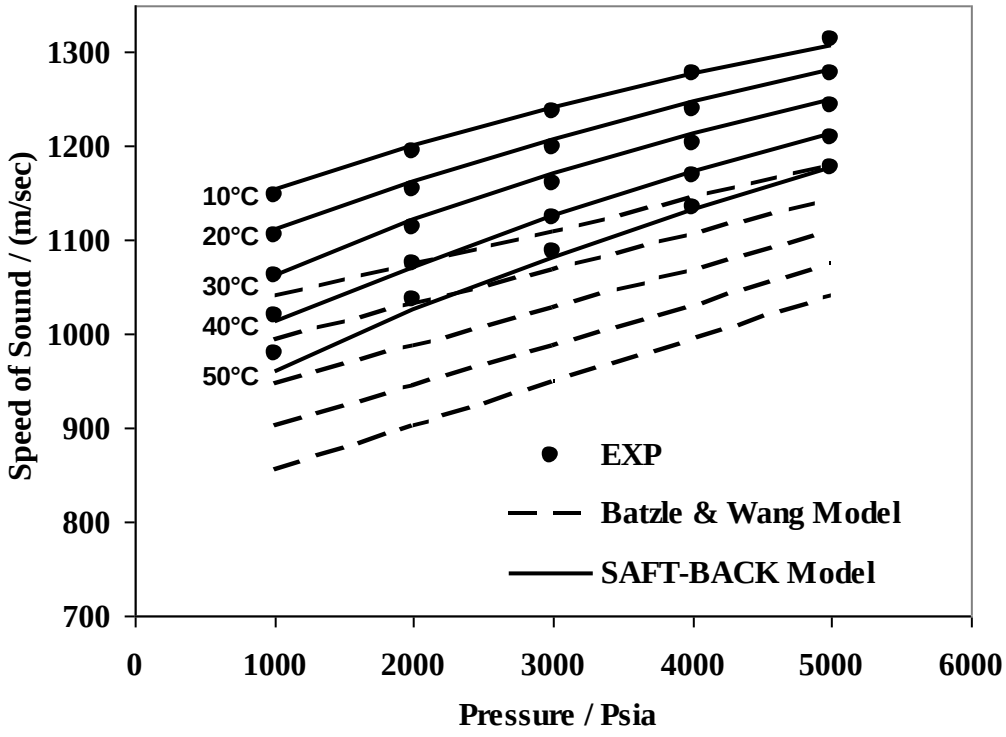

Figure 6.7 Comparison of speed of sound in a live oil ternary mixture of carbon dioxide + n-butane + n-decane in different temperatures and pressures using Batzle and Wang equations and SAFT-BACK equation of state

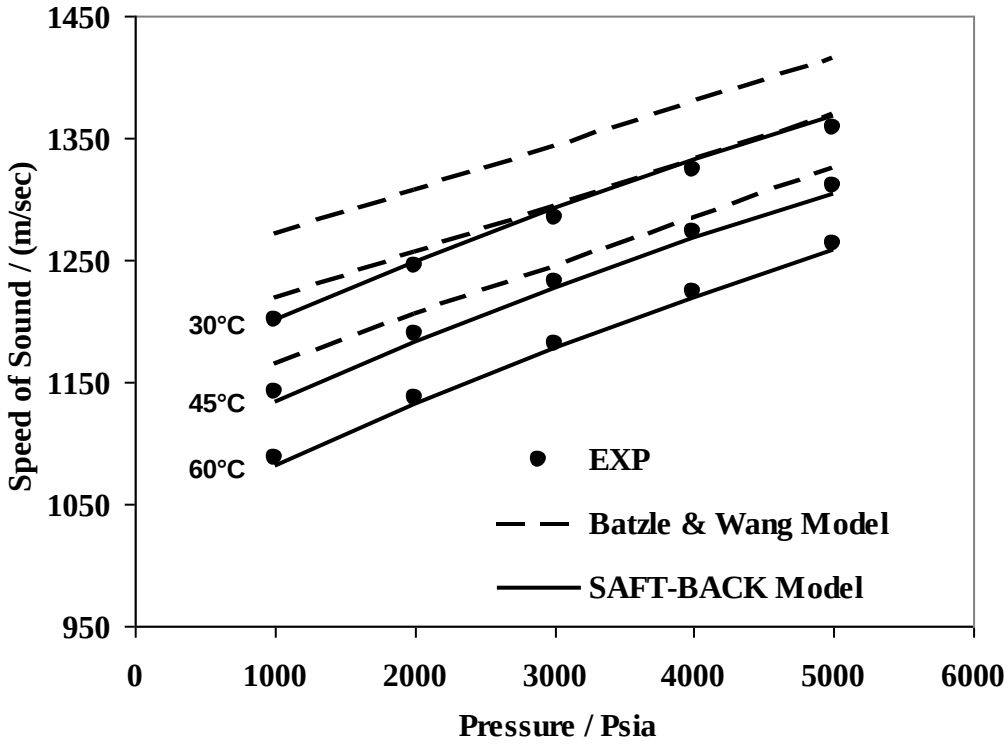

Figure 6.8 Comparison of speed of sound in a synthetic mixture of n-heptane + n-octane +n-nonane+ n-decane in different temperatures and pressures using Batzle and Wang equations and SAFT-BACK equation of state

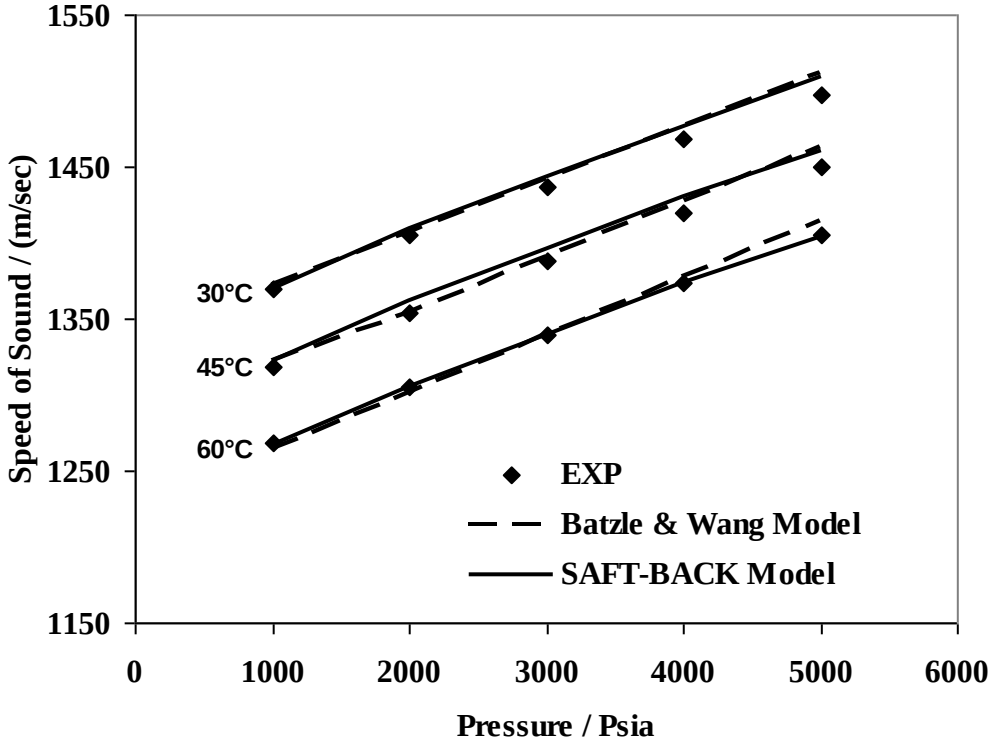

Figure 6.9 Comparison of speed of sound in Real Oil 1 in different temperatures and pressures using Batzle and Wang equations and SAFT-BACK equation of state

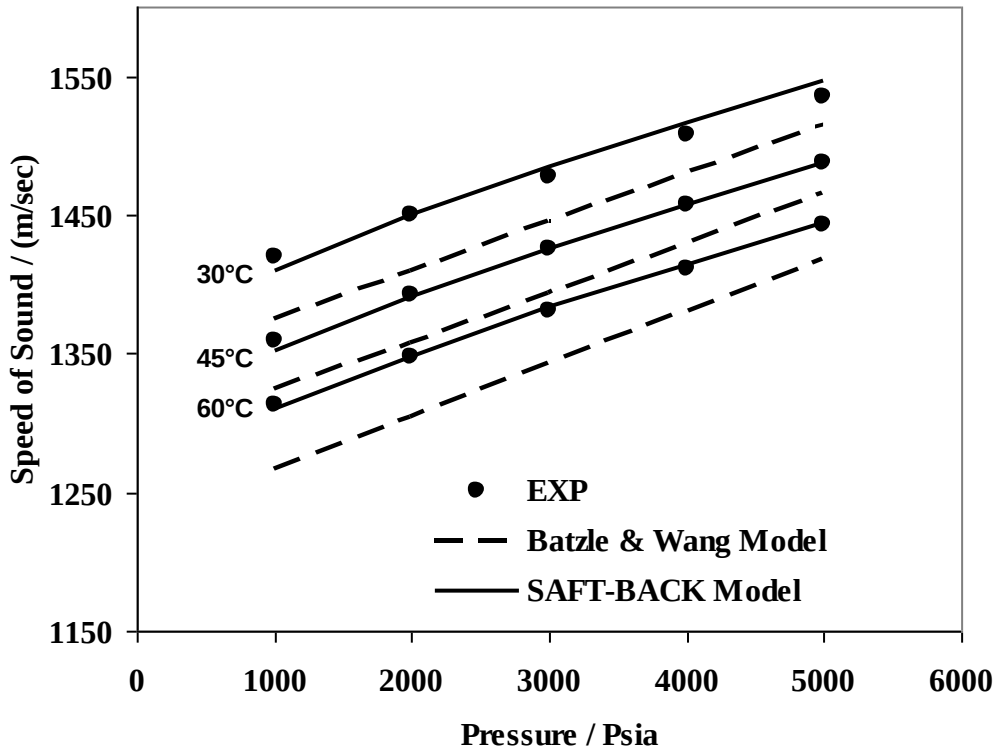

Figure 6.10 Comparison of speed of sound in Real Oil 2 in different temperatures and pressures using Batzle and Wang equations and SAFT-BACK equation of state

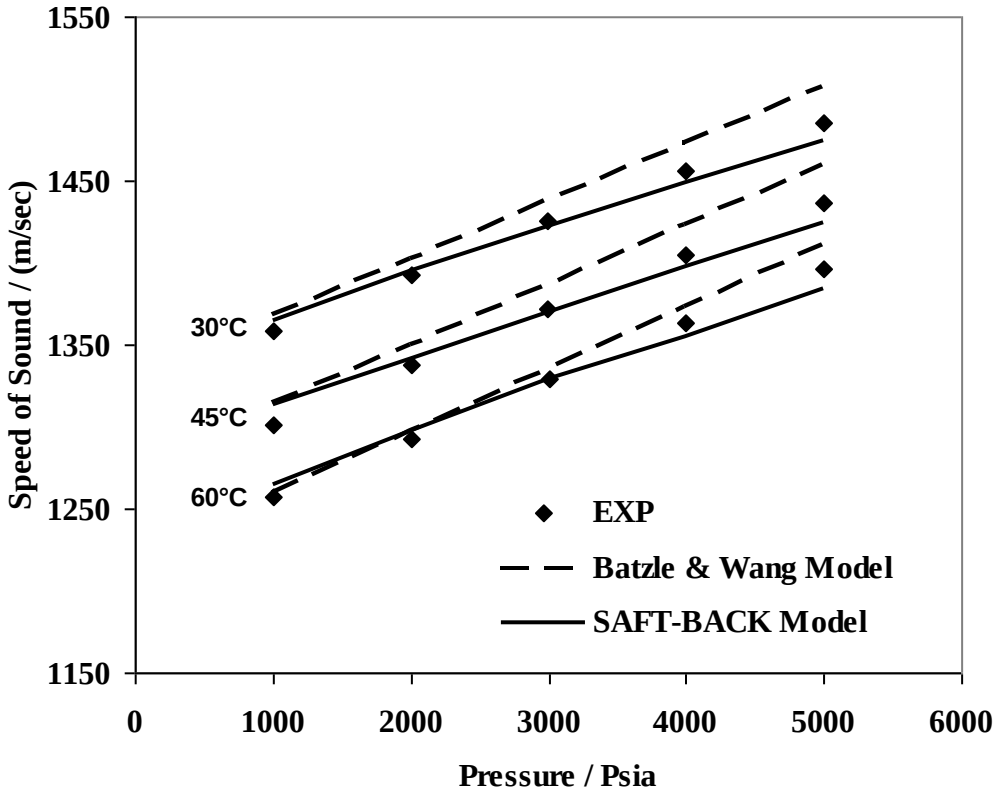

Figure 6.11 Comparison of speed of sound in Real Oil 3 in different temperatures and pressures using Batzle and Wang equations and SAFT-BACK equation of state

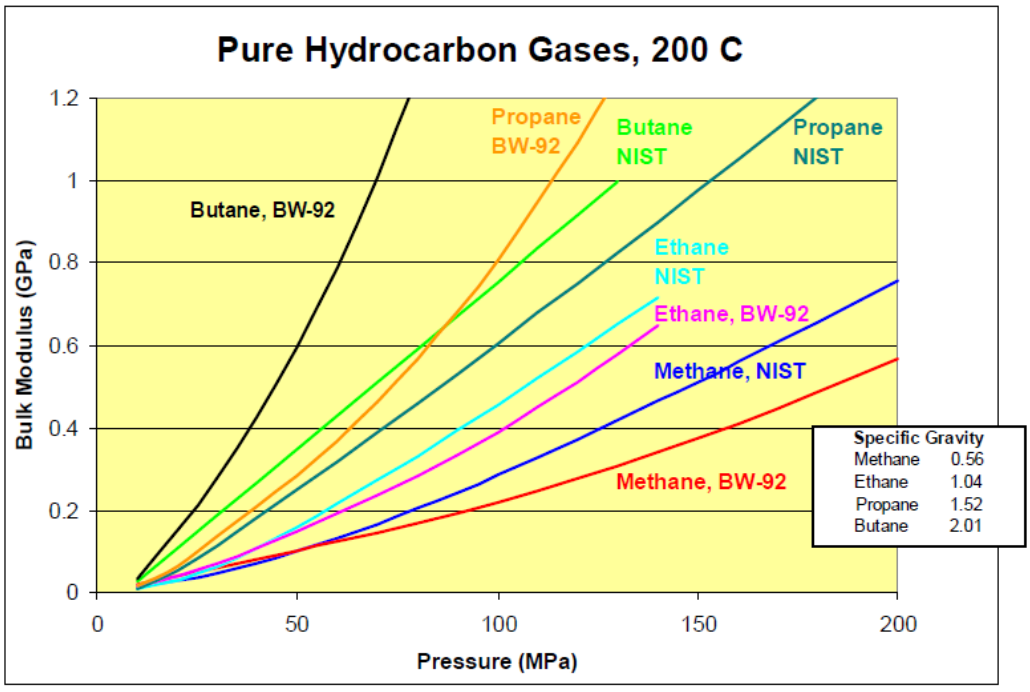

Figure 6.12 Effect of pressure on adiabatic bulk modulus of methane, ethane, propane and butane as computed by Batzle - Wang (1992) and NIST Model (200 C) (Walls, 2005)

The above figures demonstrate that the SAFT-BACK equation of state works better than the Batzle – Wang equations for calculation of the speed of sound in reservoir fluids, especially for volatile oils and live oils. The best results of Batzle – Wang equations can be observed in Real Oil 1 in Figure 6.9, which is real oil with no gases in its composition. The other figures show that this equation performs better at lower temperatures and pressures rather than in reservoir conditions. Figure 6.12 displays the deviation of the Bulk modulus for gases such as methane, ethane, propane and butane calculated by the Batzle – Wang equations from NIST data at 200 °C. These deviations have significant effects on saturated rock elastic properties and further on seismic acoustic impedance.

6.3 Effect of Temperature, Pressure and Type of Pore Fluid on Speed of Sound in Saturated Matrix

In Chapter 3, three experiments were described which explained the injection of fluids into the sediment pores and measurement of of the speed of sound in the system. First, the effects of pore pressure at constant temperature and overburden pressure on speed of sound in a saturated matrix for a binary mixture of nC_6 + nC_{10} as the pore fluid will be described. In the next step of this experiment, the same fluid is used to investigate the effects of fluid speed of sound on the saturated sediment velocity at constant temperature and different overburden pressures by keeping the effective pressure constant.

In the next experiment, the effects of temperature variations on the speed of sound in saturated sediment at constant overburden and pore pressure will be studied. CO_2 was used as the injected pore fluid. In the last experiment, both temperature and pore pressure were changed. The overburden pressure was adjusted with pore pressure in order to keep the effective pressure constant during the test. Therefore, by maintaining the effective pressure constant, it was possible to study the fluid velocity effects on saturated matrix properties.

6.3.1 Speed of Sound in Fluid Saturate Matrix (Test 1)

In Table 6.3, the measured values of speed of sound in fluid and matrix saturated with the injected fluid are indicated for different pore pressures (Chapter 3, Section 3.3.2.1). This experiment shows the variation of velocity with changes in pore pressure, while the

overburden pressure is constant. Pressure decrement often happens in reservoirs during oil recovery. The effective pressure, which is the difference between overburden and pore pressures, changes during the test and so, the porosity varies significantly during the test. This will affect the elasticity of the sediments, and compaction occurs with an increase in the effective pressure which results in higher compression velocity.

Table 6.3 Measured speed of sound in different pore pressure for sand + (nC_6 + nC_{10}) as pore fluid at 45 °C

Temperature (°C)±0.01	Overburden Pressure (psia)±0.5	Pore Pressure (psia)±0.5	V_p (EXP) (m/s)
44.94	5800.0	5000.0	1531.88
44.94	5800.0	4800.0	1534.36
44.94	5800.0	4600.0	1538.20
44.94	5800.0	4600.0	1538.56
44.94	5800.0	4400.0	1540.95
44.94	5800.0	4200.0	1548.27
44.94	5800.0	4000.0	1554.77
44.94	5800.0	3500.0	1562.60
44.94	5800.0	3000.0	1567.23
44.94	5800.0	2500.0	1592.67
44.94	5800.0	2000.0	1596.46
44.92	5800.0	1500.0	1598.94
44.92	5800.0	1000.0	1598.06
44.94	5800.0	500.0	1598.27

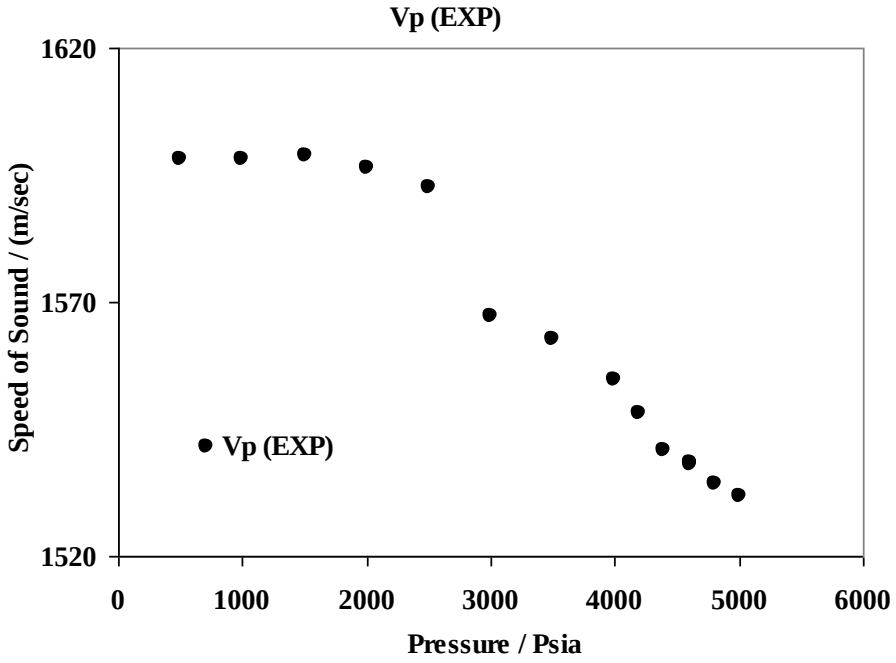

Figure 6.13 Variation of speed of sound in fluid saturated matrix [sand + (nC_6 + nC_{10})] in different pore pressures - Effective pressure increased from 800 psia to 4800 psia moving from right to left on x-axis.

In this experiment, first the overburden and pore pressure were increased to the highest possible pressures (overburden pressure: 5800 psia, pore pressure: 5000 psia). The effective pressure was maintained constant at 800 psia while fluid injection was performed. Then, the pore pressure was decreased while keeping the overburden pressure constant. The pore pressure was decreased from an initial value of 5000 psia to 500 psia. Figure 6.13 shows the speed of sound in this system for different pore pressures and effective pressure, while the overburden pressure was kept constant at 5800 psia. As it is indicated in Figure 6.13, the speed of sound has an almost a linear trend, i.e., increasing up to 2500 psia. However, at pore pressures below 2500 psia the speed of sound remains almost constant. This might be caused by compaction of sediments, resulting in porosity and permeability reduction

Table 6.4 indicates the measured speed of sound in a saturated matrix while the binary mixture of normal hexane + normal decane fluid is being injected into the pores. Overburden and pore pressures were gradually increased in order to keep the effective pressure constant.

Figure 6.14 shows the speed of sound of the binary mixture before injection and in the matrix saturated with this fluid after injection. It illustrates that by increasing pore pressure, the speed of sound is increased in both fluid and matrix increased. In this part of the experiment, the effective pressure is constant and both pore and overburden pressure change in each measurement.

Table 6.4 Measured speed of sound in nC_6 + nC_{10} and the matrix saturated with this mixture at different pressures and 45.0 °C. V_p is the velocity of the fluid-saturated matrix (fluid + matrix) and V_f is the velocity of fluid only.

Temperature (°C)±0.01	**Pore Pressure (psia)±0.5**	**V_p (EXP) (m/s)**	**V_f (EXP) (m/s)**
45.00	500.0	1367.81	1113.18
45.00	1000.2	1387.85	1137.98
45.00	1501.4	1407.32	1161.91
45.00	1999.7	1426.37	1184.83
45.00	2500.3	1444.84	1207.07
44.92	3003.3	1462.83	1228.77
44.98	3500.6	1480.39	1249.14
44.98	3998.5	1497.31	1269.12
45.02	4500.9	1513.82	1288.04
45.02	5000.2	1529.86	1306.76

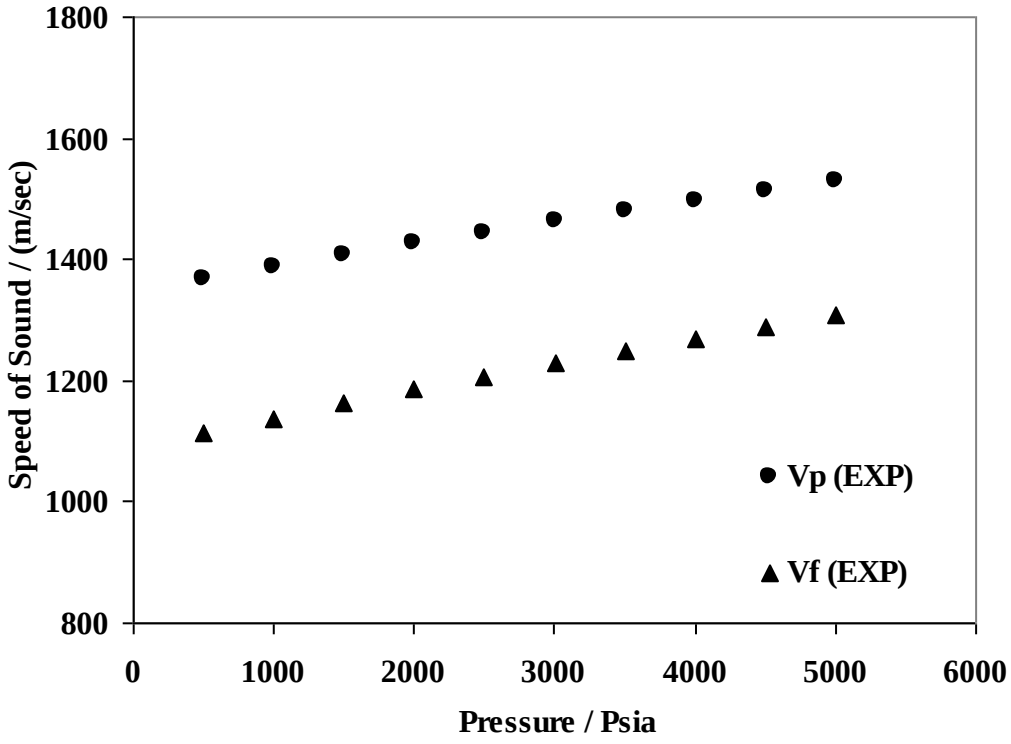

Figure 6.14 Measured speed of sound in binary mixture of nC_6 and nC_{10} in the matrix at 45 °C. V_p is the velocity of the fluid-saturated matrix (fluid + matrix) and V_f is the velocity of fluid only. The measurements were performed at a constant effective pressure.

Since the effective pressure was constant, then it is possible to assume that the porosity and pore volume are also constant.

6.3.2 Speed of Sound in Fluid Saturate Matrix (Test 2)

This experiment was performed with glass beads saturated with liquid CO_2 in different temperatures at 2500 psia. The reason of executing this test was to evaluate the measurement of the speed of sound in a volatile mixture of nC_4 + nC_{10} + CO_2, which is the next experiment. First, pure CO_2 was injected into sediments to optimise the test procedure and avoid the pore fluid to go into two-phase state.

Table 6.5 indicates the speed of sound for pure CO_2 before injection into the pores and for saturated matrix after CO_2 injection.

Figure 6.15 displays the experimental data of speed of sound at different temperatures. As shown in the figure, the temperature increment has the same reduction effects on

speed of sound of both fluid and saturated matrix. The velocity reduction rate in both cases shows a similar slope as the temperature increases. The speed of sound in the fluid and matrix is reduced by approximately 6 m/sec/°C. Since the porosity is assumed to be constant based on constant effective pressure, then it can be concluded that the speed of sound variations mostly depend on the fluid conditions.

Table 6.5 Measured speed of sound in CO_2 and the matrix saturated with this component at 2500 psia and different temperatures

Temperature (°C)±0.01	Pore Pressure (psia)±0.5	V_p (EXP) (m/s)	V_f (EXP) (m/s)
9.97	2500.3	1018.12	654.50
15.02	2499.2	981.83	634.79
25.02	2501.2	915.09	572.16
28.02	2499.4	896.94	549.83
29.00	2502.2	890.47	533.30
29.99	2499.9	884.61	530.70
30.58	2499.7	880.94	530.54
31.10	2500.1	878.23	520.21
31.58	2499.9	875.31	518.00
32.10	3200.6	872.29	514.67
35.00	2500.2	855.90	505.31
39.98	2500.9	828.67	474.37
45.00	2500.5	803.64	437.37
49.16	2499.6	783.93	412.49

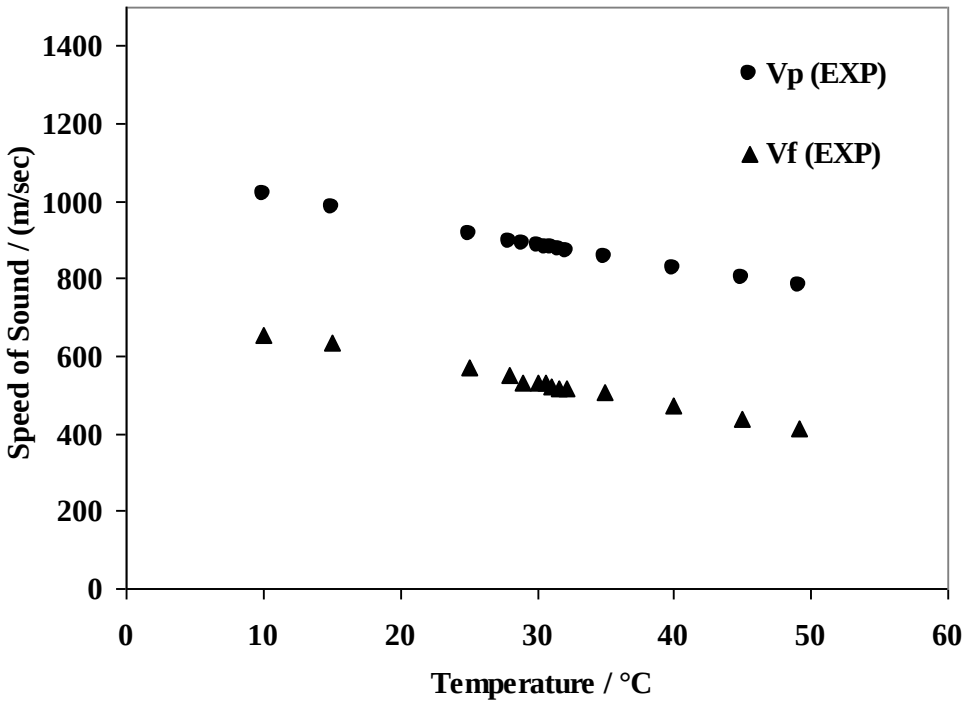

Figure 6.15 Measured speed of sound in CO_2 and within the matrix at 2500 psia and different temperatures

6.3.3 Speed of Sound in Fluid Saturate Matrix (Test 3)

In this case, speed of sound variation at different temperatures and pressures for the fluid of (nC_4 + nC_{10} + CO_2) and glass beads saturated with this fluid was investigated. Table 6.6 shows the results of this experiment.

Table 6.6 Measured speed of sound in nC_4 + nC_{10} + CO_2 and the matrix saturated with this mixture at different pressures and temperatures

Temperature (°C)±0.01	Pore Pressure (psia)±0.5	V_p (EXP) (m/s)	V_f (EXP) (m/s)
-0.04	1000.1	1339.18	-
-0.04	2001.2	1374.75	-
-0.02	3000.3	1386.89	-
-0.02	4000.4	1413.69	-
-0.02	4998.3	1432.73	-
10.03	1000.0	1294.80	1148.68
10.01	2000.1	1322.22	1195.46
9.98	3000.0	1345.56	1238.29
10.00	4000.1	1372.98	1277.54
10.04	5000.1	1395.93	1314.17
20.00	1000.0	1255.96	1104.82
20.00	2000.1	1284.10	1154.32
20.02	3000.1	1307.09	1199.22
20.02	4000.0	1332.52	1238.78
19.97	5000.0	1357.51	1278.57
29.99	1000.0	1225.99	1061.92
30.00	2000.1	1252.65	1114.13
30.00	3000.0	1278.87	1160.43
29.99	4000.0	1301.16	1203.46
30.00	5000.1	1327.49	1243.39
40.00	1000.0	1198.85	1021.12
40.02	2000.0	1225.67	1075.63
40.04	3000.0	1250.76	1124.54
40.06	4000.0	1277.25	1168.82
40.07	5000.0	1304.21	1210.28
49.96	1000.0	1173.04	979.73
50.00	2000.0	1203.42	1037.34
50.01	3000.1	1230.56	1088.51
49.99	4000.0	1256.64	1134.67
50.01	5000.0	1282.37	1177.42

Figure 6.16 displays the variations of the speed of sound in the matrix and fluid at different pressures and temperatures. P-velocities increase with increasing pore pressure and decrease with increasing temperatures.

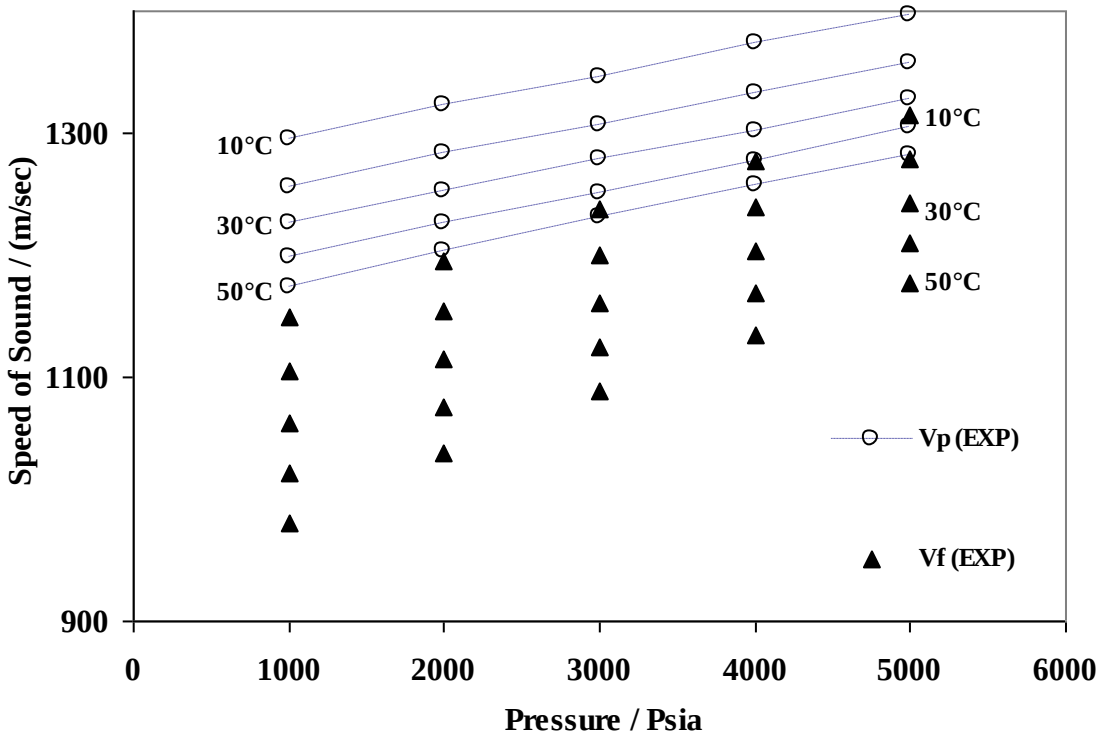

Figure 6.16 Measured speed of sound in nC_4 + nC_{10} + CO_2 and within the matrix at different pressures and temperatures

The results of the speed of sound measurements in a CO_2 - saturated matrix and a (nC_4 + nC_{10} + CO_2) - saturated matrix at different temperatures are shown in Figure 6.17. It indicates that the system of sediments with a ternary mixture of (nC_4 + nC_{10} + CO_2) as pore fluid has a higher speed of sound in comparison with the other system (the system with pure CO_2 as pore fluid). It can be concluded that the differences in the molecular weights of the two pore fluids assuming that the porosity was approximately constant, has led to different P-wave velocities.

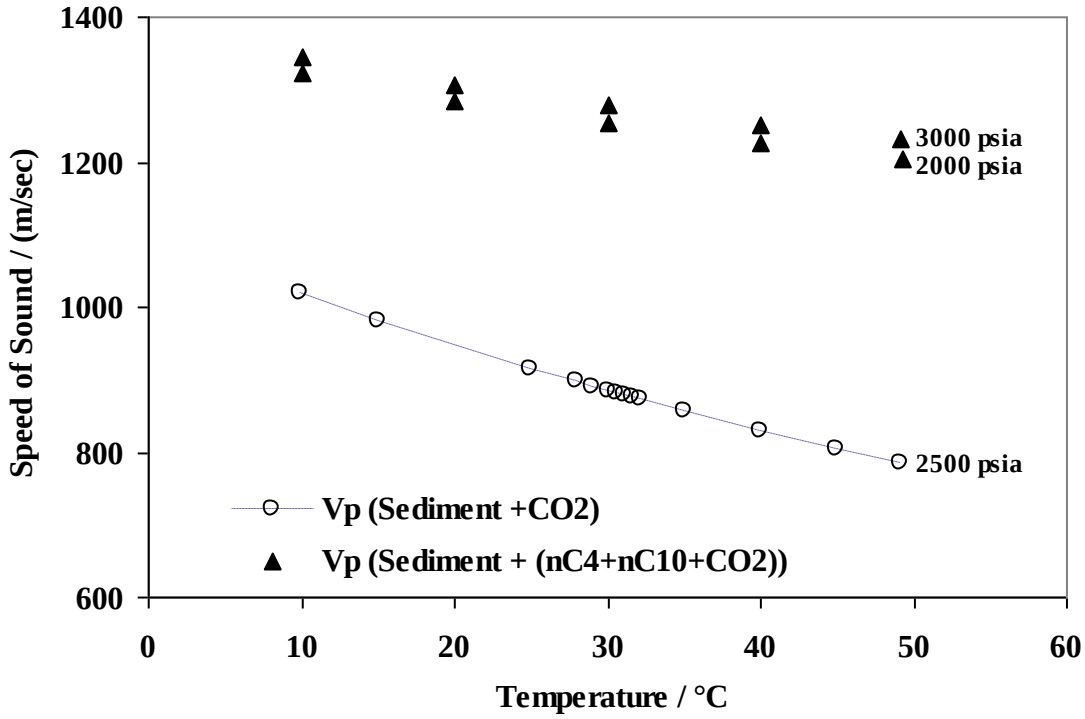

Figure 6.17 Comparison of measured speed of sound in two matrices saturated with different fluids: triangles for nC_4 + nC_{10} + CO_2 and dashed line for CO_2 at different temperatures

6.4 Conclusion

The speed of sound energy propagation depends on the physical properties of both rock and fluid. These properties are fluid content, composition, pressure, porosity and lithology of the rock. In reservoirs, oil and gas production and injection are two major causes of changes in pore pressure and fluid content/composition, which could result in changes in acoustic properties. Therefore, it is essential to have a good understanding of fluid acoustic properties.

In this work, the SAFT-BACK equation of state was used to calculate these properties, and then the results were compared with experimental data. The Batzle – Wang model has been used in the seismic industry for many years to calculate the acoustic properties of fluids.

Shams et al. (2007) studied the Batzle - Wang model (1992) for single-phase gas. They found that there is less sensitivity in the Batzle - Wang model towards the gases with

little pressure variation. They expect more problems to appear in volatile oil and gas condensate, which makes validity of Batzle - Wang model (1992) questionable.

Walls et al., (2005) showed that for the adiabatic bulk modulus, there are substantial differences between Batzle - Wang model (1992) and NIST at high pressure and temperature, and the differences depend on the gas specific gravity.

Here, the application of the SAFT-BACK equation was studied to calculate fluid properties and their effects on saturated sediments. It was observed that the SAFT-BACK equation of state can predict the results with better agreement with experimental data than the Batzle-Wang model. The Batzle-Wang equation is used by all geophysical software. This chapter illustrated the reliability and superiority of the SAFT-BACK EoS for acoustic fluid properties calculations compared to Batzle - Wang model for pure, binary, ternary mixtures and real oils. It is observed that the Batzle - Wang model fails when the molecular weight of oils is low. In addition, the Batzle - Wang model cannot predict accurate acoustic properties in gas condensates and volatile oils.

The velocity variation of a saturated matrix with three different pore fluids was also studied at various pressures and temperatures. It is observed that velocity in a saturated matrix increased with pore pressure and decreased with temperature. It is also concluded that saturated matrices with lighter hydrocarbons show lower velocity compared to those saturated with heavier hydrocarbons.

References:

Batzle M., Wang Z., 1992, *Seismic properties of pore fluids*, Geophysics, **57**, 1396-1408.

Biot M. A., 1956, *Theory of propagation of elastic waves in a fluid saturated porous solid, II, Higher frequency range,* J. Acoust. Soc. Am., **28**, 179 - 19 1.

Bulloch T.E., 1999, *The investigation of fluid propertues and seismic attributes for reservoir characterization*, a thesis submitted to Michigan Technological University

Gassmann F., 1951, *Uber die elastizitat poroser medien*: Vierteljahrsschrift der Natur. Gesselschaft, **96**, 1-23.

Shams A., Gozalpour F., MacBeth C., 2007, *Determination of the acoustic properties of hydrocarbon rich gases using PVT relations*, EAGE 69th Conference & Exhibition

Walls J., Dvorkin J., 2005, *Effects of pore fluid properties at high pressure and temperature on seismic response*, SEG Expanded Abstracts, **24**, 1617

Wang Z.W., 1988, *Wave velocities in hydrocarbons and hydrocarbon saturated rocks with applications to EOR monitoring*: Ph.D. thesis, Stanford University

Wang Z., Nur A., Batzle M.L., 1988, *Acoustic velocities in petroleum oils*, SPE paper 15646, Proceedings 61st SPE Technical Conference.

Chapter 7 – CONCLUSIONS AND RECOMMENDATIONS

7.1 Introduction

In this work, thermodynamic properties and the speed of sound of fluids were investigated. The investigations covered both experimental and modelling aspects for a wide variety of systems including pure, binary and multi-component mixtures, real reservoir fluids, CO_2 and in a wide range of temperature and density/pressure. The main achievement are summarised below:

(1) An extensive literature survey was performed in order to extract the experimental data for various hydrocarbon systems (pure and mixtures) and real fluids (Chapter 2). Also, previous modelling attemps of the speed of sound of fluids were studied and summarised in this chapter. Some binary mixtures data were used for calibrating the model.

(2) New experimental data on speed of sound in pure hydrocarbons and different type of mixtures such as binary, ternary, multi-component, volatile oil, CO_2-hydrocarbon mixtures and real fluids were generated (Chapter 3) for validating the numerical models.

(3) The velocity of sound data of fluid-saturated matrix using various fluids, sediments, temperature and pressure conditions, were also generated (Chapter 3). These data were produced for investigating the effects of different parameters on the velocity of sound in a variety of sediments and fluids. The equipments used in this work were described in detail.

(4) Thermodynamic modelling of fluid properties, using an equation of state called SAFT-BACK (Statistical Associating Fluid Theory-Boublik-Alder-Chen-Kreglewski) and an extension of the model to the mixtures has been presented. This model considered the thermodynamic properties as the derivatives of Helmholtz free energy of the molecules with respect to temperature and density. The superiorities of this equation of state over some other equations were studied. (Chapter 4).

(5) In order to improve the reliability of the equation of state to predict the speed of sound for mixtures, available experimental data generated in laboratory (Chapter 3) and extracted data from binary mixtures in the literatures (Chapter 2) and also

correlated data of the NIST webbook were used for tuning the binary interaction parameters between components.

(6) The performance of this model in predicting the speed of sound in different types of fluids in both liquid and gas states and over a wide range of temperature and pressure have been evaluated. The new experimental data measured in this work have been used for evaluation of the model (Chapter 5).

(7) To show the application of this model in reservoirs, a comparison between the results of this model and the Batzle – Wang model (which is used in all seismic fluid substitution software for determination of speed of sound in fluids) was conducted and showed the possibility of replacing Batzle – Wang model with the model developed in this work for more accurate prediction of fluid properties (Chapter 6).

(8) Some experiments were preformed in fluid-saturated sediments to measure the speed of sound (Chapter 6). The variation of velocity was studied at different temperature and pressure conditions in addition to various fluids. The speed of sound in fluids used in these experiments had been measured in advance. Changing the effective pressure in one experiment made it possible to investigate the effect of temperature and pressure on velocity of sound of the bulk frame.

The conclusions of this study and also some suggestions and recommendations for future work is presented in the following sections.

7.2 Literature Survey

One aim of the literature review was to gather and collate previous work on experimental determination and modelling of the speed of sound in fluids for pure hydrocarbons, mixtures containing light and heavy hydrocarbons and real oils. Development of a reliable thermodynamic model capable of determining various fluid properties such as heat capacities and speed of sound was another reason for this study. Data on binary mixtures were used to adjust and tune the binary interaction parameters between every two components for accurate prediction of this model (Chapter 2).

Other available models for determining these properties were studied and presented to demonstrate the requirements of industry for these calculations and positive and negative points of other thermodynamic properties.

7.3 Experimental Work

After selection of the equation of state for use in this work, the model was developed (Chapter 4) and tuned. The next step was to validate the model by using the experimental data. The existing data on the speed of sound for multi-component systems was limited in the literature. Therefore, more than 500 data points for different fluid systems have been produced experimentally (Chapter 2).

Another set of experimental data related to the measurement of the speed of sound in a bulk frame containing sediments saturated with fluids inside the pores (Chapter 2). These experiments helped to investigate the effects of temperature, pressure and effective pressure variation on speed of sound (Chapter 6).

7.4 Thermodynamic Modelling

A statistical model based on the SAFT-BACK equation of state and new proposed mixing rules for thermodynamic properties such as isobaric and isochoric heat capacities and speed of sound calculations in liquid and vapour phases was used in a model (Chapter 4). The predictions of this equation of state were compared to some other cubic EoS such as PR, SRK and VPT in predicting the thermodynamic properties. The results showed that the SAFT-BACK EoS can provide more reliable predictions. SAFT-BACK EoS has been extended to mixtures by proposing new mixing rules and binary interaction parameters.

This model was also developed for calculation of these properties for real reservoir fluids. For this purpose, the parameters of SAFT-BACK were considered as a function of molecular weight for each single carbon number and the BIPs have been established for the calculation of the dispersion energy between the segments in a mixture as a function of temperature and molecular weight of the mixture. Ideal isobaric heat capacity for each SCN was defined by their Watson Characterisation number, acentric factor and temperature (Chapter 4).

7.5 Validation of the Model

The values predicted by the model were compared with the experimental data generated in this work for a wide range of temperature, pressure and fluid samples (Chapter 5). The accuracy of the model in predicting the speed of sound for different fluids were described and displayed by comparing the results.

The main conclusions of this work can be written as follow:

- SAFT-BACK EoS has been shown to be a very strong equation of state for predicting the second order thermodynamic properties. Considering the results presented in Chapter 5 of this thesis, it is evident that the SAFT-BACK equation of state gives reasonable results for both liquid and vapour phases. The absolute average percentage deviations from experimental data for this modelling using the SAFT-BACK Equation of State are acceptable and show very good agreement with independent data.

- After modelling the speed of sound of some pure compounds and comparing the results with the data generated in the lab, small deviations were found between the experimental data and predictions. It showed the incapability of the SAFT-BACK equation of state in predicting thermodynamic properties at lower temperature with high accuracy. Therefore, it was necessary to tune the parameters of this EoS for pure compounds. Tuning of the SAFT-BACK parameters improved the results considerably.

- The modified SAFT-BACK was extended to mixtures over a wide range of temperatures by proposing four mixing rules that are defined on a segment basis. The extended modified SAFT-BACK was shown to yield good results in some derivative properties, i.e., velocity of sound and isobaric and isochoric heat capacities of multi-component mixtures containing n-alkanes from methane to *n*-decane, iC_4, iC_5, N_2 and CO_2. The capability of this equation has been checked by predicting the speed of sound over wide density and temperature ranges including the critical

temperatures. This equation proved to give better agreement with experimental data than other equations, over the temperature range 26.85-226.85 °C at pressures up to 29000 Psia.

- The Peng-Robinson EoS cannot give good and reasonable results for calculation of thermodynamic properties over a wide range of temperatures and densities, especially for binary mixtures. The deviations of the calculated speed of sound using the Peng-Robinson EoS exceeds 45% and therefore, the results are not satisfactory. A lot of attempts were conducted for tuning the parameters in the PR EoS, calculating the third parameter using different methods and using other alpha functions to improve these predictions. For this purpose, the Mathias-Copeman (1983) alpha function, the Lin and Duan (2005) method and some other correlations were used, but no significant improvement was observed in the calculation of pressure of pure compounds. This certainly affects the other properties which are obtained by differentiation of pressure with respect to density and temperature like C_p, C_v and V_s.

- To extend the developed model to real oils with petroleum fractions, Katz (1983) equation was used to define the composition of a synthetic oil to determine the speed of sound. The exponential molar distribution is the simplest method for splitting the C_7^+ fraction into a number of pseudo-components.

- A full description of the real reservoir fluid by identifying all its constituents may not be possible. Distillation and gas chromatography determine the hydrocarbon groups in a real fluid by measuring some of their properties such as average boiling point temperature, molecular weight and density (Danesh, 1998). The experimental results of speed of sound of real fluids were used to develop this correlation for mixtures. Comparison between the measured values and predictions show the accuracy of this model.

- Calculation of fluid density, fluid velocity and fluid bulk modulus has made directly using Batzle-Wang model (1992) and SAFT-BACK model (this work). Other seismic properties such as P-wave velocity, S-wave velocity, acoustic impedance and Poisson ratio are calculated using the Biot (1956) – Gassmann (1951) model. Any small deviation in predicted density, velocity and bulk modulus of the fluids from the experimental data, could lead to significant effect on rock properties, especially P-wave velocity and acoustic impedance. These deviations will change AVO responses and in some cases may cause a change in AVO class (Bulloch, 1999). The differences between calculated and experimental fluid properties have a small effect on S-wave velocity and much smaller effect on Poisson ratio at high pressure conditions.

7.6 Recommendations for Future Work

One of the main fluids in reservoirs is water/brine. SAFT-BACK EoS should be developed for mixtures of water - hydrocarbons and the binary interaction parameters of polar components need to be tuned. Salinity is another area of research for developing this model as the reservoir water is usually saline. A lot of experimental data for tuning and extension of this model should be generated for mixtures of water and hydrocarbons. This model can be developed to water / brine – real reservoir fluids by using the experimental data.

Measurement of the velocity of sound in sediment saturated with fluids can be continued by using various synthetic and fluids. In order to idealize the conditions of experiments and get closer to reservoir properties, porosity of the bulk frame can be reduced by using various sizes of sediments to fill the empty spaces between the larger particles.

In order to investigate the effects of fluid changes on seismic properties more accurately using the Gassmann model, knowledge of some properties of fluid, dry rock framework and evacuated porous media is necessary. The input variables necessary for the Gassmann - Biot model calculations include the solid material grain bulk modulus and density that are determined from the mineralogy of the reservoir matrix. The water/brine

and hydrocarbon bulk modulus and density values can be computed at reservoir temperature and pressure conditions using SAFT-BACK model. The P-wave and S-wave velocities and bulk density of the matrix should be measured in the laboratory to calculate the saturated bulk modulus and the dry frame shear modulus. Gassmann's relations can be used to calculate the dry frame bulk modulus using the saturated bulk modulus. Also, the bulk density can be calculated by using a volume weighted average density for the saturated matrix. Finally, P-wave and S-wave velocities can be calculated using a velocity form of Gassmann's relation suggested by Murphy, Schwartz, and Hornby (1991).

The speed of sound has been increasingly employed to model fluid properties. The measurements can be made quickly and with a high accuracy over wide ranges of temperature and pressure for the liquid and vapour phases. It might be possible to obtain a good knowledge about other properties of fluids such as composition, molar fraction and constituent components of fluids from measured speed of sound. It can be a significant improvement in seismic industry to know the phase behaviour of pore fluids in the reservoirs either during production or before and after improved oil recovery methods using speed of sound in fluids.

It is possible to use well log data to derive the velocity of sound in fluids in the reservoirs. Fluid elastic properties which are used in Gassmann equations might be obtained from P-wave and S-wave velocity and density well logs. Calculated fluid velocity by Gassmann model can be used for determination of fluid composition.

References

Batzle M., Wang Z., 1992, *Seismic properties of pore fluids*, Geophysics, **57**, 1396-1408

Biot M. A., 1956, *Theory of propagation of elastic waves in a fluid saturated porous solid, II, Higher frequency range,* J. Acoust. Soc. Am., **28**, 179 - 191

Bulloch T.E., 1999, *The investigation of fluid propertues and seismic attributes for reservoir characterization*, a thesis submitted to Michigan Technological University

Gassmann F., 1951, *Uber die elastizitat poroser medien*: Vierteljahrsschrift der Natur. Gesselschaft, **96**, 1-23

Murphy W.F., Schwartz L.M., Hornby B., 1991, *Interpretation physics of V_p and V_s in sedimentary rocks*: Transactions SPWLA 32nd Annual Logging Symposium, 1-24